Tutorial 3:

Continuous domain sparse recovery of biomedical imaging data using structured low-rank approaches

JONG CHUL YE, KAIST
MATHEWS JACOB, UNIV. OF IOWA

Joint work by several authors

CBIG, Univ. Iowa

1. Dr. Gregory Ongie
2. Dr. Merry Mani
3. Mr. Arvind Balachandrasekaran
4. Ms. Ipshita Bhattacharya
5. Ms. Sampurna Biswas

KAIST

1. Dr. Kyong Hwan Jin
2. Mr. Juyoung Lee
3. Dongwook Lee
4. Junhong Min

Overview

Part 1: Theory & Algorithms

Part 2: Applications

Overview

1. Introduction
2. Review of Compressive Sensing
3. FRI extrapolation from uniform samples
4. Structured low-rank interpolation for non-uniform samples
5. Fast implementations
6. Biomedical applications

Overview

1. Introduction
2. Review of Compressive Sensing
3. FRI extrapolation from uniform samples
4. Structured low-rank interpolation for non-uniform samples
5. Fast implementations
6. Biomedical applications

Motivation: MRI reconstruction

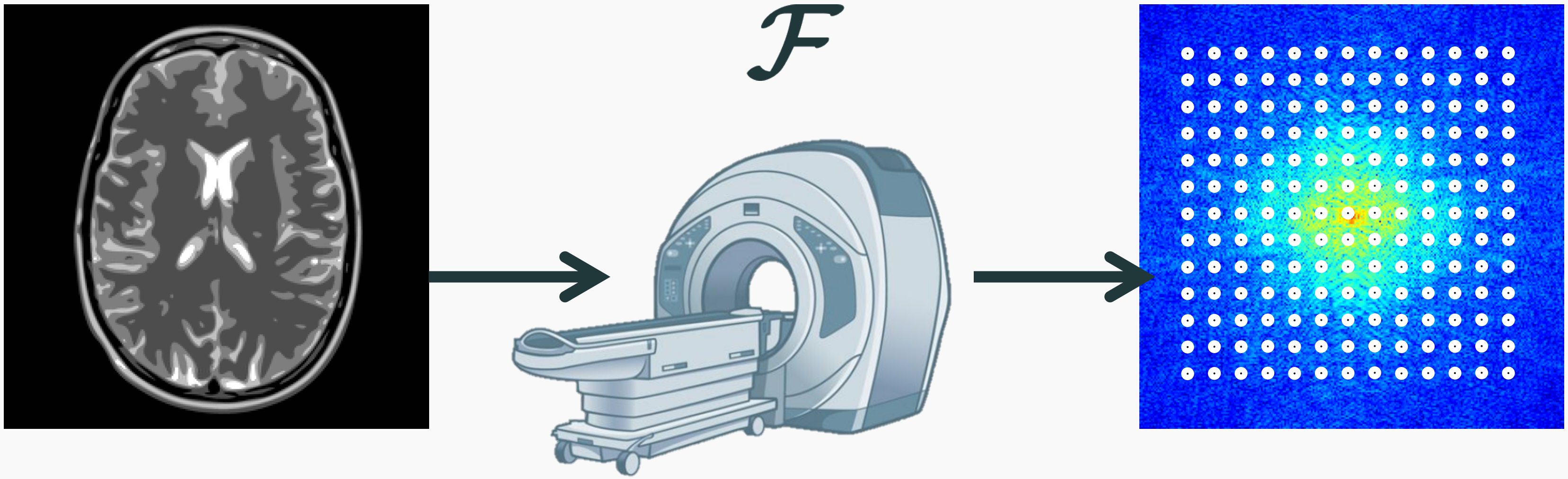

Main Problem:

Reconstruct image from Fourier domain samples

Related: Computed Tomography, Florescence Microscopy

Motivation: MRI Reconstruction

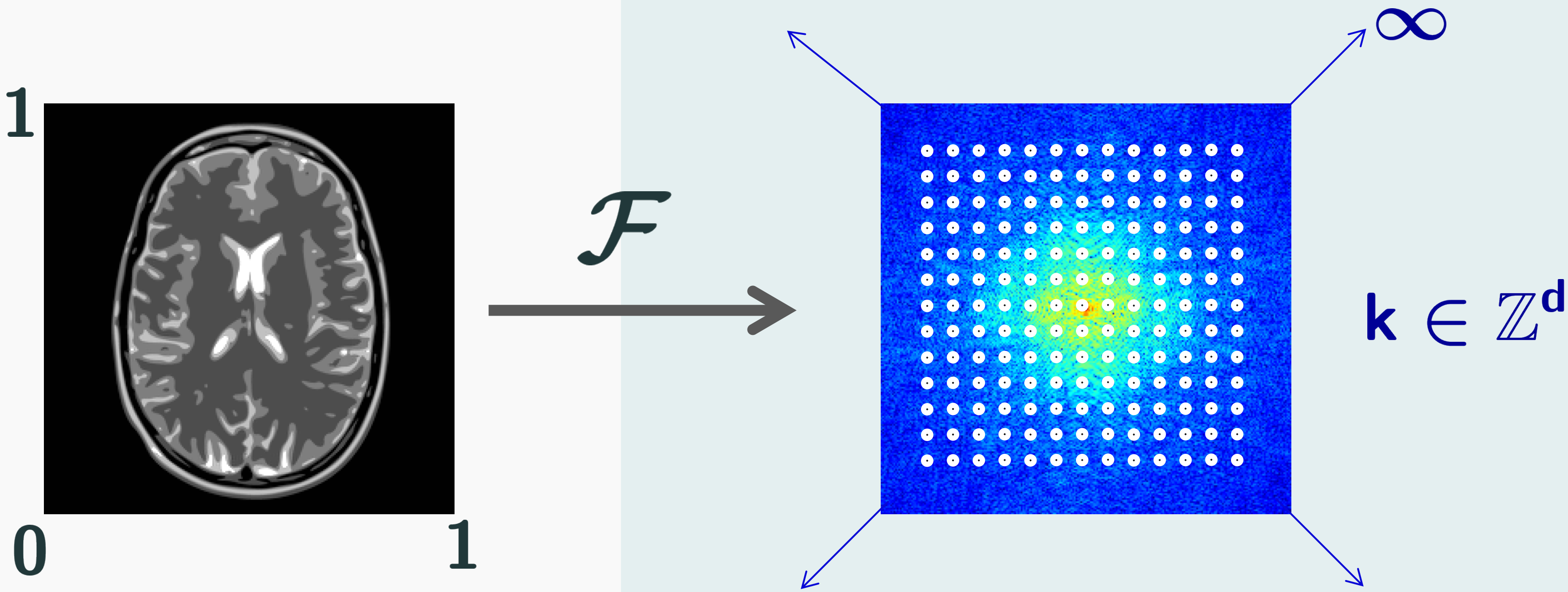

$$f(x), \quad x \in [0,1]^d$$

$$\widehat{f}[k] := \int_{[0,1]^d} f(x) e^{-j2\pi k \cdot x} dx$$

Uniform Fourier Samples =
Fourier Series Coefficients

Types of “Compressive” Fourier Domain Sampling

low-pass

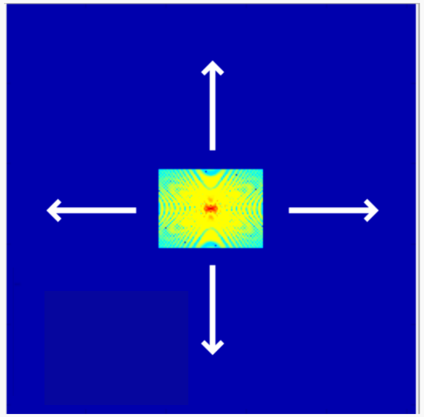

Fourier
Extrapolation

↓

Super-resolution
recovery

radial

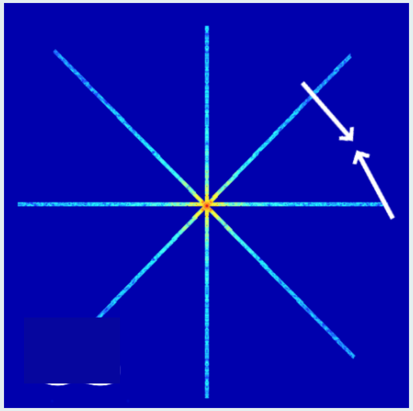

random

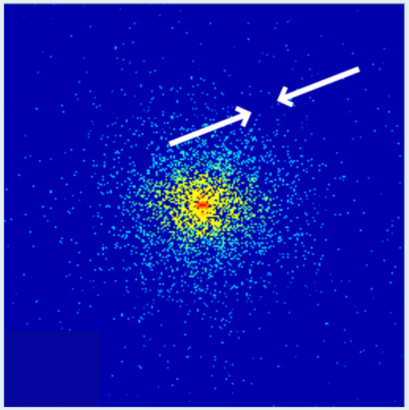

Fourier
Interpolation

↓

“Compressed Sensing”
recovery

Extrapolation: super-resolution microscopy

The Nobel Prize in Chemistry 2014

Photo: Matt Staley/HHMI

Eric Betzig

Prize share: 1/3

© Bernd Schuller, Max-Planck-Institut

Stefan W. Hell

Prize share: 1/3

Photo: K. Lowder via Wikimedia Commons, CC-BY-SA-3.0

William E. Moerner

Prize share: 1/3

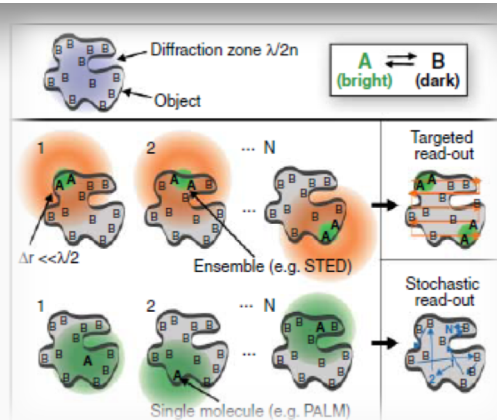

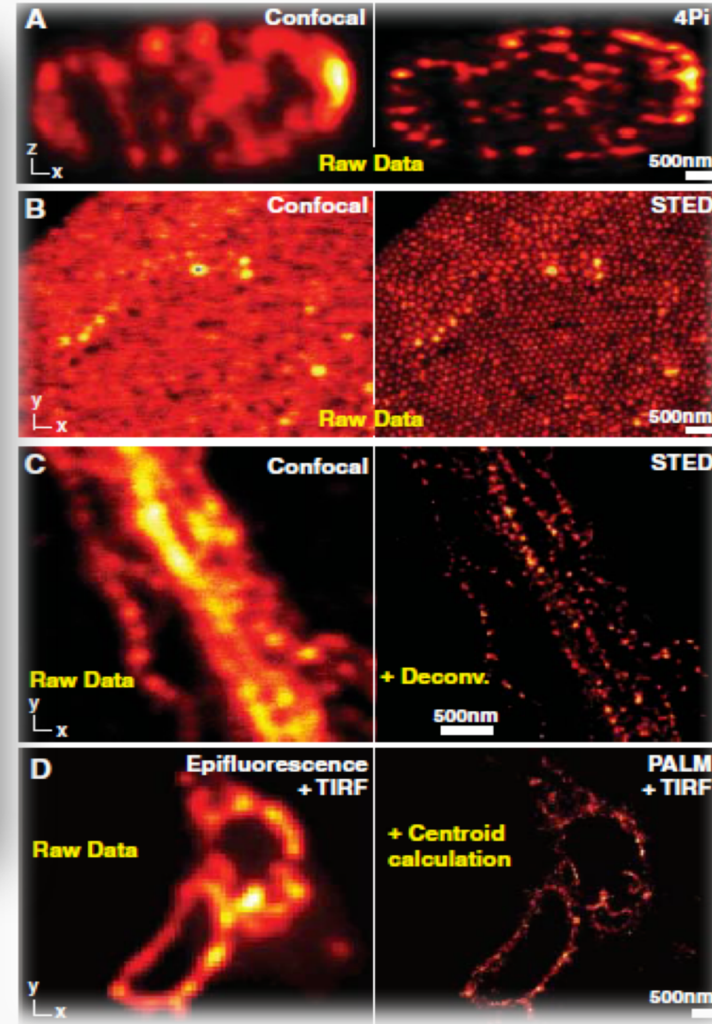

S. Hell et al, Science 2007.

Interpolation: accelerated MRI

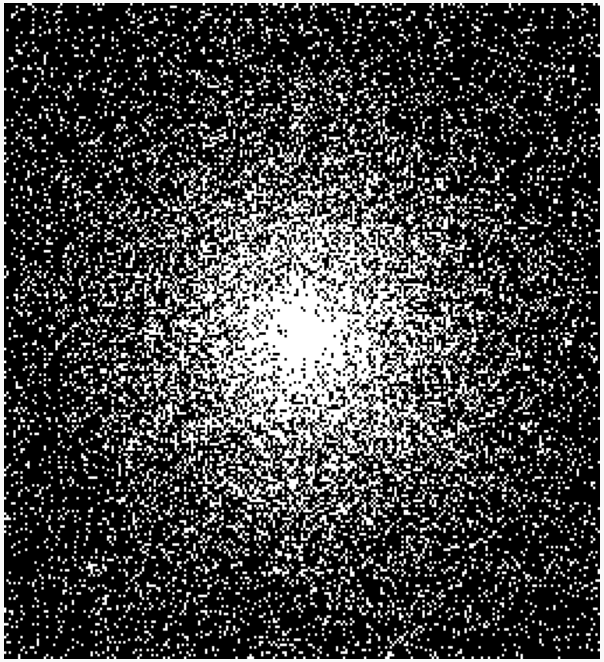

25% Random
Fourier samples
(variable density)

TV-min →

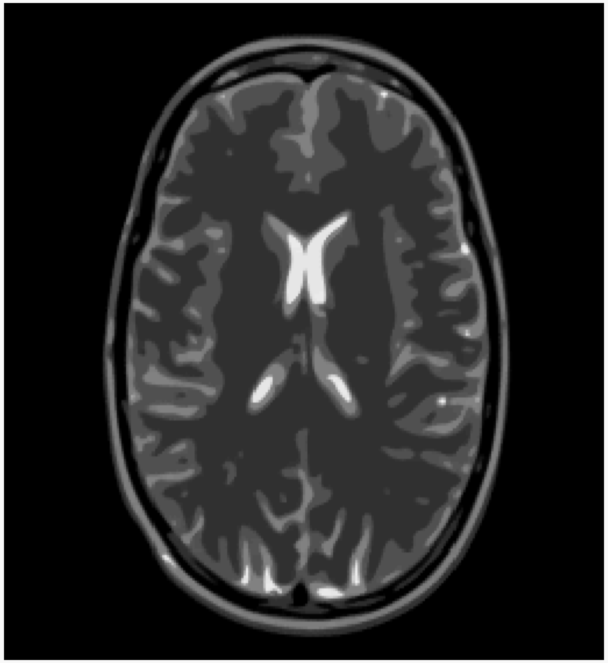

Rel. Error = 5%

Overview

1. Introduction
2. Review of Compressive Sensing
3. FRI extrapolation from uniform samples
4. Structured low-rank interpolation for non-uniform samples
5. Fast implementations
6. Biomedical applications

Compressed Sensing (CS)

- Incoherent projection
- Underdetermined system
- Sparse unknown vector

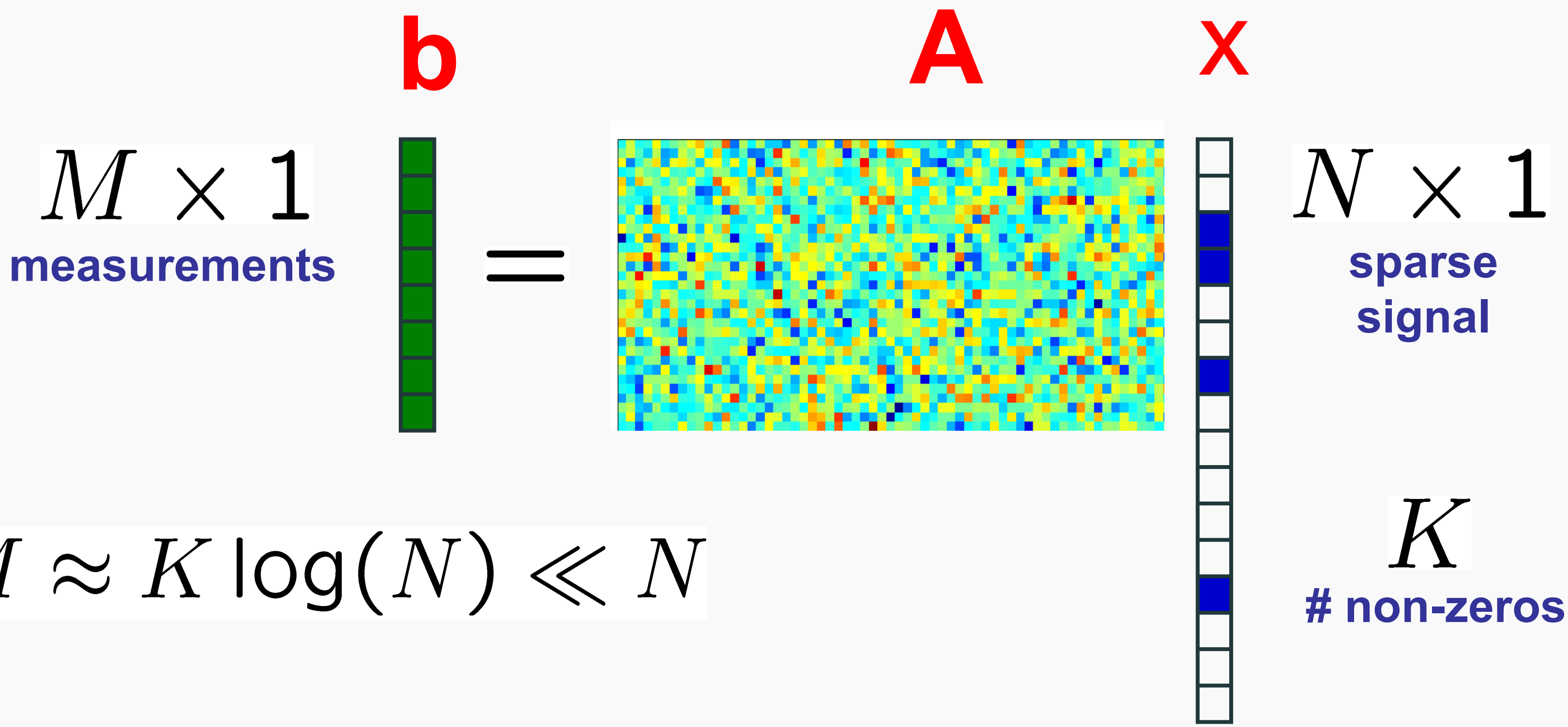

$$M \approx K \log(N) \ll N$$

Courtesy of Dr. Dror Baron

Sparse-Low Rank Recovery in Nutshell

Reconstructed image

Forward mapping
By physics

$$\hat{x} = \arg\min_{x} \|y - Ax\|_2^2 + R(x)$$

Measurement data

Prior Knowledge
(smoothness, sparsity,etc)

Application to biomedical imaging

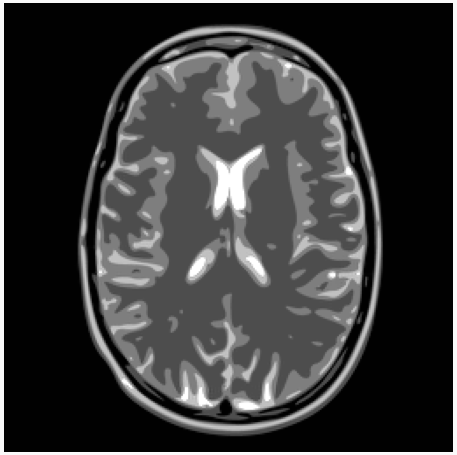

$\mathcal{F}$

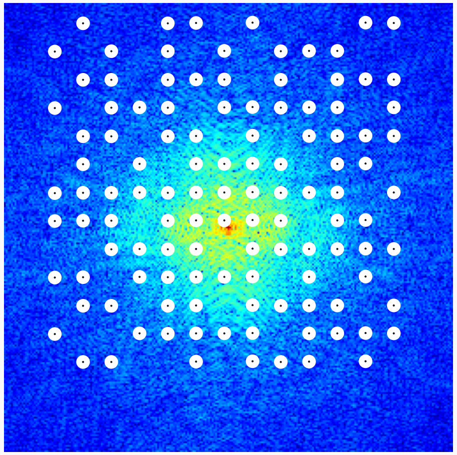

Full sampling is costly!

Randomly undersample

Application to biomedical imaging

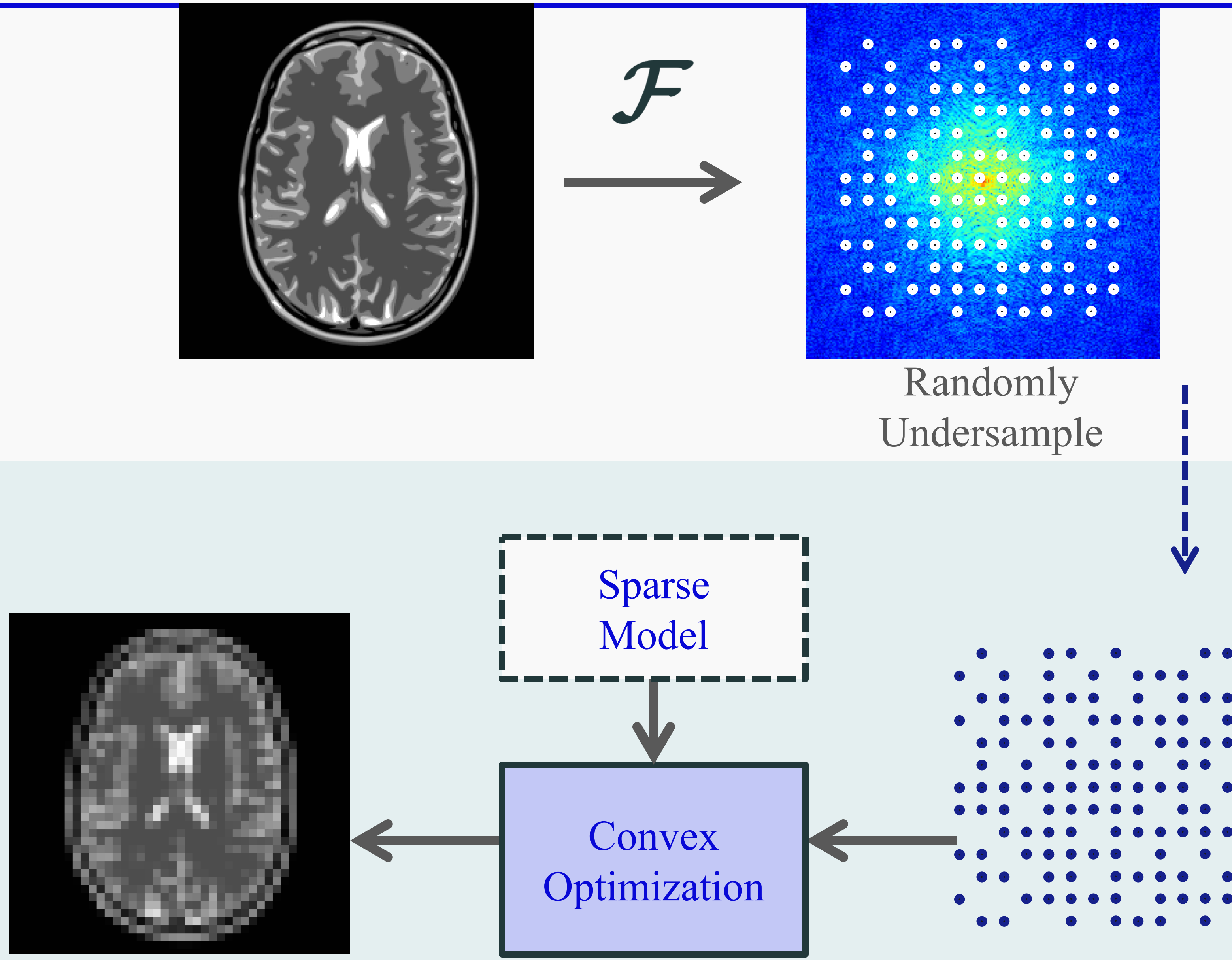

Analysis formulation of Compressed Sensing

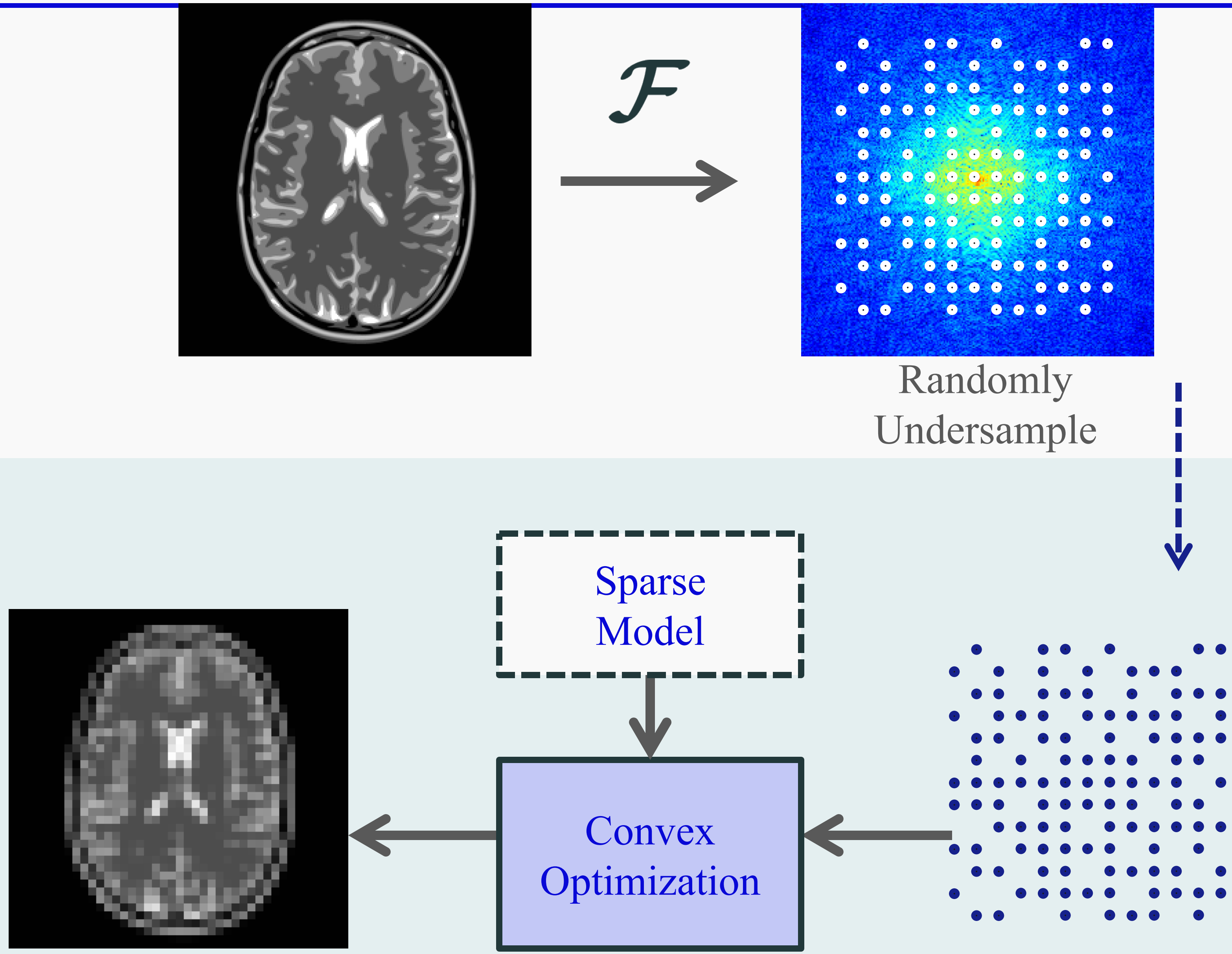

Example:

Assume discrete gradient of image is sparse

↕

Piecewise constant model

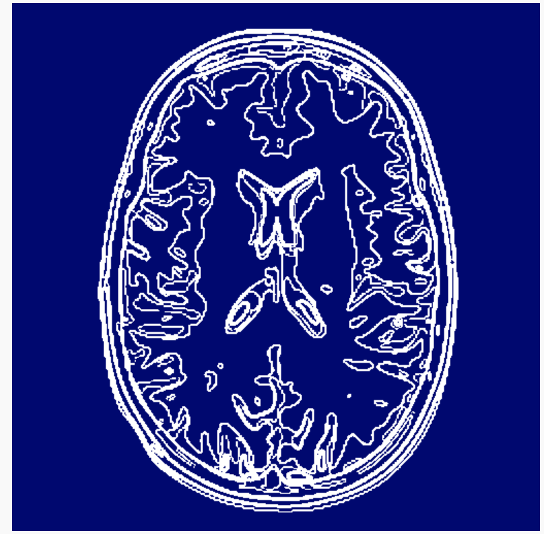

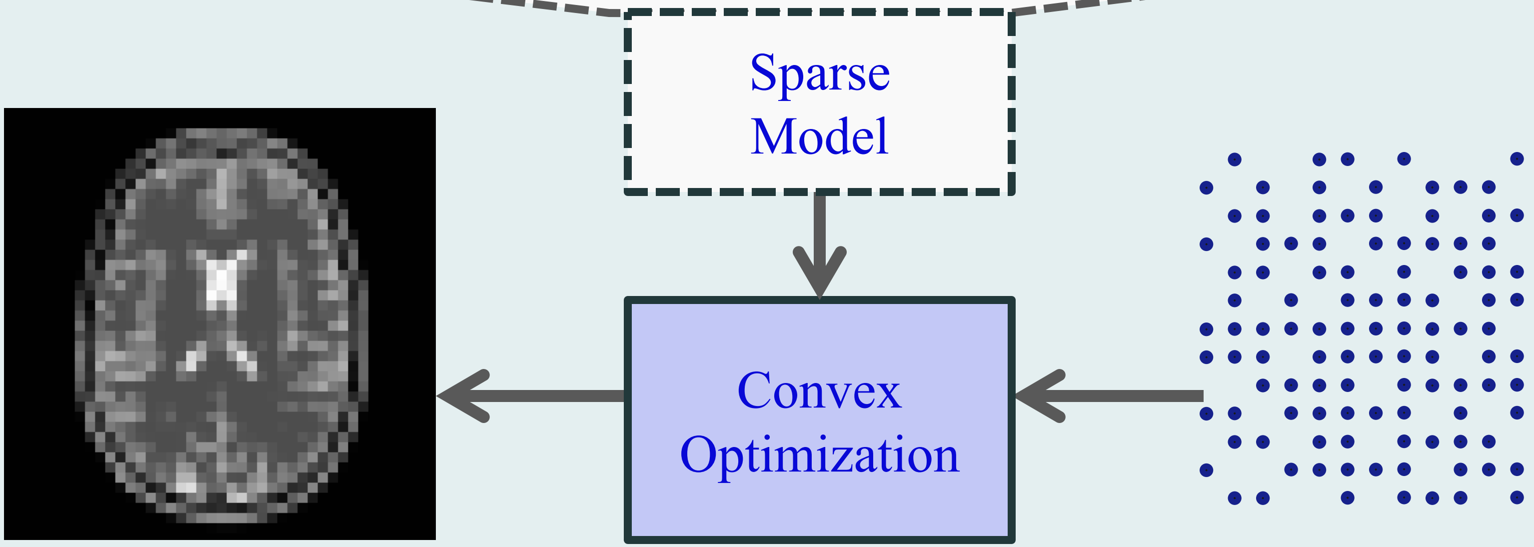

Recovery by Total Variation (TV) minimization

TV semi-norm: $\|\mathbf{g}\|_{TV} = \sum_{i,j} \sqrt{|g_{i+1,j} - g_{i,j}|^2 + |g_{i,j+1} - g_{i,j}|^2}$

i.e., L1-norm of discrete gradient magnitude

$\sum_{i,j}$ 

Recovery by Total Variation (TV) minimization

TV semi-norm: $\|\mathbf{g}\|_{\mathbf{TV}} = \sum_{\mathbf{i},\mathbf{j}} \sqrt{|\mathbf{g}_{\mathbf{i}+1,\mathbf{j}} - \mathbf{g}_{\mathbf{i},\mathbf{j}}|^2 + |\mathbf{g}_{\mathbf{i},\mathbf{j}+1} - \mathbf{g}_{\mathbf{i},\mathbf{j}}|^2}$

i.e., L1-norm of discrete gradient magnitude

$\sum_{\mathbf{i},\mathbf{j}}$ 

$$\min_{\mathbf{g}\in\mathbb{C}^{\mathbf{N}\times\mathbf{N}}} \|\mathbf{g}\|_{\mathbf{TV}} \quad \text{subject to} \quad \mathbf{F}_{\Omega}\mathbf{g} = \mathbf{F}_{\Omega}\mathbf{f} \qquad (\mathbf{TV}\text{-min})$$

Recovery by Total Variation (TV) minimization

TV semi-norm: $$\|\mathbf{g}\|_{TV} = \sum_{i,j} \sqrt{|g_{i+1,j} - g_{i,j}|^2 + |g_{i,j+1} - g_{i,j}|^2}$$

i.e., L1-norm of discrete gradient magnitude

$$\sum_{i,j}$$

$$\min_{\mathbf{g}\in\mathbb{C}^{N\times N}} \|\mathbf{g}\|_{TV} \quad \text{subject to} \quad \mathbf{F}_\Omega \mathbf{g} = \mathbf{F}_\Omega \mathbf{f} \qquad (\mathbf{TV}\text{-min})$$

Restricted DFT

$$\Omega =$$

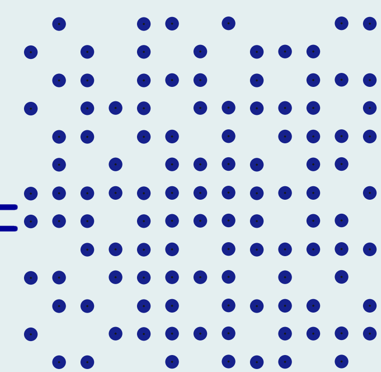

Sample locations

Recovery by Total Variation (TV) minimization

TV semi-norm: $$\|\mathbf{g}\|_{TV} = \sum_{i,j} \sqrt{|g_{i+1,j} - g_{i,j}|^2 + |g_{i,j+1} - g_{i,j}|^2}$$

i.e., L1-norm of discrete gradient magnitude

$$\sum_{i,j}$$

$$\min_{\mathbf{g}\in\mathbb{C}^{N\times N}} \|\mathbf{g}\|_{TV} \text{ subject to } \mathbf{F}_\Omega \mathbf{g} = \mathbf{F}_\Omega \mathbf{f} \qquad (\mathbf{TV}\text{-min})$$

Restricted DFT

Convex optimization problem

Fast iterative algorithms:

ADMM/Split-Bregman, FISTA, Primal-Dual, etc.

$\Omega =$

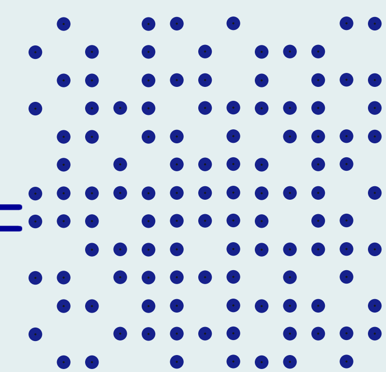

Sample locations

Recovery using zero filled IFFT

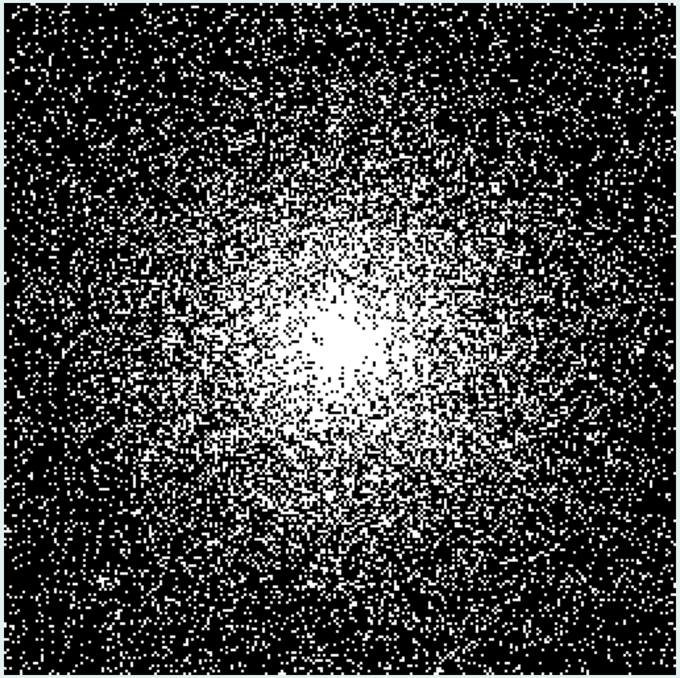

25% Random
Fourier samples
(variable density)

$\xrightarrow{\mathbf{DFT}^{-1}}$

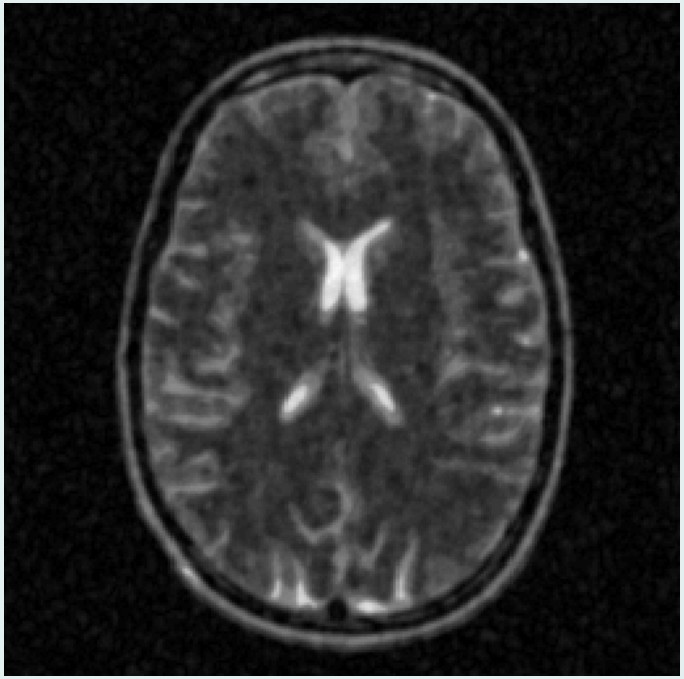

Rel. Error = 30%

Recovery using TV minimization

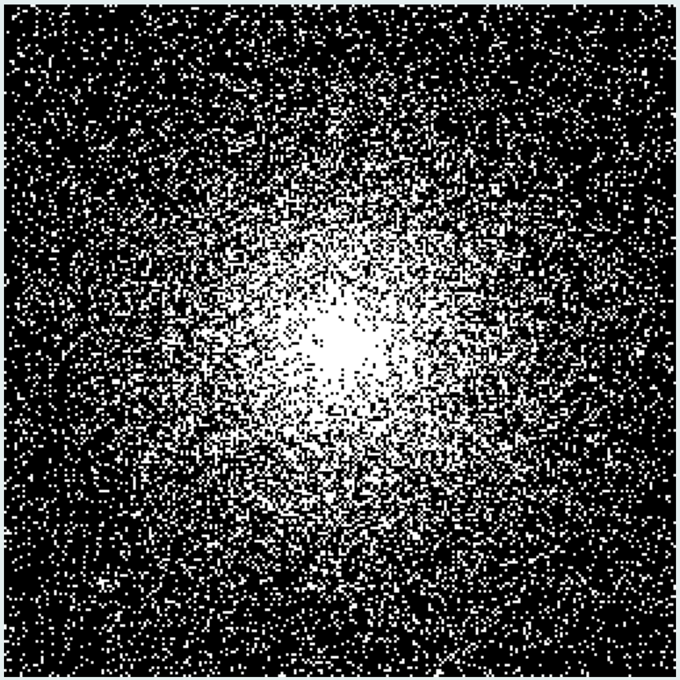

25% Random
Fourier samples
(variable density)

TV-min

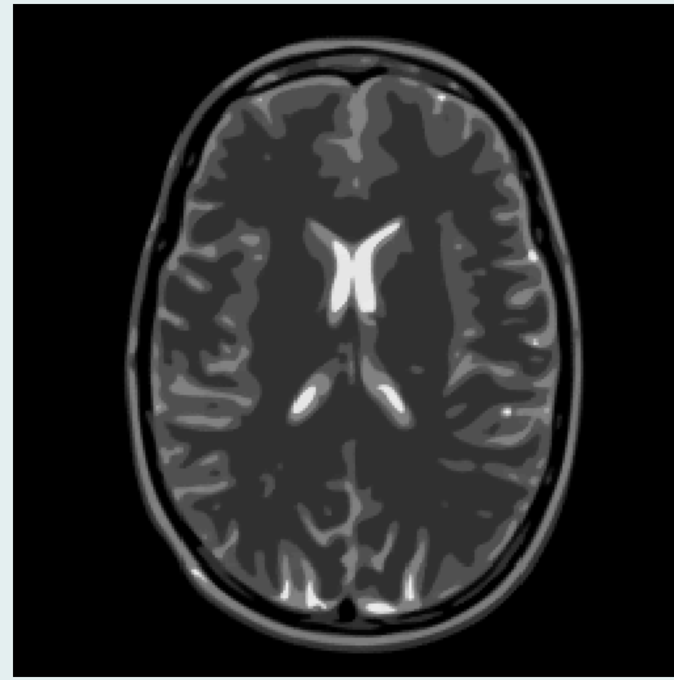

Rel. Error = 5%

Limitations of CS

- Discrete domain theory
- Explicit form of sensing matrix
- RIP issue → no direct interpolation

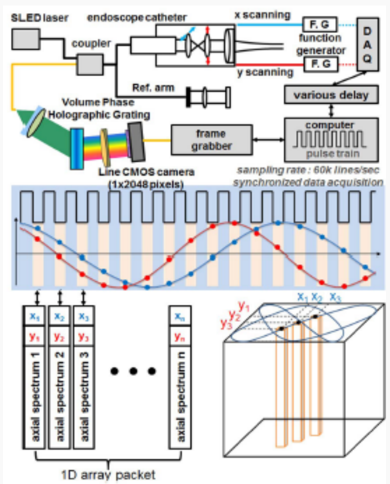

ig. 2. (Color online) 3D SD-OCT image reconstruction

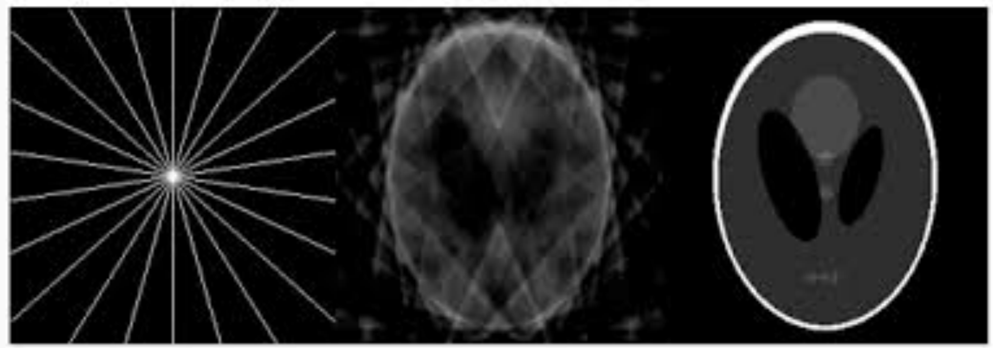

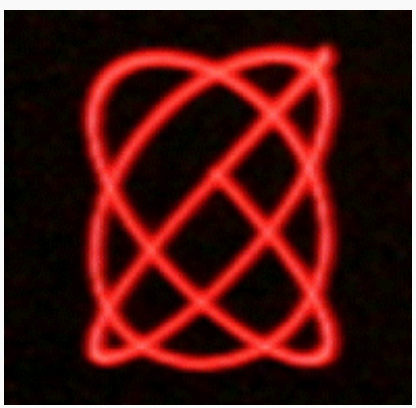

Analytic Reconstruction

Beautiful analytic reconstruction results from fully sampled data

(a) MR Imaging

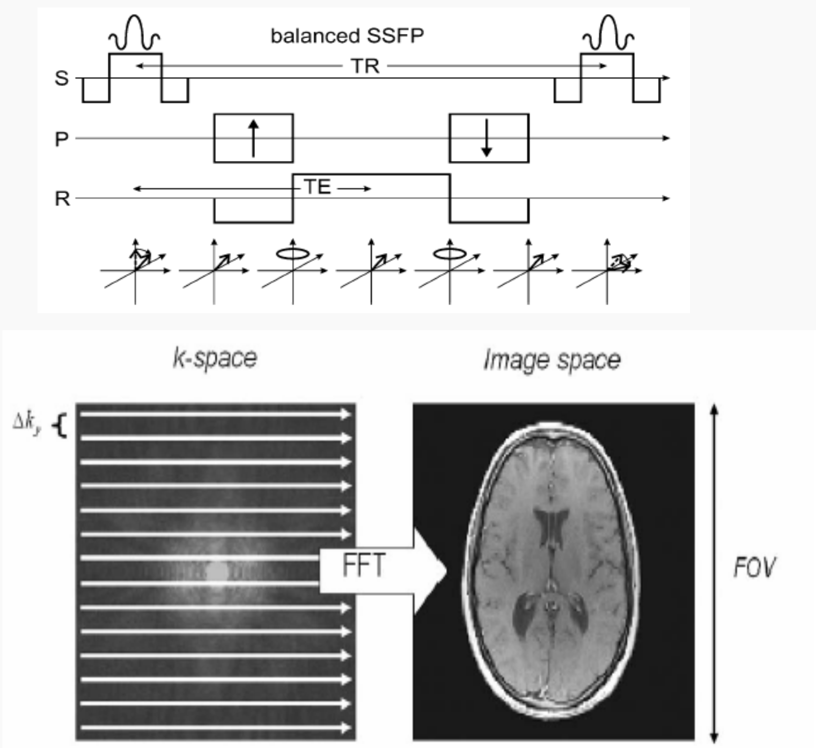

(b) Time-reversal of a scattered wave

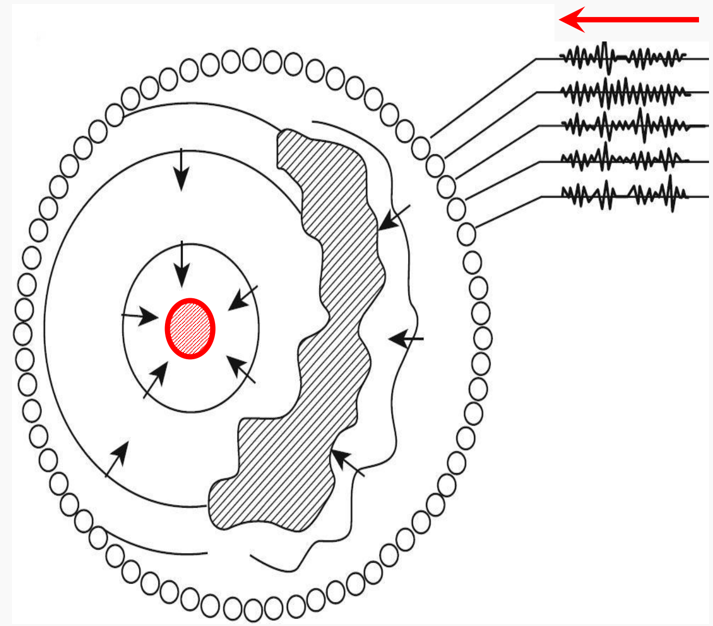

$$\mathcal{I}_1(x) = \int_\Omega f(z) \int_0^T \int_{\partial\Omega} \frac{\partial G(x,y,T,t)}{\partial \nu_y} \frac{\partial \Gamma}{\partial t}(z,y,0,T-t)\, d\sigma(y)\, dt\, dz.$$

Project Goal: Unification of CS and analytic reconstruction for biomedical imaging using a 2-layer approach

Dense samples

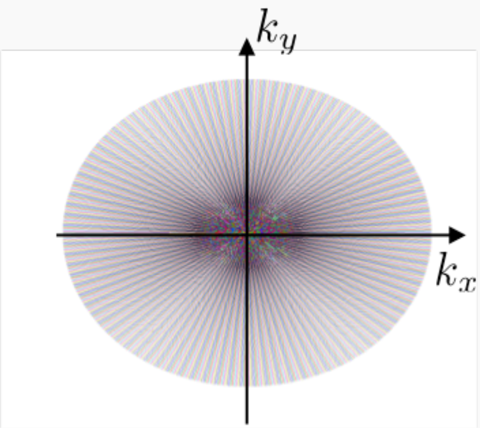

"The Missing Link"

?

Sparse samples

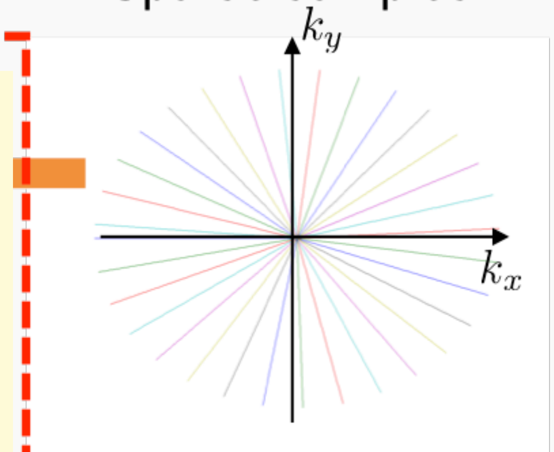

Analytic Reconstruction

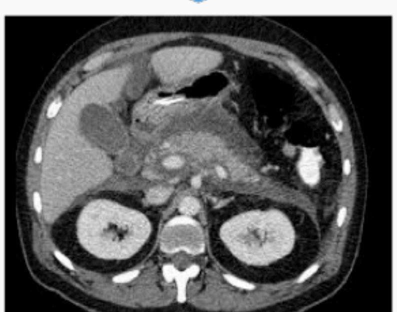

Compressed Sensing

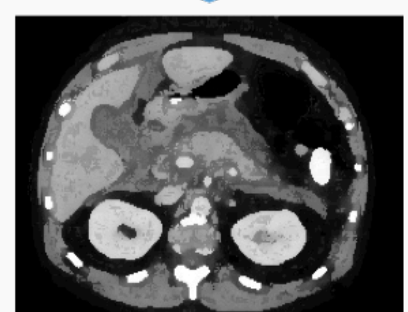

Rank $H(x)$ ⟷ *dual* ⟷ $\|x\|_0$

"True" measurement model:

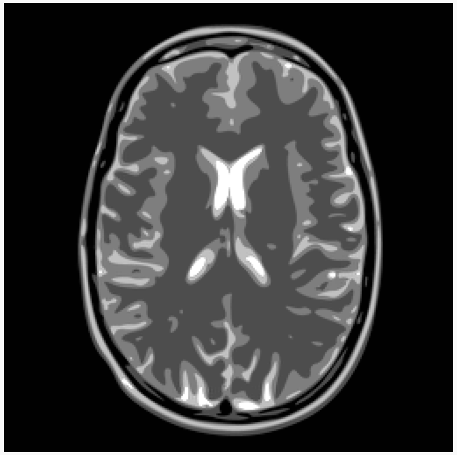

Continuous

$\mathcal{F}$

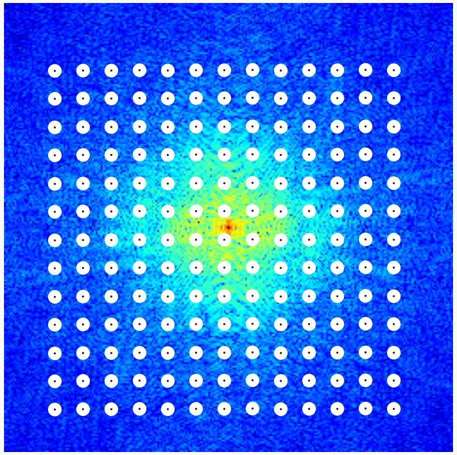

Continuous

“True” measurement model:

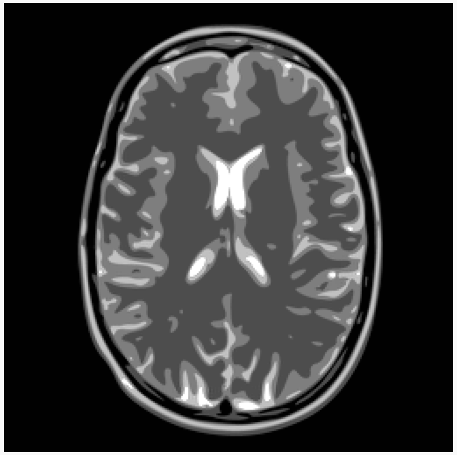

$\mathcal{F}$ $\longrightarrow$

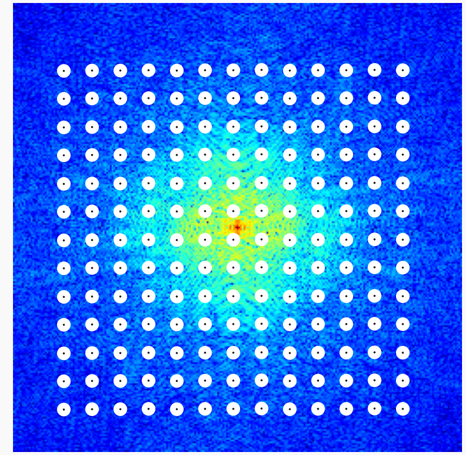

Continuous

Continuous

Approximated measurement model:

$\approx$

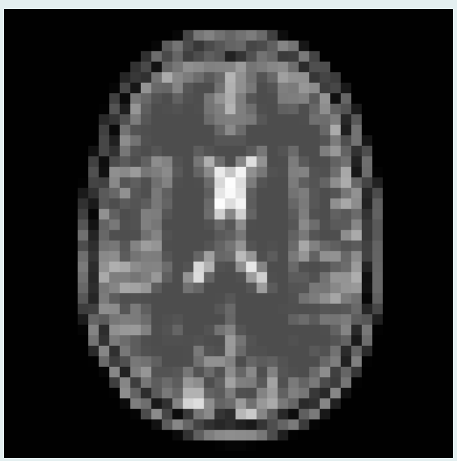

DFT $\longrightarrow$

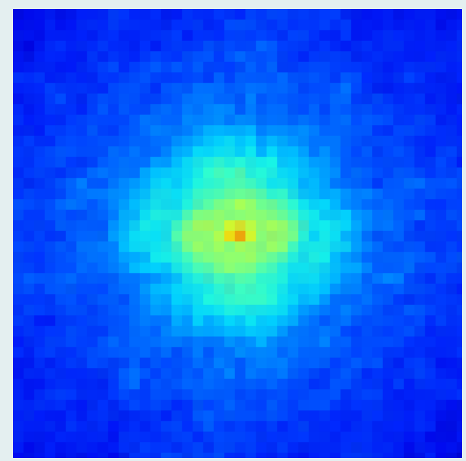

DISCRETE

DISCRETE

DFT Reconstruction

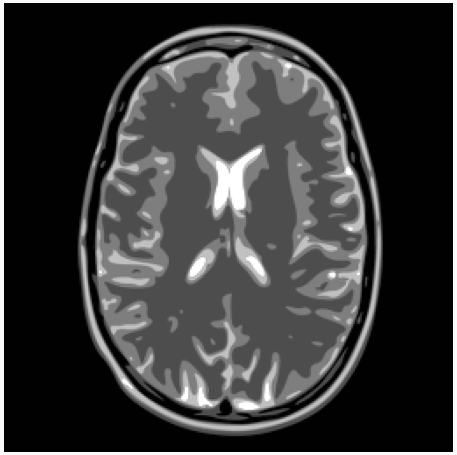

Continuous

$\mathcal{F}$

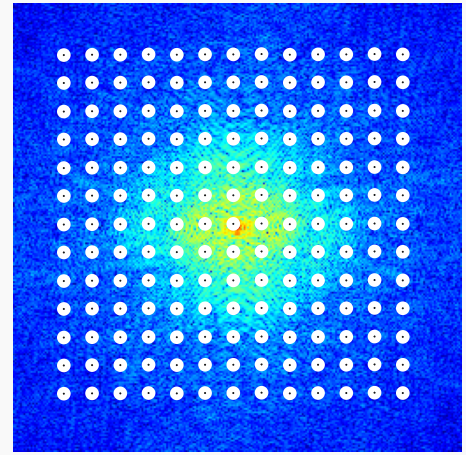

Continuous

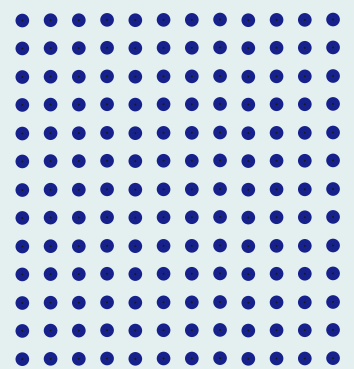

DFT Reconstruction

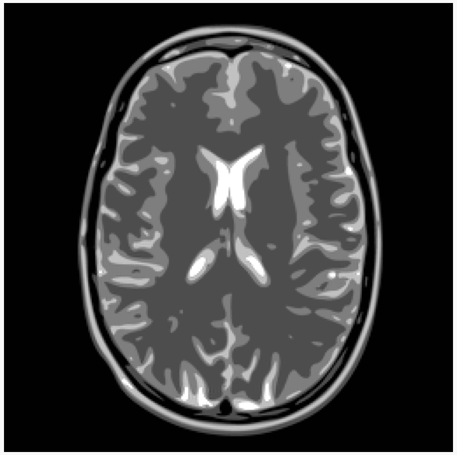

Continuous

$\mathcal{F}$ →

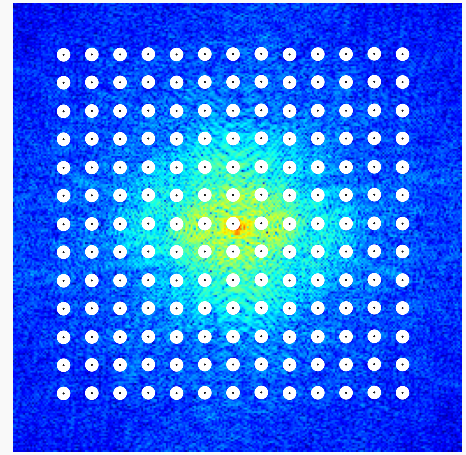

Continuous

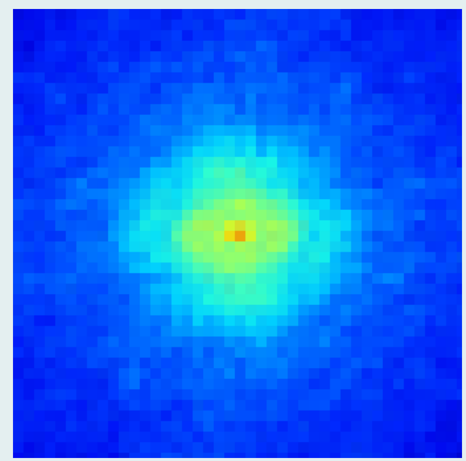

DISCRETE

DFT Reconstruction

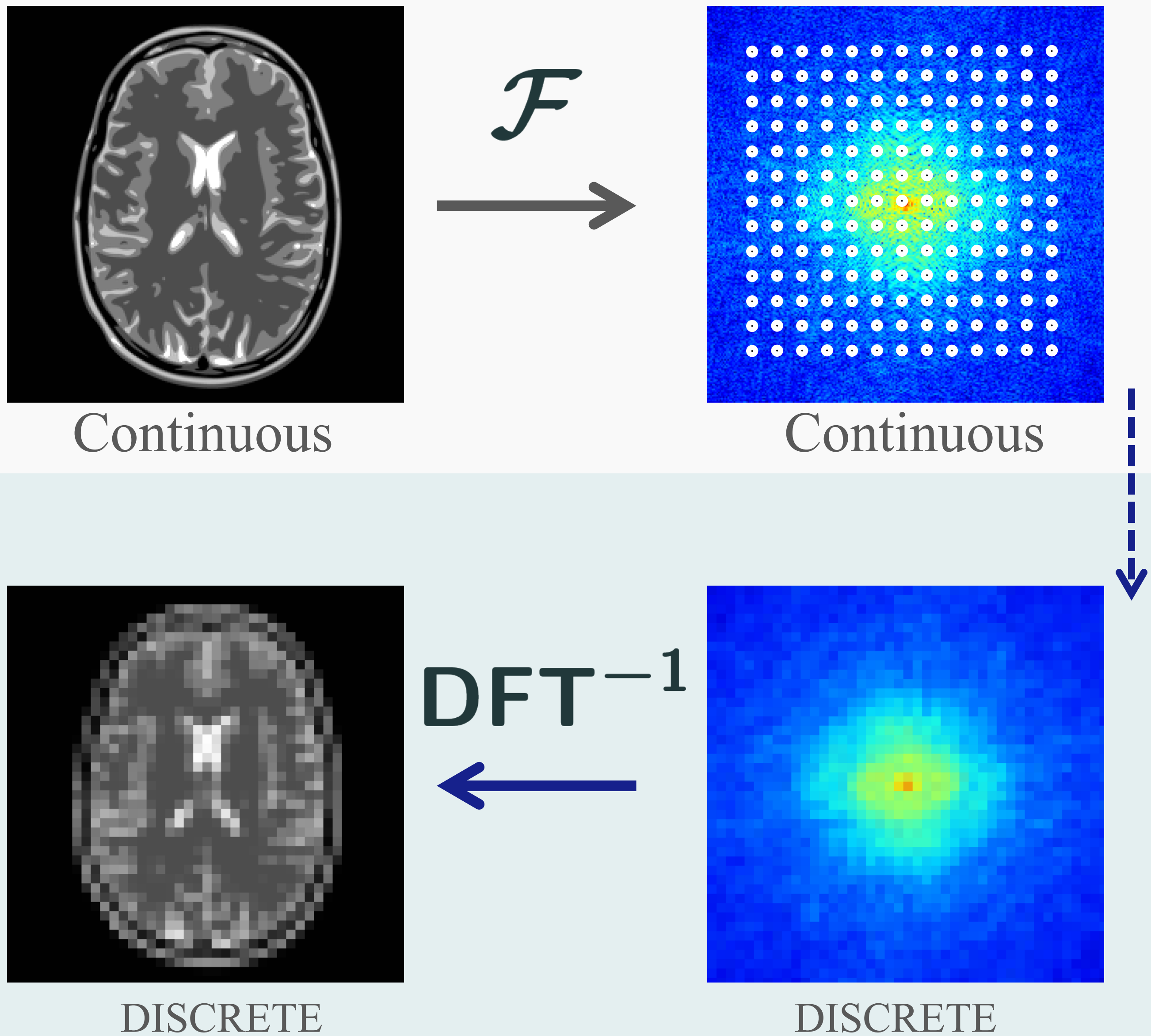

Challenge: Discrete approximation destroys sparsity!

Continuous

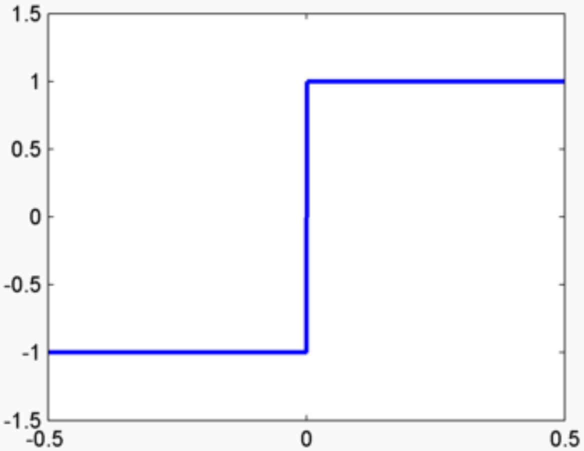

Challenge: Discrete approximation destroys sparsity!

Continuous

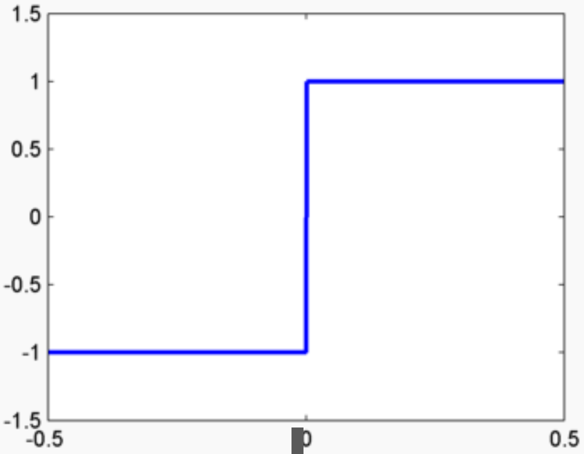

∂

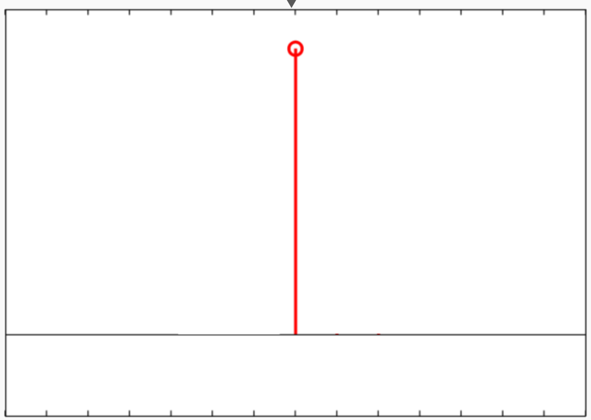

Exact Derivative

Challenge: Discrete approximation destroys sparsity!

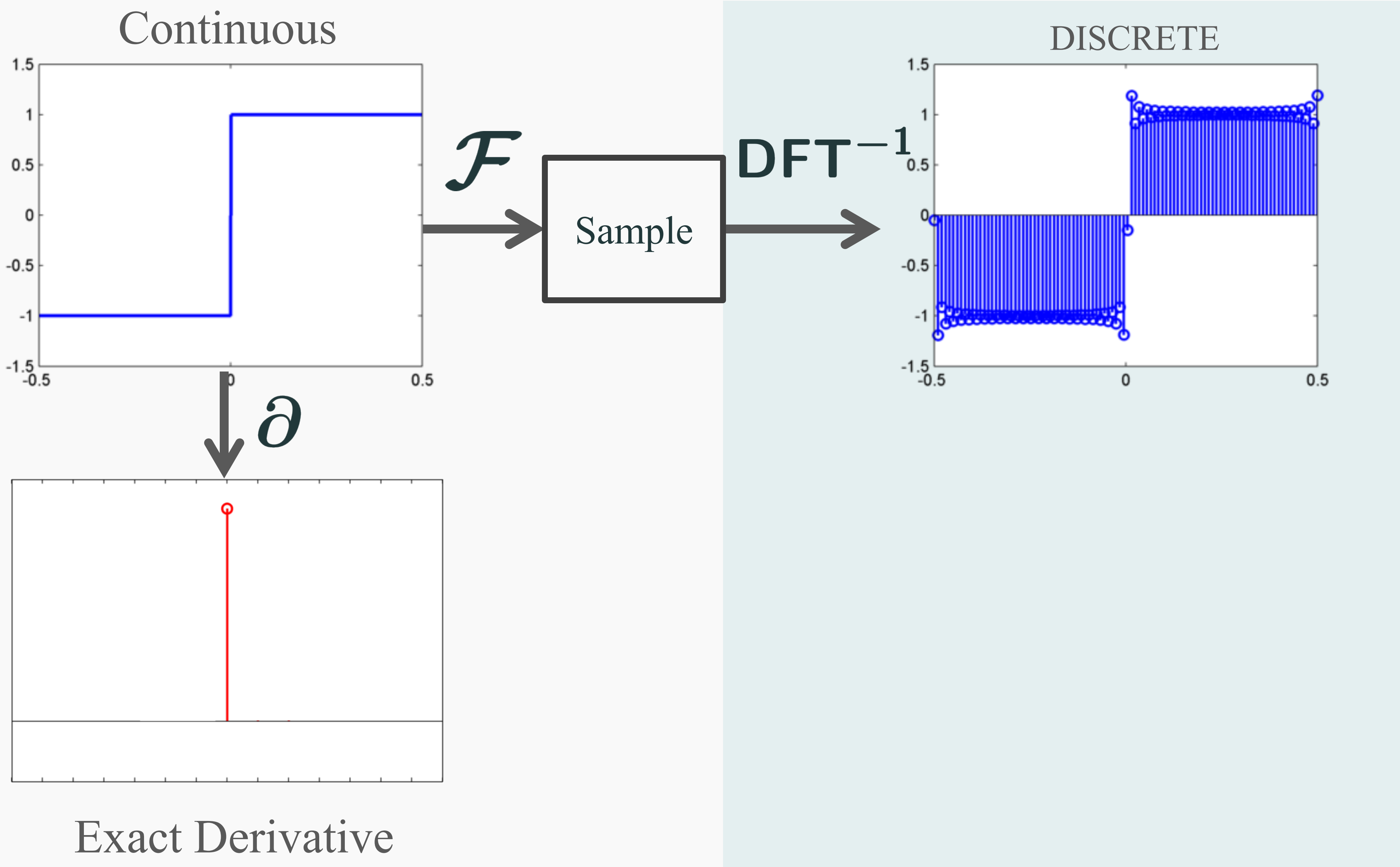

Challenge: Discrete approximation destroys sparsity!

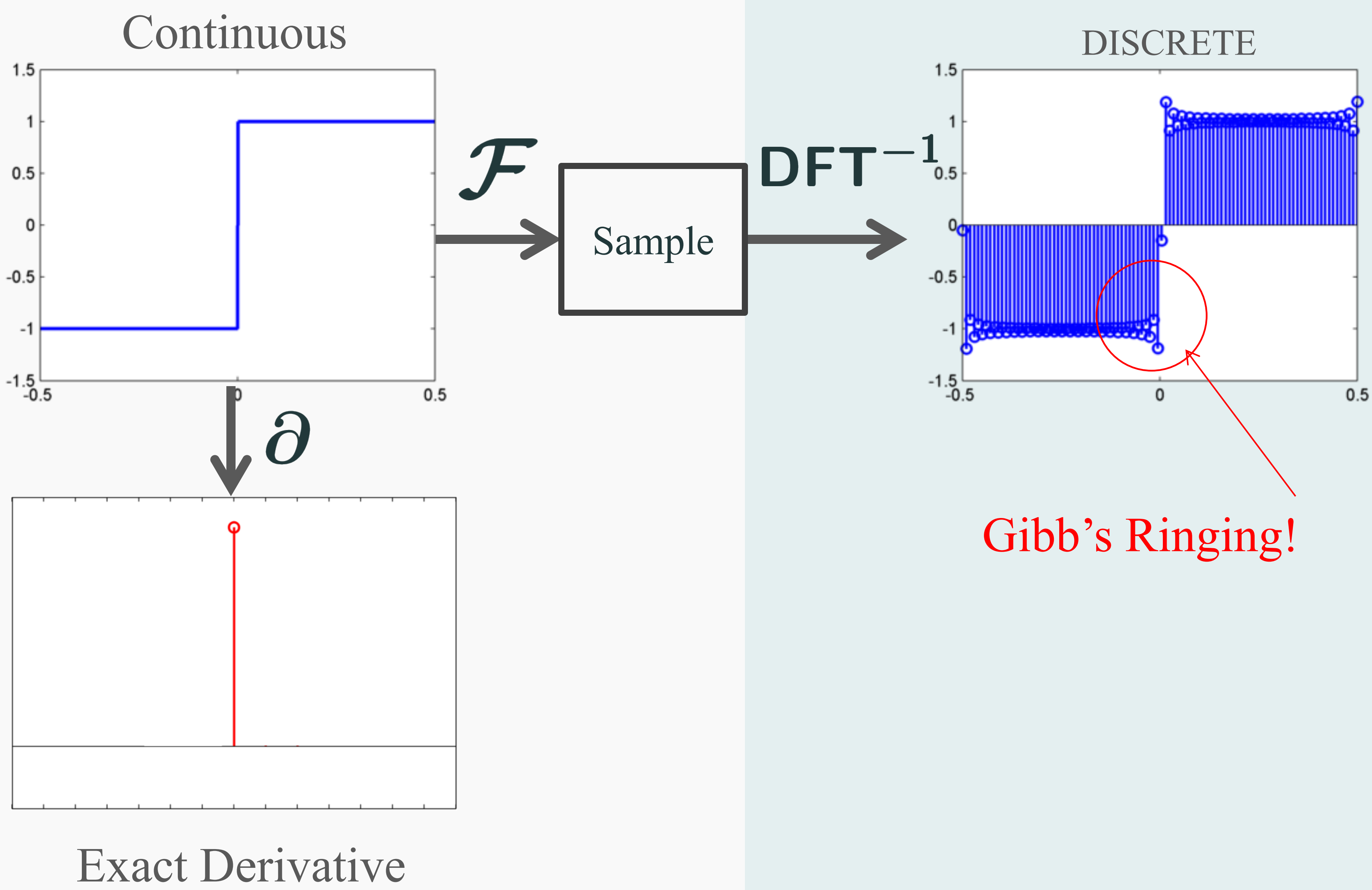

Challenge: Discrete approximation destroys sparsity!

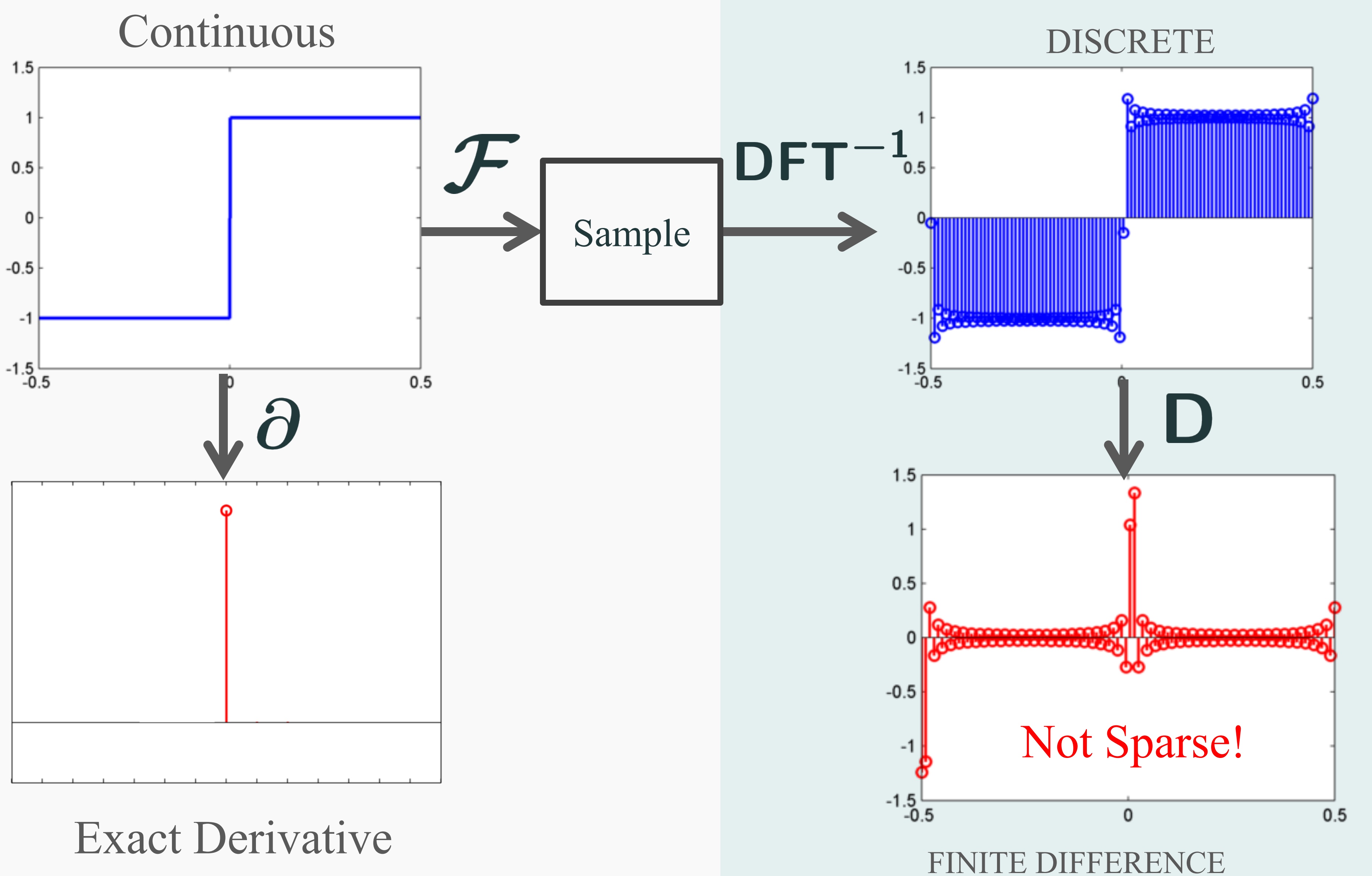

Super-resolution setting: ringing artifacts !!

Fourier

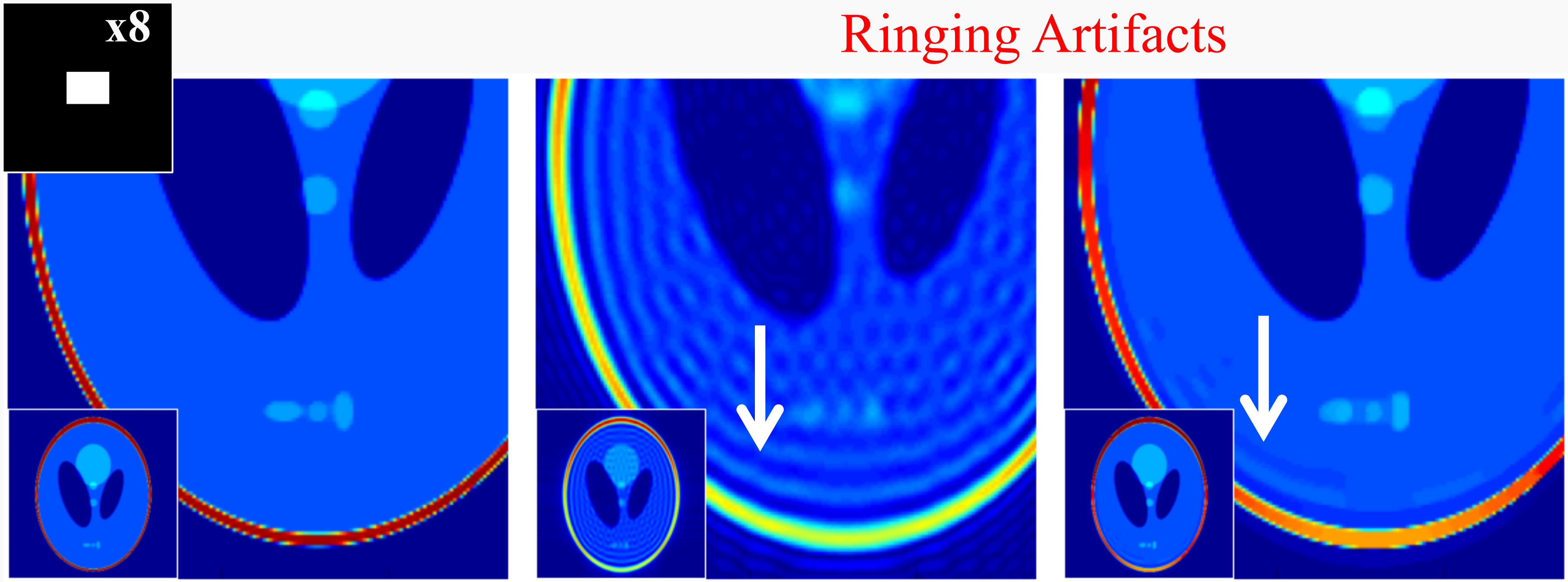

(a) Fully sampled (b) IFFT, SNR=10.8dB (c) TV, SNR=16.6dB

Overview

1. Introduction

2. Review of Compressive Sensing

3. FRI extrapolation from uniform samples

    1-D Theory

4. Structured low-rank interpolation for non-uniform samples

5. Fast implementations

6. Biomedical applications

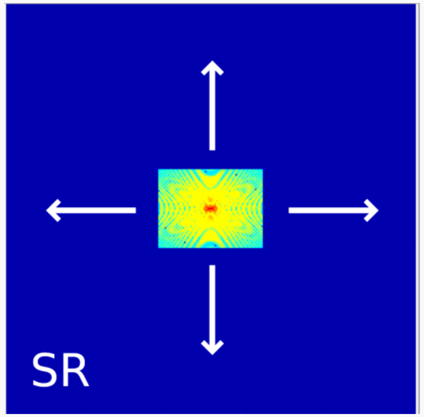

Classical Off-the-Grid Method: Prony (1795)

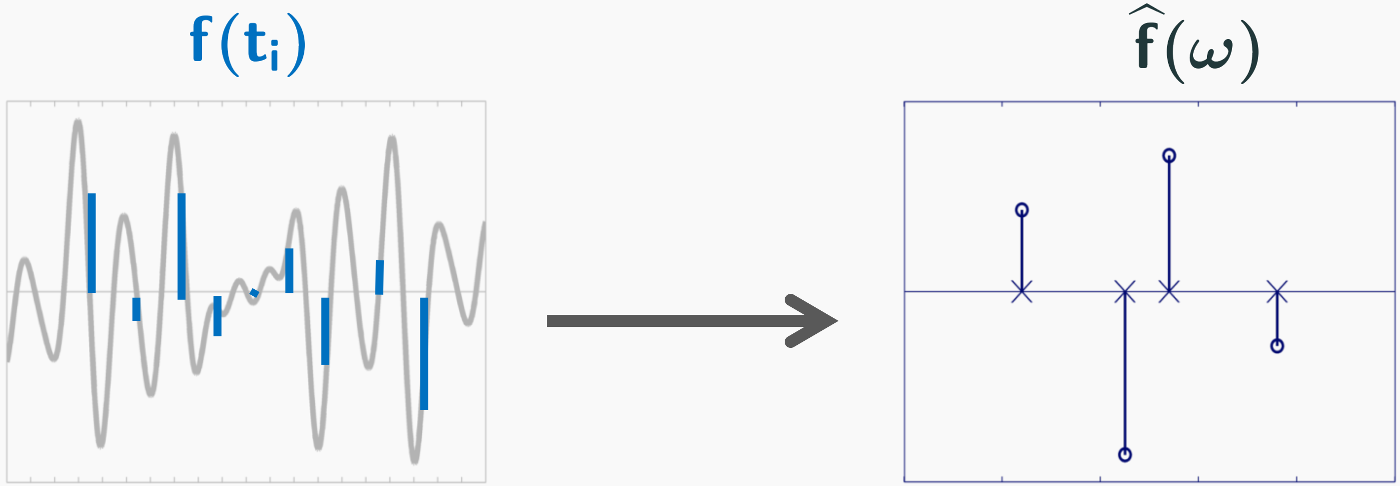

Uniform time samples

Off-the-grid frequencies

- Robust variants:

  Pisarenko (1973), MUSIC (1986), ESPRIT (1989),

  Matrix pencil (1990) . . . Atomic norm (2011)

Main inspiration: Finite-Rate-of-Innovation (FRI)

[Vetterli et al., 2002]

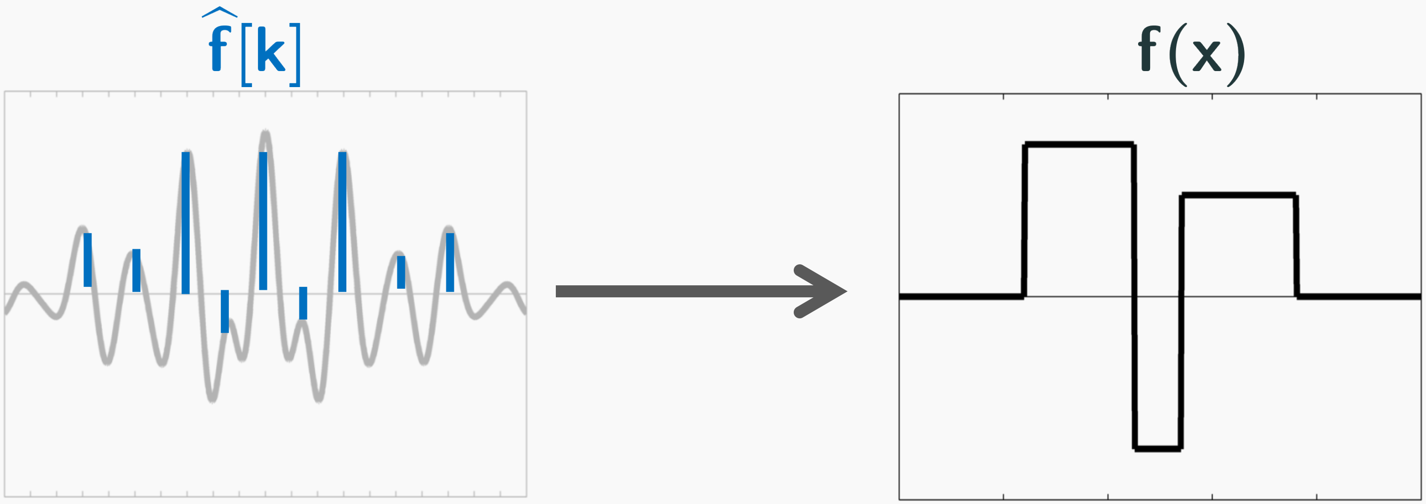

Uniform
Fourier samples

Off-the-grid
PWC signal

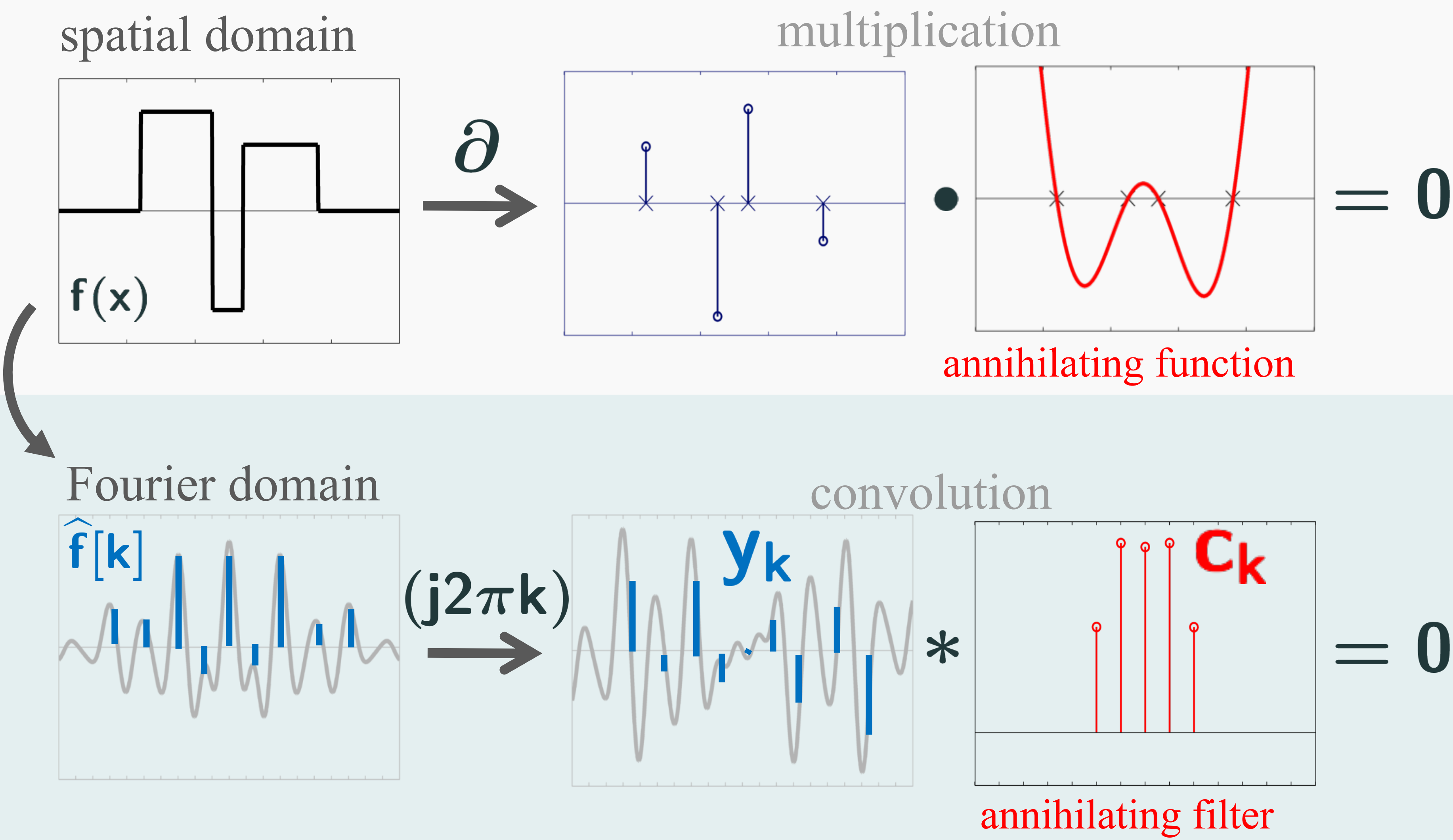

Annihilation Relation: $\sum_k y_{\ell-k} c_k = 0$

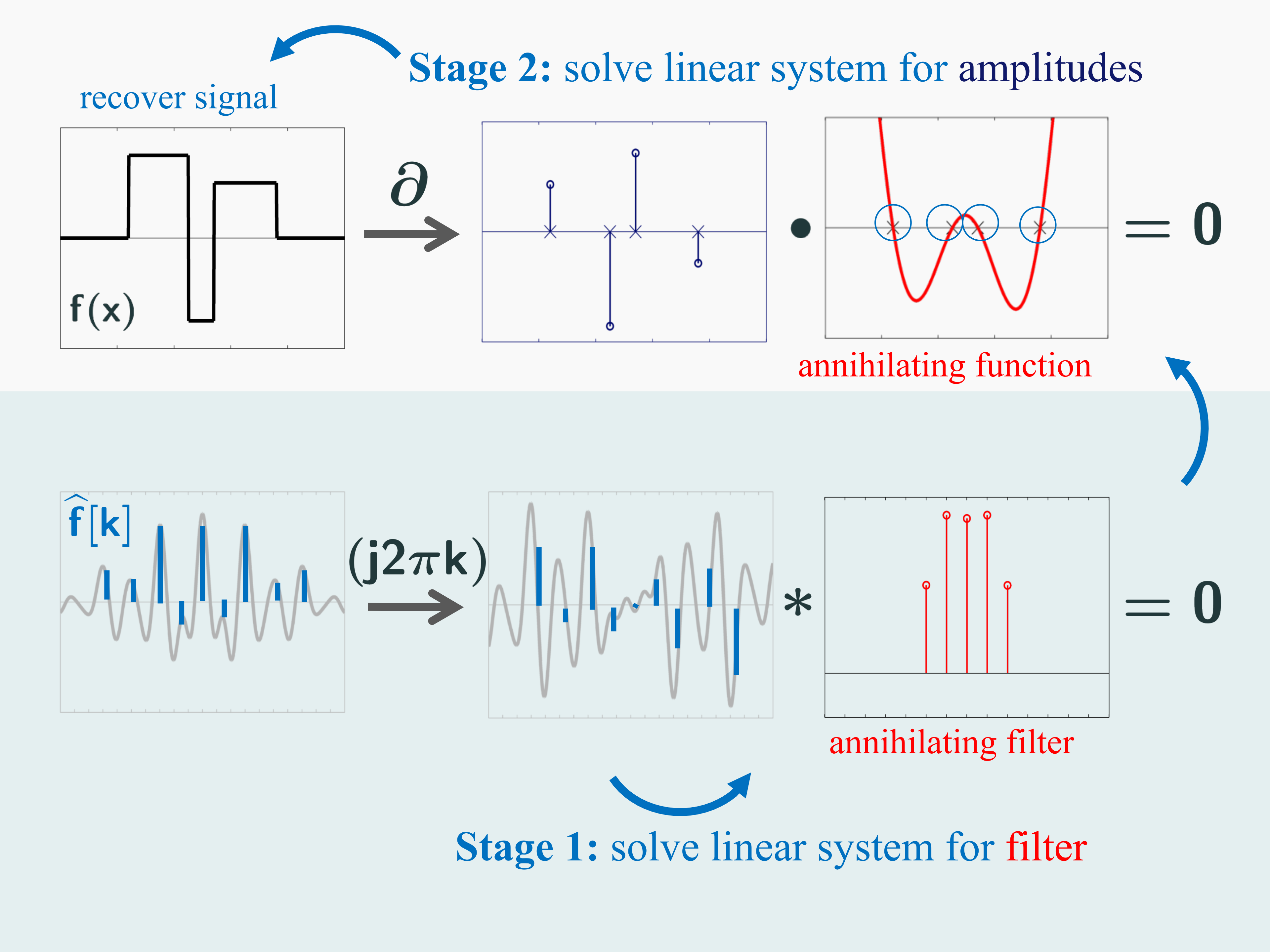
Stage 2: solve linear system for amplitudes
recover signal
f(x)
∂
annihilating function
= 0
f̂[k]
(j2πk)
*
annihilating filter
= 0
Stage 1: solve linear system for filter

Similar 1-D FRI idea by [Liang & Hacke 1989]

IEEE TRANSACTIONS ON ACOUSTICS, SPEECH, AND SIGNAL PROCESSING, VOL. 37, NO. 4, APRIL 1989

Superresolution Reconstruction Through Object Modeling and Parameter Estimation

E. MARK HAACKE, ZHI-PEI LIANG, AND STEVEN H. IZEN

***Abstract*—Fourier transform reconstruction with limited data is often encountered in tomographic imaging problems. Conventional techniques, such as FFT-based methods, the spatial-support-limited extrapolation method, and the maximum entropy method, have not been optimal in terms of both Gibbs ringing reduction and resolution enhancement. In this correspondence, a new method based on object modeling and parameter estimation is proposed to achieve superresolution reconstruction.**

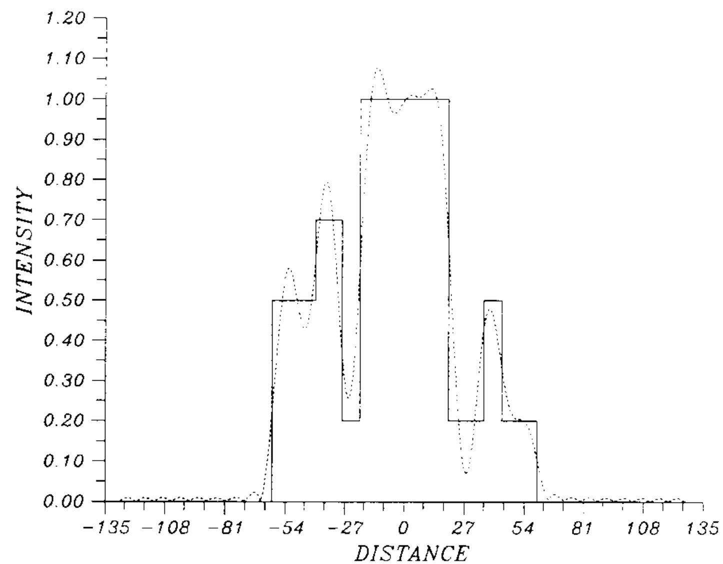

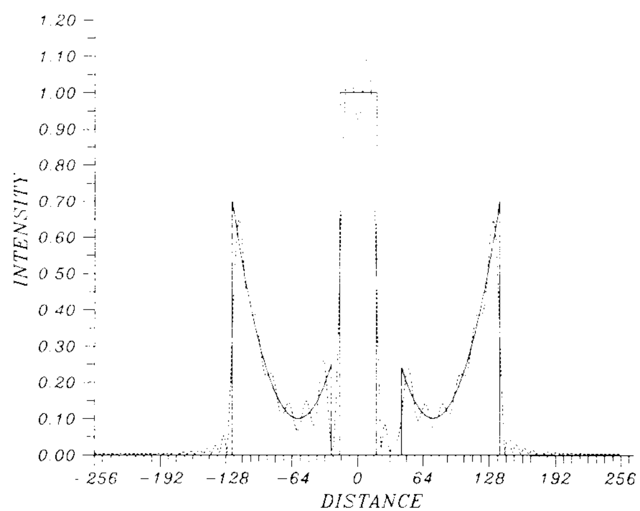

(a)

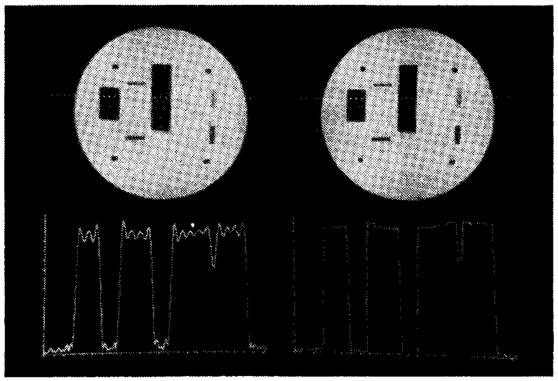

(a) (b)

Fig. 2. (a) Fourier reconstruction of a phantom from real magnetic resonance data using 256 data points in the vertical direction and 64 points in the horizontal direction. (b) Same as (a), but vertical direction is reconstructed using the proposed method. An example profile through the phantom shows the improvement in image behavior.

Overview

1. Introduction

2. Review of Compressive Sensing

3. FRI extrapolation from uniform samples

2-D Theory

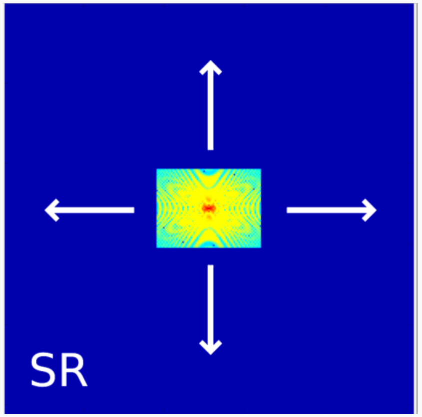

4. Structured low-rank interpolation for non-uniform samples

5. Fast implementations

6. Biomedical applications

Extension to higher dims: Singularities not isolated

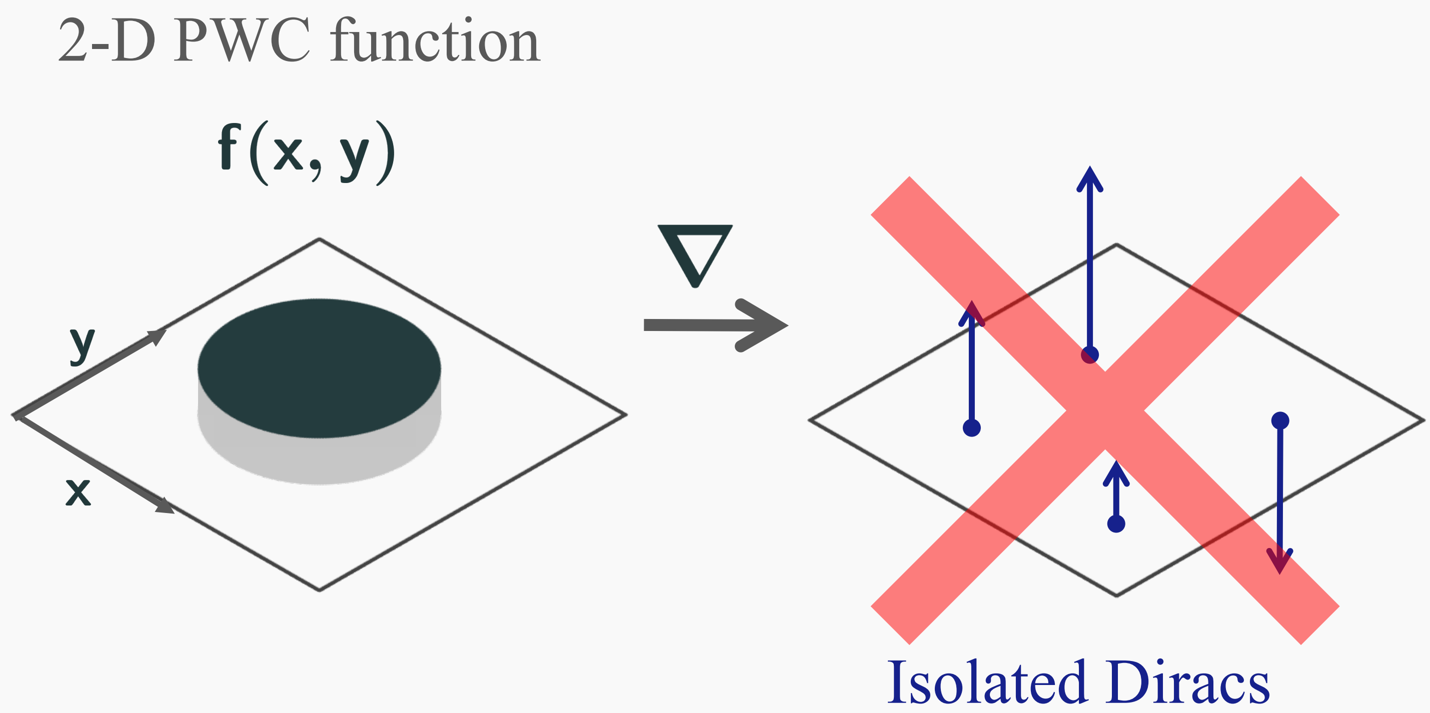

Extension to higher dims: Singularities not isolated

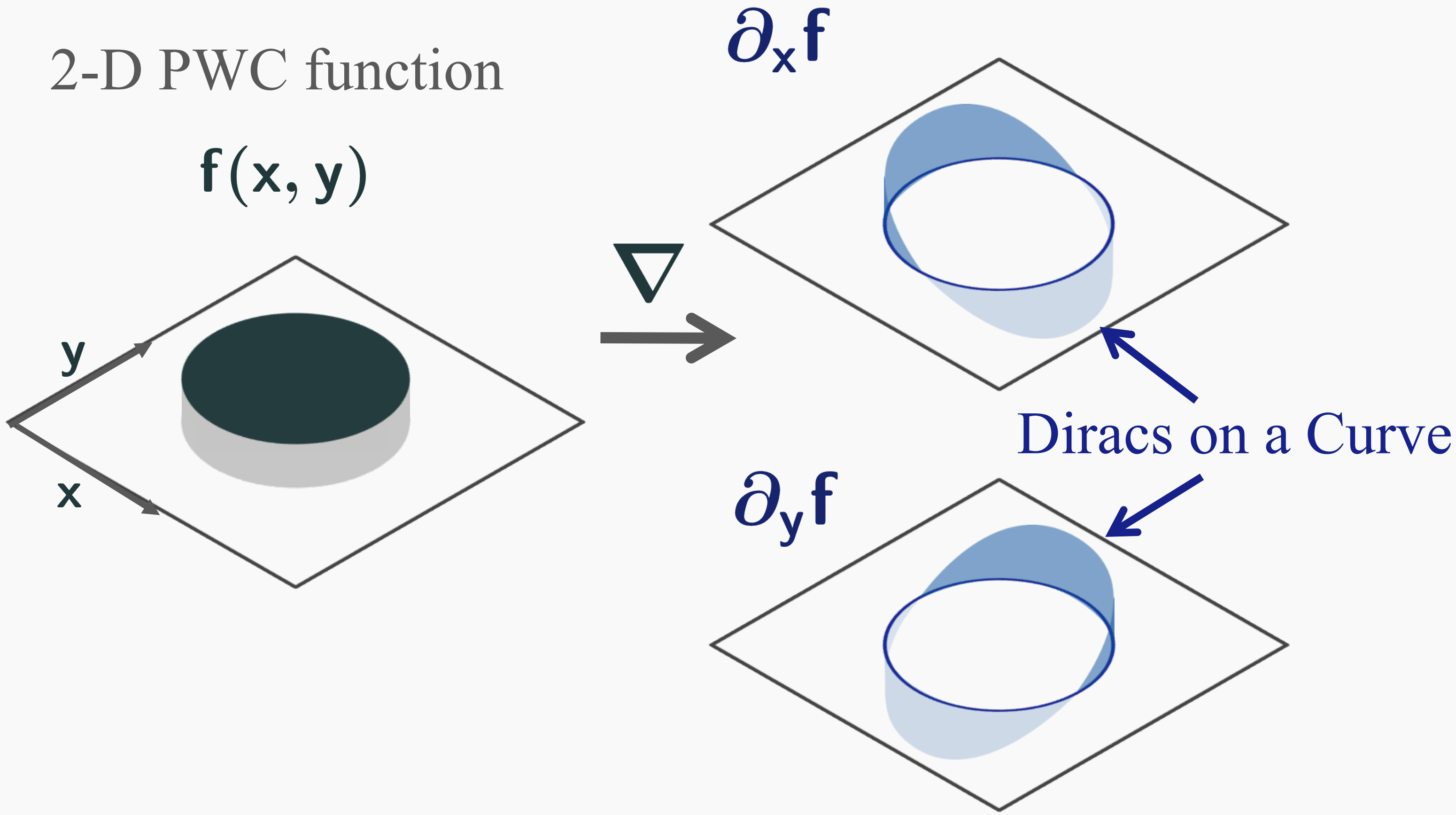

2-D PWC functions satisfy an annihilation relation

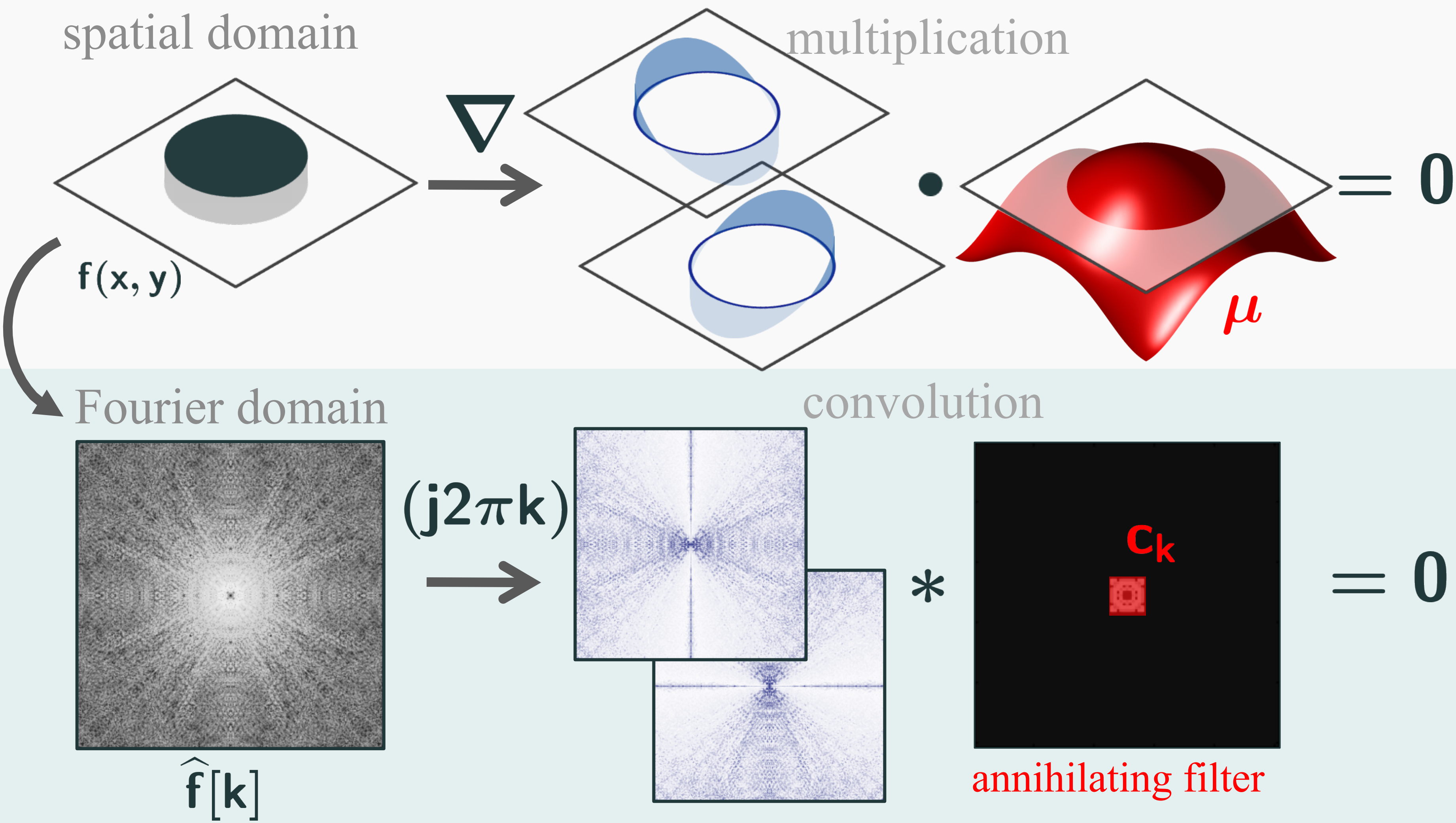

Annihilation relation: $\sum_k \widehat{\nabla f}[\ell - k] c_k = 0$

Image recovery

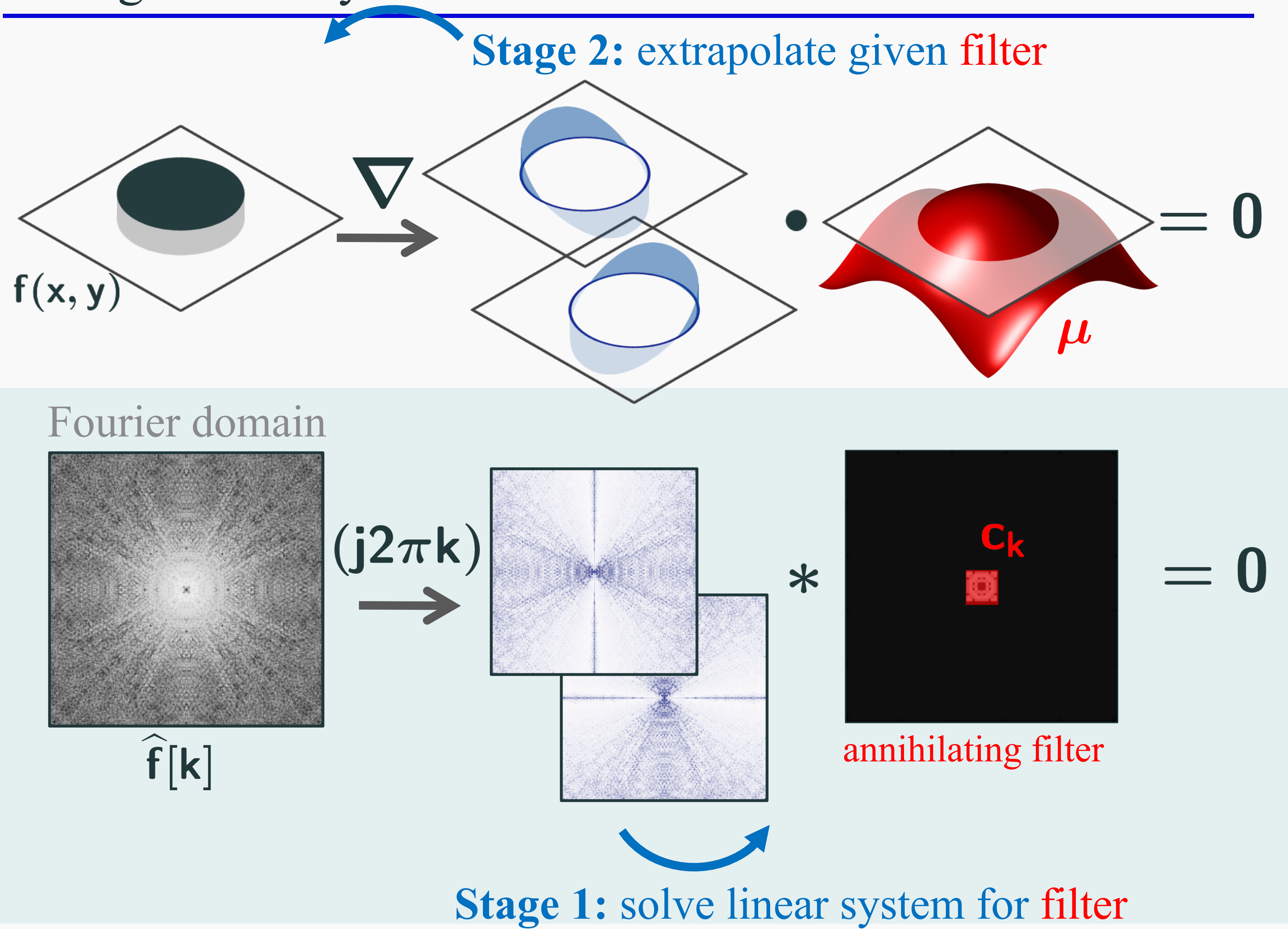

Bandlimited curves

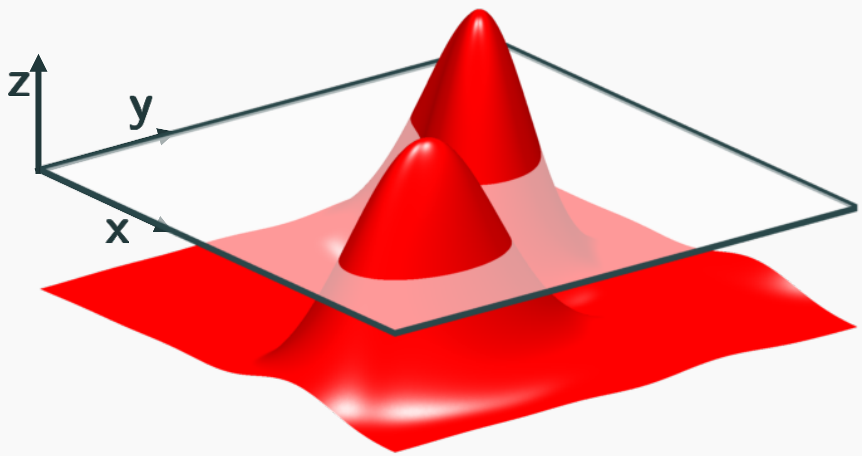

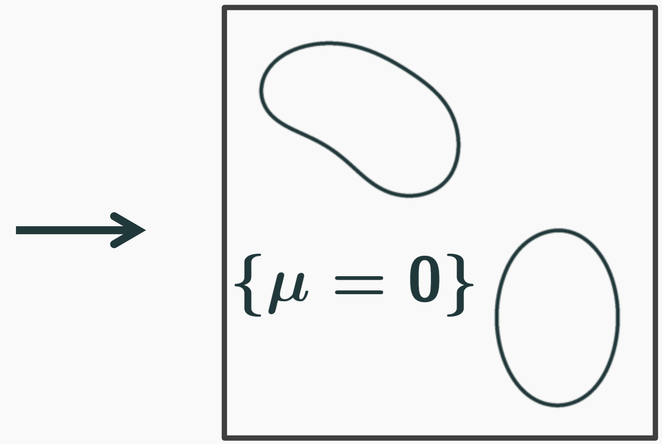

"FRI Curve"

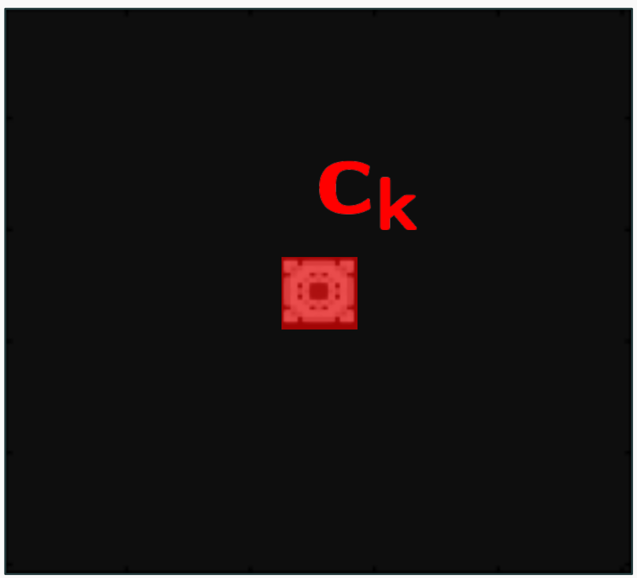

[Pan, Vetterli & Blu, IEEE Trans IP, 2015](#)

Bandlimited curves can represent complex shapes

Multiple curves
& intersections

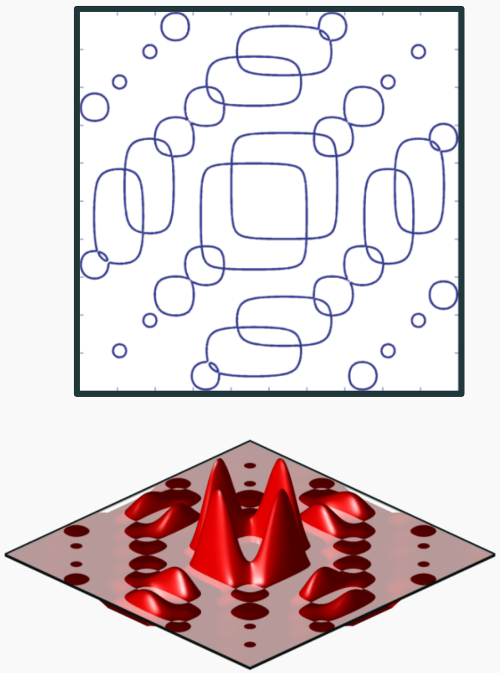

13x13 coefficients

Non-smooth
points

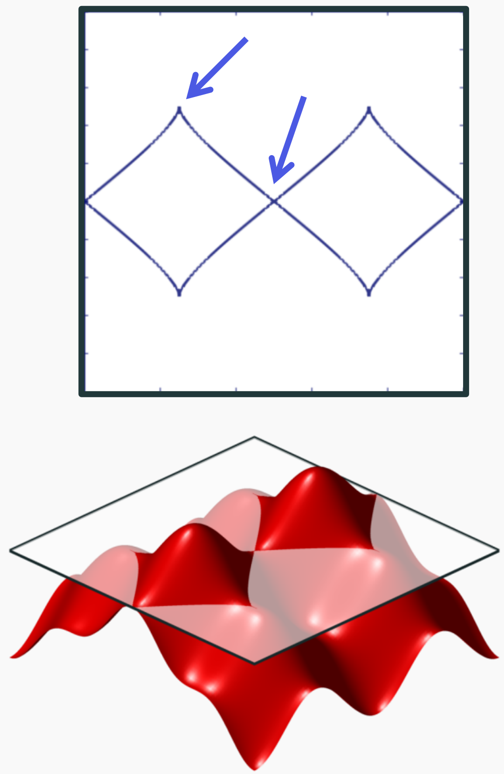

7x9 coefficients

Approximate
arbitrary curves

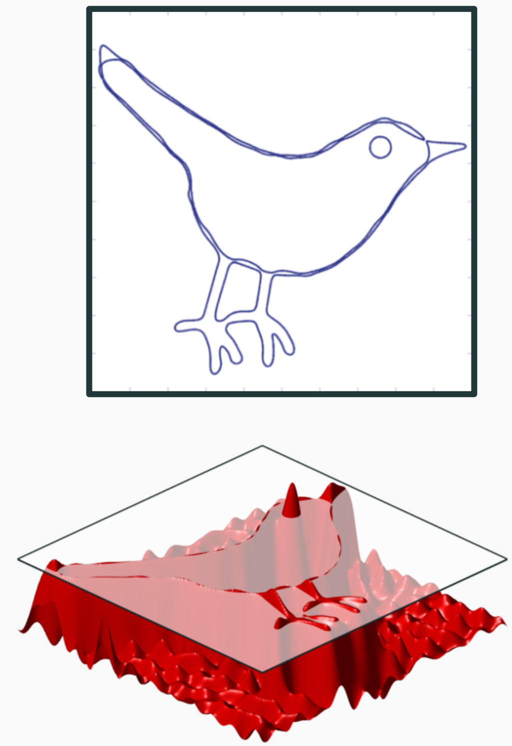

25x25 coefficients

Piecewise analytic model

- Signal model: piecewise analytic signal

$$f(z) = \sum_{i=1}^{N} g_i(z) \cdot 1_{\Omega_i}(z)$$

$$\text{s.t.} \quad g_i \text{ analytic in } \Omega_i$$

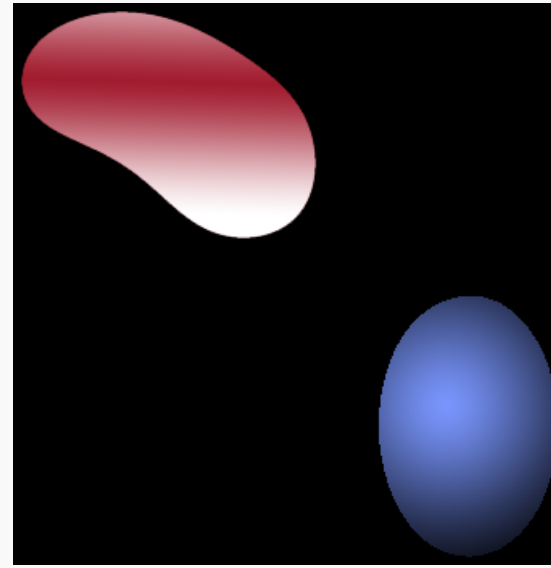

- Not suitable for natural images
- 2-D only
- Recovery is ill-posed: Infinite DoF

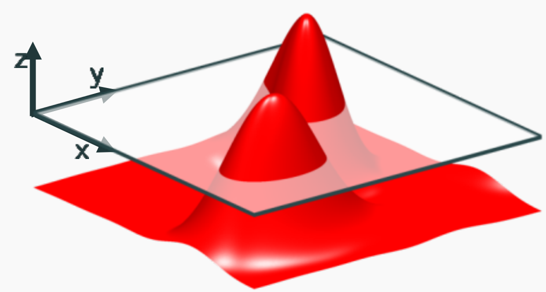

Pan, Vetterli & Blu, IEEE Trans IP, 2015

Piecewise smooth model

- New model: piecewise smooth signals

$$f(x) = \sum_{i=1}^{N} g_i(x) \cdot 1_{\Omega_i}(x)$$

$$\text{s.t.} \quad g_i \text{ smooth in } \Omega_i$$

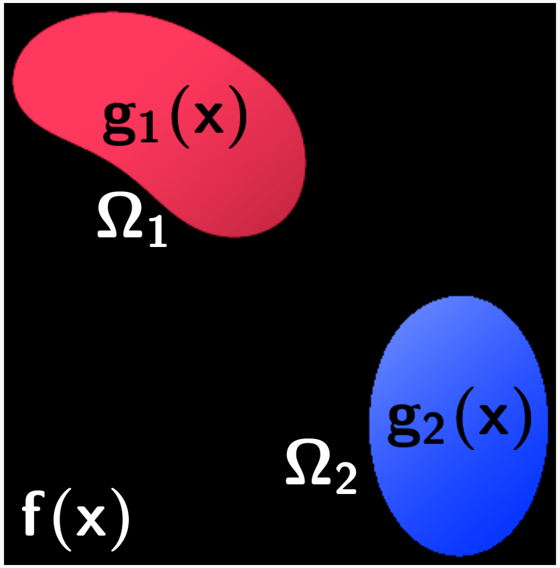

- Extends easily to n-D
- Provable sampling guarantees
- Fewer samples necessary for recovery

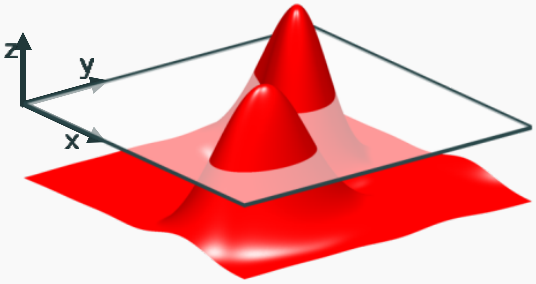

[Ongie & Jacob, SIAM J Imag. Science, in press]

Eg. Piecewise constant functions: annihilation

Prop: If f is PWC with edge set $\mathbf{E} \subseteq \{\mu = 0\}$

for μ bandlimited to $\boldsymbol{\Lambda}$ then

$$\sum_{\mathbf{k} \in \boldsymbol{\Lambda}} \mathbf{c}[\mathbf{k}]\,\widehat{\nabla \mathbf{f}}[\ell - \mathbf{k}] = 0 \text{ for all } \ell$$

any 1st order partial derivative

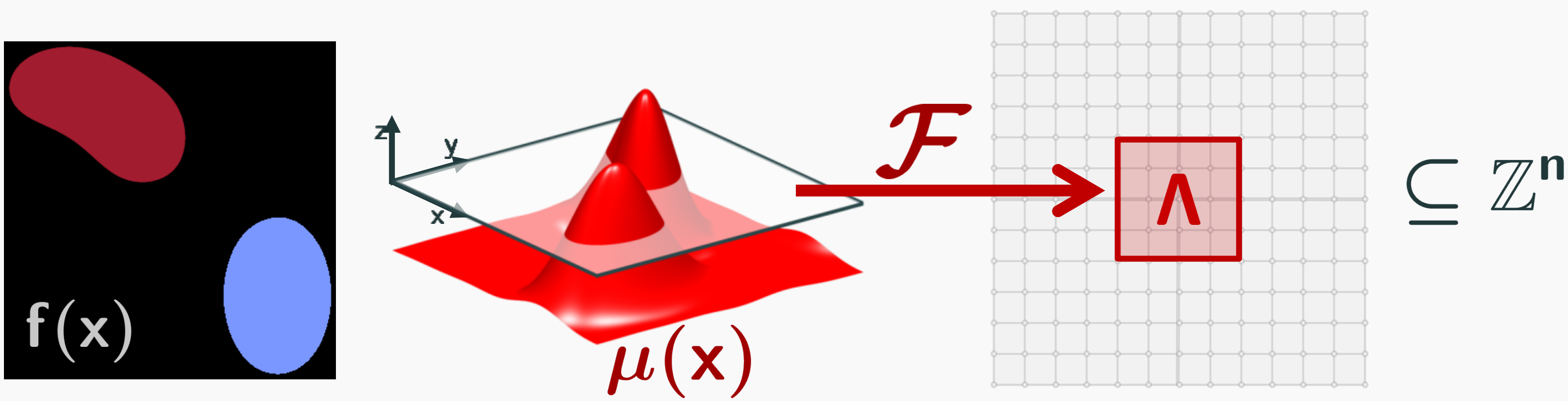

Eg. Piecewise linear functions: annihilation

Prop: If **f** is PW linear, with edge set $\mathbf{E} \subseteq \{\mu = \mathbf{0}\}$

and μ bandlimited to $\mathbf{\Lambda}$ then

$$\sum_{\mathbf{k} \in 2\mathbf{\Lambda}} \widehat{\mu^2}[\mathbf{k}]\widehat{\partial^2 \mathbf{f}}[\ell - \mathbf{k}] = \mathbf{0}, \quad \forall \ell \in \mathbb{Z}^{\mathbf{n}}$$

any 2^{nd} order partial derivative

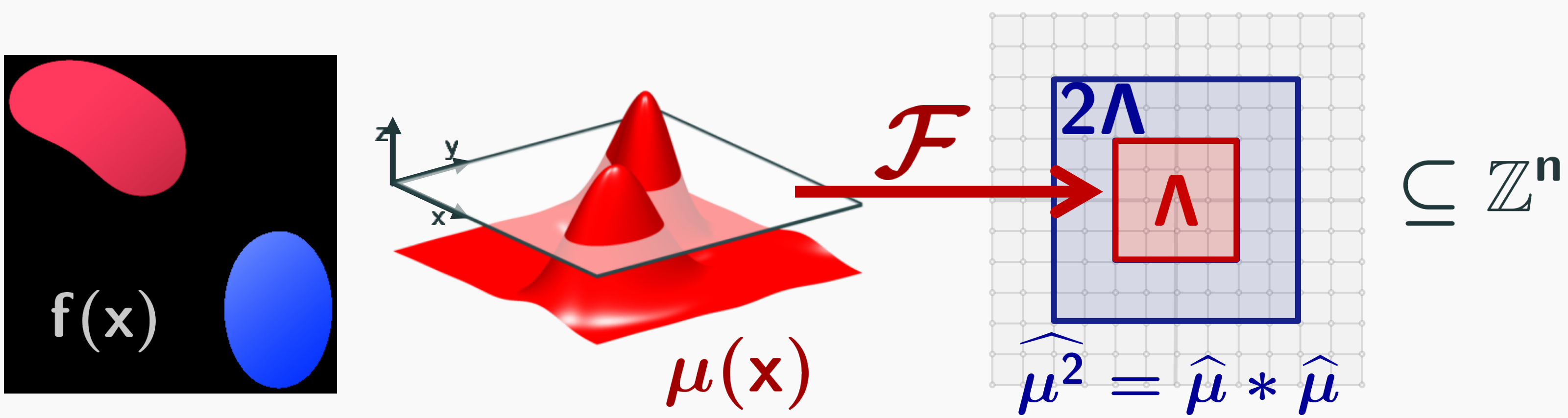

General signal models

$$\mathbf{f(x)} = \sum_{i=1}^{N} \mathbf{g_i(x)} \cdot \mathbf{1}_{\Omega_i}(\mathbf{x})$$

$$\text{s.t.} \quad \mathbf{Dg_i} = \mathbf{0} \text{ in } \mathbf{\Omega_i}$$

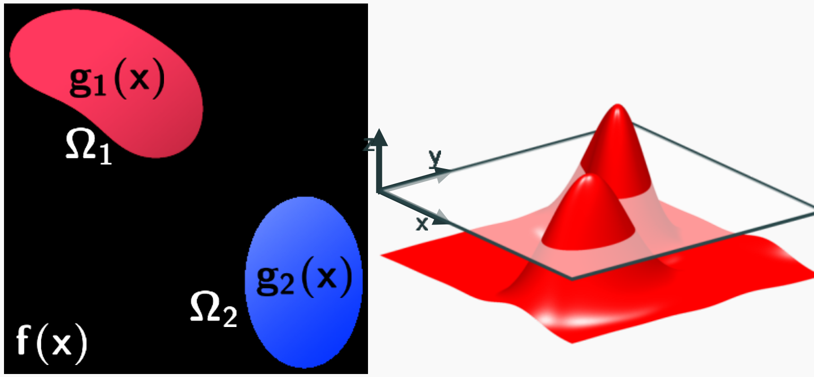

Signal Model:	Choice of Diff. Op.:	
PW Constant	$\mathbf{D} = \nabla$	1st order
PW Analytic*	$\mathbf{D} = \partial_x + j\partial_y$	
PW Harmonic	$\mathbf{D} = \Delta$	2nd order
PW Linear	$\mathbf{D} = \{\partial_{xx}, \partial_{xy}, \partial_{yy}\}$	
PW Polynomial	$\mathbf{D} = \{\partial^\alpha\}_{\lvert\alpha\rvert=n}$	nth order

Can we extrapolate ?

Piecewise smooth signals satisfy annihilation conditions

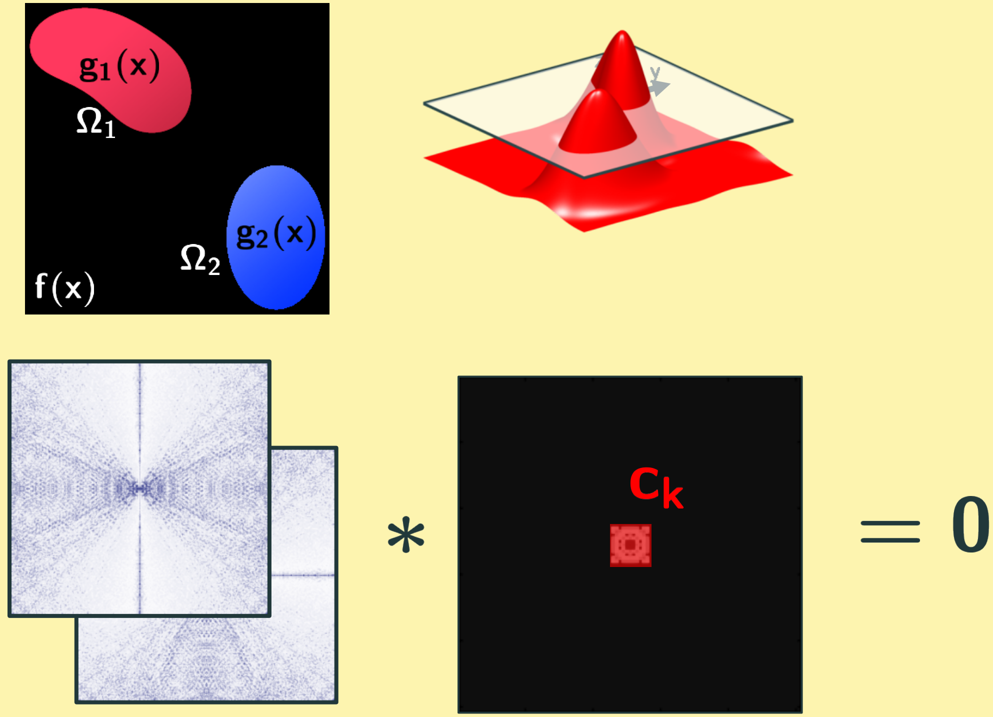

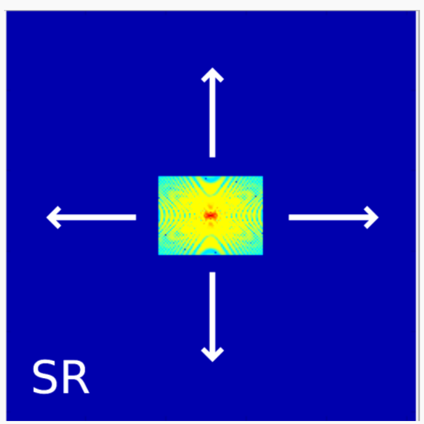

How much should we sample to extrapolate?

Recovery guarantees: challenges

1-D FRI Sampling Theorem [Vetterli et al., 2002]:

A continuous-time PWC signal with K jumps can be uniquely recovered from 2K+1 uniform Fourier samples.

Proof (a la Prony's Method):

Form Toeplitz matrix T from samples, use uniqueness of Vandermonde decomposition: $\mathbf{T} = \mathbf{V}\mathbf{D}\mathbf{V}^H$

"Caratheodory Parametrization"

Recovery guarantees: challenges

Extends to *n*-D if singularities isolated [Sidiropoulos, 2001]

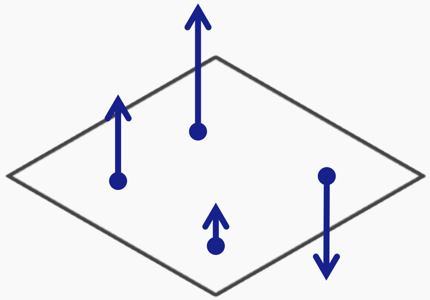

$$\xrightarrow{\mathcal{F}} \quad \hat{\mathbf{f}}[\mathbf{k}] = \sum_{\mathbf{i}} \mathbf{a_i} \mathbf{e}^{-\mathbf{j}2\pi\mathbf{k}\cdot\mathbf{x_i}}$$

Not true when singularities supported on curves:

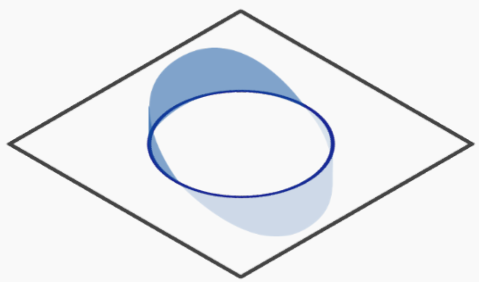

$$\xrightarrow{\mathcal{F}} \quad \widehat{\nabla \mathbf{f}}[\mathbf{k}] = \oint_{\partial\Omega} \mathbf{e}^{-\mathbf{j}2\pi\mathbf{k}\cdot\mathbf{x}} \mathbf{n}\, \mathbf{ds}$$

Requires new techniques:

- Spatial domain interpretation of annihilation relation
- Algebraic geometry of trigonometric polynomials

Image recovery

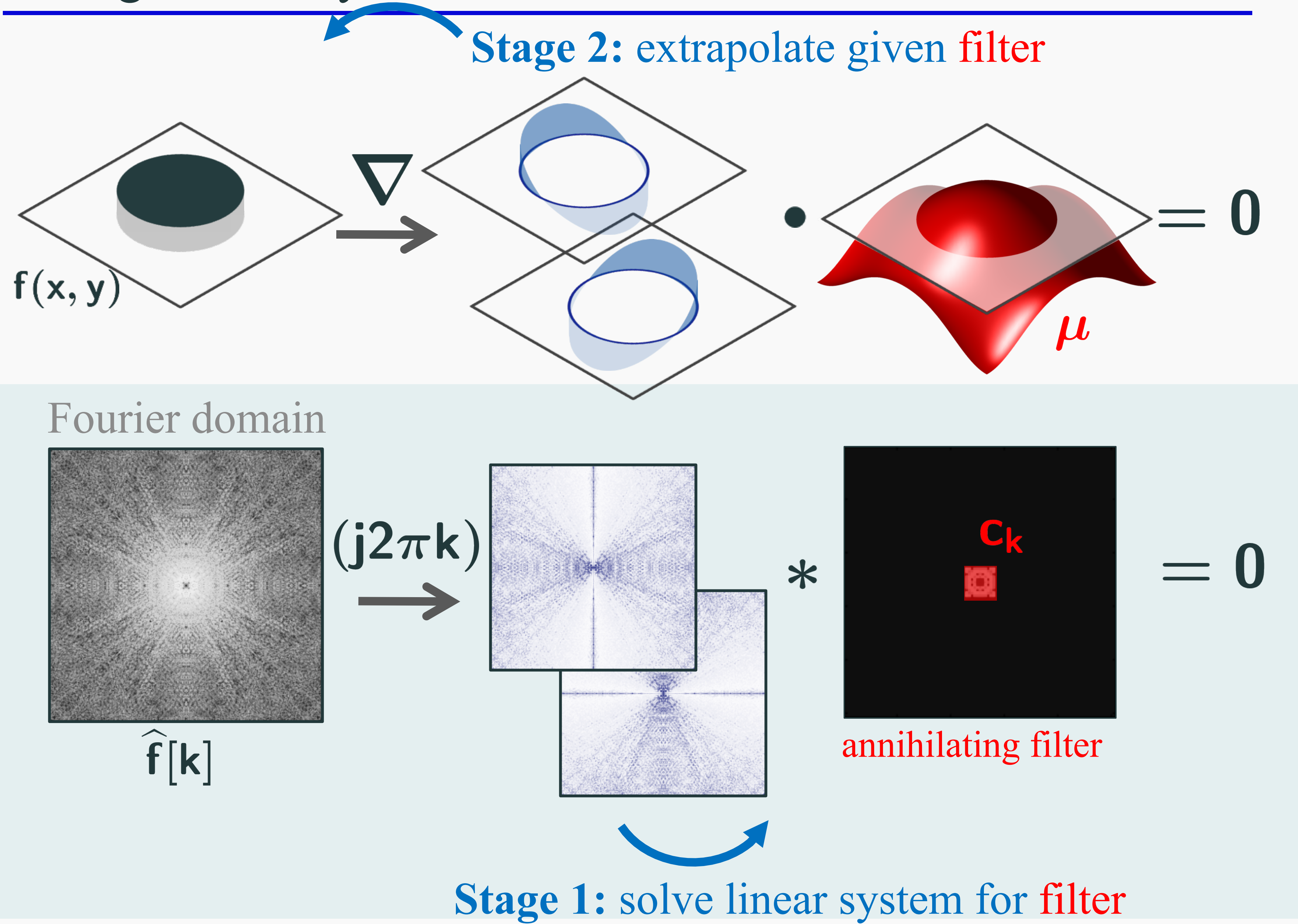

Step 1. When can you recover the filter ?

Theorem: If **f** is PWC* with edge set $\mathbf{E} = \{\mu = 0\}$ with μ minimal and bandlimited to Λ then $\mathbf{c} = \widehat{\mu}$ is the unique solution to

$$\sum_{\mathbf{k} \in \Lambda} \mathbf{c}[\mathbf{k}] \widehat{\nabla \mathbf{f}}[\ell - \mathbf{k}] = 0 \text{ for all } \ell \in 2\Lambda$$

*Some geometric restrictions apply

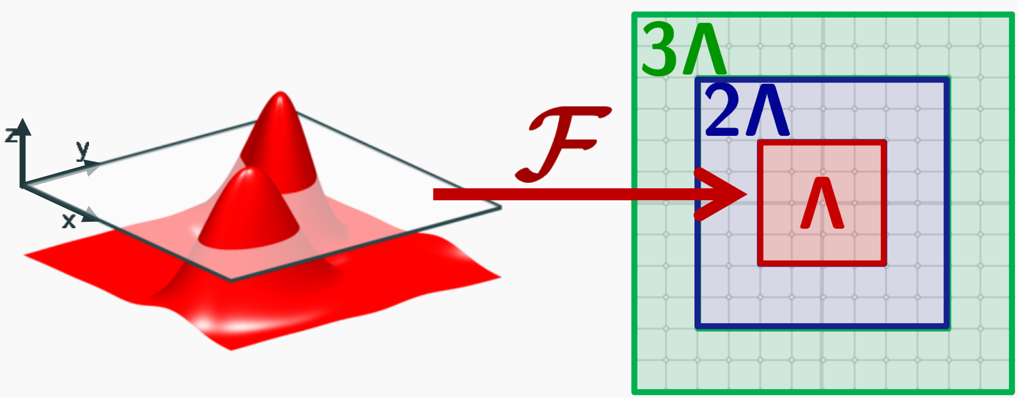

$\subseteq \mathbb{Z}^2$

Requires samples of $\widehat{\mathbf{f}}$ in 3Λ to build equations

Ongie & Jacob, SIAM J Imag. Science, in press

Step 2. When can you recover the signal given the filter ?

Theorem: If **f** is PWC* with edge set $\mathbf{E} = \{\mu = 0\}$

with μ minimal and bandlimited to $\mathbf{\Lambda}$ then

$\mathbf{g} = \mathbf{f}$ is the unique solution to

$$\mu \cdot \nabla \mathbf{g} = 0 \;\; \text{s.t.} \;\; \widehat{\mathbf{f}}[\mathbf{k}] = \widehat{\mathbf{g}}[\mathbf{k}], \mathbf{k} \in \mathbf{\Gamma}$$

when the sampling set $\mathbf{\Gamma} \supseteq 3\mathbf{\Lambda}$

Ongie & Jacob, SIAM J Imag. Science, in press

Step 2. When can you extrapolate given the filter ?

Theorem: If **f** is PWC* with edge set $\mathbf{E} = \{\mu = 0\}$

with μ minimal and bandlimited to Λ then

$\mathbf{g} = \mathbf{f}$ is the unique solution to

$$\mu \cdot \nabla \mathbf{g} = 0 \ \text{ s.t. } \ \widehat{\mathbf{f}}[\mathbf{k}] = \widehat{\mathbf{g}}[\mathbf{k}], \mathbf{k} \in \Gamma$$

when the sampling set $\Gamma \supseteq 3\Lambda$

Equivalently,

$$\mathbf{f} = \arg\min_{\mathbf{g}} \|\mu \cdot \nabla \mathbf{g}\| \ \text{ s.t. } \ \widehat{\mathbf{f}}[\mathbf{k}] = \widehat{\mathbf{g}}[\mathbf{k}], \mathbf{k} \in \Gamma$$

Ongie & Jacob, SIAM J Imag. Science, in press

Super-resolution image recovery

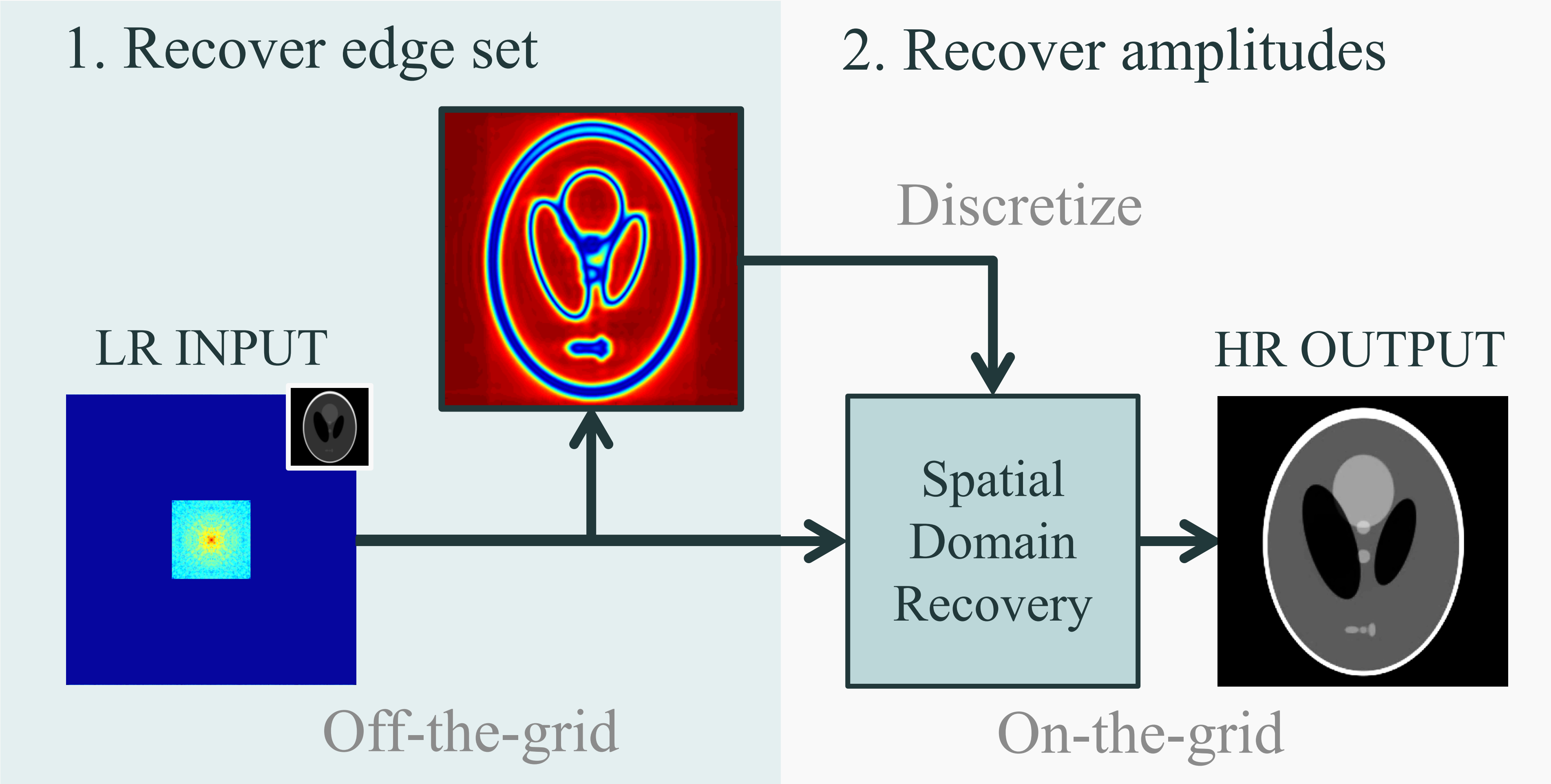

Ongie & Jacob, SIAM J Imag. Science, in press

Super-resolution of MRI Medical Phantoms

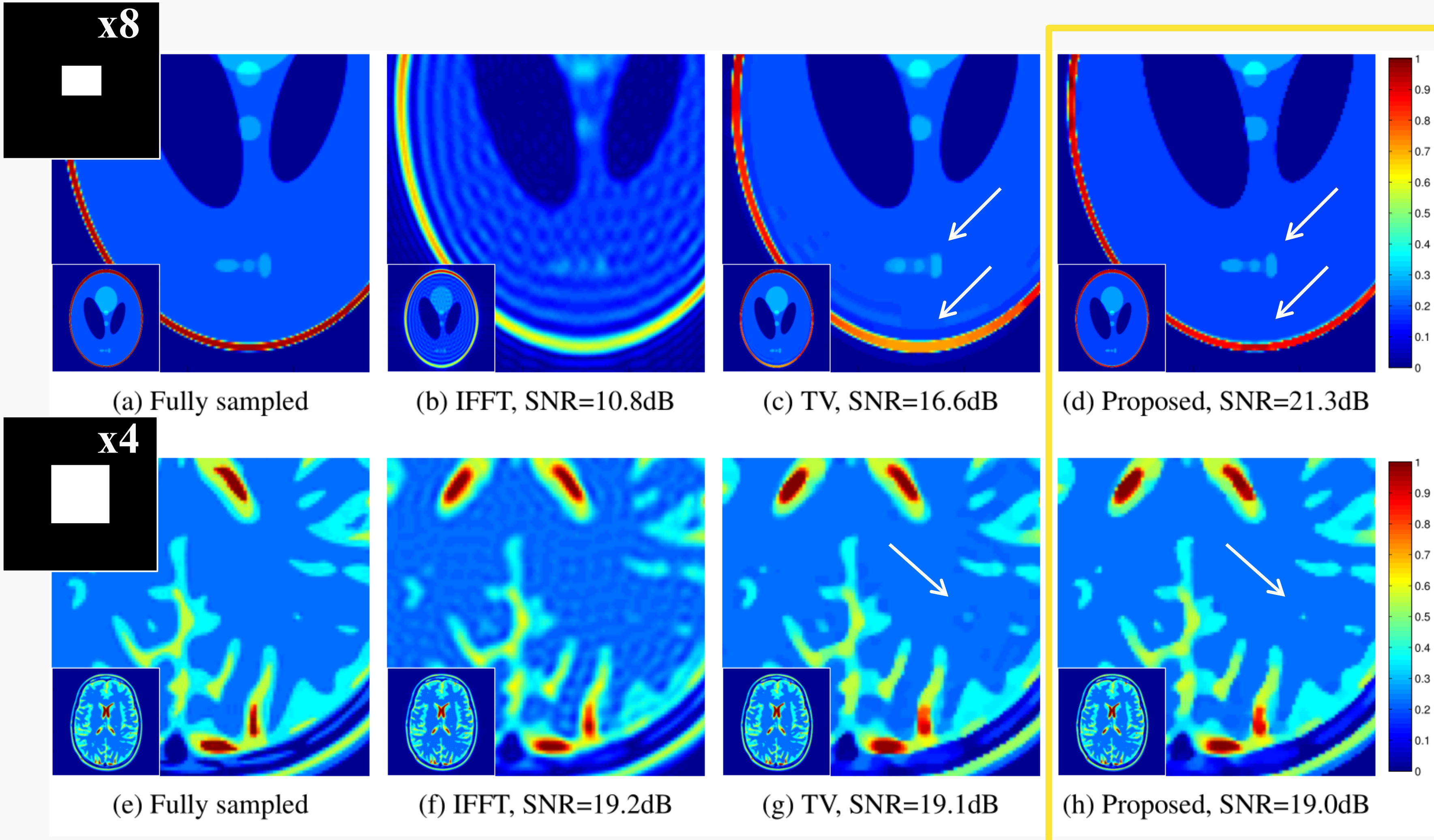

(a) Fully sampled (b) IFFT, SNR=10.8dB (c) TV, SNR=16.6dB (d) Proposed, SNR=21.3dB

(e) Fully sampled (f) IFFT, SNR=19.2dB (g) TV, SNR=19.1dB (h) Proposed, SNR=19.0dB

Ongie & Jacob, SIAM J Imag. Science, in press

Can we generalize to non-uniform setting ??

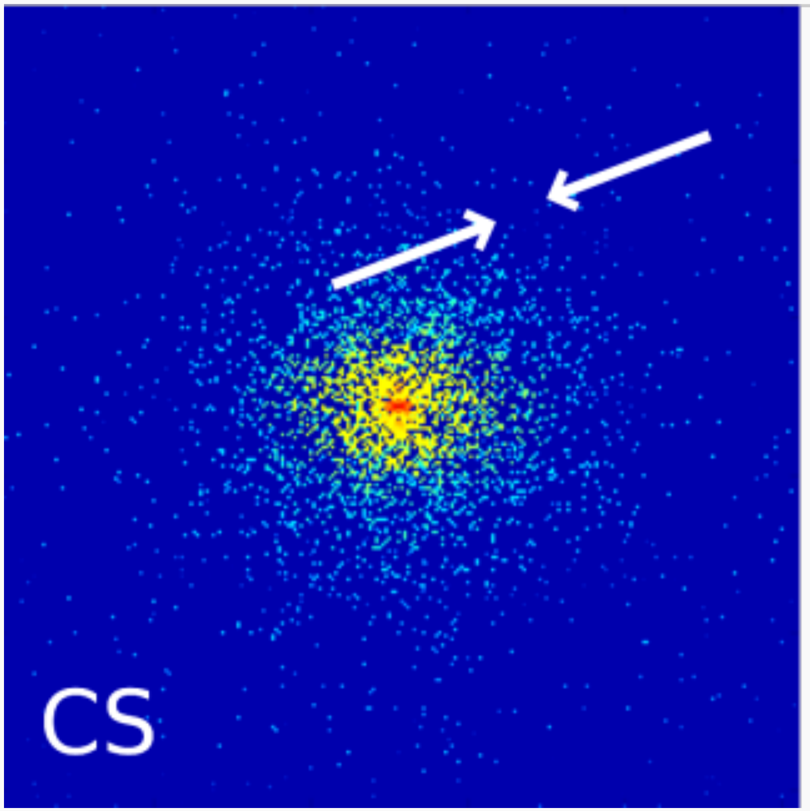

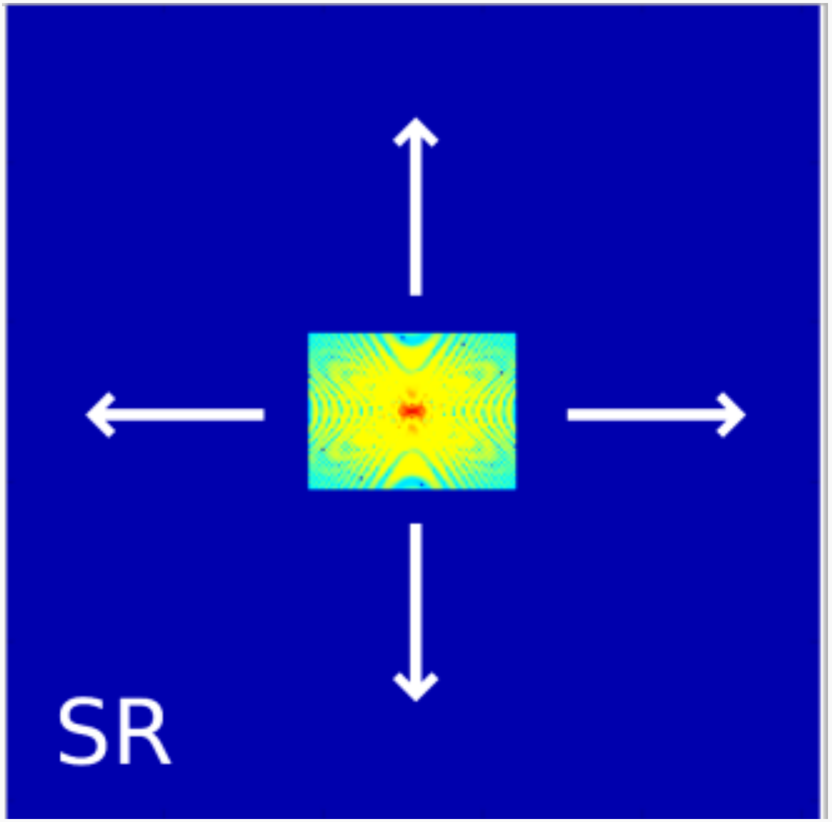

Improve recovery using non-uniform sampling

Overview

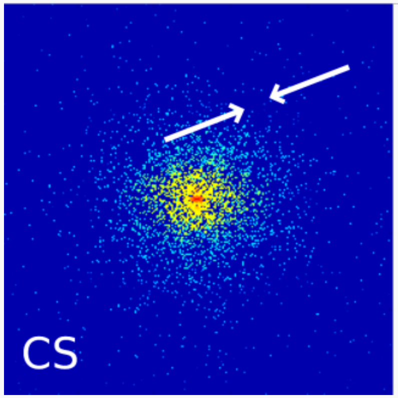

1. Introduction

2. Review of Compressive Sensing

3. FRI extrapolation from uniform samples

4. Structured low-rank interpolation for non-uniform samples

- 1-D Theory

5. Fast implementations

6. Biomedical applications

Sampling vs low-rank interpolation

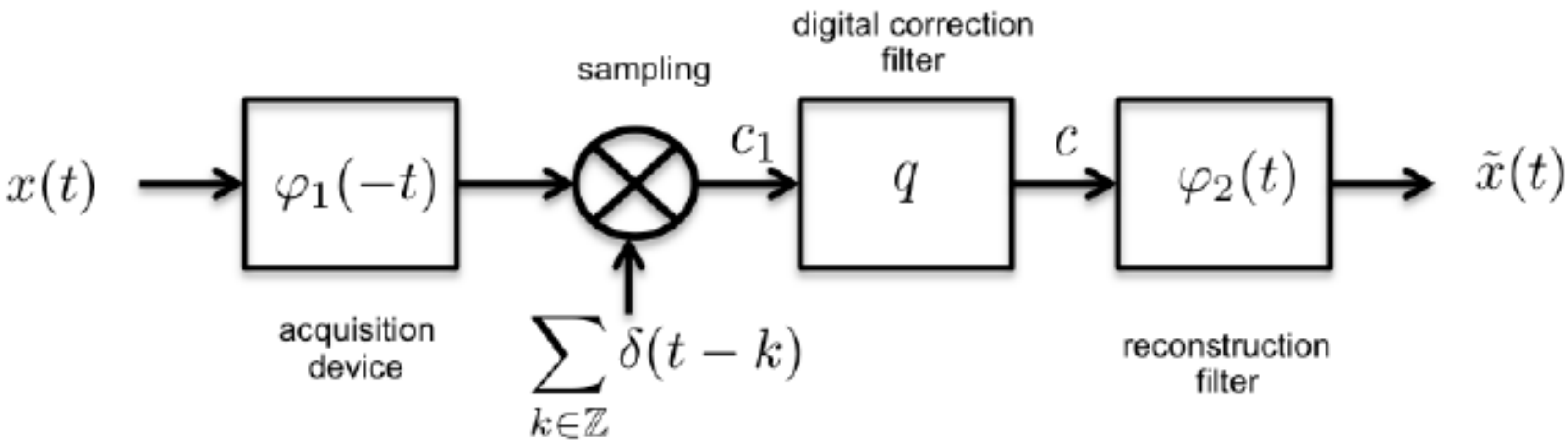

(a)

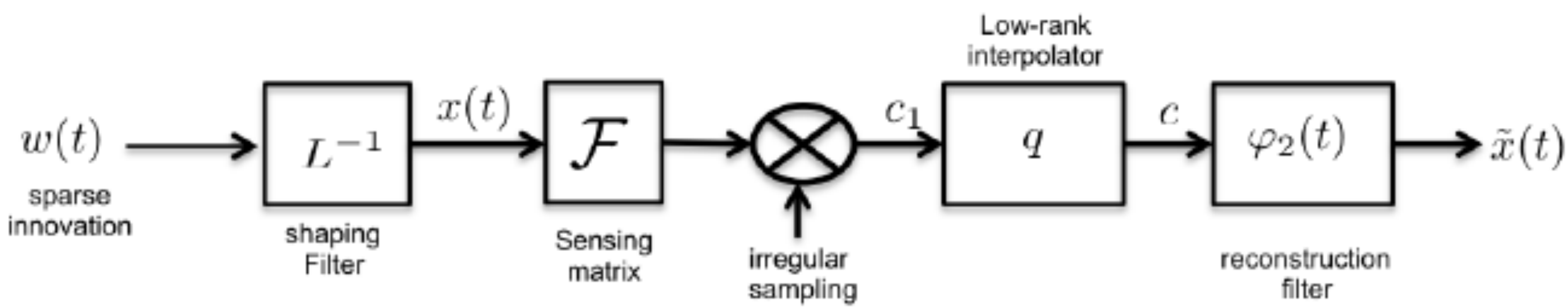

(b)

Key idea: annihilating filter

*** FRI Sampling theory**

$f(x)$: periodic stream of K Diracs

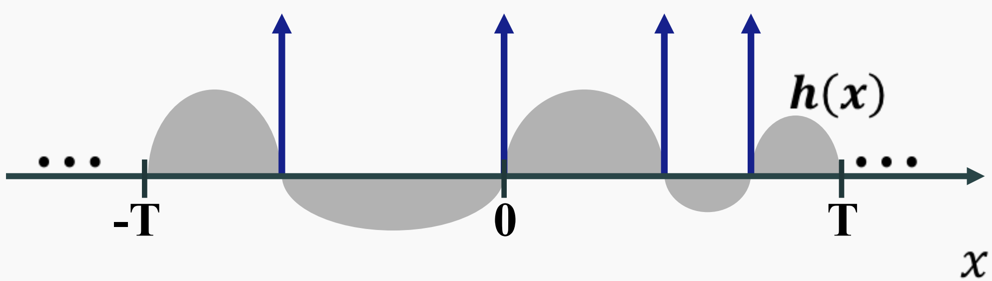

$h(x)$: annihilating function

$$f(x) \cdot h(x) = 0$$

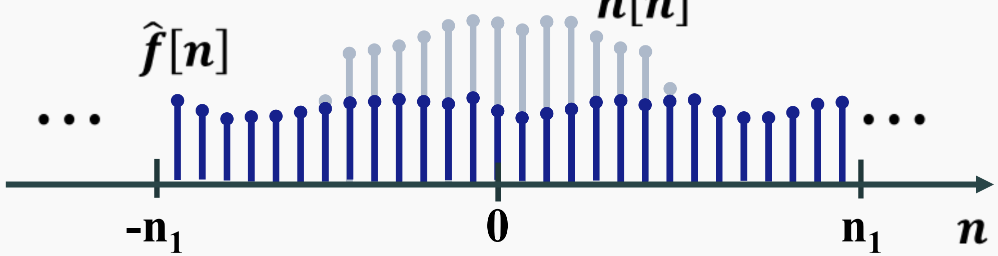

$\hat{h}[n]$: annihilating filter

$$\hat{f}[n] * \hat{h}[n] = 0$$

Length of $\hat{h}[n] \geq$ k+1

Low rank Hankel matrix

[* Jin KH et al. IEEE TCI (to appear)](#) [* Ye JC et al. IEEE TIT, 2016](#) [* Jin KH et al.,IEEE TIP, 2015](#)

*** ALOHA : Annihilating filter based LOw rank Hankel matrix Approach**

Finite length convolution

$$(\hat{h} * \hat{f})[n] = \sum_{I=0}^{\kappa-1} \hat{h}[I]\hat{f}[n-I] = 0$$

κ : # of annihilating filter coef.

Matrix Representation

$$\mathscr{C}(\hat{f})\bar{\hat{h}} = 0$$

$$\mathscr{C}(\hat{f})\bar{\hat{h}} = \quad (n_1 = 11, \kappa = 5)$$

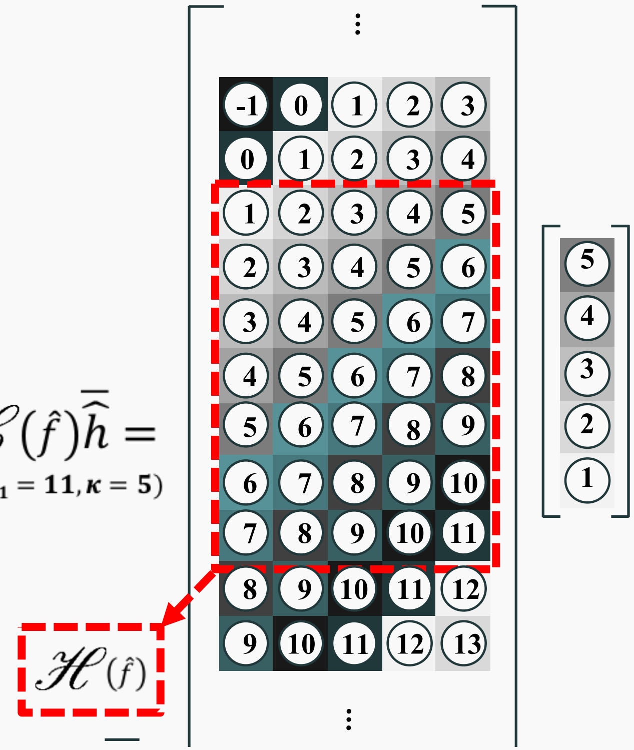

Sparsity in spatial domain ⇔ low rankness in k-space

Low-Rank Hankel matrix minimization

$$\mathrm{Rank}\,\mathcal{H}(\hat{\boldsymbol{f}}) = k$$

[* Jin KH et al IEEE TCI, 2016](#)
[* Jin KH et al.,IEEE TIP, 2015](#)
[* Ye JC et al., IEEE TIT, 2016](#)

Missing elements can be found by low rank Hankel structured matrix completion

$$\min_{\mathbf{m}} \quad \|\mathcal{H}(\mathbf{m})\|_*$$
$$\text{subject to} \quad P_\Omega(\mathbf{m}) = P_\Omega(\hat{f})$$

$\|\cdot\|_*$ Nuclear norm $\qquad P_\Omega$ Projection on sampling positions

General TV Signals

$$\mathrm{L}f(x) = \sum_{j=0}^{k-1} a_j \delta(x - x_j), \quad x_j \in [0, \tau].$$

$$\mathrm{L} := a_K \mathrm{D}^K + a_{K-1}\mathrm{D}^{K-1} + \ldots + a_1 \mathrm{D} + a_0$$

Piecewise smooth
Splines, polynomials

Weighted Fourier data

$$\mathcal{F}\{\mathrm{L}f(x)\} = \hat{l}(\omega)\hat{f}(\omega) = \sum_{j=0}^{k-1} a_j e^{-i\omega x_j}$$

$$\hat{l}(\omega) = a_K (i\omega)^K + a_{K-1}(i\omega)^{K-1} + \ldots + a_1 (i\omega) + a_0$$

Existence of Annihilating Filter

Annihilating filter for weighted Fourier data

$$\hat{h}(\omega) * \left(\hat{l}(\omega)\hat{f}(\omega)\right) = 0$$

General Low-Rank Hankel Matrix Completion

$$\begin{aligned} (P) \quad & \min_{\mathbf{m}\in\mathbb{C}^n} \quad \textsc{rank}\,\mathscr{H}(\mathbf{m}) \\ & \text{subject to} \quad P_\Omega(\mathbf{m}) = P_\Omega(\hat{\mathbf{l}} \odot \hat{\mathbf{f}}) \ , \end{aligned}$$

Extension to general signal models

Stream of Diracs

$$x(t) = \sum_{l\in\mathbb{Z}}\sum_{i=0}^{r-1} c_i \delta(t - t_i - l\tau) \ ,$$

$$rank = r$$

$$\hat{h}(z) \ = \ \sum_{l=0}^{r} \hat{h}[l] z^{-l} = \prod_{j=0}^{r-1}(1 - e^{-i2\pi t_j/\tau} z^{-1})$$

Stream of differentiated Diracs

$$x(t) = \sum_{l\in\mathbb{Z}}\sum_{j=0}^{d_j} c \ldots \delta^{(j)}(t - \ldots t \ldots)$$

$$rank = \sum_j d_j$$

$$\hat{h}(z) \ldots \prod^{r-1} (1 - \ldots z^{-1})^{d_j}$$

With a proper weighting, the Hankel matrix of the weighted k-space data → low ranked.

Non-uniform spline

$$\mathrm{L}x = \sum_{j=0}^{r-1} c_j \delta\left(t - t_j\right)$$

$$\mathrm{L} := a_K \partial^K + a_{K-1}\partial^{K-1} + \ldots + a_1 \partial + a_0$$

$$rank = r$$

$$\hat{h}(z) \ = \ \sum_{l=0}^{r} \hat{h}[l] z^{-l} = \prod_{j=0}^{r-1}(1 - e^{-i2\pi t_j/\tau} z^{-1})$$

Piecewise smooth polynomial

$$x^{(q+1)}(t) = \sum_{l\in\mathbb{Z}}\sum_{j=0}^{q} c_{lj} \delta^{(j)}(t - t_l)$$

$$rank = rq$$

$$\hat{h}(z) = \prod_{j=0}^{r-1} (1 - u_j z^{-1})^q \ .$$

* Ye JC et al., IEEE TIT 2016

Performance Guarantees

Exact Recovery

$$\min_{\mathbf{m}} \|\mathcal{H}(\mathbf{m})\|_*$$
$$\text{subject to} \quad P_\Omega(\mathbf{m}) = P_\Omega(\hat{\mathbf{f}})$$

$$m \geq c_1 \mu c_s k \log^\alpha n$$

$$\alpha = \begin{cases} 2, & \text{on grid} \\ 4, & \text{off grid} \end{cases}$$

Stable Recovery

$$\min_{\mathbf{m}} \|\mathcal{H}(\mathbf{m})\|_*$$
$$\text{subject to} \quad \|P_\Omega(\mathbf{m}) - P_\Omega(\hat{\mathbf{f}})\| \leq \delta$$

$$\|\mathcal{H}(\mathbf{m}) - \mathcal{H}(\hat{\mathbf{f}})\|_F \leq c_2 n^2 \delta$$

* Ye JC et al.,IEEE TIT 2016

Mutual Coherence for FRI

$$\mu \quad \leq \quad \max\left\{\frac{\zeta_{n-d+1}}{\sigma_{\min}\left(\mathcal{V}_{n-d+1}^{*}\mathcal{V}_{n-d+1}\right)}, \frac{\zeta_d}{\sigma_{\min}\left(\mathcal{V}_d^{*}\mathcal{V}_d\right)}\right\}$$

Confluent Vandermonde matrix

$$\mathscr{H}(\hat{\mathbf{x}}) = \mathcal{V}_{n-d+1}\,\mathcal{B}\,\mathcal{V}_d^T,$$

$$\zeta_N \quad = \quad N\left[\frac{(N-1)!}{(N-l_{\max})!}\right]^2$$

Multiplicity of roots

$$\mu \leq \frac{n/2}{n/2 - 1/\Delta - 1}$$

Using extreme function
for bounding singular value
See Moitra (2015)

* Ye JC et al.,IEEE TIT 2016

Relation to Super-resolution: Minimum separation

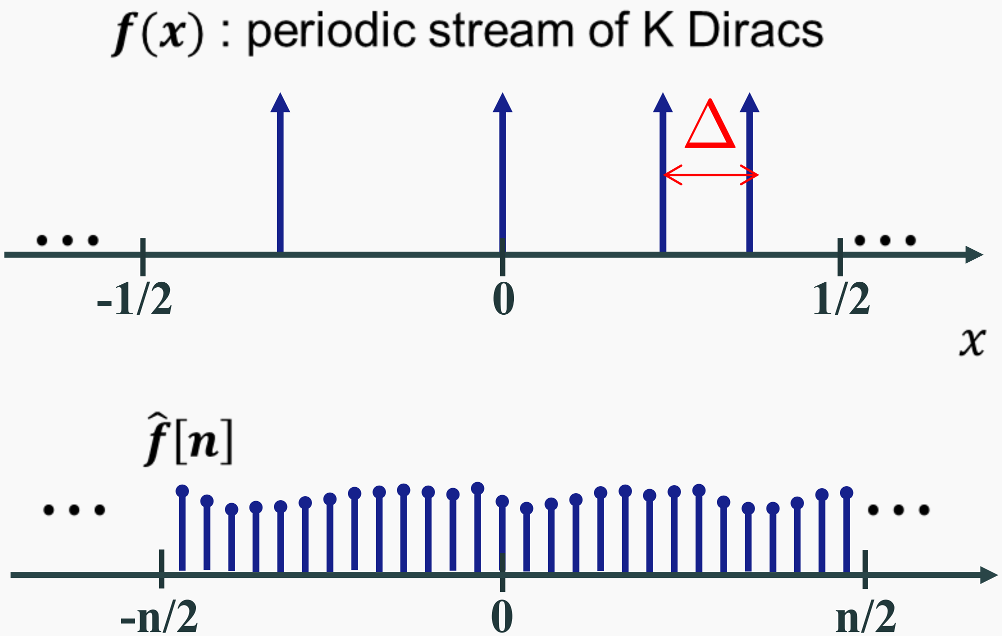

$$\Delta > \frac{2}{n}$$

Same as
Candes et al (2013)
Tang et al (2015)

$$\mu \leq \frac{n/2}{n/2 - 1/\Delta - 1}$$

Using extreme function
for bounding singular value
See Moitra (2015)

** Ye JC et al.,IEEE TIT 2016*

Link to discrete domain CS

* Ye JC et al.,IEEE TIT 2016

On grid model using cardinal setup

- ***Unknown singularities are located on integer grid***

$$\mathrm{L}x(t) = \sum_{l \in \mathbb{Z}} a[l]\delta(t-l)$$

- ***Discrete whiting filter with uniform sampling accounts for the sparsity***

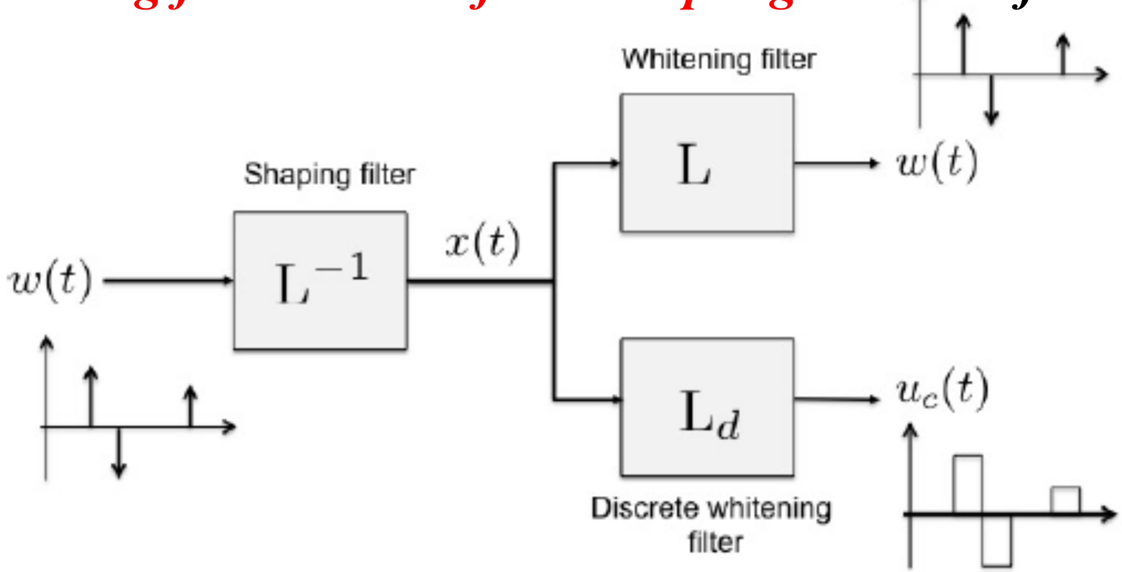

Off-Grid vs On-Grid : Hankel

* Ye JC et al.,IEEE TIT 2016

Hankel Matrix: off-grid

$$\begin{bmatrix} \hat{y}[0] & \hat{y}[1] & \cdots & \hat{y}[d-1] \\ \hat{y}[1] & \hat{y}[2] & \cdots & \hat{y}[d] \\ \vdots & \vdots & \ddots & \vdots \\ \hat{y}[n-d] & \hat{y}[n-d+1] & \cdots & \hat{y}[n-1] \end{bmatrix}$$

Wrap-around Hankel Matrix: on-grid

$$\begin{bmatrix} \hat{w}_0[0] & \hat{w}_0[1] & \cdots & \hat{w}_0[d-1] \\ \hat{w}_0[1] & \hat{w}_0[2] & \cdots & \hat{w}_0[d] \\ \vdots & \vdots & \ddots & \vdots \\ \hat{w}_0[n-d] & \hat{w}_0[n-d+1] & \cdots & \hat{w}_0[n-1] \\ \hline \hat{w}_0[n-d+1] & \hat{w}_0[n-d+2] & \cdots & \hat{w}_0[0] \\ \vdots & \vdots & \ddots & \vdots \\ \hat{w}_0[n-1] & \hat{w}_0[0] & \cdots & \hat{w}_0[d-2] \end{bmatrix}$$

Periodic repetition

$$m \geq c_1 \mu c_s k \log^{\alpha} n$$

$$\alpha = \begin{cases} 2, & \text{on grid} \\ 4, & \text{off grid} \end{cases}$$

Off-grid vs On-grid: weighting

Regularized Weighting → more stable

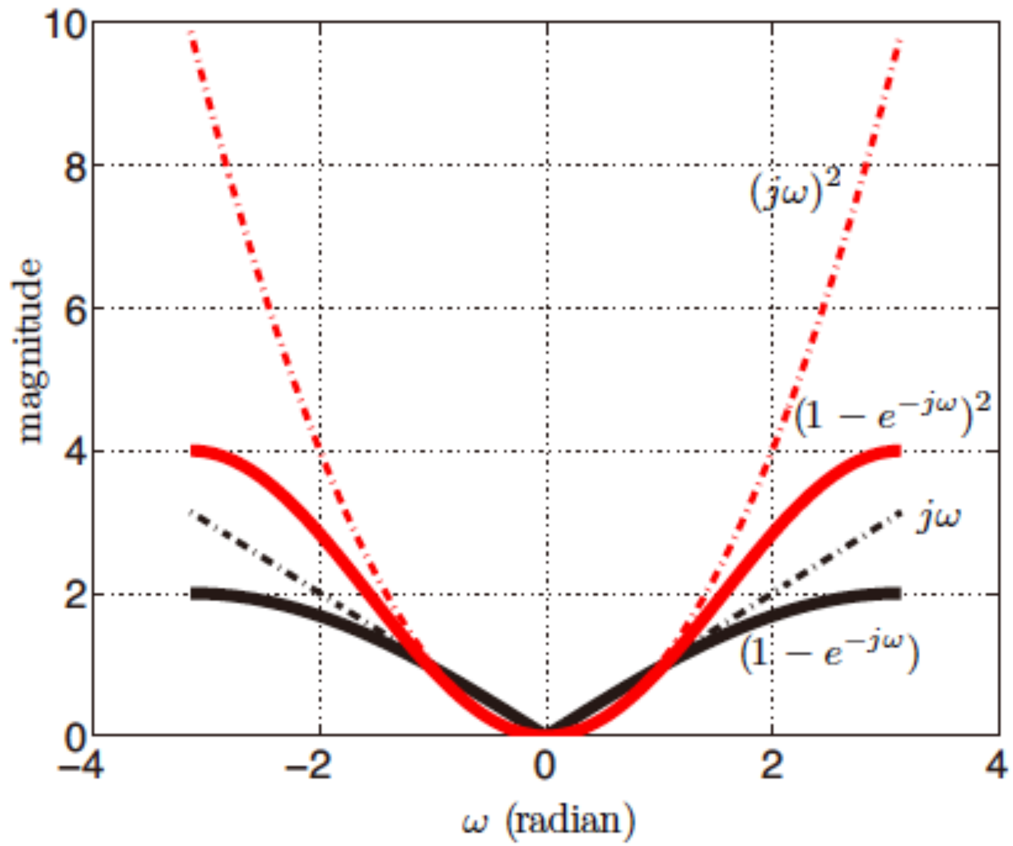

* Ye JC et al.,IEEE TIT 2016

Phase transition:
piecewise constant signals

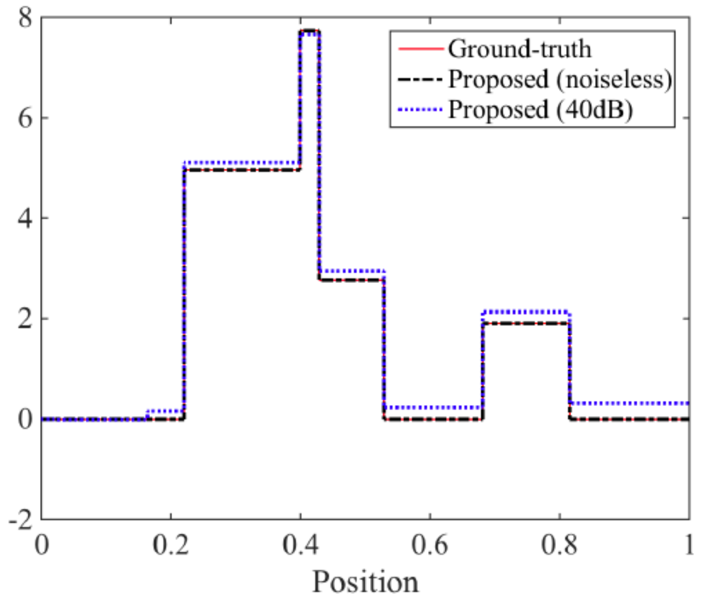

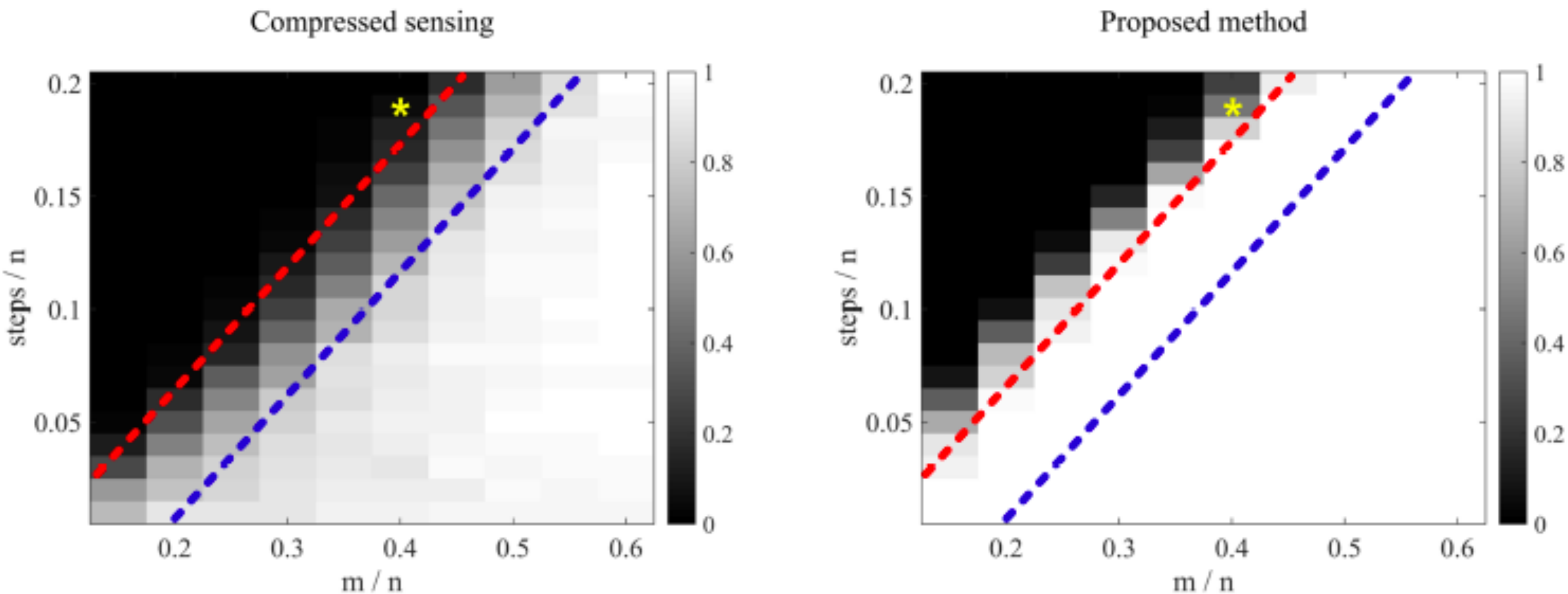

Overview

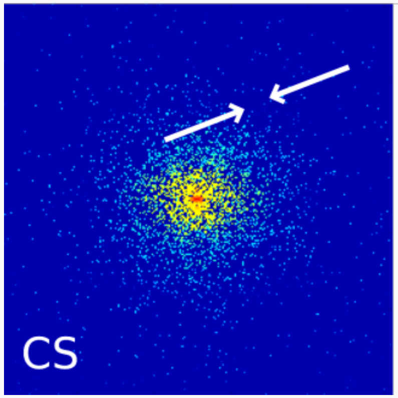

1. Introduction
2. Review of Compressive Sensing
3. FRI extrapolation from uniform samples
4. Structured low-rank interpolation for non-uniform samples
   - 2-D Theory
5. Fast implementations
6. Biomedical applications

2-D PWC functions satisfy an annihilation relation

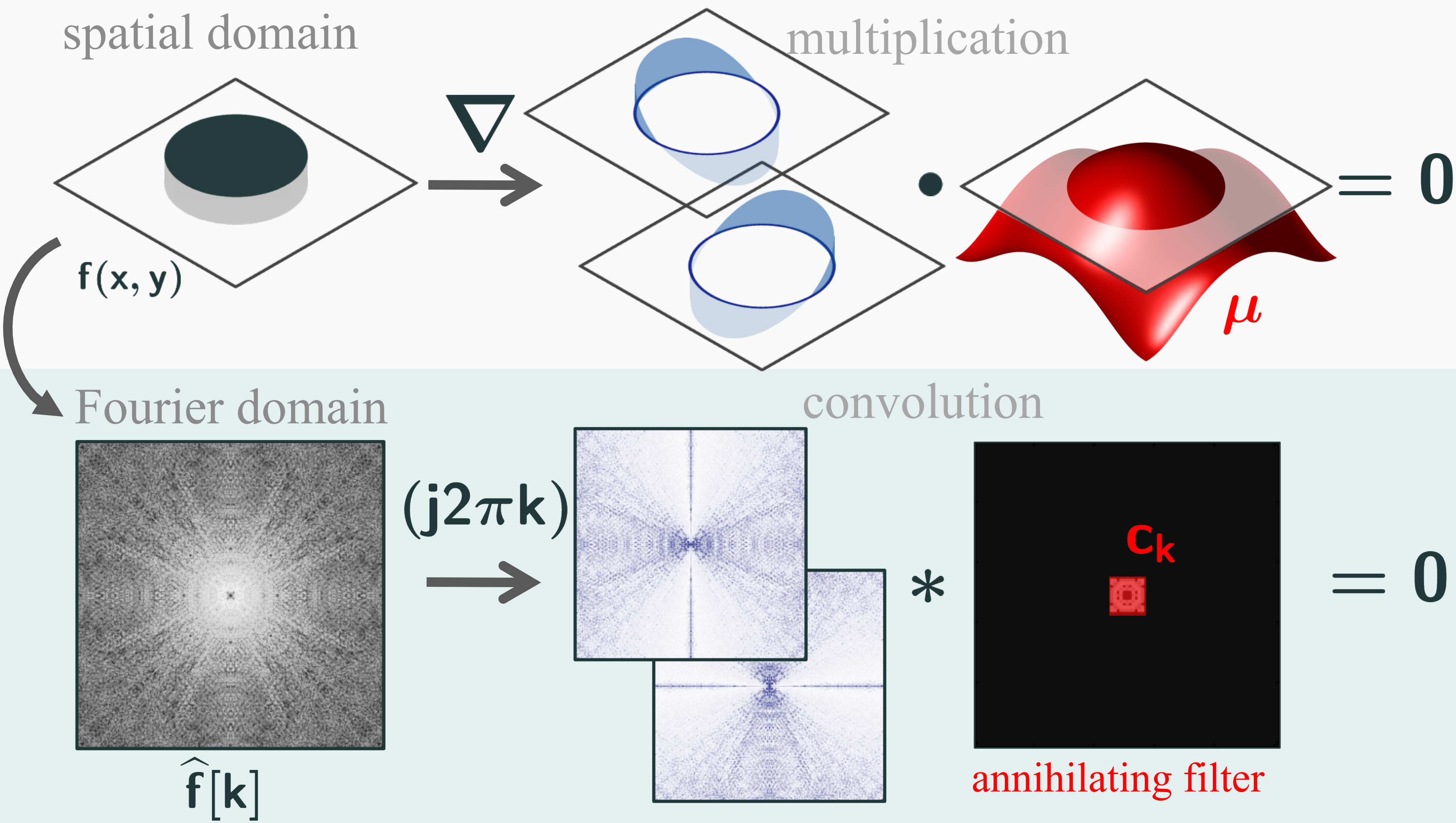

Annihilation relation: $\sum_k \widehat{\nabla f}[\ell - k] c_k = 0$

Matrix representation of annihilation

$$\mathcal{T}(\widehat{f})\,\boldsymbol{c} = 0$$

2-D convolution matrix (block Toeplitz)

vector of filter coefficients

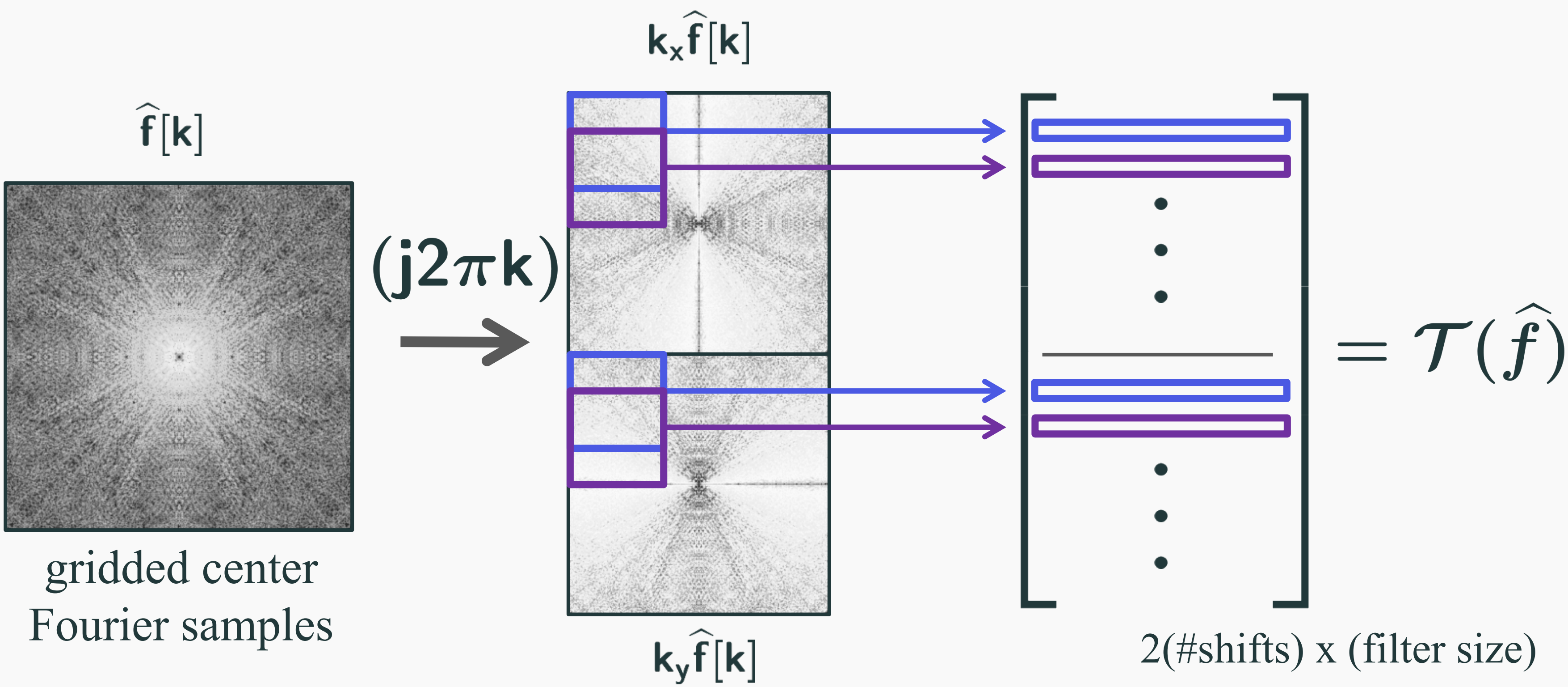

Basis of algorithms: Annihilation matrix is low-rank

Prop: If the level-set function is bandlimited to Λ and the assumed filter support $\Lambda' \supset \Lambda$ then

$$\operatorname{rank}[\mathcal{T}(\widehat{\mathbf{f}})] \leq |\Lambda'| - (\#\text{shifts } \Lambda \text{ in } \Lambda')$$

Fourier domain

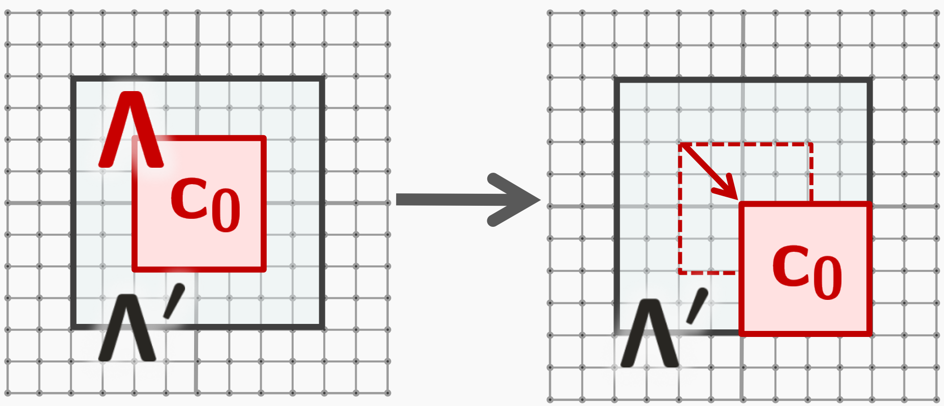

Spatial domain

$$\mu(x, y) \longrightarrow e^{j2\pi(kx+ly)}\mu(x, y)$$

Basis of algorithms: Annihilation matrix is low-rank

Prop: If the level-set function is bandlimited to Λ and the assumed filter support $\Lambda' \supset \Lambda$ then

$$\mathrm{rank}[\mathcal{T}(\widehat{\mathbf{f}})] \leq |\Lambda'| - (\#\text{shifts } \Lambda \text{ in } \Lambda')$$

Example:
Shepp-Logan

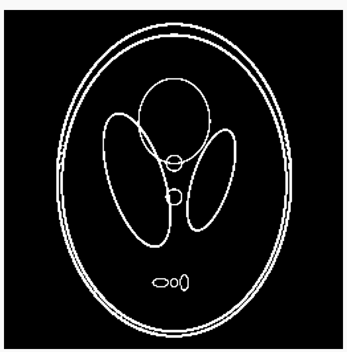

Fourier domain

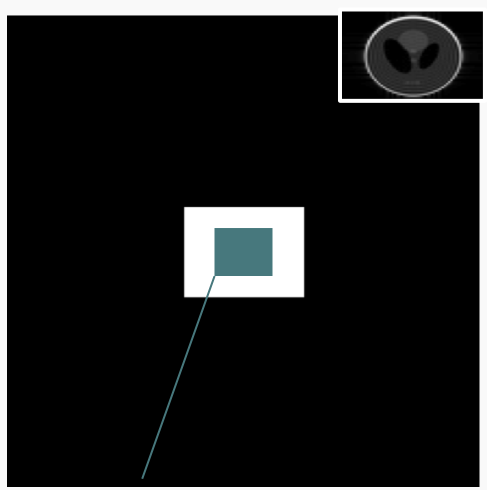

Assumed filter: 33x25

Samples: 65x49

$\sigma(\mathcal{T}(\widehat{f}))$

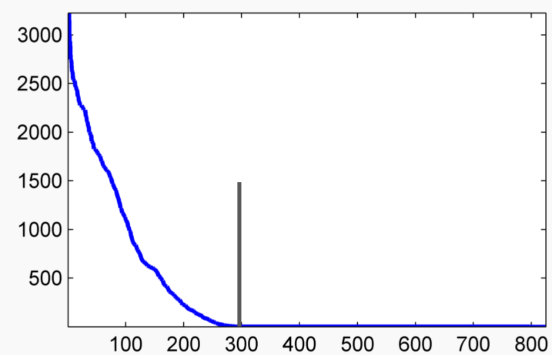

Rank ≈ 300

One Step Algorithm

Jointly estimate edge set and amplitudes

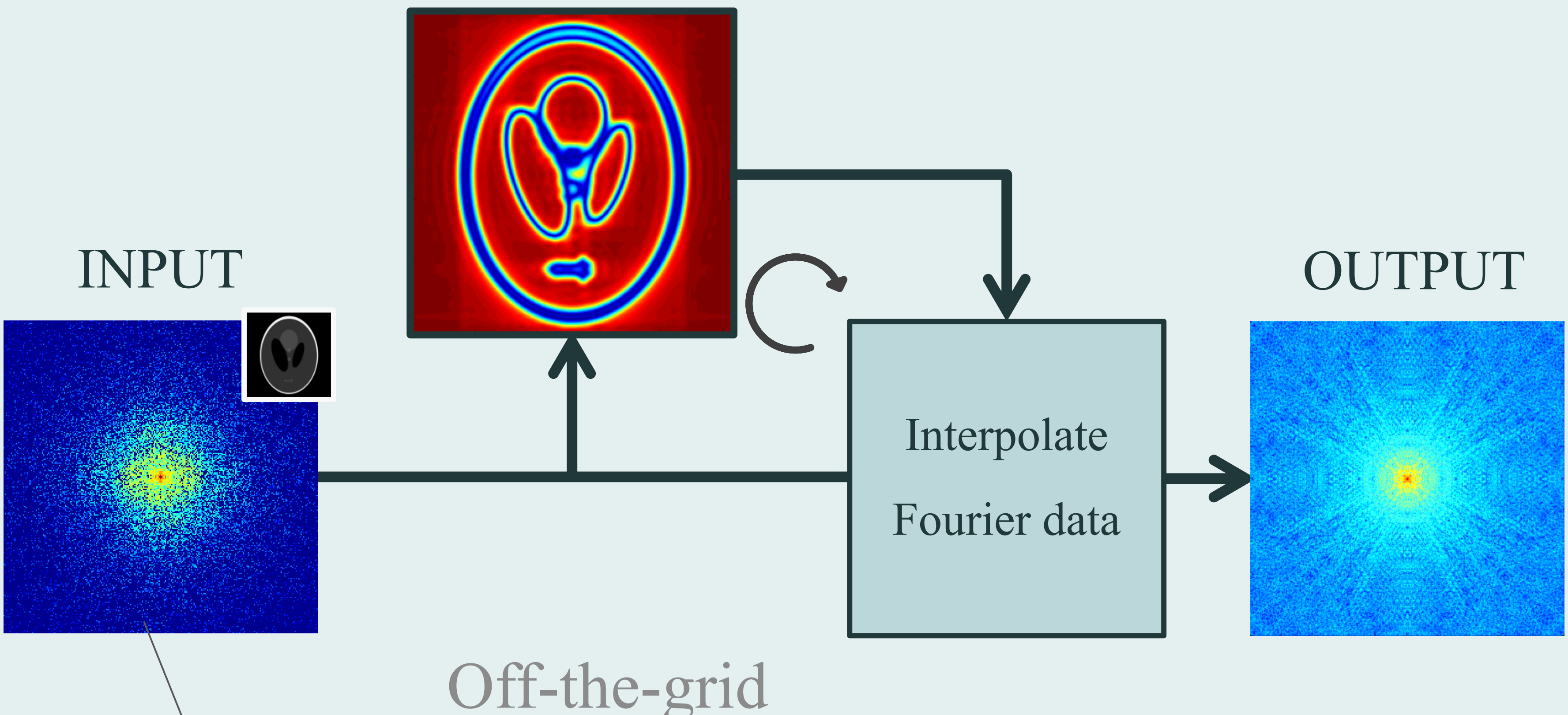

Accommodate random samples

Recovery as a structured low-rank matrix completion

$$\min_{\widehat{\mathbf{f}}} \quad \operatorname{rank}[\mathcal{T}(\widehat{\mathbf{f}})] \;\; \textbf{s.t.} \;\; \widehat{\mathbf{f}}[\mathbf{k}] = \widehat{\mathbf{b}}[\mathbf{k}], \mathbf{k} \in \mathbf{\Gamma}$$

Recovery as a structured low-rank matrix completion

$$\min_{\widehat{\mathbf{f}}} \quad \mathrm{rank}[\mathcal{T}(\widehat{\mathbf{f}})] \quad \textbf{s.t.} \quad \widehat{\mathbf{f}}[\mathbf{k}] = \widehat{\mathbf{b}}[\mathbf{k}], \mathbf{k} \in \Gamma$$

1-D Example:

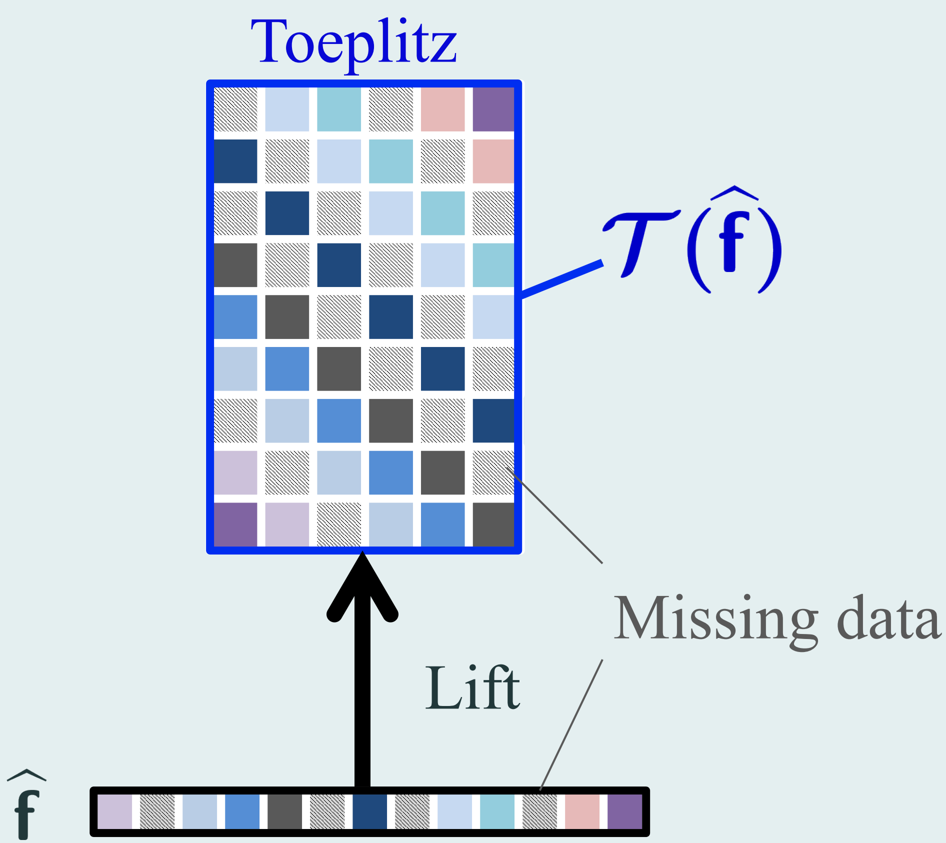

Recovery as a structured low-rank matrix completion

$$\min_{\widehat{\mathbf{f}}} \quad \text{rank}[\mathcal{T}(\widehat{\mathbf{f}})] \quad \textbf{s.t.} \quad \widehat{\mathbf{f}}[\mathbf{k}] = \widehat{\mathbf{b}}[\mathbf{k}], \mathbf{k} \in \mathbf{\Gamma}$$

1-D Example:

Complete matrix

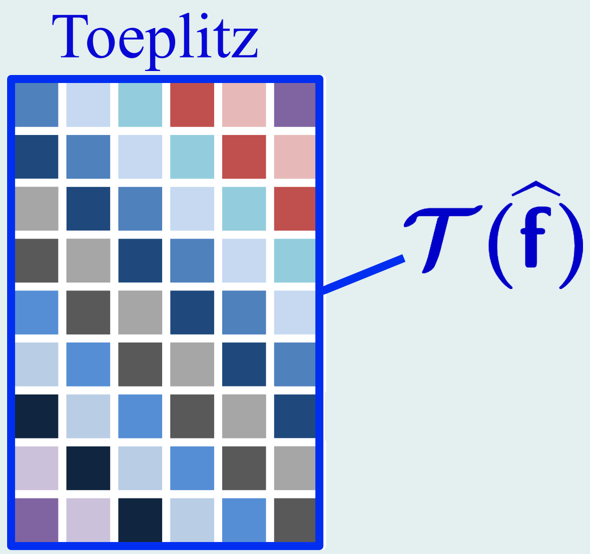

$\widehat{\mathbf{f}}$

Recovery as a structured low-rank matrix completion

$$\min_{\widehat{\mathbf{f}}} \quad \mathrm{rank}[\mathcal{T}(\widehat{\mathbf{f}})] \quad \textbf{s.t.} \quad \widehat{\mathbf{f}}[\mathbf{k}] = \widehat{\mathbf{b}}[\mathbf{k}], \mathbf{k} \in \boldsymbol{\Gamma}$$

1-D Example:

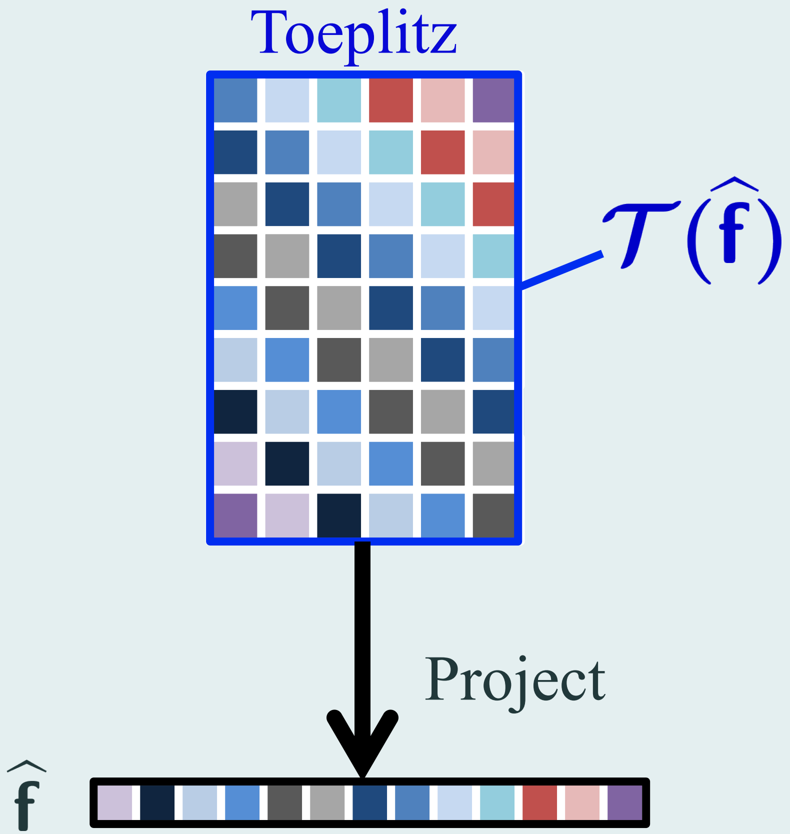

Recovery as a structured low-rank matrix completion

$$\min_{\widehat{\mathbf{f}}} \quad \mathrm{rank}[\mathcal{T}(\widehat{\mathbf{f}})] \;\; \textbf{s.t.} \;\; \widehat{\mathbf{f}}[\mathbf{k}] = \widehat{\mathbf{b}}[\mathbf{k}], \mathbf{k} \in \boldsymbol{\Gamma}$$

NP-Hard!

Recovery as a structured low-rank matrix completion

$$\min_{\widehat{\mathbf{f}}} \quad \mathrm{rank}[\mathcal{T}(\widehat{\mathbf{f}})] \quad \textbf{s.t.} \quad \widehat{\mathbf{f}}[\mathbf{k}] = \widehat{\mathbf{b}}[\mathbf{k}], \mathbf{k} \in \mathbf{\Gamma}$$

↓ *Convex Relaxation*

$$\min_{\widehat{\mathbf{f}}} \quad \|\mathcal{T}(\widehat{\mathbf{f}})\|_* \quad \textbf{s.t.} \quad \widehat{\mathbf{f}}[\mathbf{k}] = \widehat{\mathbf{b}}[\mathbf{k}], \mathbf{k} \in \mathbf{\Gamma}$$

Nuclear norm – sum of singular values

Recovery from 20-fold random undersampled data

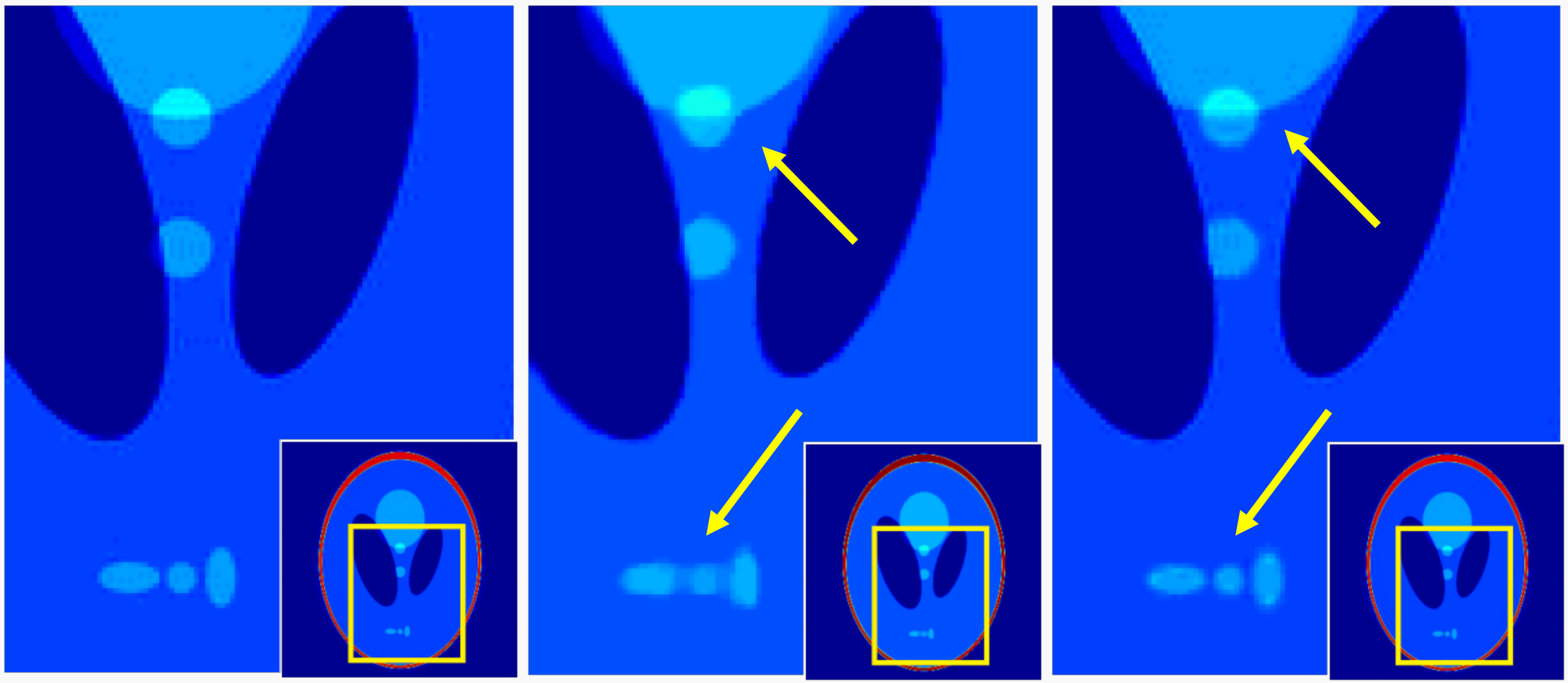

Fully sampled | TV regularized recovery | Structured low-rank recovery

[Ongie & Jacob, SAMPTA 15](https://arxiv.org/abs/1609.07429)
https://arxiv.org/abs/1609.07429

Fully sampled TV (SNR=17.8dB) GIRAF (SNR=19.0)

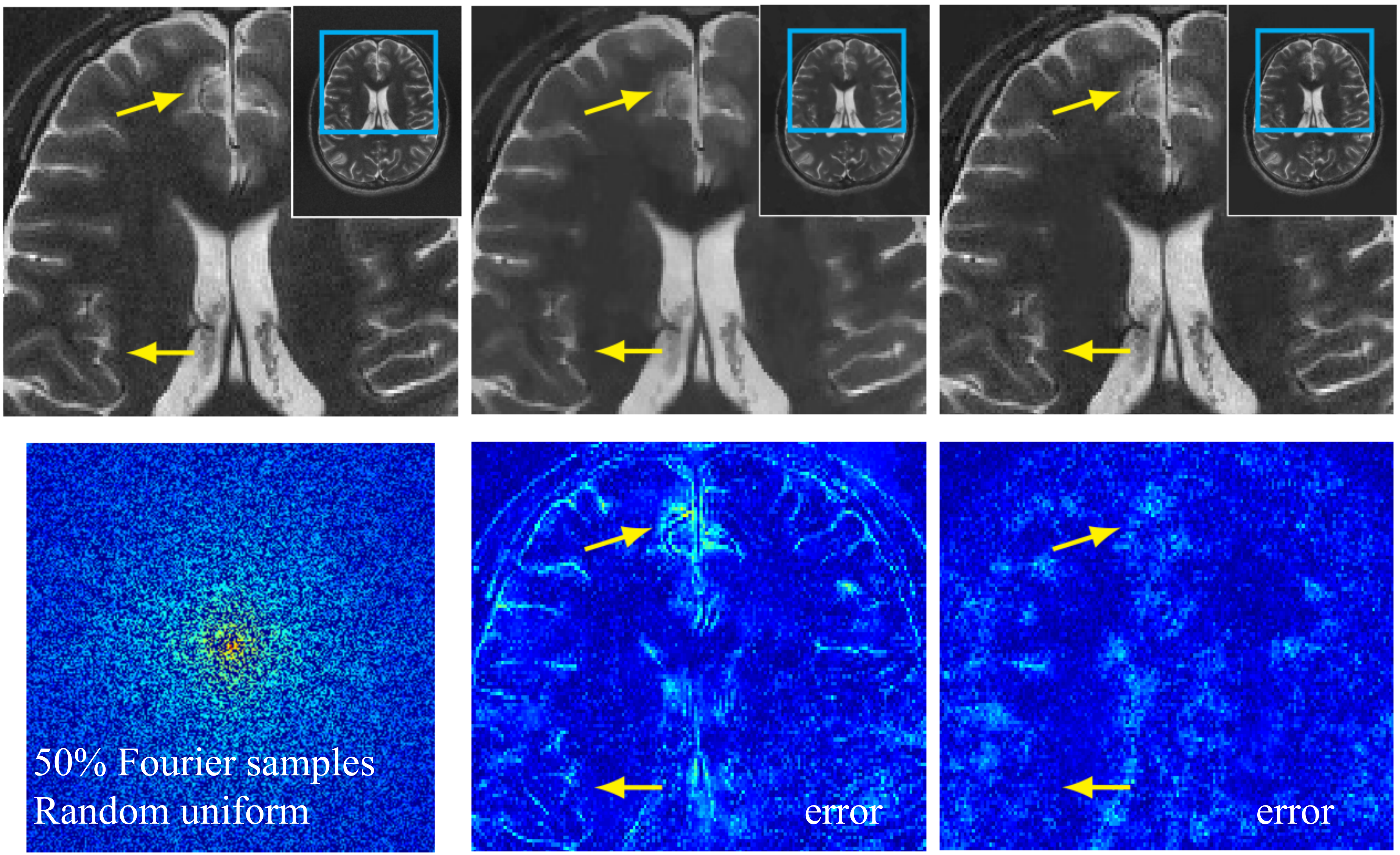

Ongie & Jacob, SAMPTA 15
https://arxiv.org/abs/1609.07429

Performance guarantee

Let f be a piecewise constant signal with edge set, which is the zero level set of a bandlimited function. Assume that f is sampled uniformly at m locations random on a Fourier domain grid Γ. Then, f can be recovered from the samples using a SLR approach if

$$\mathsf{m} > \rho_1 \, \mathsf{c_s} \, \mathsf{r} \, \log^4 |\Gamma|$$

$\boldsymbol{\rho_1}$ = incoherence measure of edge-set

$\mathbf{r}$ = rank of $\mathcal{T}(\widehat{\mathbf{f}})$

$\mathbf{c_s}$ = ratio of grid size to filter size

Ongie & Jacob, ICIP16, https://arxiv.org/abs/1703.01405

Incoherency measure ρ_1

Intuition: minimum separation distance when packing r points on the edge-set curve, where $\mathbf{r} = \textbf{rank}\, \mathcal{T}(\widehat{\mathbf{f}})$

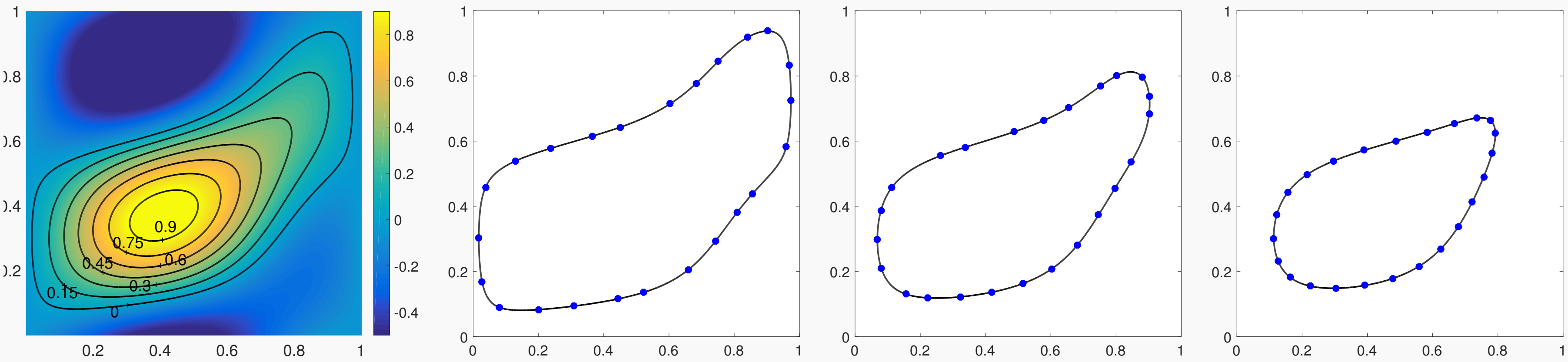

(a) Level-sets of μ_0 (b) $\rho \leq 8.0$ (c) $\rho \leq 264.9$ (d) $\rho \leq 5.0 \times 10^4$

Small regions: high incoherence & more measurements

Complex boundaries: high rank/bandwidth

Phase transitions

Randomly generated synthetic PWC images

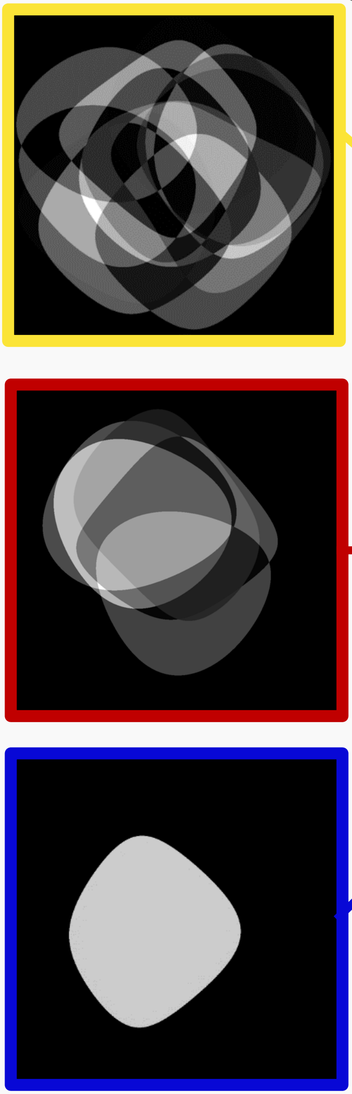

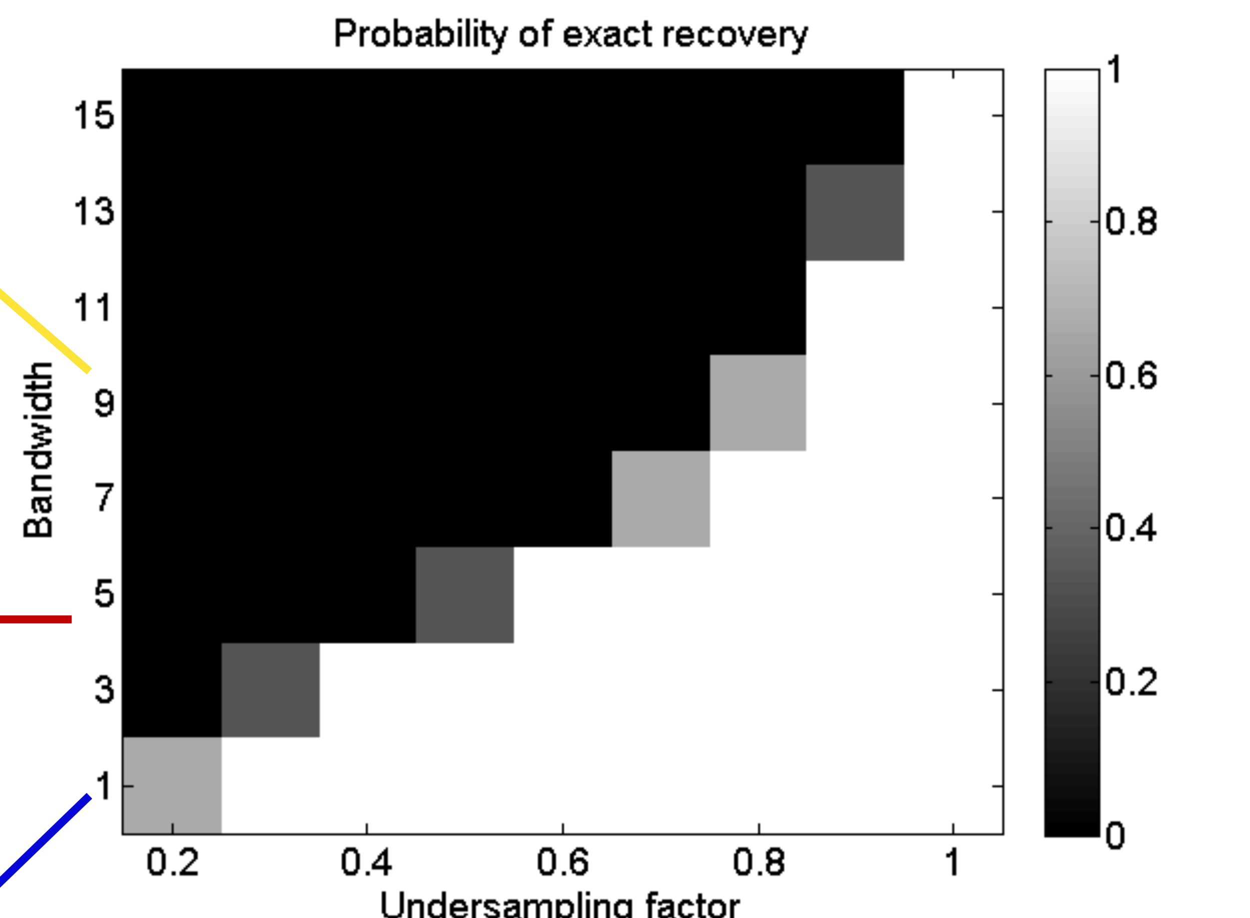

- 10 trials
- Uniform random Fourier samples
- 64x64 Fourier sampling window

[Ongie & Jacob, ICIP16, https://arxiv.org/abs/1703.01405](https://arxiv.org/abs/1703.01405)

Related structured low-rank methods in MRI

Magnetic Resonance in Medicine 64:457–471 (2010)

SPIRiT: Iterative Self-consistent Parallel Imaging Reconstruction From Arbitrary *k*-Space

Michael Lustig[1,2]* and John M. Pauly[2]

Discrete formulation exploiting multichannel acquisition

668 IEEE TRANSACTIONS ON MEDICAL IMAGING, VOL. 33, NO. 3, MARCH 2014

Low-Rank Modeling of Local k-Space Neighborhoods (LORAKS) for Constrained MRI

Justin P. Haldar, *Member, IEEE*

Discrete formulation exploiting sparsity, smoothly varying phase, and multichannel acquisition

Overview

1. Introduction
2. Review of Compressive Sensing
3. FRI extrapolation from uniform samples
4. Structured low-rank interpolation for non-uniform samples
5. Fast algorithms
6. Biomedical applications

Nuclear norm minimization

$$\min_{\widehat{\mathbf{f}}} \|\mathbf{A}\widehat{\mathbf{f}} - \mathbf{b}\|^2 + \lambda\|\mathbf{X}\|_* \quad \text{s.t.} \quad \mathbf{X} = \mathcal{T}(\widehat{\mathbf{f}})$$

ADMM = Singular value thresholding (SVT)

1. Singular value thresholding step

   -compute *full SVD* of X!

2. Solve linear least squares problem

   -analytic solution or CG solve

Alternating projections ["SAKE," Shin 14], ["LORAKS," Haldar, 14]

$$\min_{\widehat{\mathbf{f}}} \|\mathbf{A}\widehat{\mathbf{f}} - \mathbf{b}\|^2 \quad \text{s.t.} \quad \boxed{\mathbf{X} = \mathcal{T}(\widehat{\mathbf{f}})}$$

$$\boxed{\text{rank } \mathbf{X} \leq \mathbf{r}}$$

Alternating projection algorithm (Cadzow)

1. Project onto space of rank r matrices

   -Compute *truncated SVD:* $\mathbf{X}^\star = \mathbf{U}\boldsymbol{\Sigma}_r\mathbf{V}^H$

2. Project onto space of structured matrices

   -Average along "diagonals"

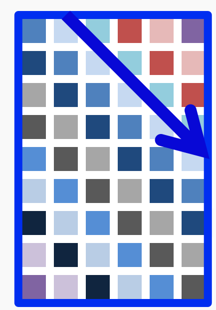

U,V factorization [O.& Jacob, SampTA 15, Jin et al., ISBI 15]

$$\min_{\widehat{\mathbf{f}}} \|\mathbf{A}\widehat{\mathbf{f}} - \mathbf{b}\|^2 + \lambda\|\mathbf{X}\|_* \;\; \text{s.t.} \;\; \mathbf{X} = \mathcal{T}(\widehat{\mathbf{f}})$$

"U,V factorization trick"

$$\|\mathbf{X}\|_* = \min_{\mathbf{X}=\mathbf{U}\mathbf{V}^H} \frac{1}{2}\left(\|\mathbf{U}\|_F^2 + \|\mathbf{V}\|_F^2\right)$$

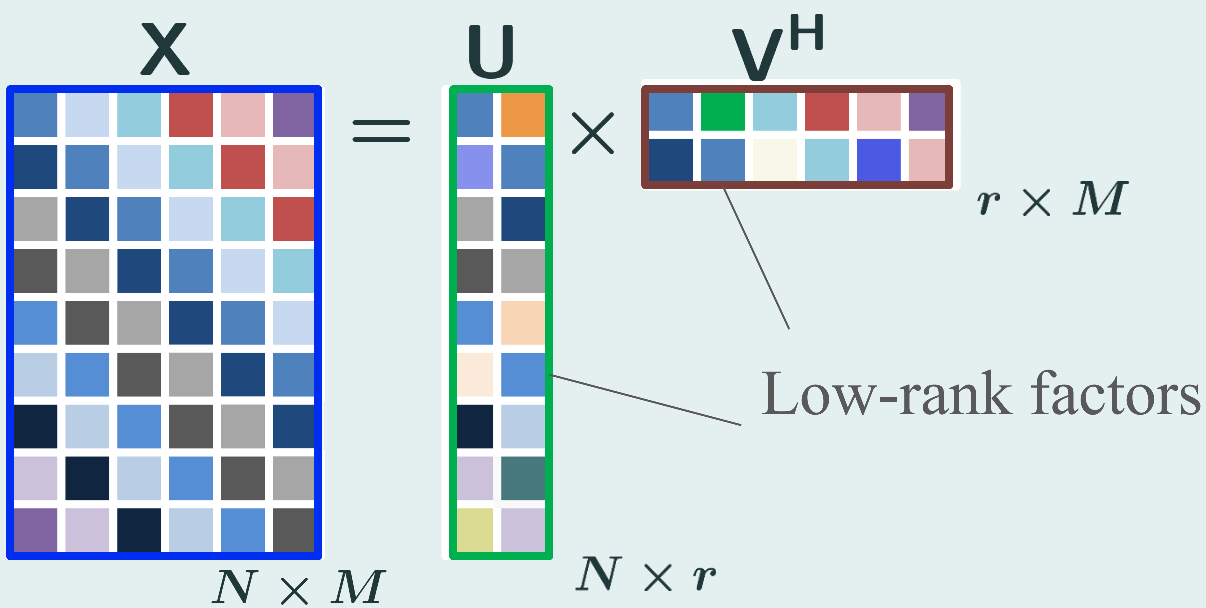

U,V factorization [O.& Jacob, SampTA 15, Jin et al., ISBI 15]

$$\min_{\hat{\mathbf{f}},\mathbf{U},\mathbf{V}} \|\mathbf{A}\hat{\mathbf{f}} - \mathbf{b}\|^2 + \frac{\lambda}{2}\left(\|\mathbf{U}\|_F^2 + \|\mathbf{V}\|_F^2\right)$$

$$\text{s.t. } \mathbf{U}\mathbf{V}^H = \mathcal{T}(\hat{\mathbf{f}})$$

UV factorization approach

~~1. Singular value thresholding step~~

~~-compute *full SVD* of X!~~

SVD-free → fast matrix inversion steps

2. Solve linear least squares problem

-analytic solution or CG solve

Main challenge : Computational complexity & memory

2-D

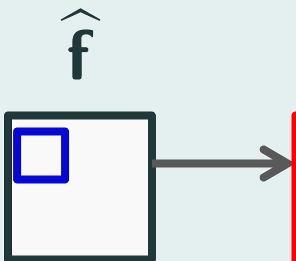

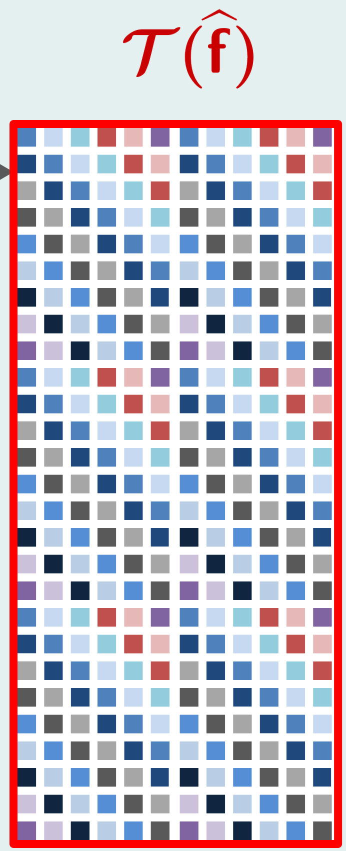

Image: 256x256

Filter: 32x32

$\sim 10^6 \times 1000$

3-D

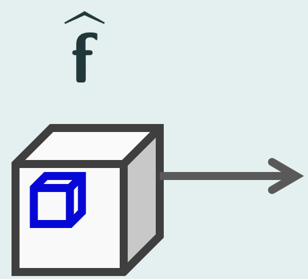

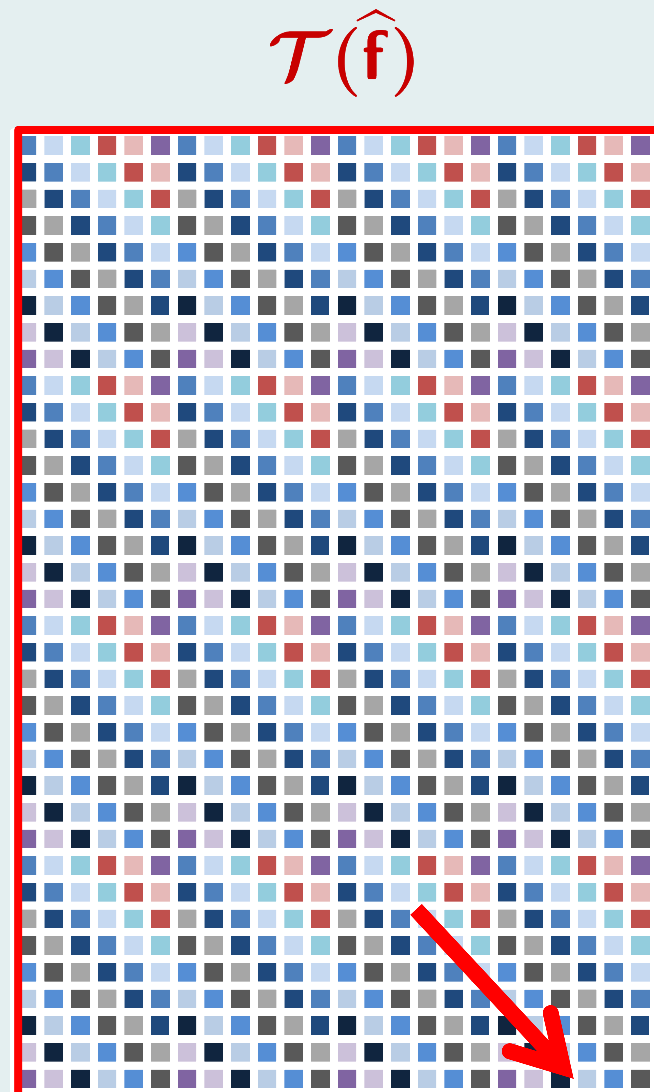

256x256x32

32x32x10

$\sim 10^8 \times 10^5$

Cannot Hold

in Memory!

Exploit convolutional structure of the matrix

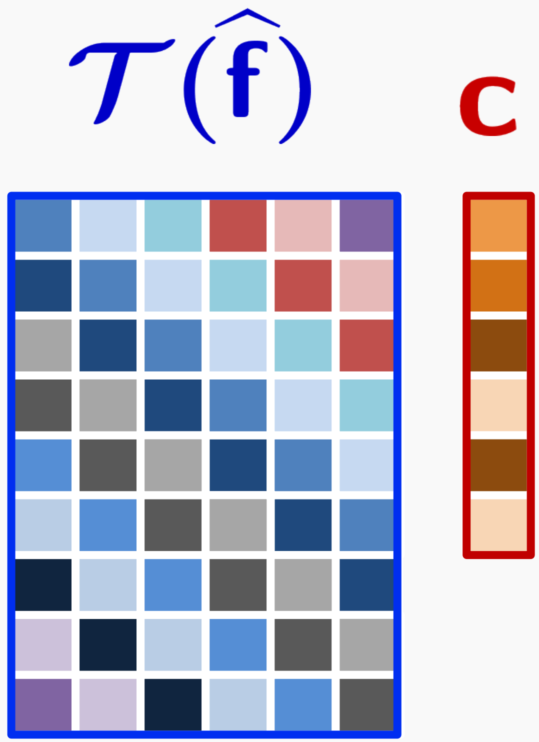

$$\approx \hat{\mathbf{f}} * \mathbf{c}$$

Fast evaluation using FFT

Direct computation of small Gram matrix: avoid storage

IRLS algorithm along with structure exploitation

- Original IRLS: To recover low-rank matrix X, iterate

$$\mathbf{W} \leftarrow (\mathbf{X}^{\mathbf{H}}\mathbf{X} + \epsilon\mathbf{I})^{-\frac{1}{2}}$$

$$\mathbf{X} \leftarrow \arg\min_{\mathbf{X}} \|\mathbf{X}\mathbf{W}^{\frac{1}{2}}\|_{\mathbf{F}}^2 + \lambda\|\mathbf{A}\mathbf{X} - \mathbf{B}\|_{\mathbf{F}}^2$$

IRLS

- Original IRLS: To recover low-rank matrix X, iterate

$$\mathbf{W} \leftarrow (\mathbf{X}^{\mathsf{H}}\mathbf{X} + \epsilon \mathbf{I})^{-\frac{1}{2}}$$

$$\mathbf{X} \leftarrow \arg\min_{\mathbf{X}} \|\mathbf{X}\mathbf{W}^{\frac{1}{2}}\|_{\mathsf{F}}^2 + \lambda \|\mathbf{A}\mathbf{X} - \mathbf{B}\|_{\mathsf{F}}^2$$

- We adapt to structured case: $\mathbf{X} = \mathcal{T}(\widehat{f})$

$$\mathbf{W} \leftarrow (\mathcal{T}(\widehat{\mathbf{f}})^{\mathsf{H}}\mathcal{T}(\widehat{\mathbf{f}}) + \epsilon \mathbf{I})^{-\frac{1}{2}}$$

$$\widehat{\mathbf{f}} \leftarrow \arg\min_{\widehat{\mathbf{f}}} \|\mathcal{T}(\widehat{\mathbf{f}})\mathbf{W}^{\frac{1}{2}}\|_{\mathsf{F}}^2 + \lambda \|\mathbf{A}\widehat{\mathbf{f}} - \mathbf{b}\|^2$$

IRLS algorithm

- Original IRLS: To recover low-rank matrix X, iterate

$$\mathbf{W} \leftarrow (\mathbf{X}^H\mathbf{X} + \epsilon\mathbf{I})^{-\frac{1}{2}}$$

$$\mathbf{X} \leftarrow \arg\min_{\mathbf{X}} \|\mathbf{X}\mathbf{W}^{\frac{1}{2}}\|_F^2 + \lambda\|\mathbf{A}\mathbf{X} - \mathbf{B}\|_F^2$$

- We adapt to structured case: $\mathbf{X} = \mathcal{T}(\widehat{f})$

$$\mathbf{W} \leftarrow (\mathcal{T}(\widehat{\mathbf{f}})^H\mathcal{T}(\widehat{\mathbf{f}}) + \epsilon\mathbf{I})^{-\frac{1}{2}}$$

$$\widehat{\mathbf{f}} \leftarrow \arg\min_{\widehat{\mathbf{f}}} \|\mathcal{T}(\widehat{\mathbf{f}})\mathbf{W}^{\frac{1}{2}}\|_F^2 + \lambda\|\mathbf{A}\widehat{\mathbf{f}} - \mathbf{b}\|^2$$

Without modification, this approach is still slow!

Ongie & Jacob, ISBI16
https://arxiv.org/abs/1609.07429

Idea 1: Embed Toeplitz lifting in circulant matrix

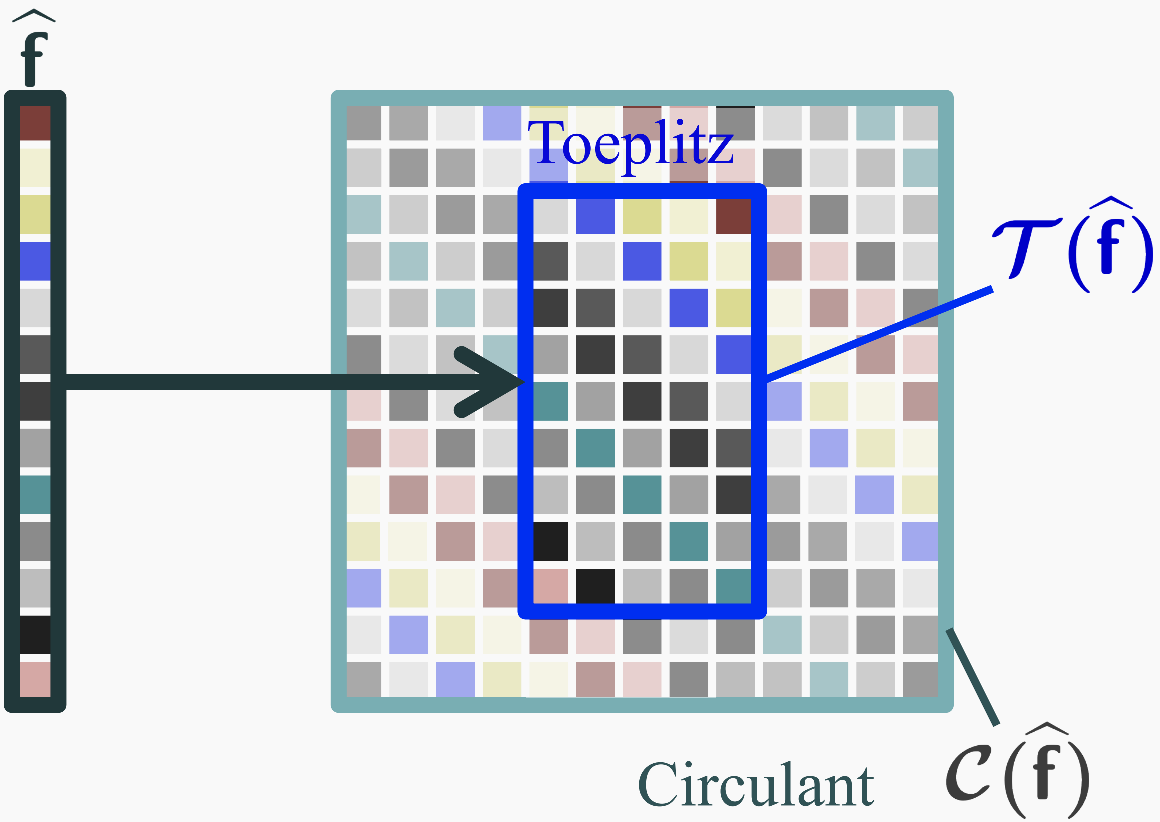

*Fast matrix-vector products with $\mathcal{T}(\hat{\mathbf{f}})$ by FFTs

[Ongie & Jacob, ISBI16](https://arxiv.org/abs/1609.07429)
https://arxiv.org/abs/1609.07429

Idea 2: Approximate matrix lifting

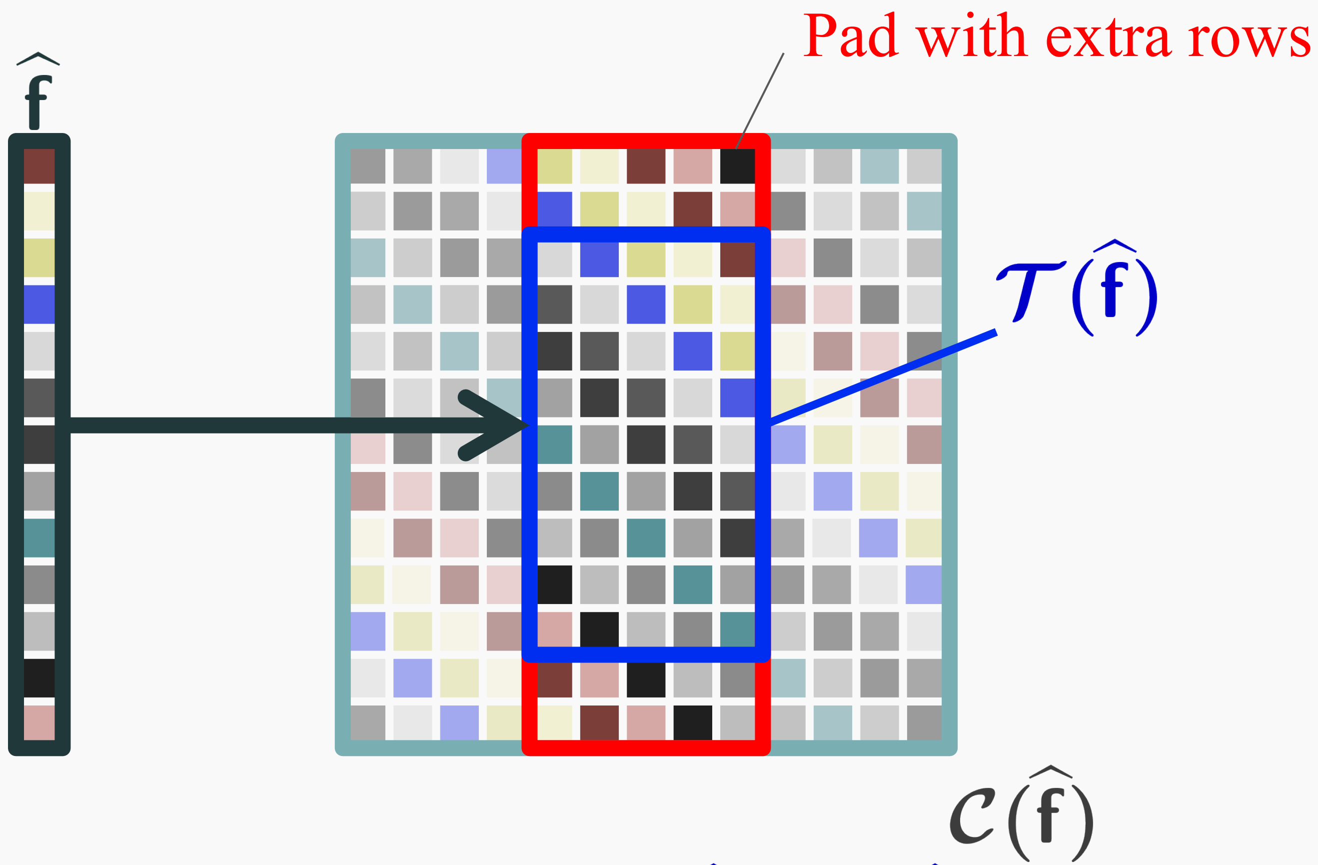

*Fast computation of $\mathcal{T}(\widehat{\mathbf{f}})^H\mathcal{T}(\widehat{\mathbf{f}})$ by FFTs

Ongie & Jacob, ISBI16
https://arxiv.org/abs/1609.07429

GIRAF: fast [O. & Jacob, 2016 (arXiv)]

Complexity similar to IRLS for TV minimization

IRLS TV-minimization

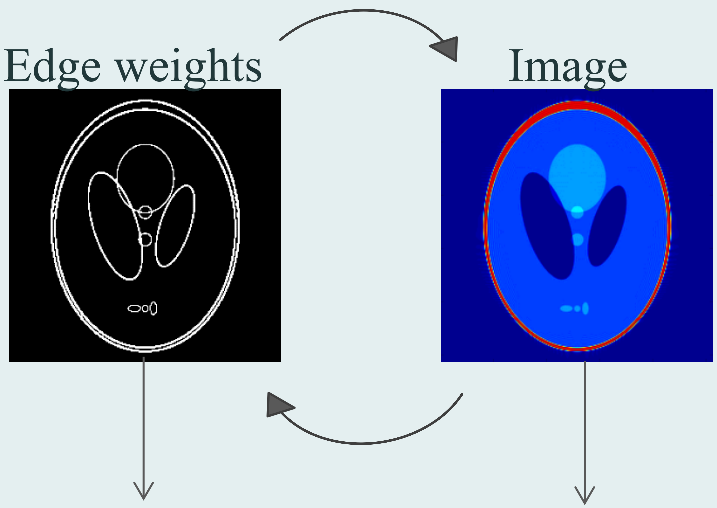

Local update:

$$w_{i,j} = \frac{1}{|(\nabla f)_{i,j}| + \epsilon}$$

Least-squares problem

GIRAF algorithm

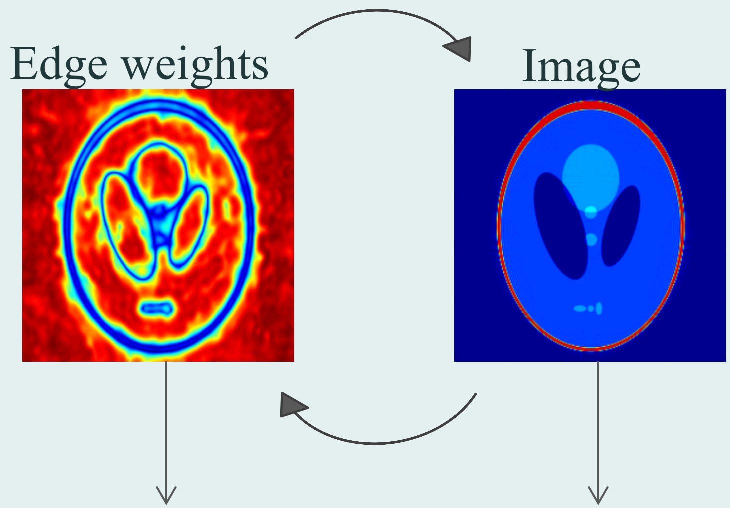

Global update w/small SVD

Least-squares problem

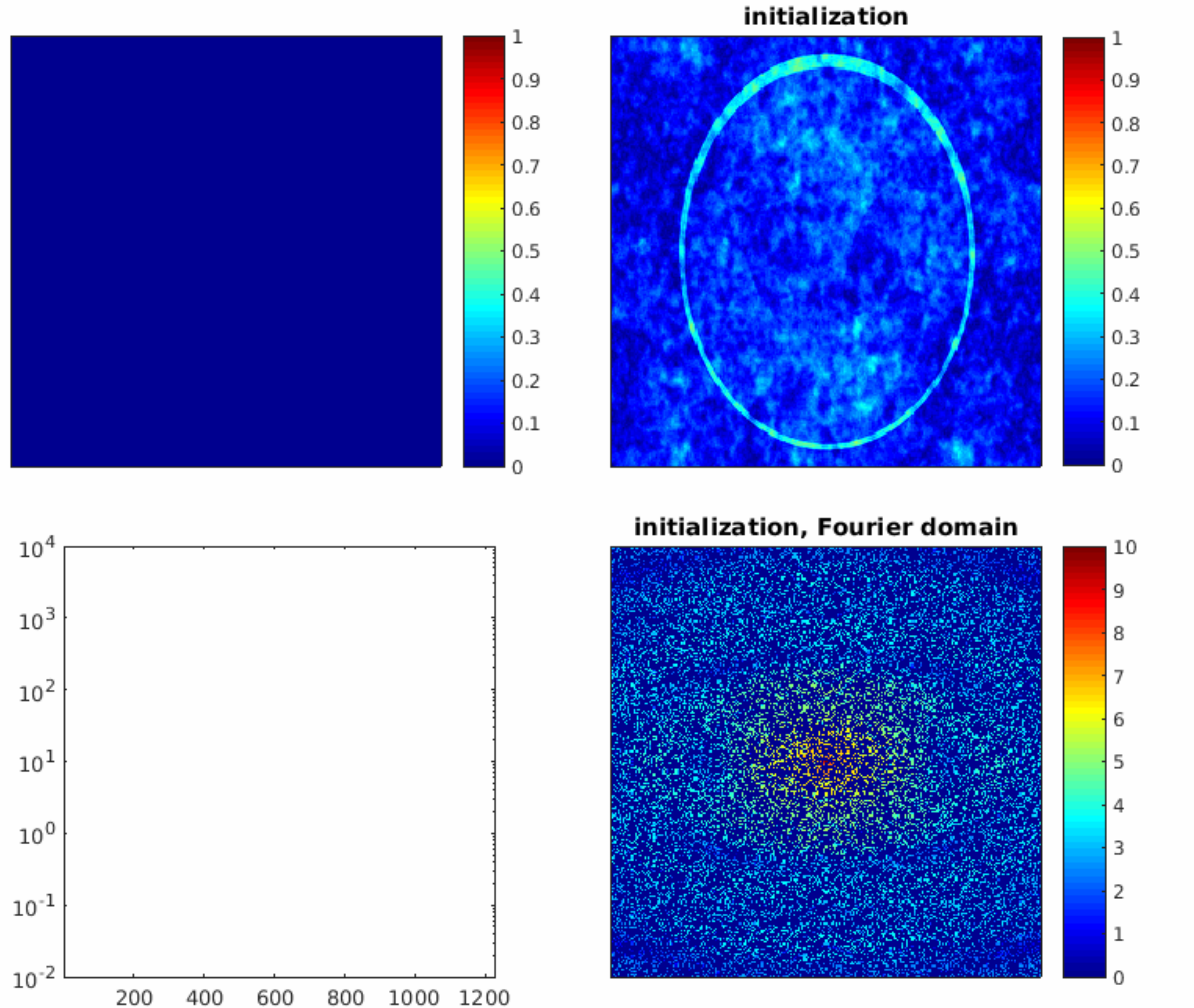
initialization
initialization, Fourier domain
0 0.1 0.2 0.3 0.4 0.5 0.6 0.7 0.8 0.9 1
0 1 2 3 4 5 6 7 8 9 10
10^{-2} 10^{-1} 10^{0} 10^{1} 10^{2} 10^{3} 10^{4}
200 400 600 800 1000 1200

Convergence speed of GIRAF

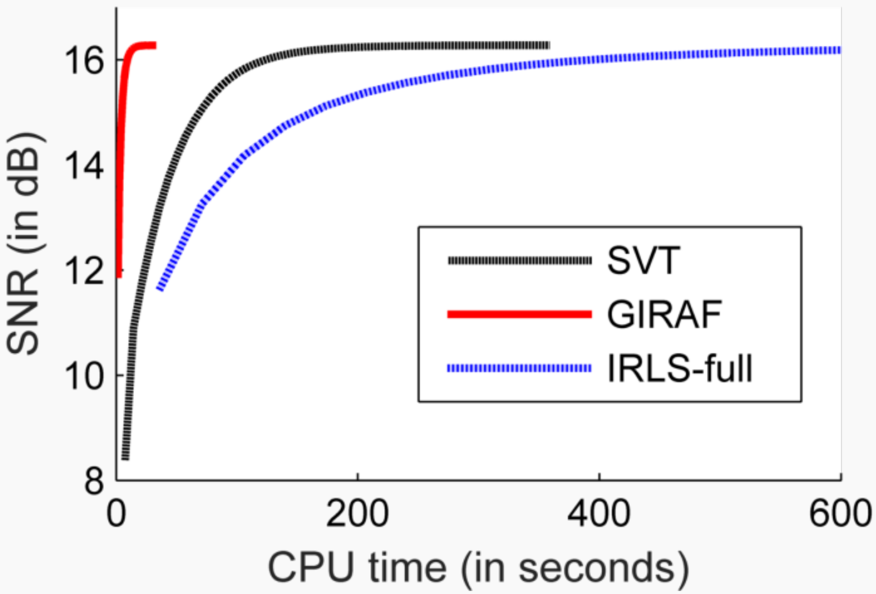

	15×15 filter		31×31 filter	
Algorithm	# iter	total	# iter	total
SVT	7	110s	11	790 s
GIRAF	6	20s	7	44 s

Table: iterations/CPU time to reach convergence tolerance of NMSE < 10^{-4}.

[Ongie & Jacob, ISBI16](https://arxiv.org/abs/1609.07429)
https://arxiv.org/abs/1609.07429
Software available at https://research.engineering.uiowa.edu/cbig/software

Convergence speed of GIRAF

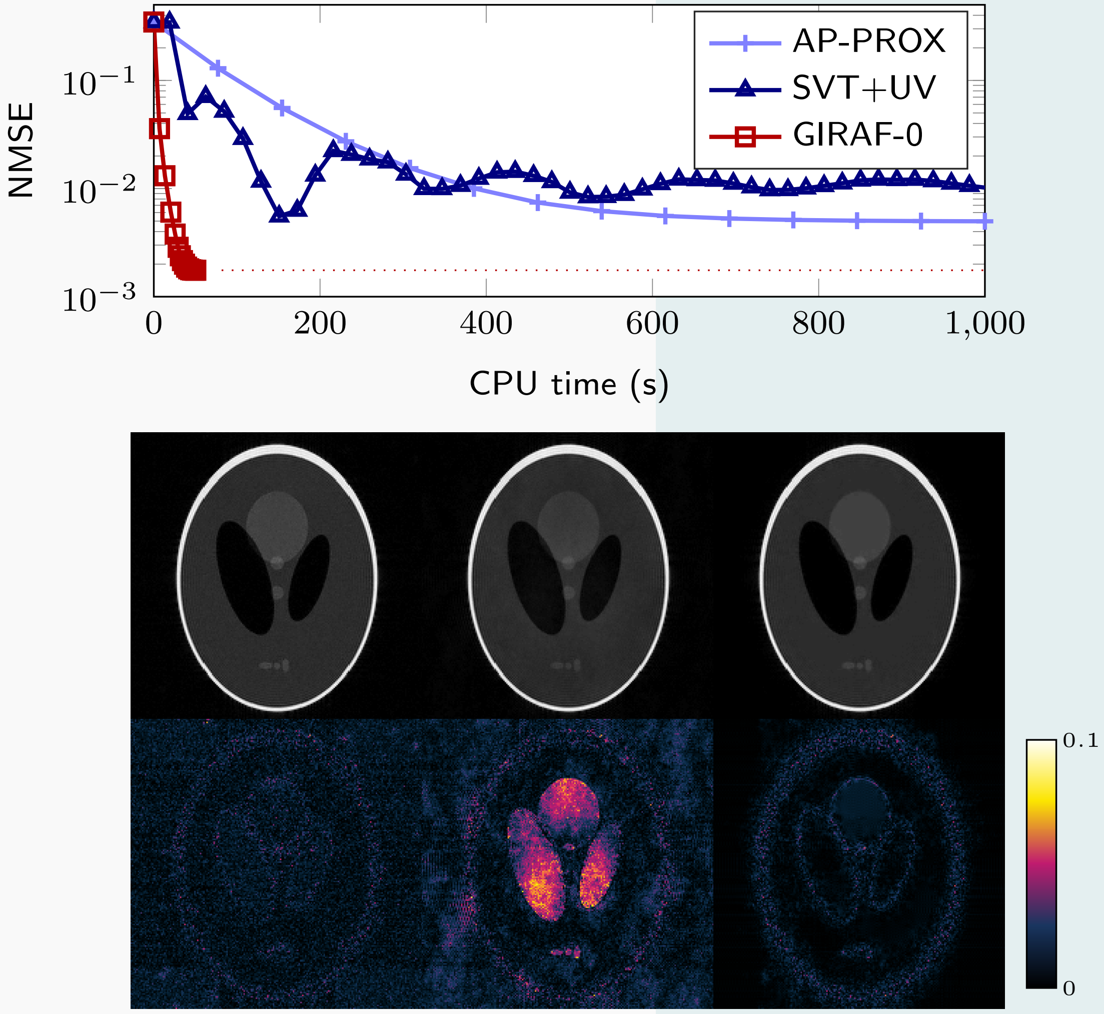

AP-PROX	SVT+UV	GIRAF-0
NMSE = $4.9e{-3}$	NMSE = $11.6e{-3}$	NMSE = $1.8e{-3}$
Runtime: 1000 s	Runtime: 1090 s	Runtime: 49 s

Overview

1. Introduction
2. Review of Compressive Sensing
3. FRI extrapolation from uniform samples
4. Structured low-rank interpolation for non-uniform samples
5. Fast implementations
6. Biomedical applications
   a. Applications to MRI
   b. Other applications

TV-domain sparse signal cases

y
(PE)

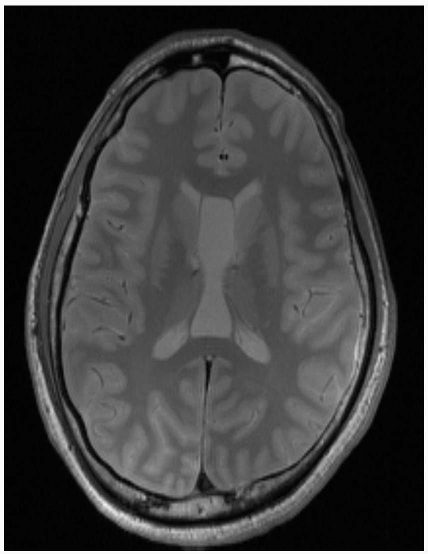

x (RO)

Sparse In
TV
domain

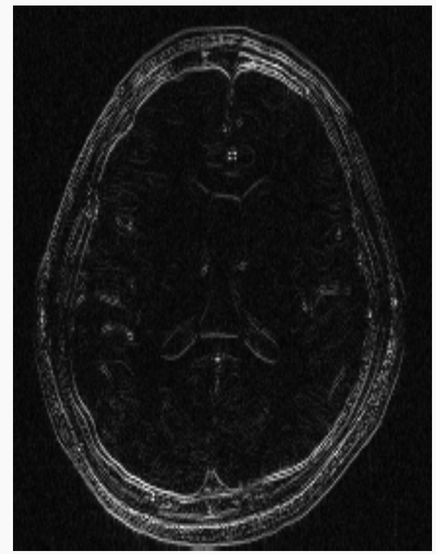

x (RO)

y
(PE)

TV-domain sparse signal cases

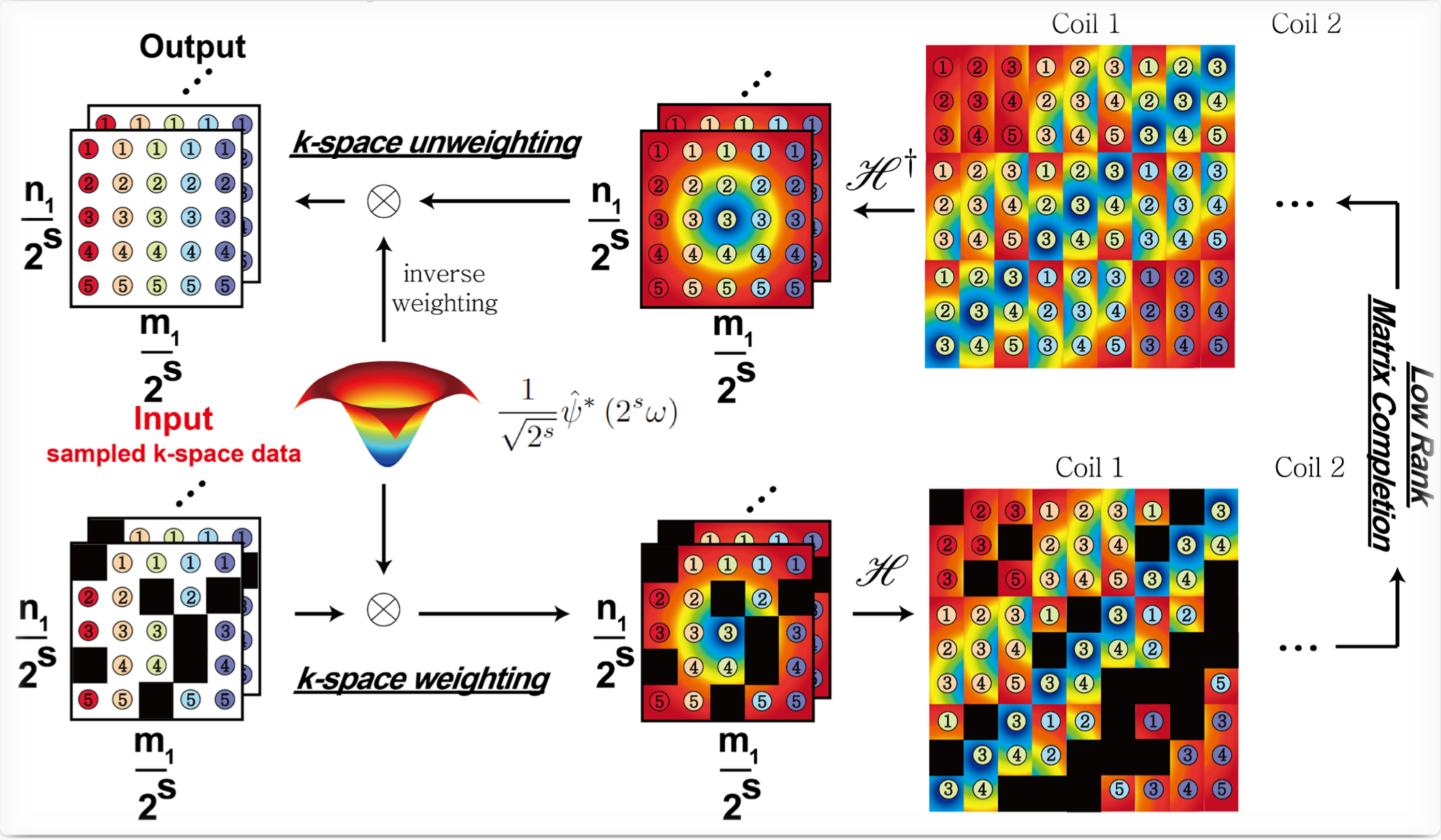

k-t dynamic sparse signal cases

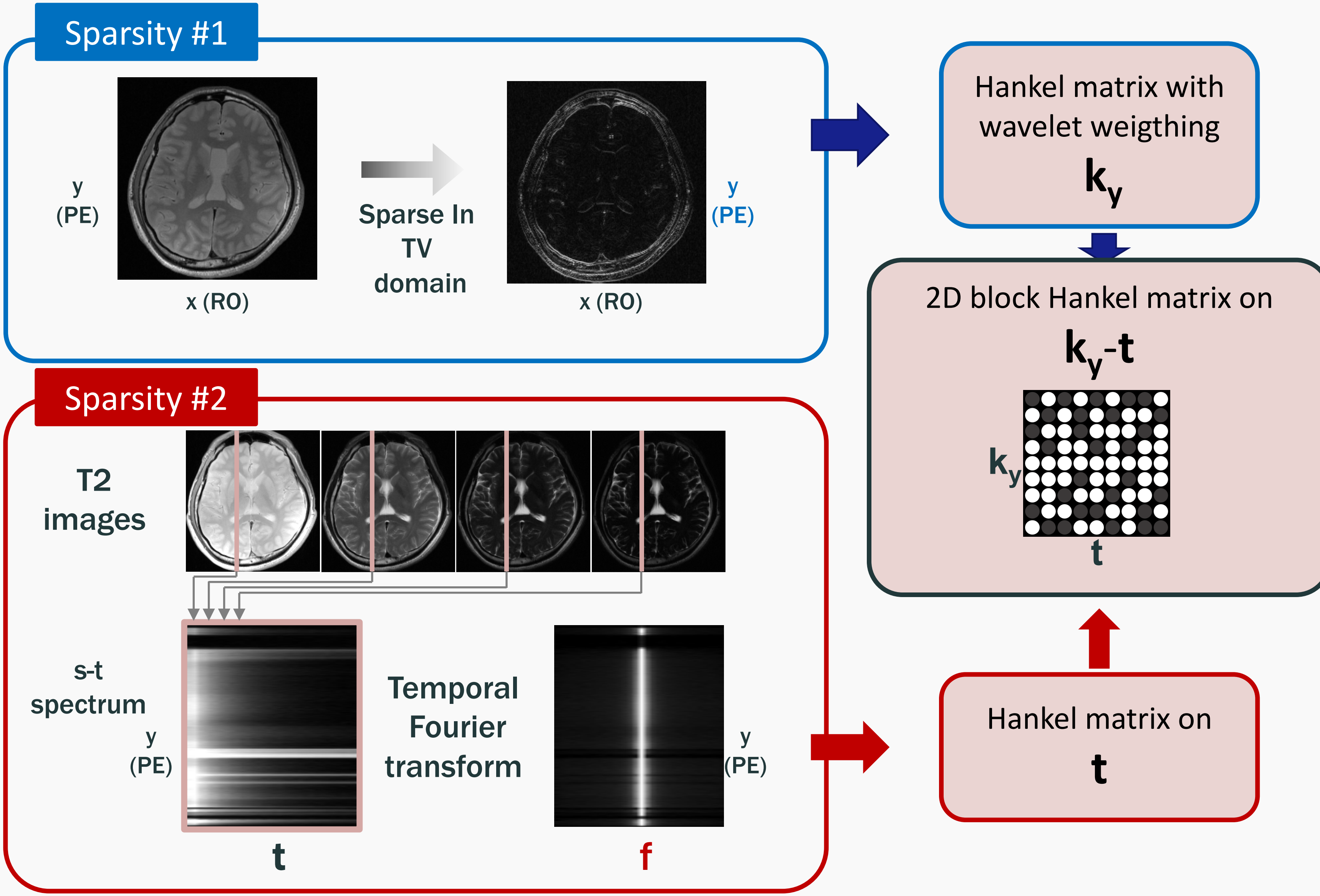

k-t dynamic sparse signal cases

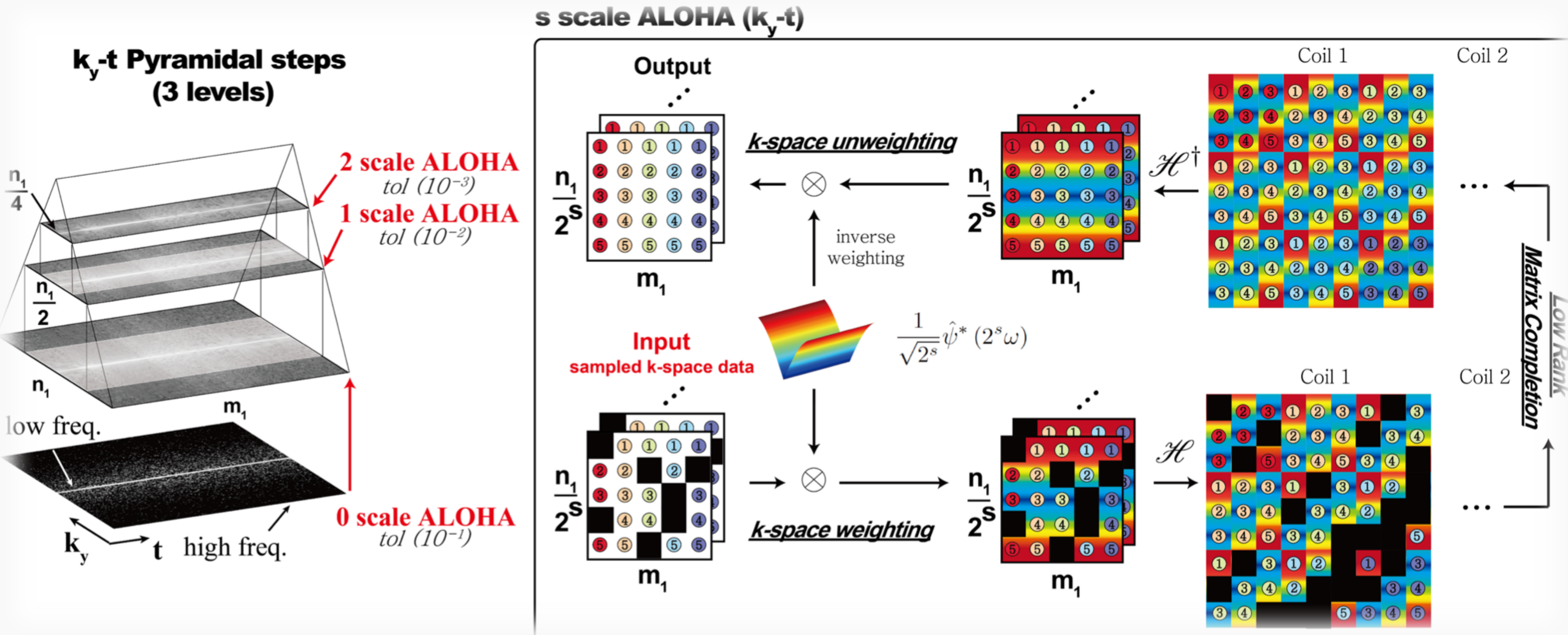

Single coil static MRI

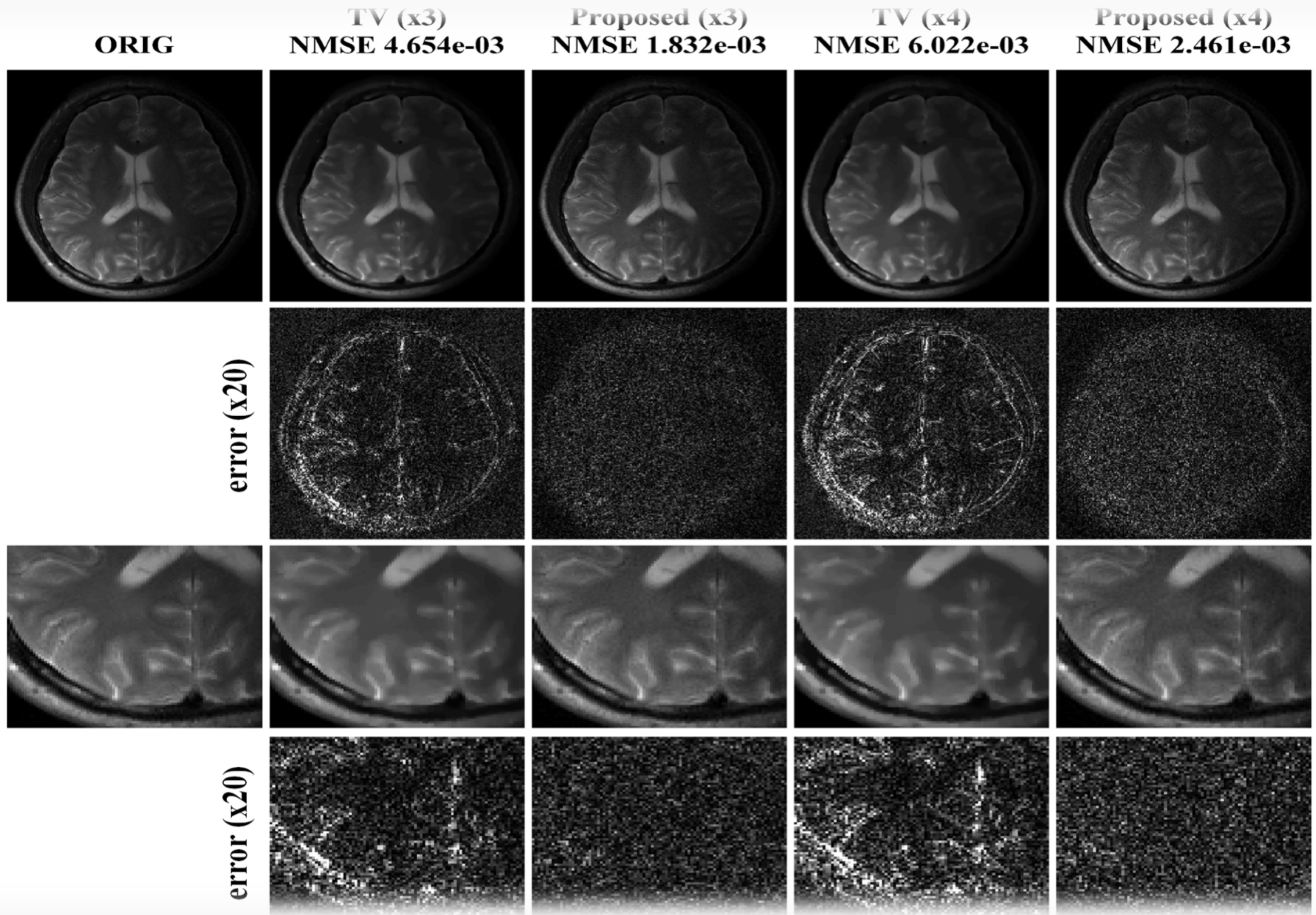

Rank Bound for Parallel Imaging

$$\mathcal{Y}_h = \begin{bmatrix} \mathscr{H}_c(\hat{\mathbf{l}} \odot \hat{\mathbf{g}}_1) & \cdots & \mathscr{H}_c(\hat{\mathbf{l}} \odot \hat{\mathbf{g}}_{N_c}) \end{bmatrix}$$

$$\textsc{rank}\,\mathcal{Y}_h \leq \textsc{rank}\,\mathscr{H}_c(\hat{\mathbf{w}}) + \textsc{rank}\,\mathscr{H}_c(\hat{\mathbf{f}}_{tr})$$

Sparsity of common image
In transform domain

Sparsity of sensitivity map
In Fourier domain

Jin et al, IEEE TCI, 2016

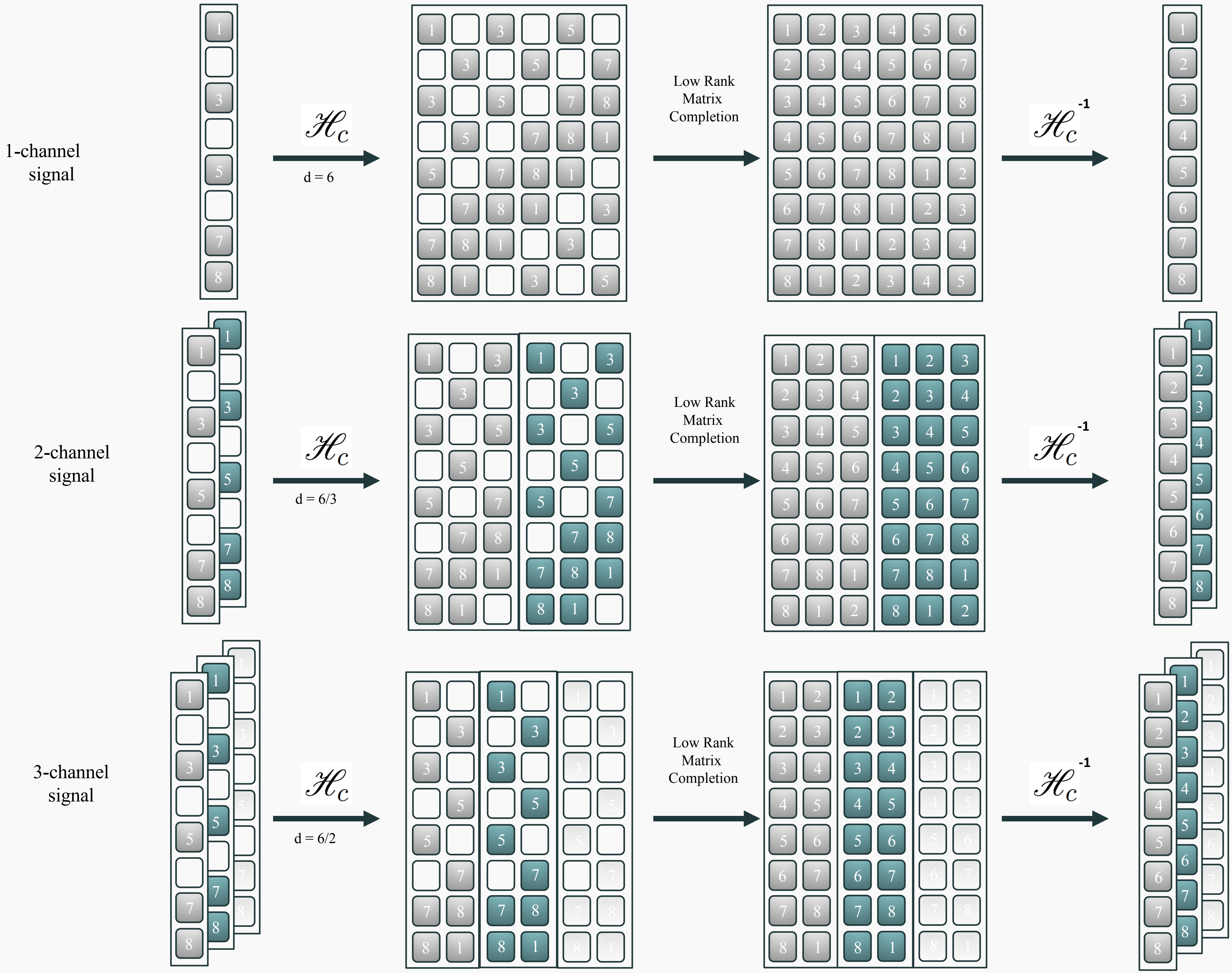
1-channel signal
d = 6
Low Rank Matrix Completion
2-channel signal
d = 6/3
Low Rank Matrix Completion
3-channel signal
d = 6/2
Low Rank Matrix Completion

Parallel MRI

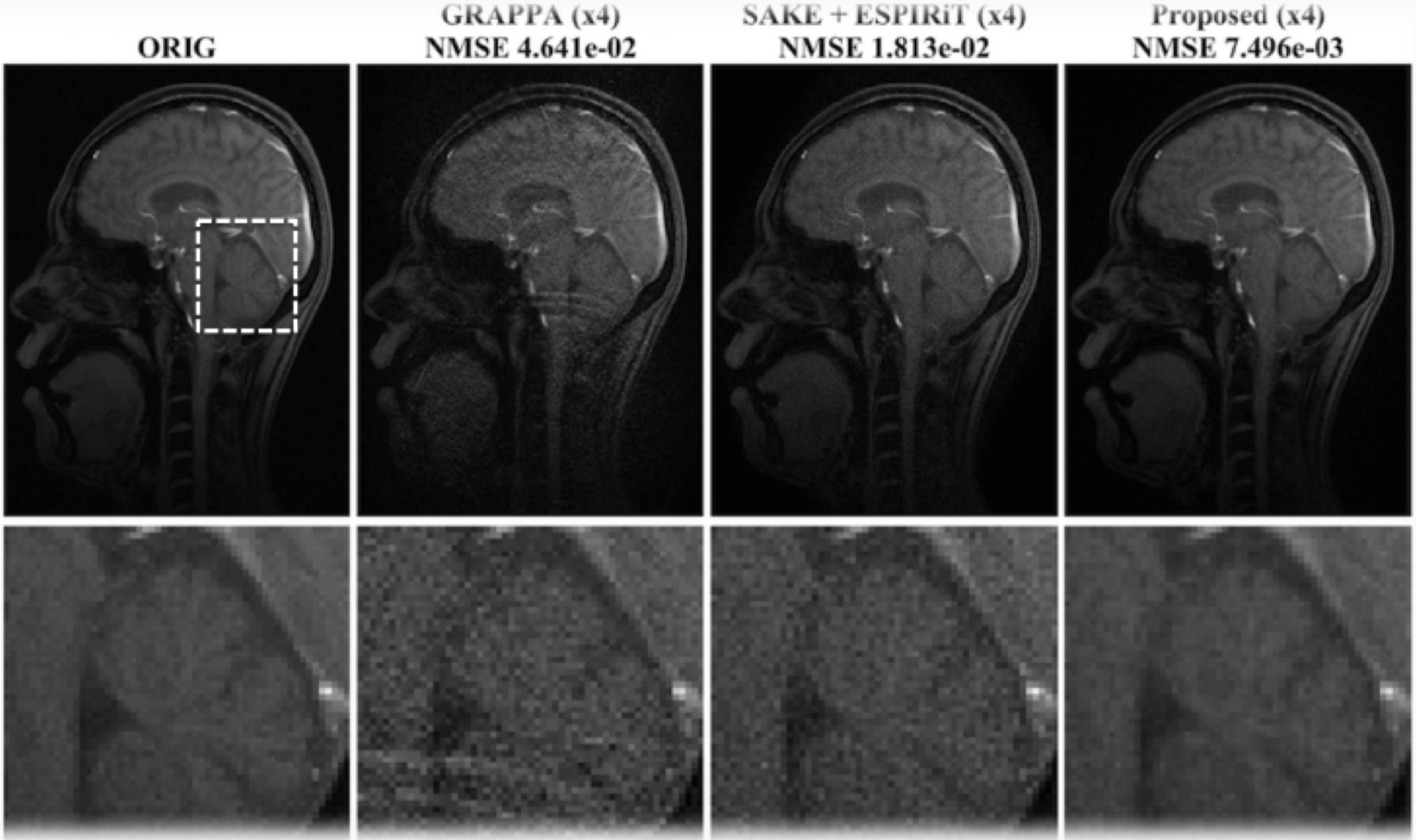

Dynamic MRI – multi coil

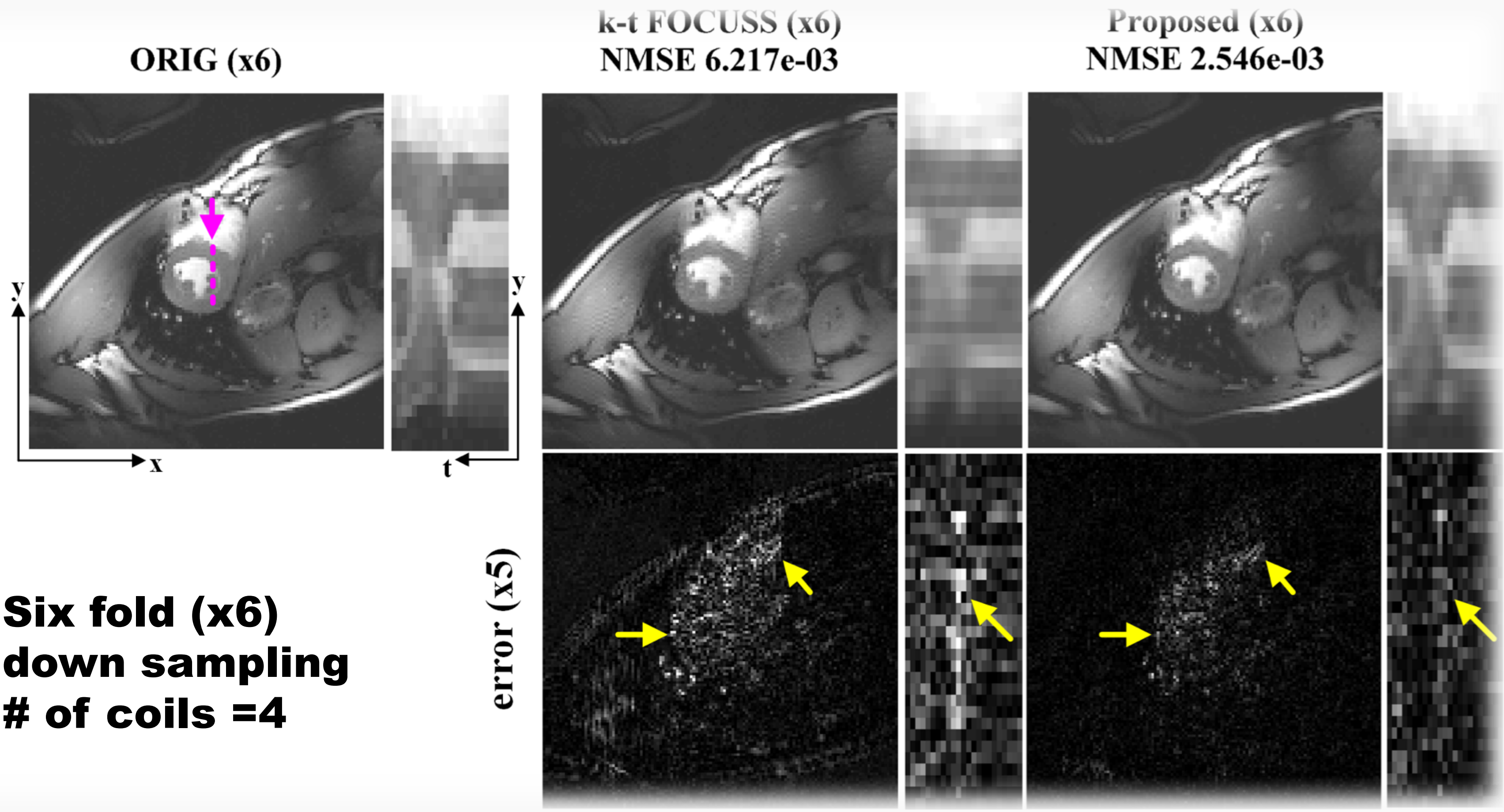

Six fold (x6)
down sampling
# of coils =4

MR Parameter Mapping

What is MR parameter mapping?

$$SI = SI_0 e^{-t/T_2}$$

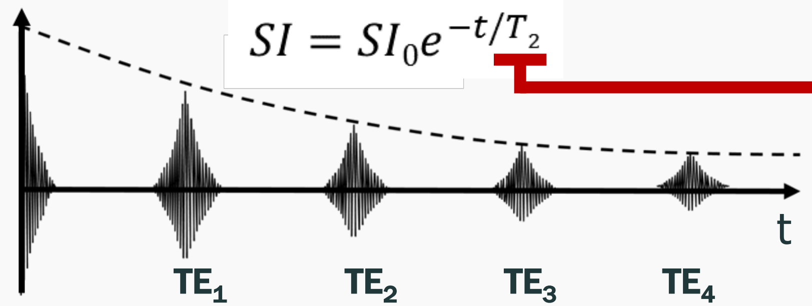

Finding the **quantitative** value of each tissue

e.g. Multi-Echo Spin-Echo (ME-SE, T2 mapping)

Pros | Cons

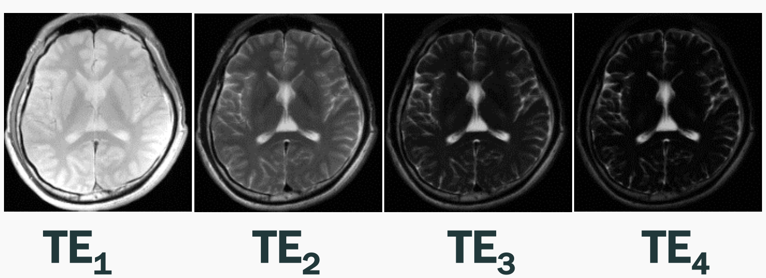

e.g. Multi-echo images for T2 mapping

Long scan time

- Needs multiple scans
- Variation of TI, TE, FA, etc.

[1] Siemonsen, S et al., Radiology, 2008 [2] Rugg-Gunn, F. J., et al. *NEUROLOGY*, 2005

Result : in vivo acceleration study (ME-SE, T2)

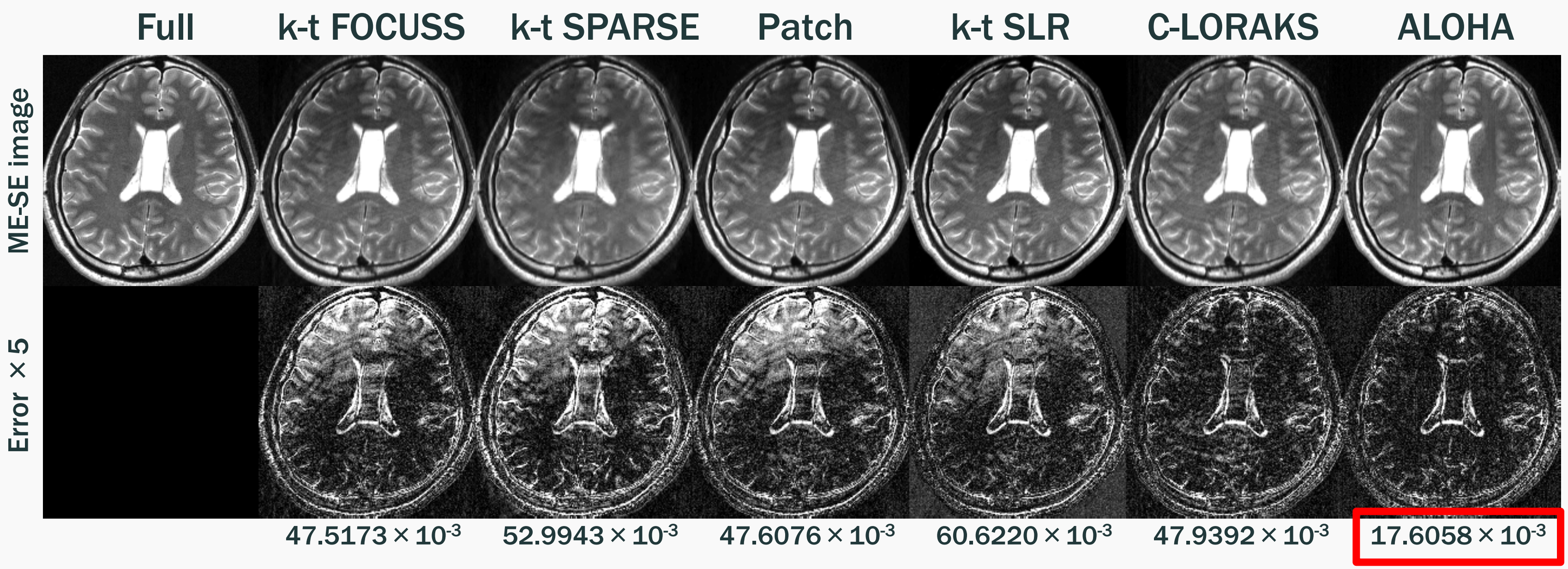

Reconstruction of x12.8 accelerated scan – ME-SE (4th echo)

Lee et al, MRM, 2015

Result : in vivo acceleration study (ME-SE, T2)

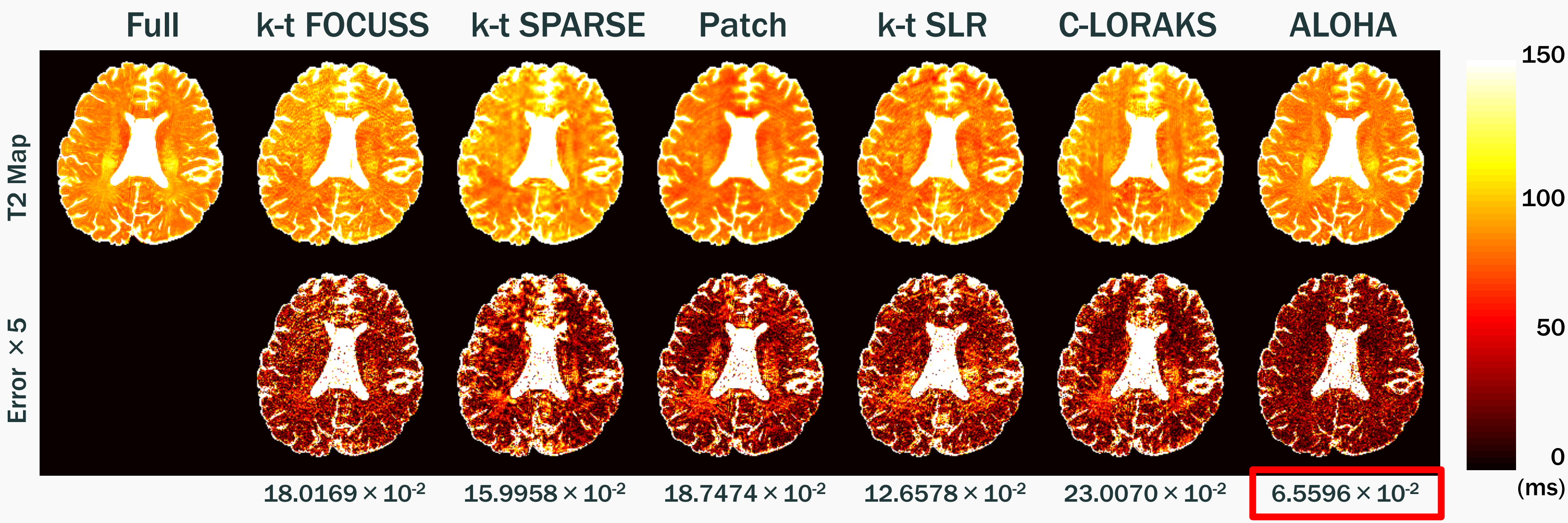

Mapping from the reconstruction of x12.8 accelerated scan – T2 mapping

Lee et al, MRM, 2015

Result : Signal intensity curves (SE-IR, T1)

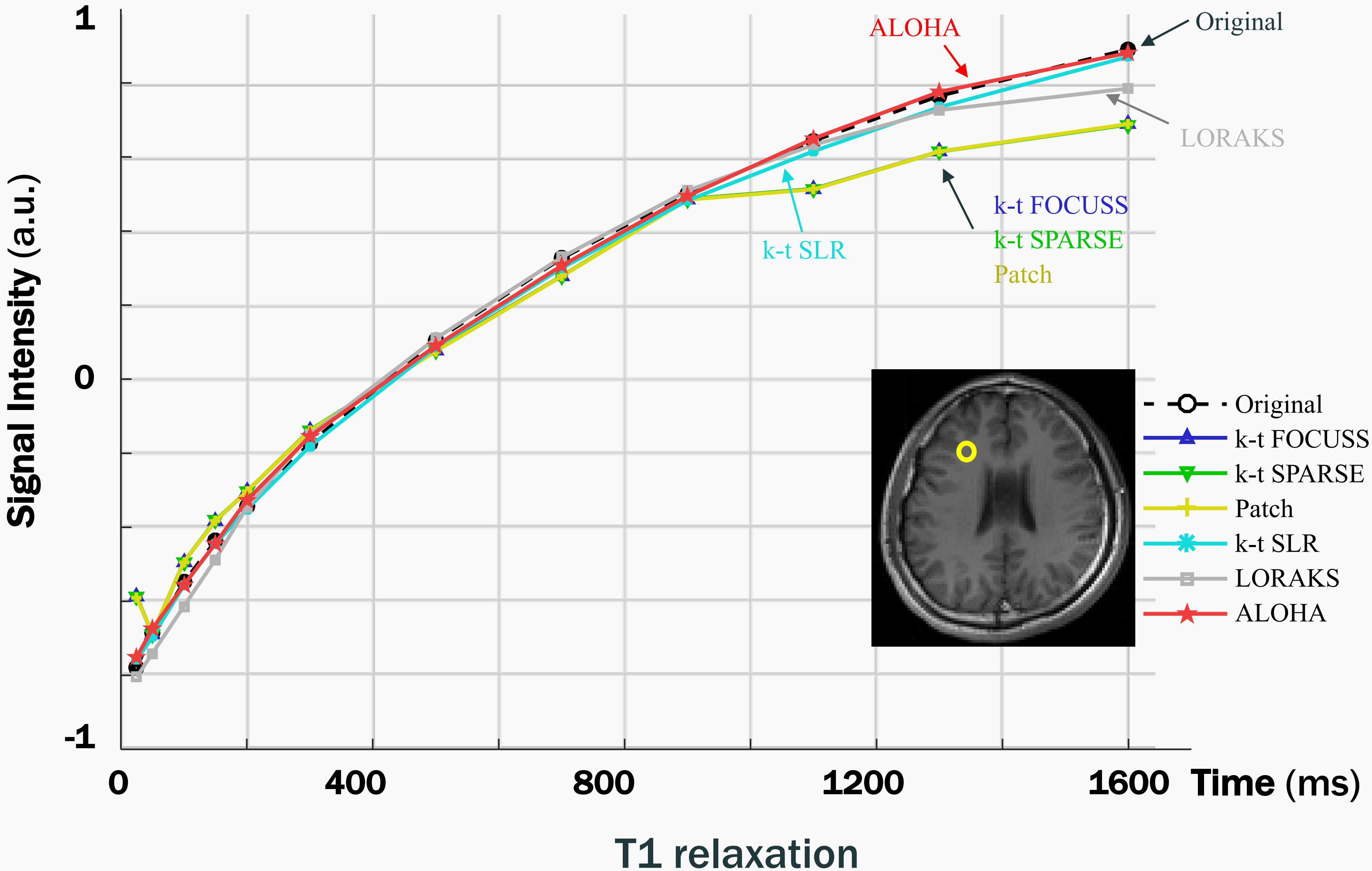

Lee et al, MRM, 2015

Summary of Results

- **Goal : Acceleration of MR Parameter mapping by undersampling and reconstruction**

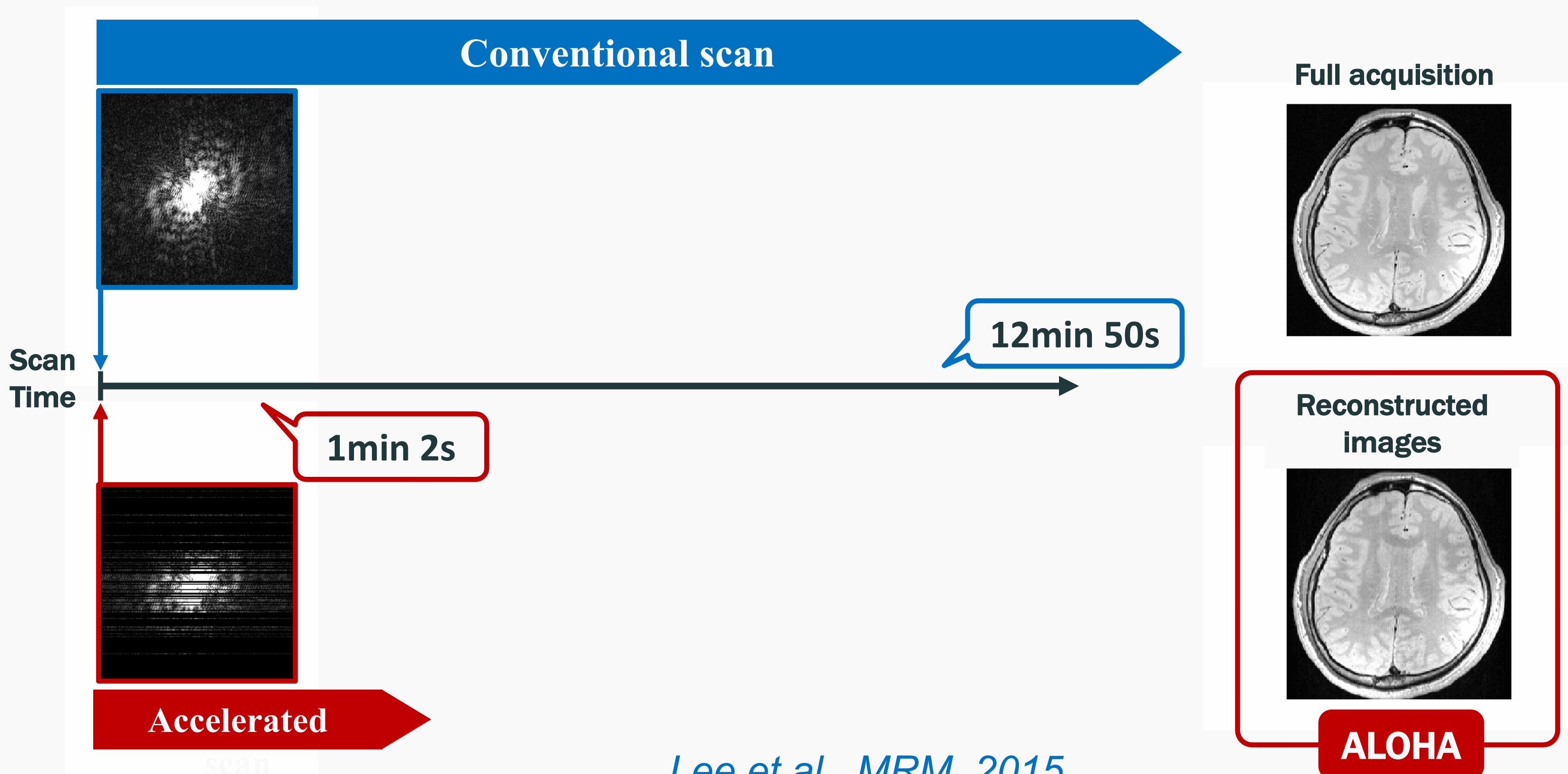

Lee et al, MRM, 2015

Extension to 3-D applications using GIRAF

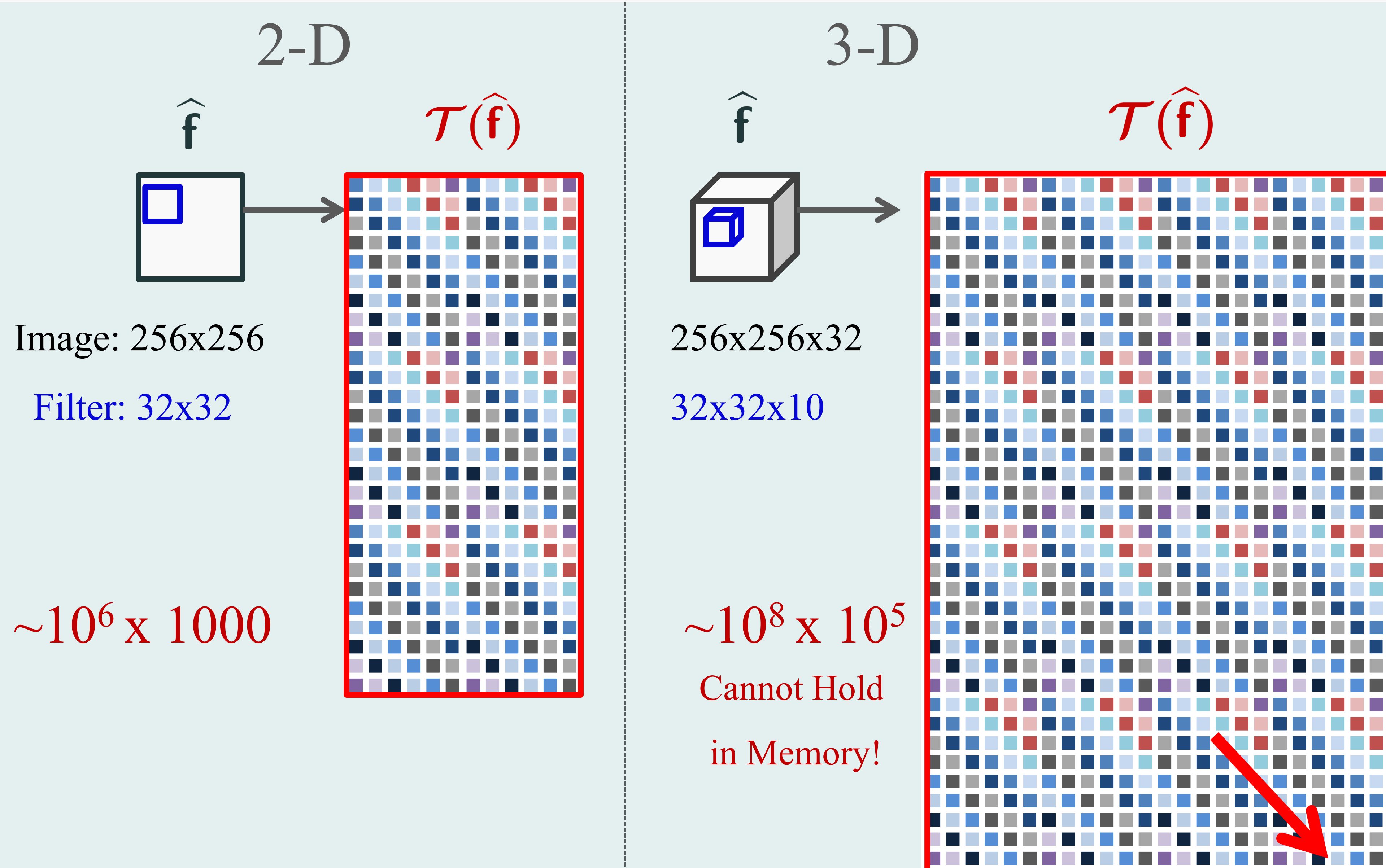

3D applications: dynamic MRI

Lifting in 3D

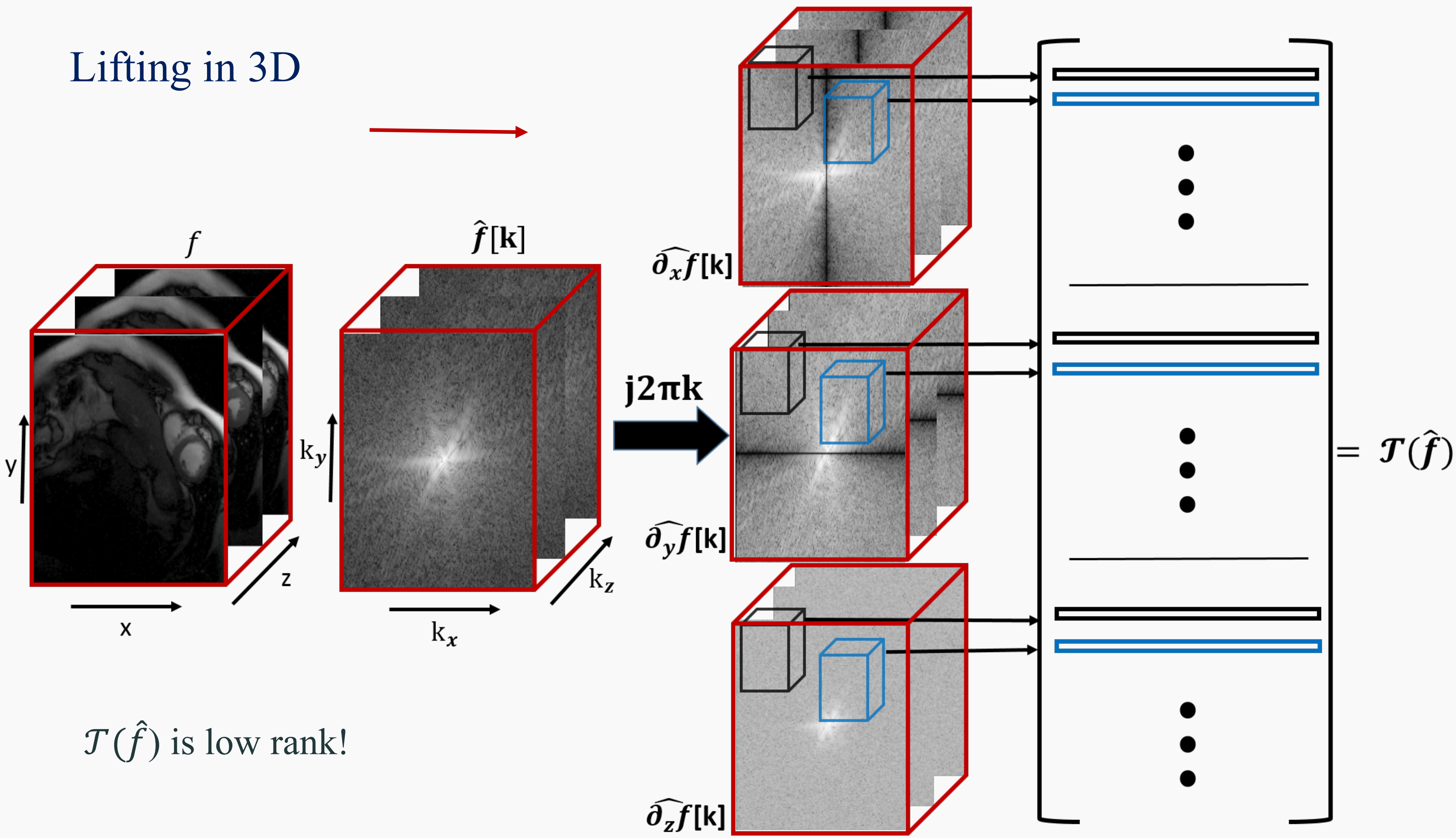

$\mathcal{T}(\hat{f})$ is low rank!

Fast 3-D implementation using GIRAF

Weight Update:

Gram matrix: 2 FFTs and no matrix product.

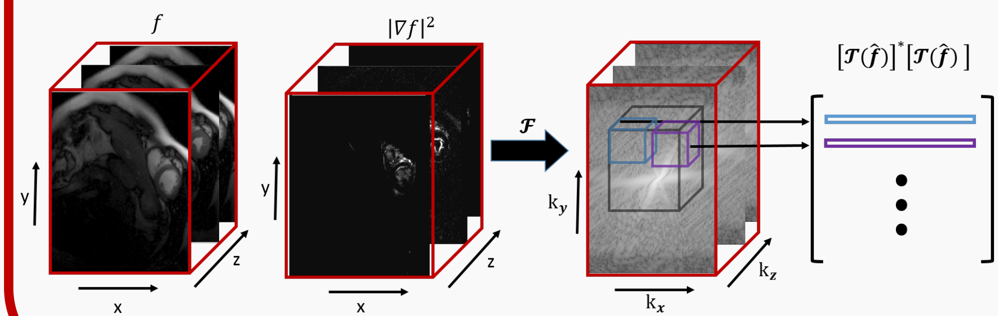

Square root - one small eigen decomposition

Fourier data update:

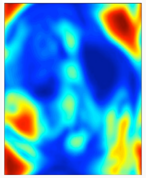

1 frame of $\boldsymbol{\mu}_{\mathbf{sos}}$

$$\|\mathcal{T}(\mathcal{Q}\mathcal{F}_t\hat{\mathbf{f}})\mathbf{W}^{\frac{1}{2}}\|_F^2 \rightarrow \text{ simplifies to } \|\mathcal{Q}(\mathcal{F}_t\hat{\mathbf{f}}) \star \hat{\mu}_{sos}\|_F^2$$

Where, $\boldsymbol{\mu}_{\mathbf{sos}} = \sqrt{\sum_{\mathbf{i=1}}^{\mathbf{N}} |\boldsymbol{\mathcal{F}}^{-1}(\mathbf{w_i})|^2}$

Need few iterations of CG to solve.

Cardiac CINE MRI

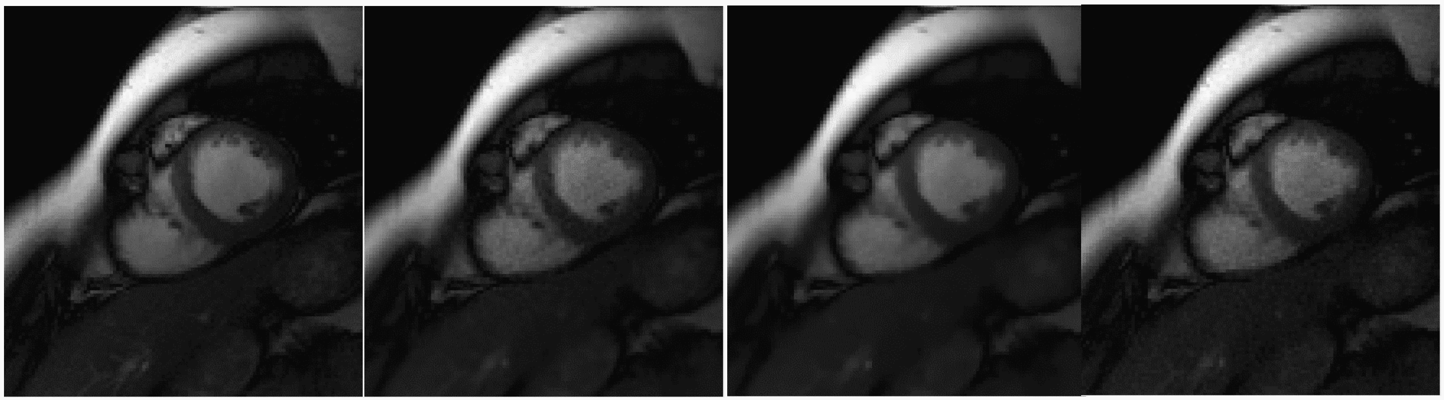

Truth

Proposed
SNR – 23.32
HFEN– 0.109

TV
SNR – 23.27
HFEN– 0.121

Fourier Sparsity
SNR – 21.52
HFEN– 0.15

Golden angle (14lines)

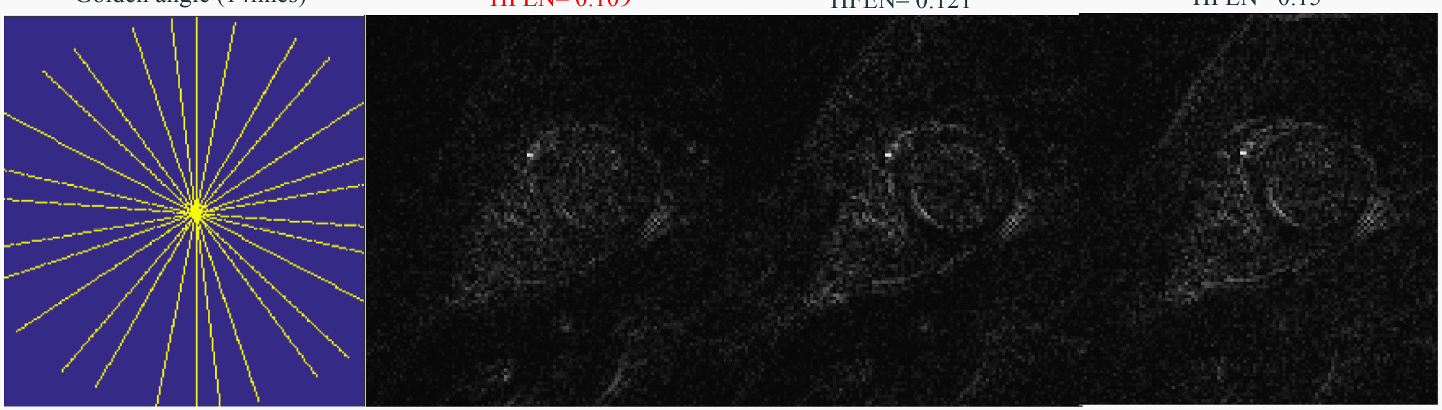

Balachandrasekaran & Jacob, ICIP 16

Exponential signal model

Linear combination of exponentials

$$\rho[\mathbf{r}, \mathbf{n}] = \sum_{\mathbf{i}=1}^{\mathbf{L}} \alpha_{\mathbf{i}}(\mathbf{r})\ \beta_{\mathbf{i}}(\mathbf{r})^{\mathbf{n}}$$

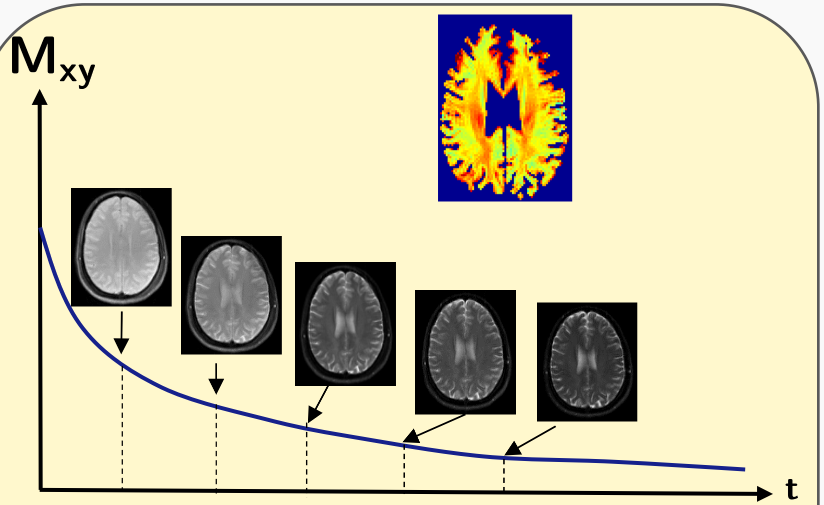

Parameter mapping

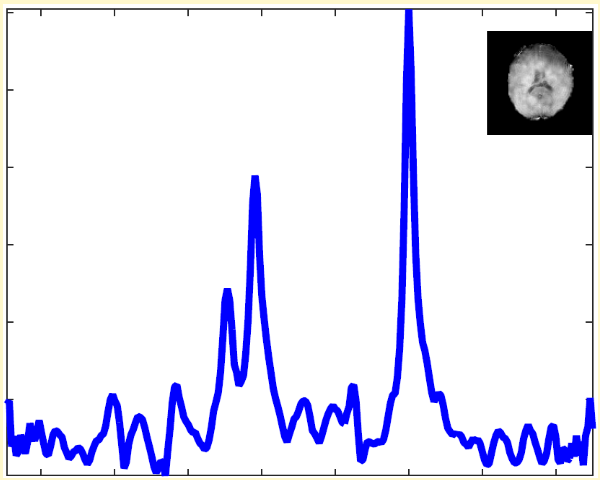

MR spectroscopic imaging

Acceleration the acquisition of exponentials

$$\rho[\mathbf{r}, \mathbf{n}] = \sum_{i=1}^{L} \alpha_i(\mathbf{r})\ \beta_i(\mathbf{r})^n$$

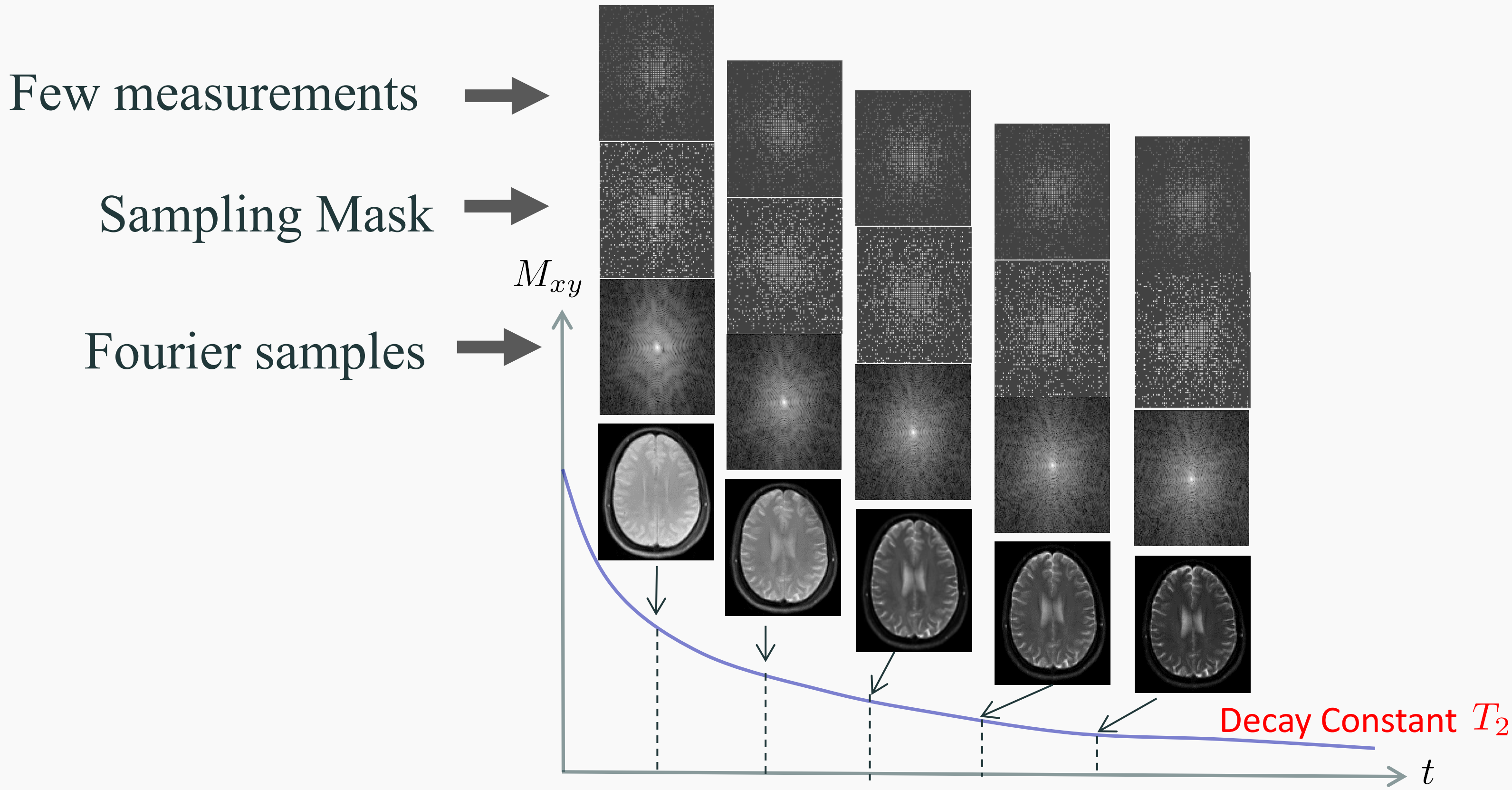

MR parameter mapping

State of the art

Exploit correlations between voxel profiles

- Low rank methods [Doneva et al,..]
- Dictionary learning methods [BCS;Bhave et al]

Exploit correlations within an exponential voxel profile

- Pixel by pixel structured low-rank [MORASSA: Peng et al,2016]

Structured low-rank with wavelet models

- Exploit sparsity of kx-t planes in wavelet domain [ALOHA]

Unify above strategies !!

1-D signal satisfies an annihilation relation

$$\mathbf{y[n]} = \sum_{\mathbf{m=0}}^{\mathbf{L}} \rho[\mathbf{n-m}]\mathbf{h[m]} = \mathbf{0}$$

$\rho[n] = \alpha^n$

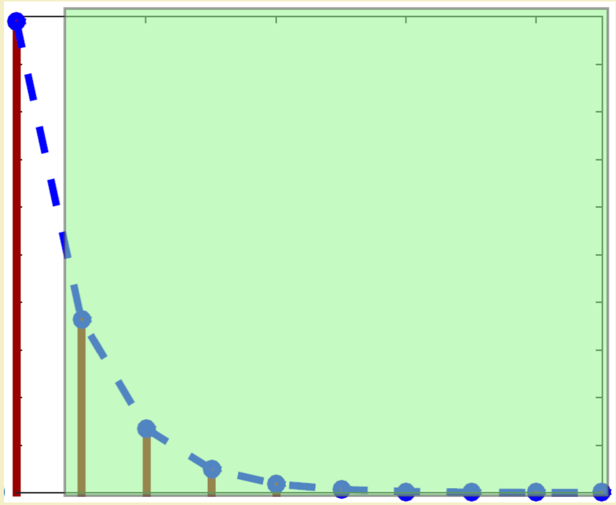

Possible shifts of filter

$* \; h[n] = [1, -\alpha^{-1}] \quad =$

$y[n] = 0$

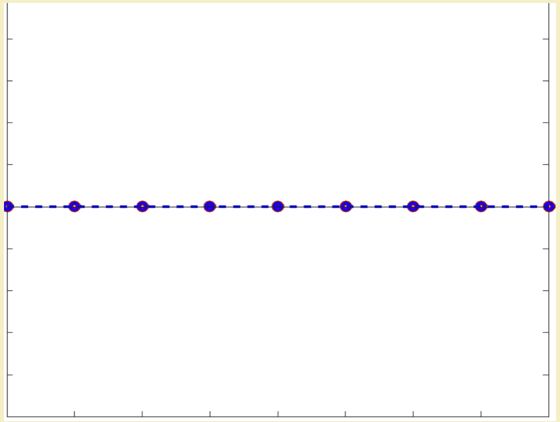

Exponential parameters are spatially smooth

Filter coefficients are spatially smooth

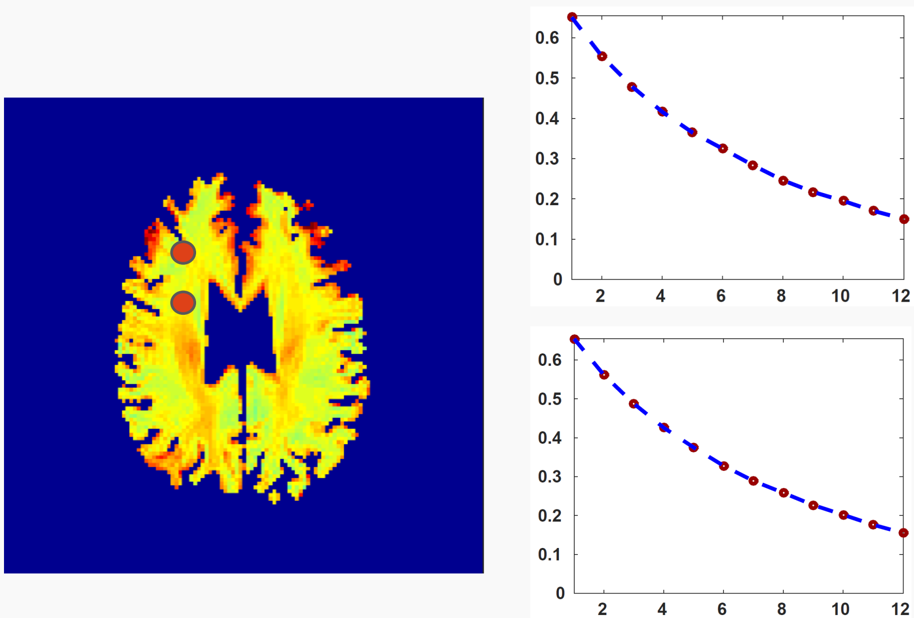

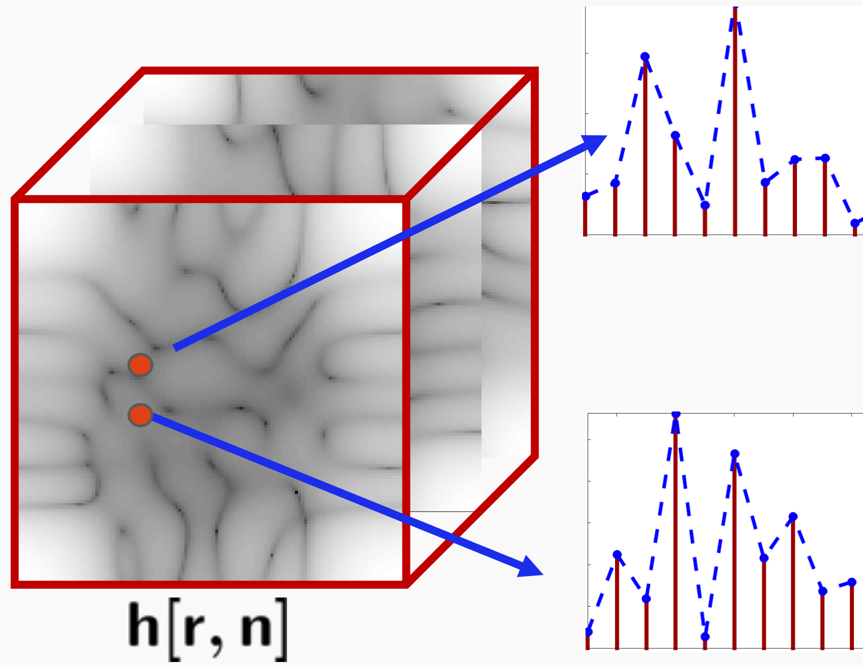

Spatially smooth filters: FIR in Fourier domain

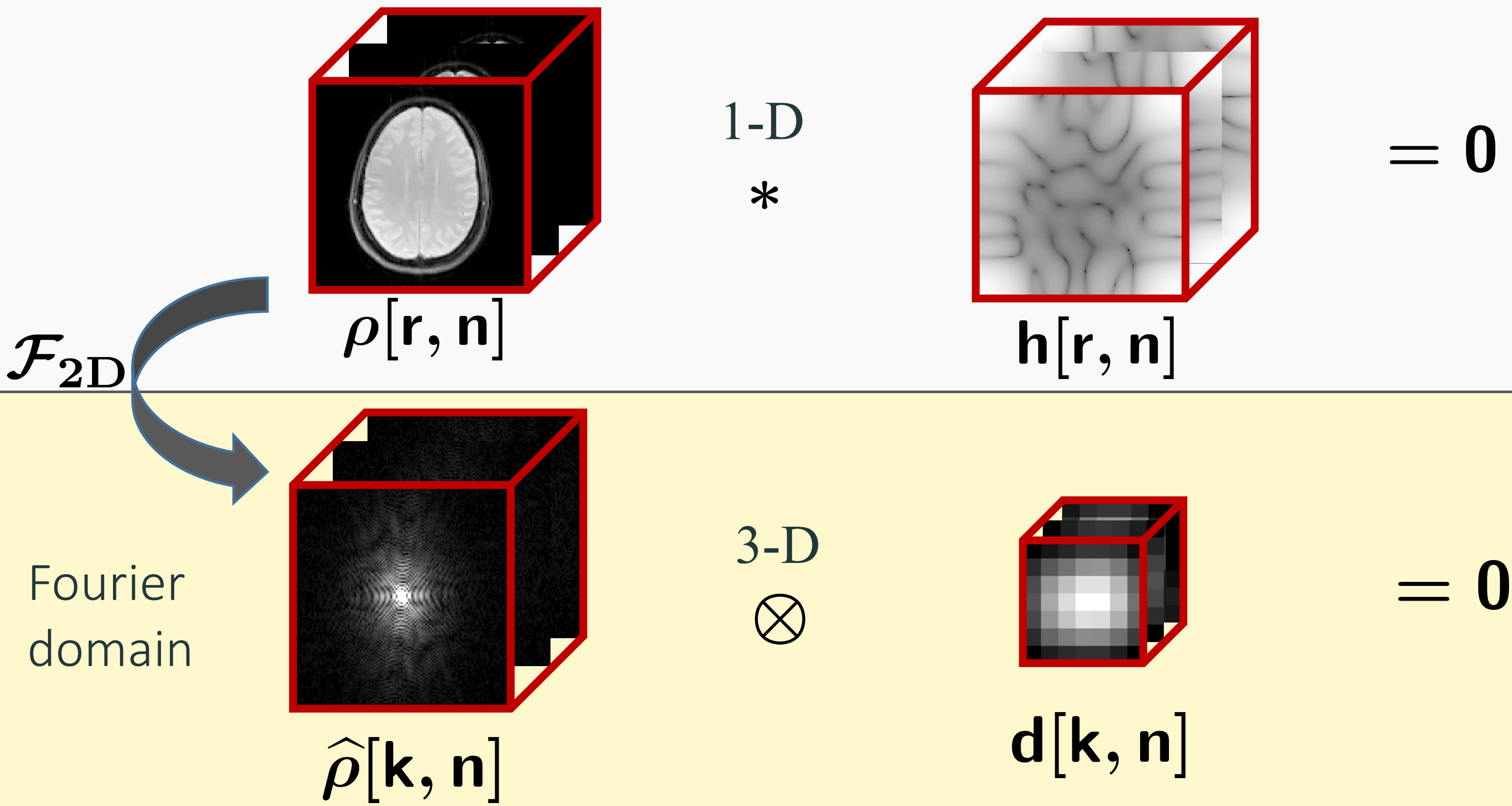

Annihilation relation: $\widehat{\rho}[\mathbf{k}, \mathbf{n}] \otimes \mathbf{d}[\mathbf{k}, \mathbf{n}] = \mathbf{0}$

Bandwidth of filter & spatial smoothness

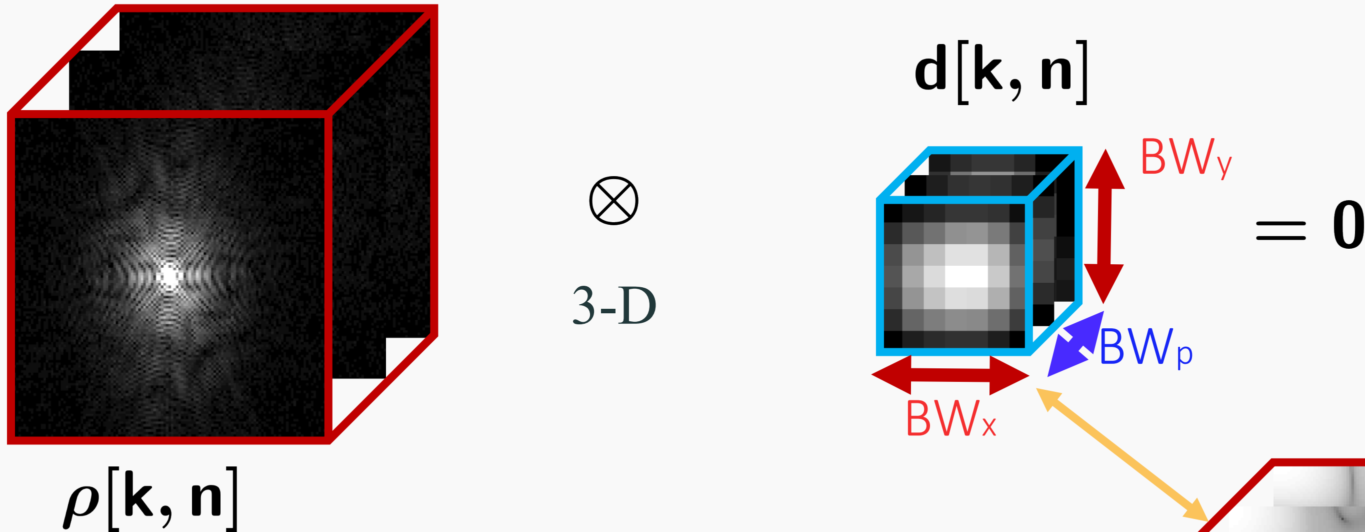

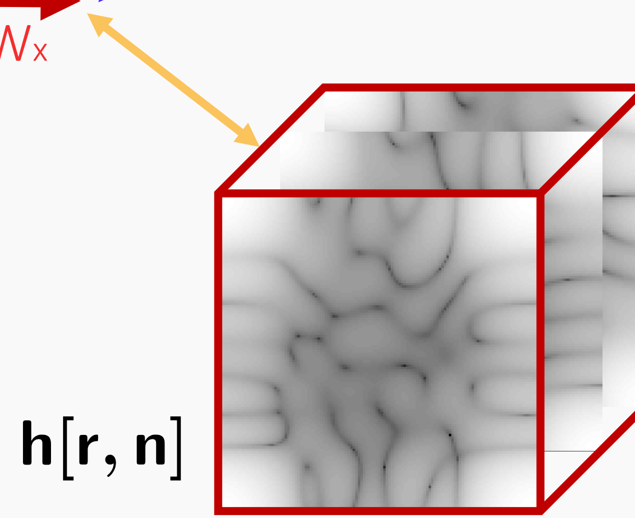

BW_x & BW_y: spatial smoothness of parameters.

BW_p: number of exponentials.

Annihilation as a matrix-vector product

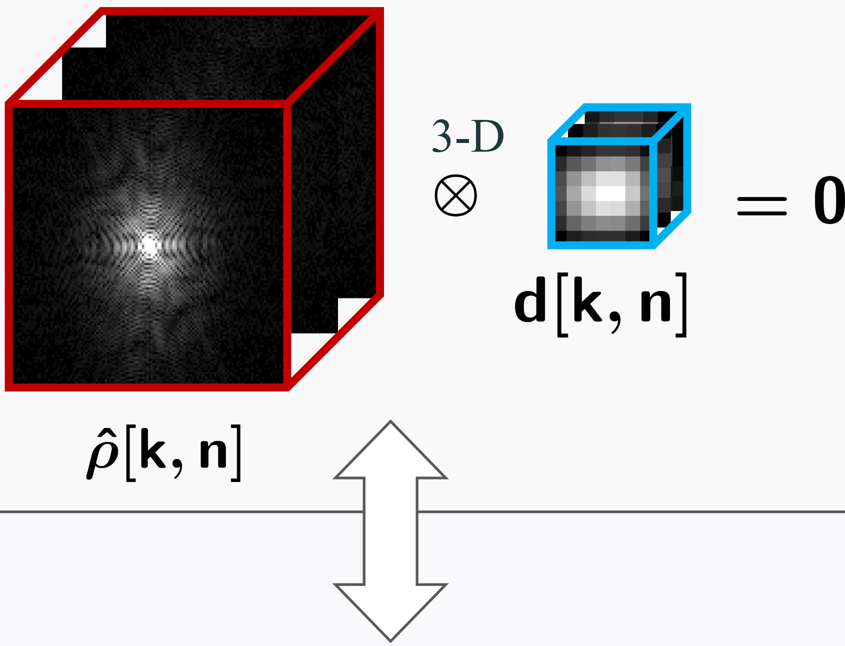

$$\mathcal{T}(\hat{\rho})\,\mathbf{d} = \mathbf{0}$$

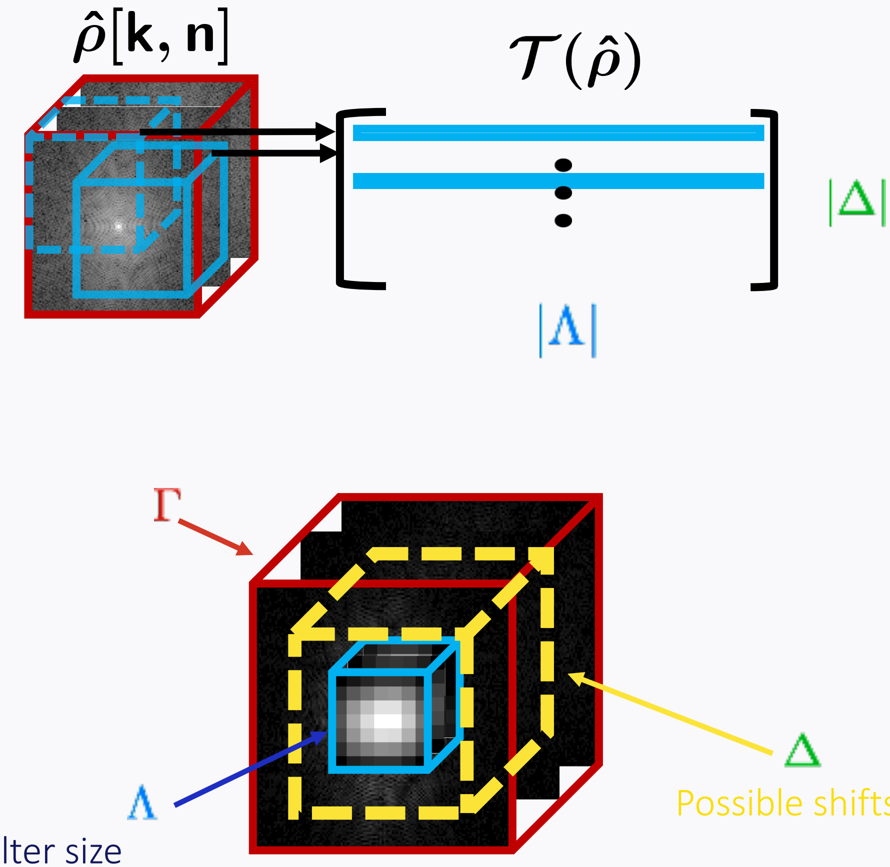

Minimal filter & assumed filter size

Minimal filter: exact size is unknown

Assumed filter: larger than minimal filter

⇨ Several possible annihilating filters

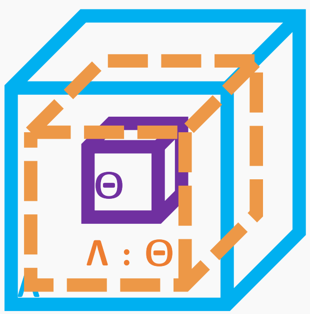

$$\underbrace{d[k,n]}_{\text{Assumed filter}} = \underbrace{c[k,n]}_{\text{Minimal filter}} \otimes \underbrace{e[k,n]}_{\text{FIR filter}}$$

Dimension of annihilating subspace $\geq \quad |\Lambda : \Theta|$

Rank of the matrix

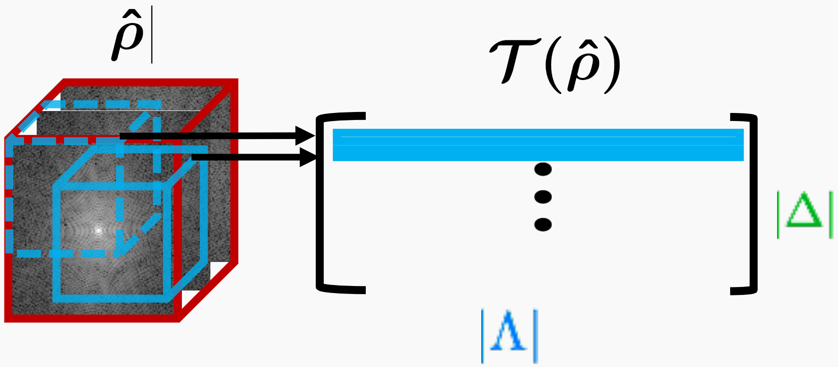

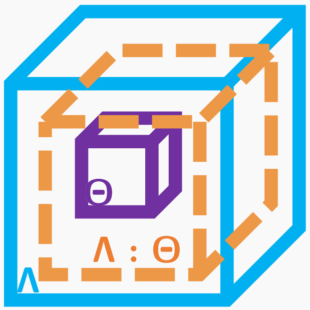

Dimension of annihilating subspace $\geq \quad |\Lambda : \Theta|$

$$\Rightarrow \quad \text{Rank}(\mathcal{T}(\hat{\rho})) \leq |\Lambda| - |\Lambda : \Theta|$$

Structured low-rank optimization problem

Find the signal that satisfies data consistency & minimizes rank

$$\hat{\rho}^{\star} = \arg\min_{\hat{\rho}} \|\mathcal{T}(\hat{\rho})\|_{\mathbf{p}} + \frac{\mu}{2}\|\mathcal{A}(\hat{\rho}) - \mathbf{b}\|_2^2$$

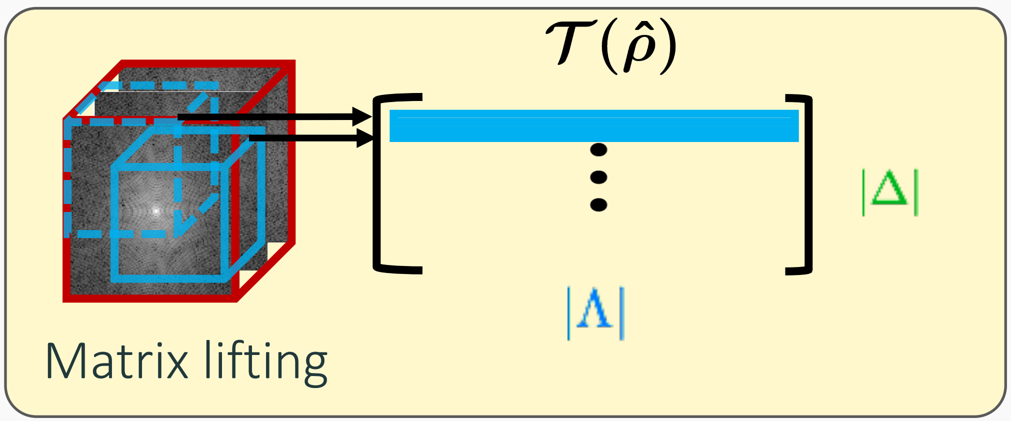

Special case: no spatial smoothness

Spatial dimension of filter is the same as Γ

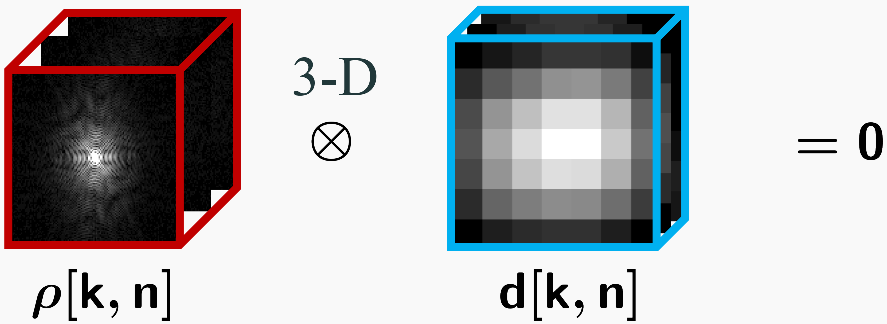

Lifting: concatenation of pixel-by pixel Toeplitz matrices

$$\mathcal{T}(\rho) = [\mathcal{T}(\rho_1)| \ldots |\mathcal{T}(\rho_N)]$$

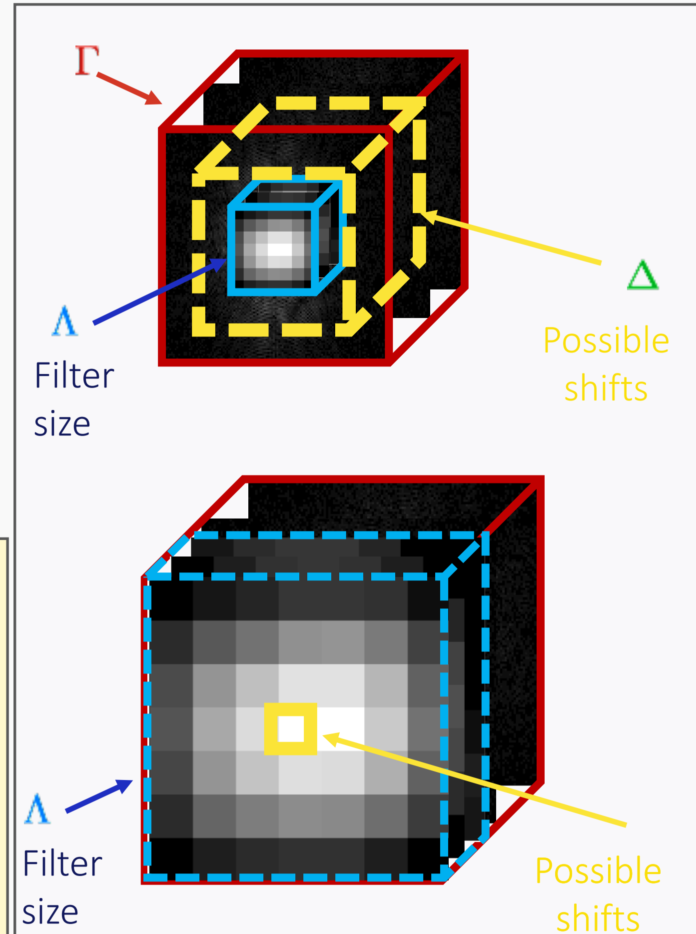

Relation to other structured low-rank priors

Pixel independent structured low-rank prior [MORASSA,Peng et al.,2016]

$$\{\rho_{\mathsf{m}}\} = \arg\min_{\{\rho_{\mathsf{m}}\}} \sum_{\mathsf{m}} \|\mathcal{T}(\rho_{\mathsf{m}})\|_* + \|\mathcal{A}(\boldsymbol{\rho}) - \mathsf{b}\|^2$$

Does not exploit spatial correlations

Proposed special case: nuclear norm of concatenated matrices

$$\mathcal{T}(\rho) = [\mathcal{T}(\rho_1)|\ldots|\mathcal{T}(\rho_N)]$$

Combination of low-rank & exponential priors: exploit spatial correlations

Only one small EVD per iteration: considerably faster

ALOHA based solution discussed earlier ..

2-D prior: fills in kx-t planes using structured low-rank interpolation

Signal sparse in wavelet domain

Does not exploit exponential decay of signal

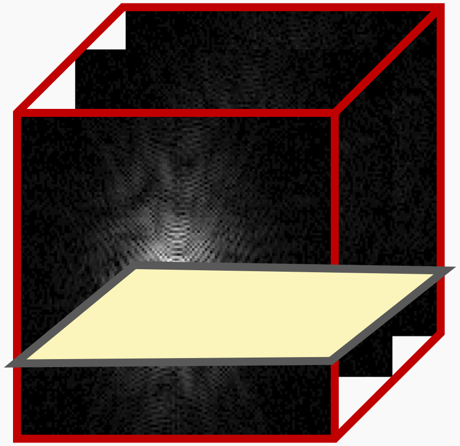

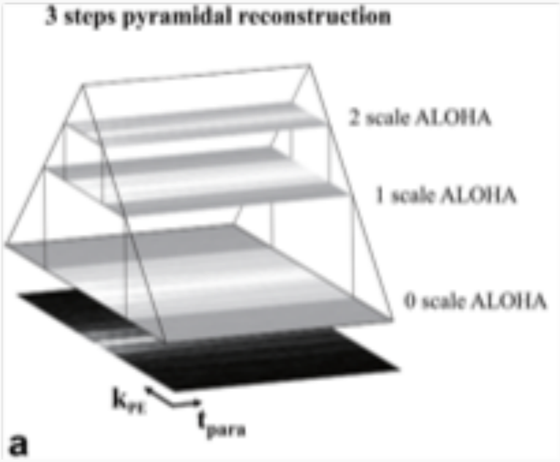

Use signal weighting: ALOHA-like prior

GIRAF: Circulant approximation is not accurate

Approximation is good if signal amplitude is negligible at boundaries

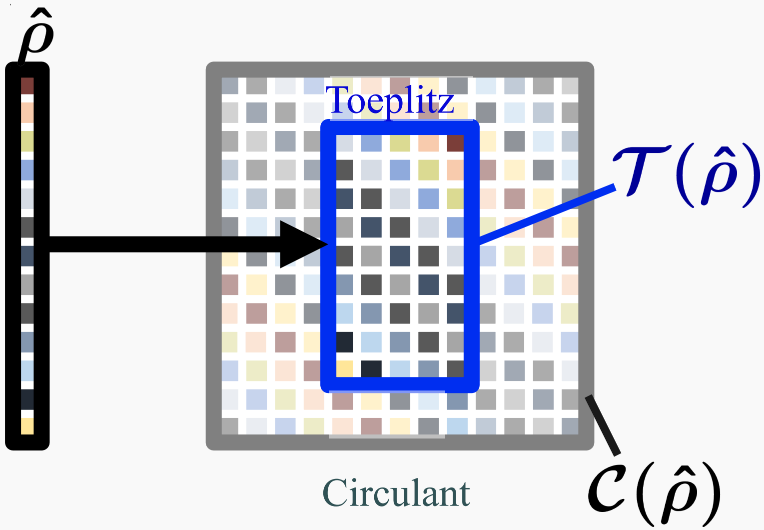

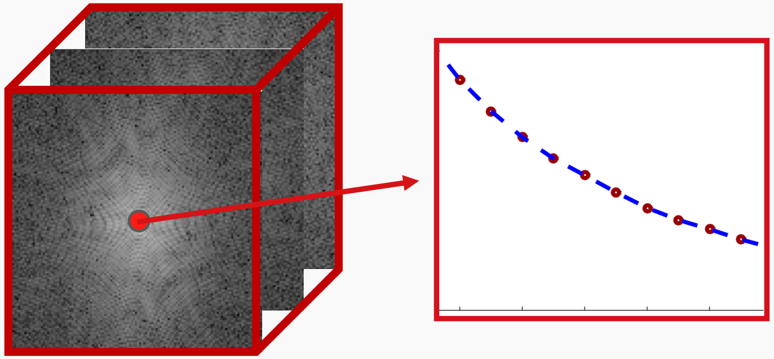

High signal amplitude: poor approximation

Solution: hybrid approach

Circular convolution in space

Linear convolution along parameter dimension

$$\mathbf{w}[\mathbf{k},\mathbf{n}] \otimes \hat{\rho}[\mathbf{k},\mathbf{n}] = \sum_{\mathbf{m}} \underbrace{\sum_{p} \hat{\rho}[\mathbf{k}-\mathbf{p}, n-m] h[\mathbf{p}, m]}_{\approx\, \mathbf{g}_{\mathbf{n}-\mathbf{m},\mathbf{m}} = \hat{\rho}_{\mathbf{n}-\mathbf{m}} \,*\, \mathbf{h}_{\mathbf{m}}}$$

Sum of spatial circular convolutions: computed using FFT

Weight evaluation

$$\mathbf{W} \leftarrow (\underbrace{\mathcal{T}(\hat{\rho})\mathcal{T}(\hat{\rho})^{H}}_{\mathbf{R}} + \epsilon\mathbf{I})^{\frac{p}{2}-1}$$

$$\mathbf{R} = \begin{pmatrix} \mathbf{R}_{1,1} & \mathbf{R}_{1,2} & \cdots & \mathbf{R}_{1,M} \\ \mathbf{R}_{2,1} & \mathbf{R}_{2,2} & \cdots & \mathbf{R}_{2,M} \\ \vdots & \vdots & \cdots & \vdots \\ \vdots & \vdots & \cdots & \vdots \\ \mathbf{R}_{M,1} & \mathbf{R}_{M,2} & \cdots & \mathbf{R}_{M,M} \end{pmatrix}$$

Sum of spatial circular convolutions: computed using FFT

$$\mathbf{R}_{\mathbf{p},\mathbf{q}} = \sum_{\mathbf{i}=1}^{\mathbf{k}} \underbrace{\mathbf{T}(\hat{\rho}_{p+i-1})\mathbf{T}(\hat{\rho}_{q+i-1})^{*}}$$

Validation using single channel data (sim)

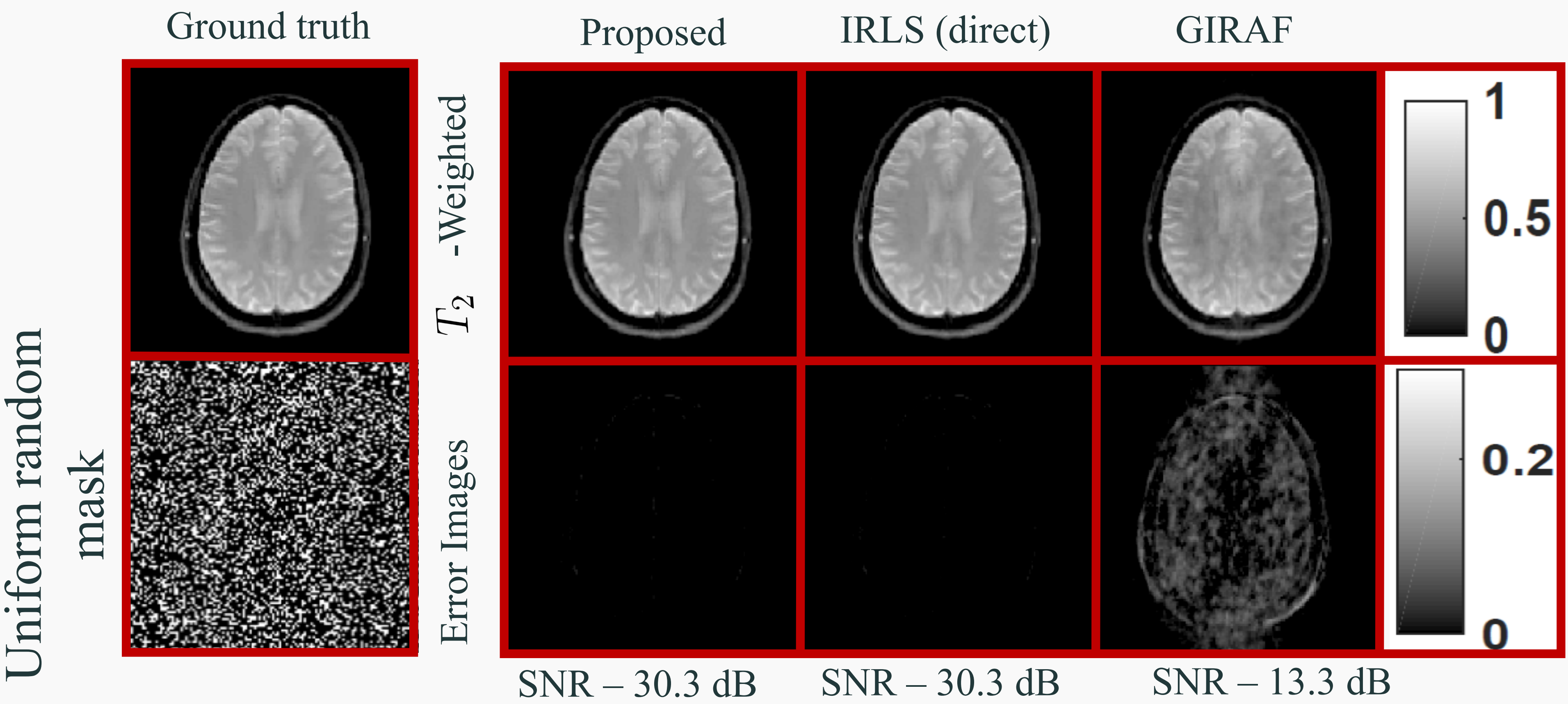

Validation using single channel data (simulation)

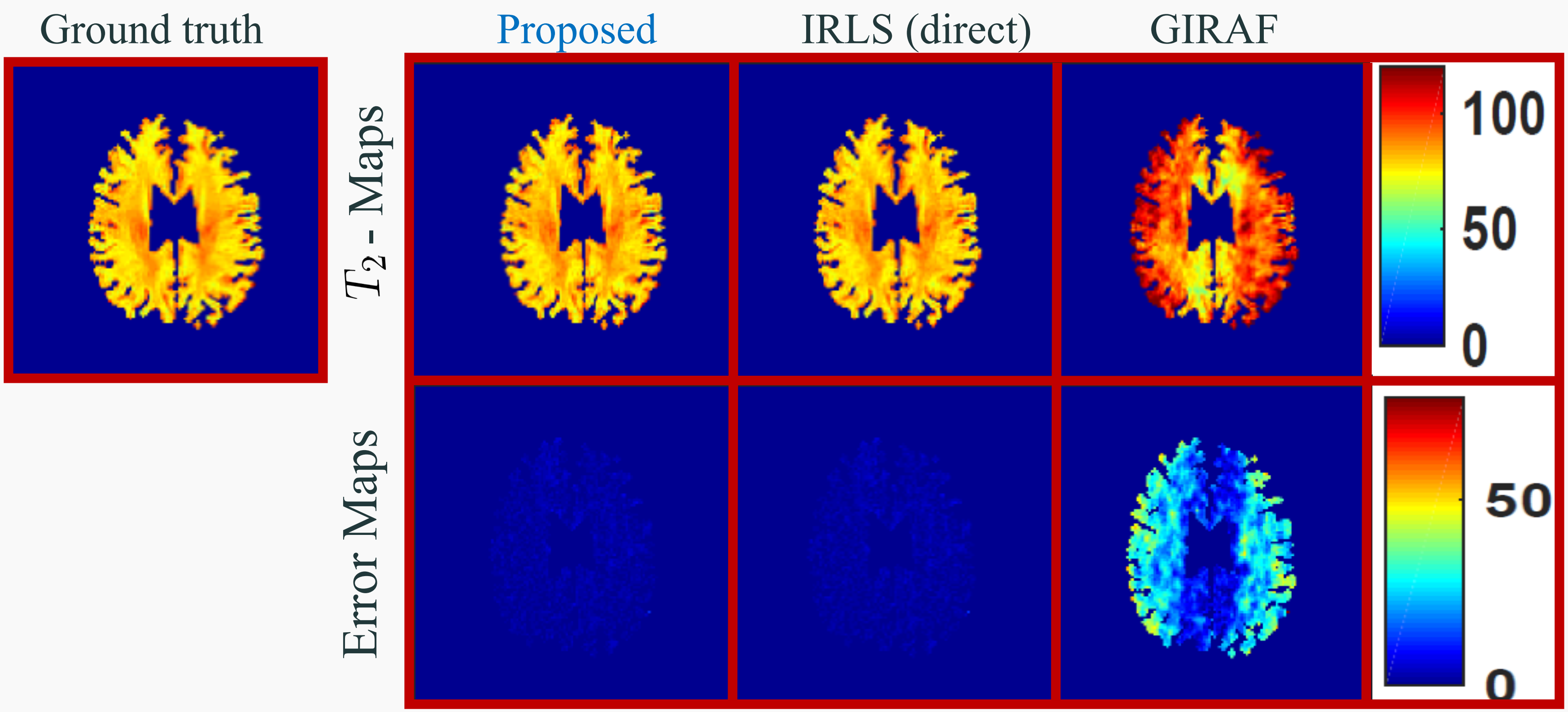

SER – 31.4 dB SER – 31.4 dB SER – 10.4 dB

Fast convergence

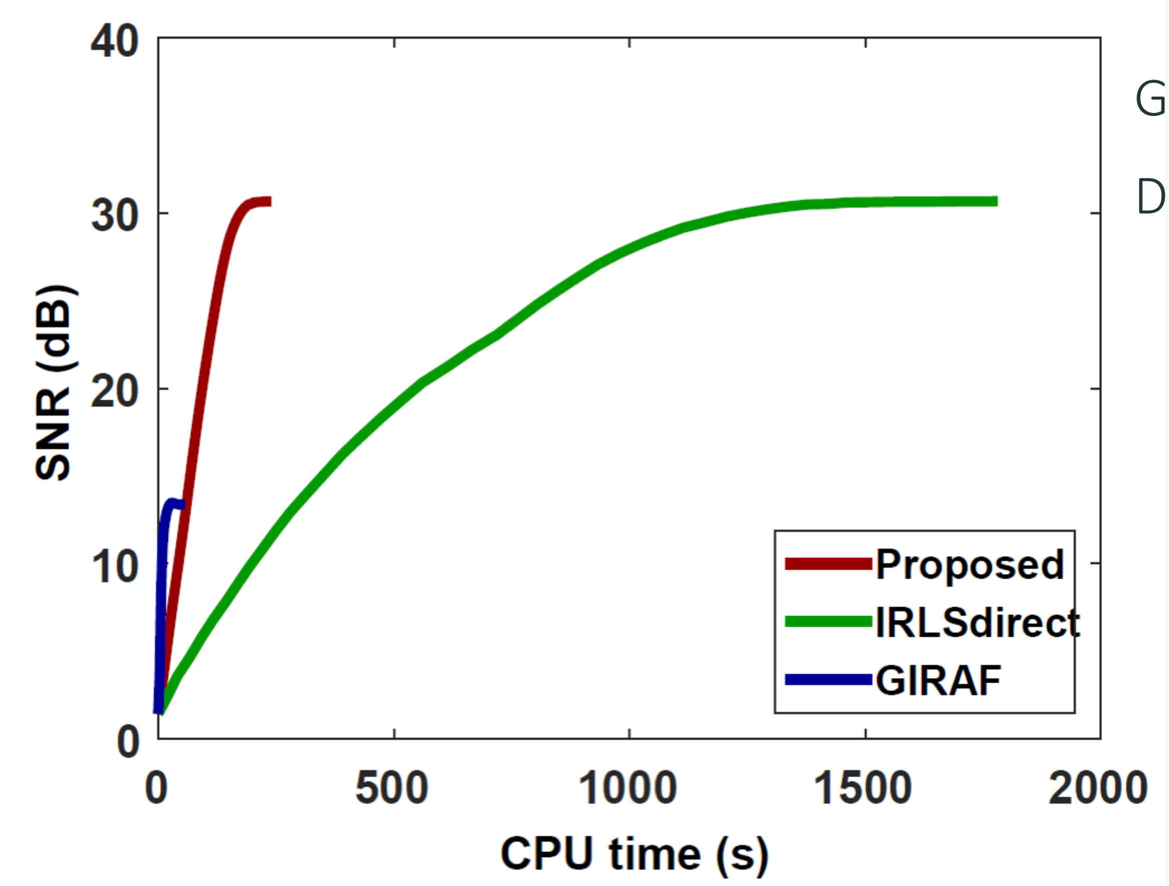

GIRAF: poor approximation

Direct IRLS: slow

Comparison with state of the art

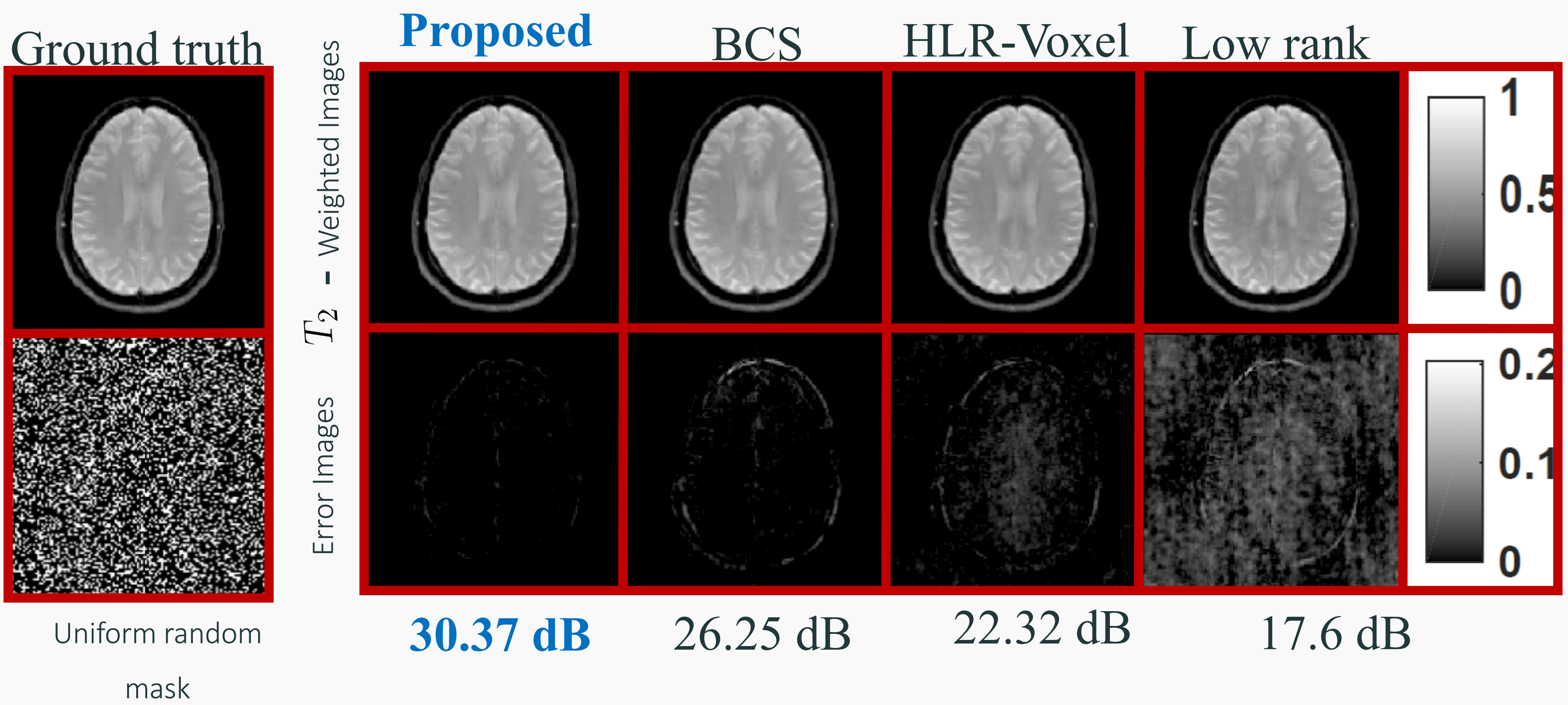

Comparison with state of the art

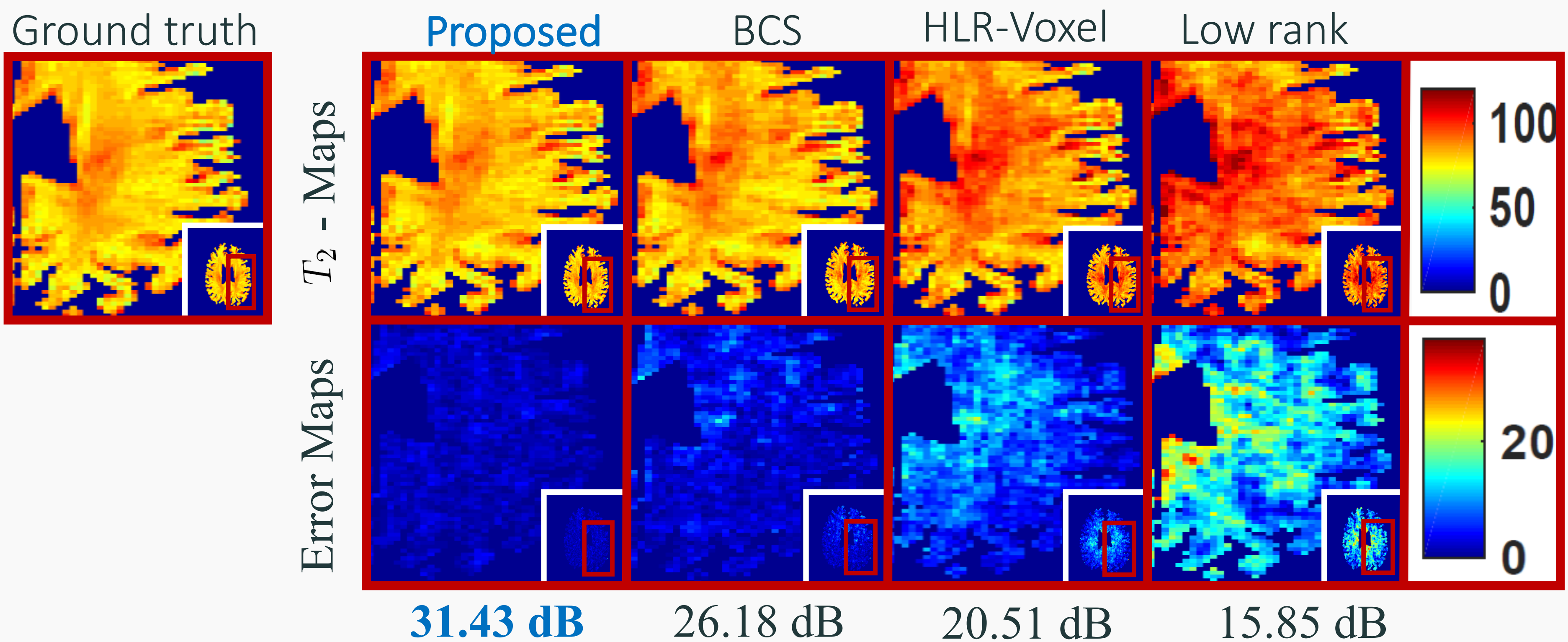

Multichannel acquisitions

- TR=2500 ms,
- slice thickness = 5mm
- FOV = 22x22 cm^2
- Matrix size : 128x128,
- No of coils = 12,
- TE = 10 to 120 ms

Smaller filters provide better results

filter size	SNR
128x128x10	28.05
122x122x10	30.30
114x114x10	31.00
108x108x10	31.12
102x102x10	**31.21**
100x100x10	31.20

(a) Varying spatial dimension

filter size	SNR (dB)
102x102x11	30.80
102x102x10	**31.21**
102x102x7	31.13
102x102x4	30.96
102x102x2	30.78
102x102x1	29.88

(b) Varying temporal dimensions

Smaller filters: spatial regularization

Multichannel acq: T2 weighted images

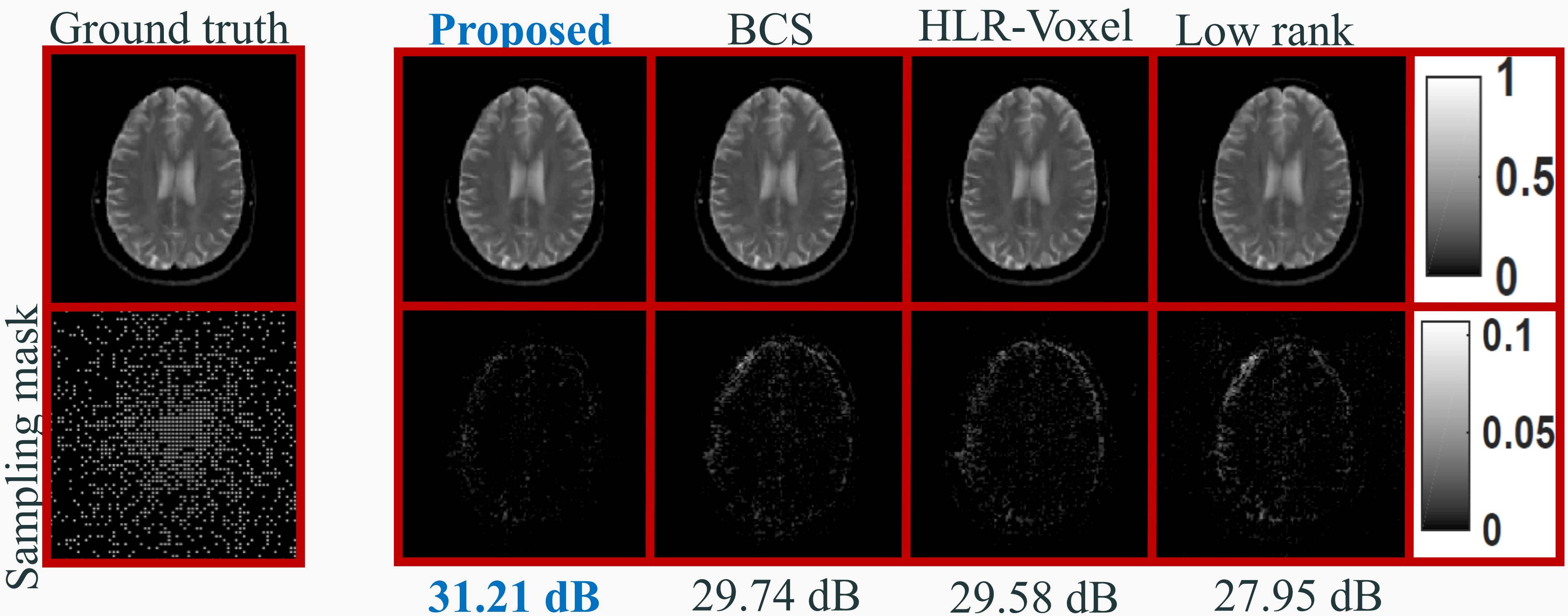

Multichannel acquisition: parameter maps

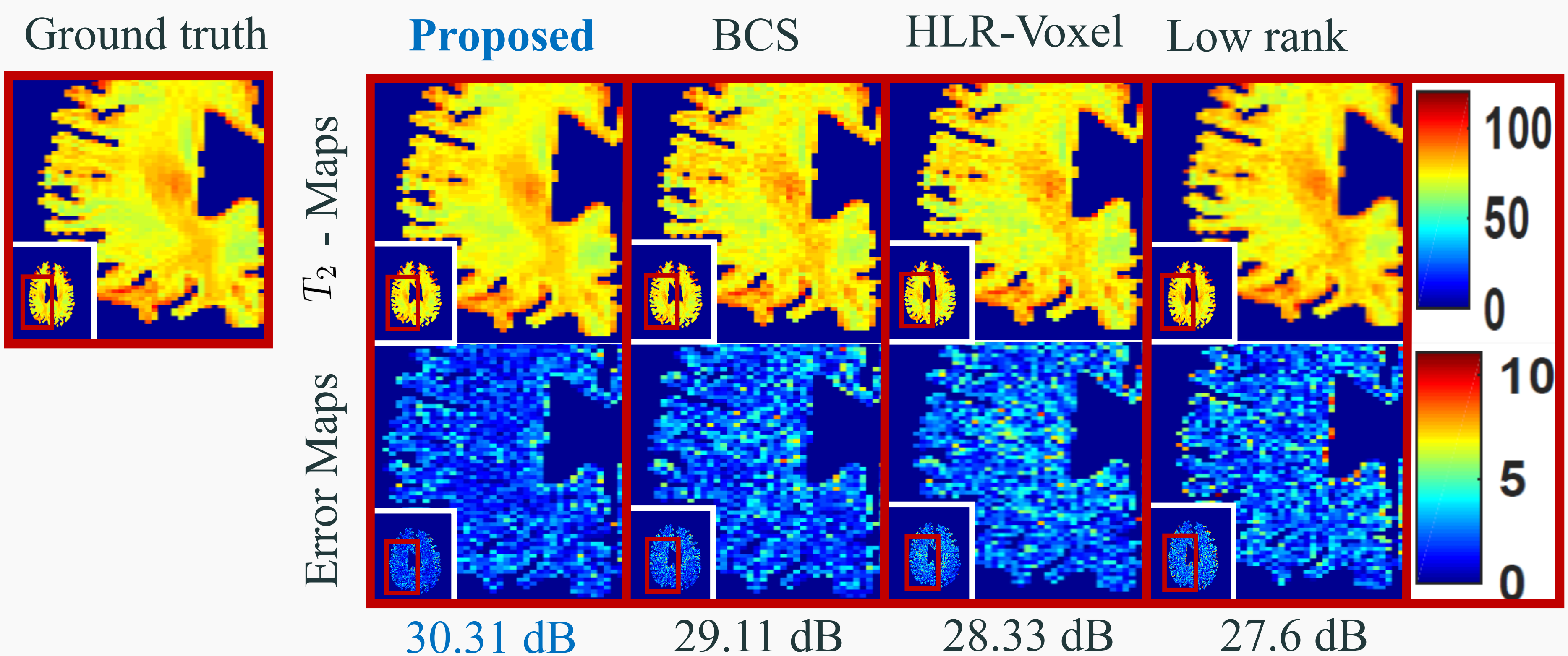

Infrared spectroscopy

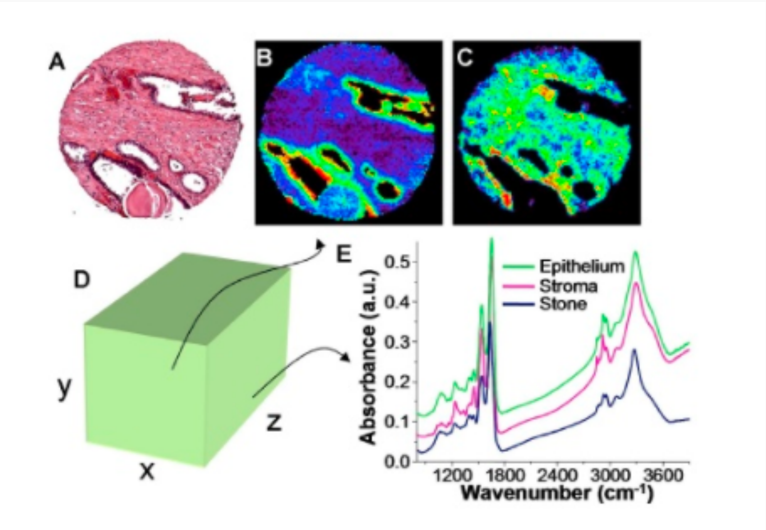

1D IR spectroscopy

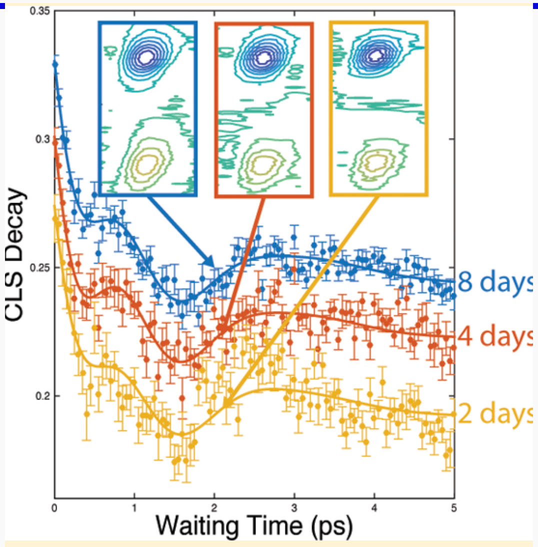

2D IR spectroscopy

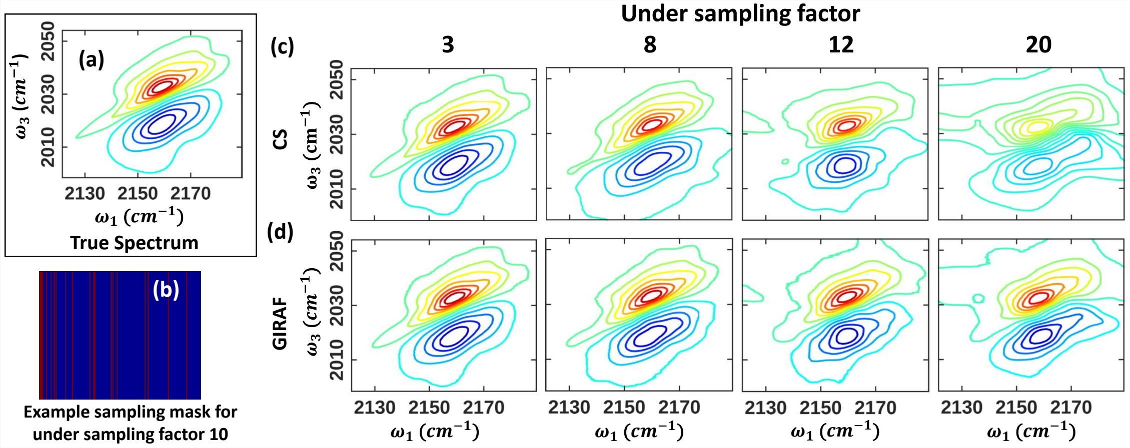

Accelerated imaging using GIRAF

[Humston et al, Journal of Physical Chemistry]

[Bhattacharya et al, Optics Letters, submitted]

Correction of Nyquist ghosts in multishot MRI [MUSSELS]

Motion-induced inter-shot phase errors

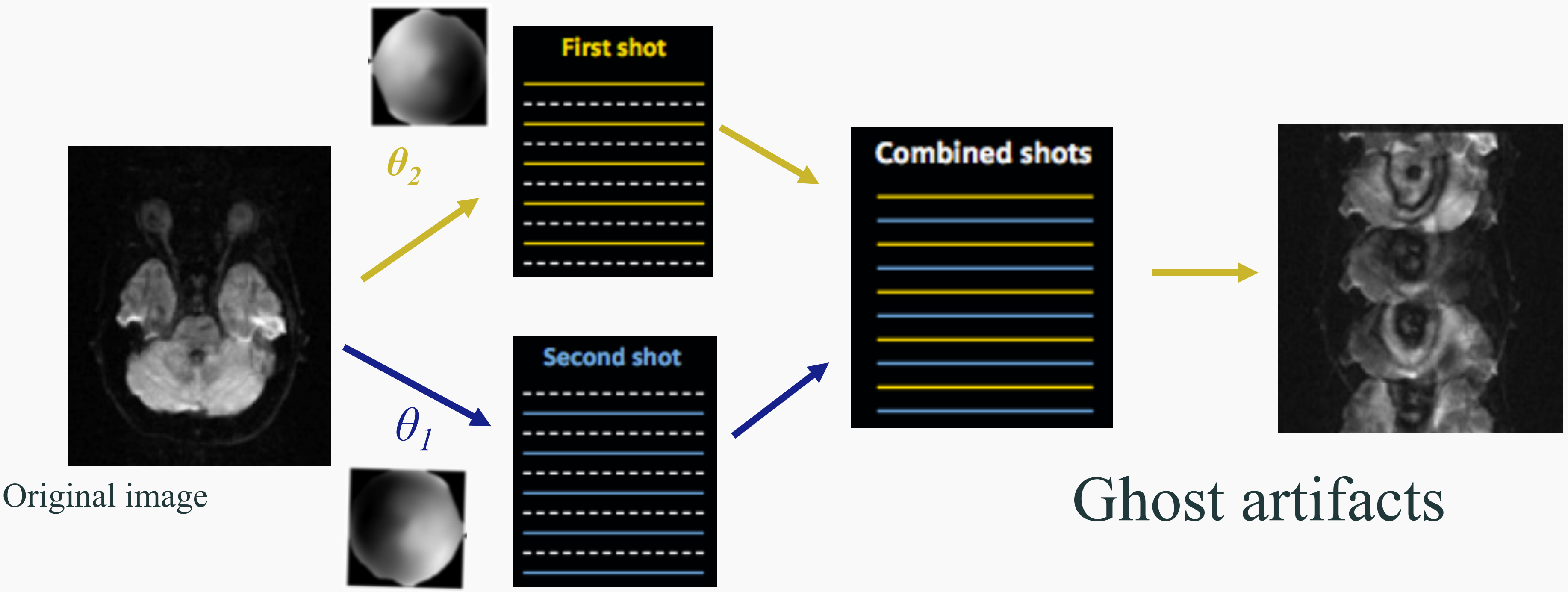

Self calibration methods: Image domain

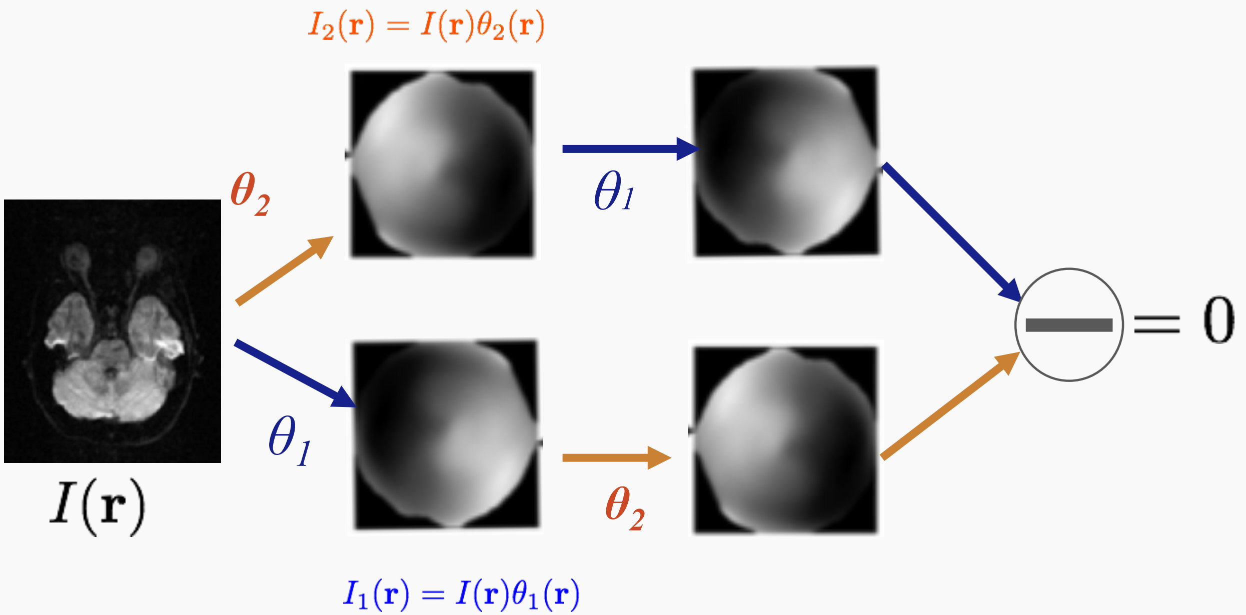

Image domain annihilation relation [Morrisson, Do & Jacob 2007]

$$I_2(\mathbf{r}) \cdot \theta_1(\mathbf{r}) - \hat{I}_1(\mathbf{r}) \cdot \hat{\theta}_2(\mathbf{r}) = 0$$

Model sensitivities as polynomials: EVD

Better than SOS estimates

Self calibration methods: Fourier domain

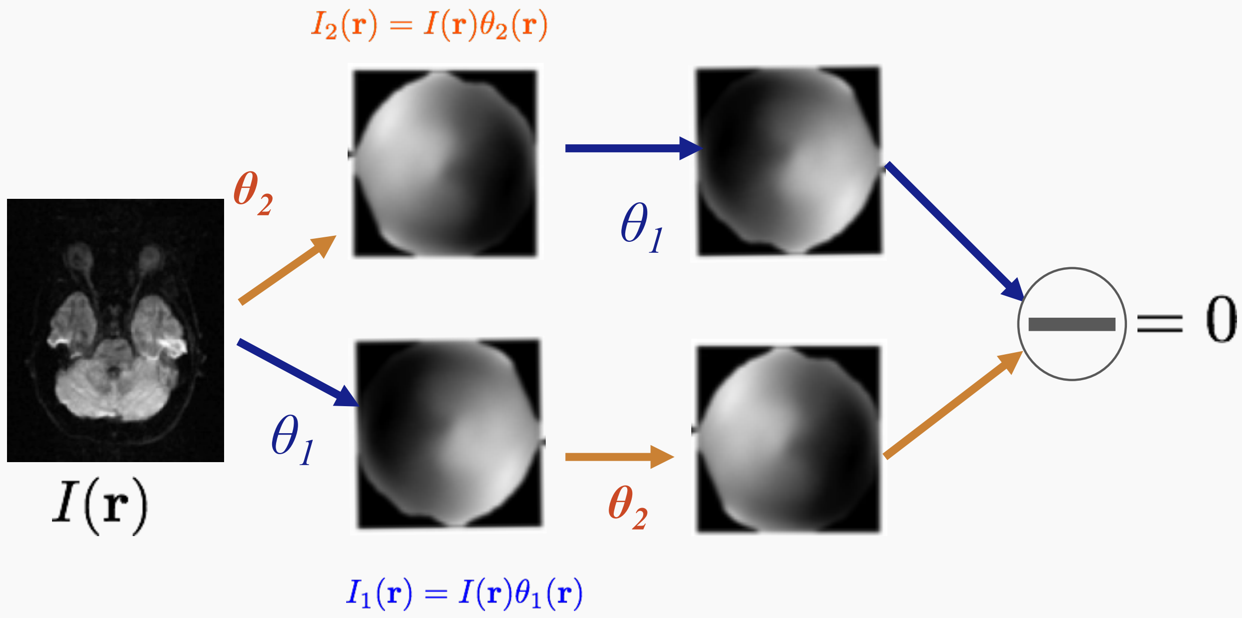

Fourier domain relation [Lustig 2012, Haldar 2014]

$$\hat{I}_2[\mathbf{k}] * \hat{\theta}_1[\mathbf{k}] - \hat{I}_1[\mathbf{k}] * \hat{\theta}_2[\mathbf{k}] = 0$$

Phase: linear combination of exponentials → FIR filter

Self calibration methods: matrix form

Fourier domain relation

$$\hat{I}_2[\mathbf{k}] * \hat{\theta}_1[\mathbf{k}] - \hat{I}_1[\mathbf{k}] * \hat{\theta}_2[\mathbf{k}] = 0$$

Convolution: matrix multiplication

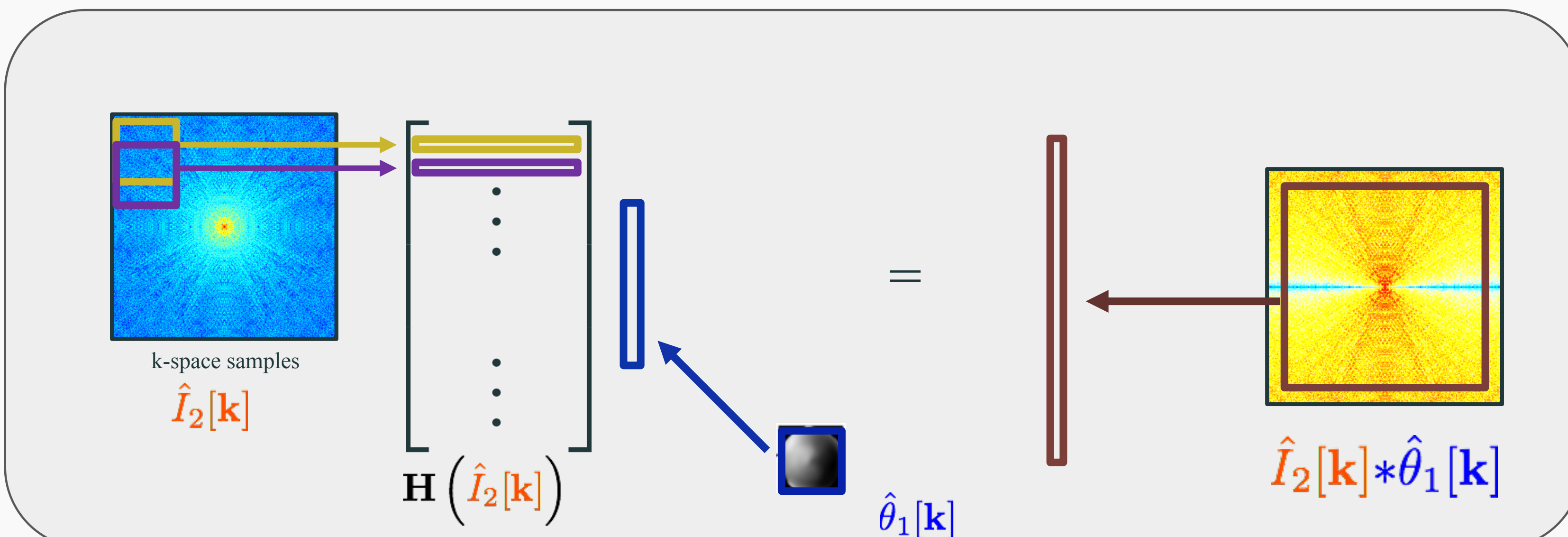

Self calibration methods: Fourier domain

Fourier domain relation

$$\hat{I}_2[\mathbf{k}] * \hat{\theta}_1[\mathbf{k}] - \hat{I}_1[\mathbf{k}] * \hat{\theta}_2[\mathbf{k}] = 0$$

Compact matrix representation

$$\underbrace{\left[\mathbf{H}\left(\hat{I}_2[\mathbf{k}]\right), \mathbf{H}\left(\hat{I}_1[\mathbf{k}]\right)\right]}_{\mathbf{Q}(I_1, I_2)} \begin{bmatrix} \hat{\theta}_1[\mathbf{k}] \\ -\hat{\theta}_2[\mathbf{k}] \end{bmatrix} = 0$$

N shots: $\binom{N}{2}$ null space vectors

$\mathbf{Q}$ is low-rank & structured

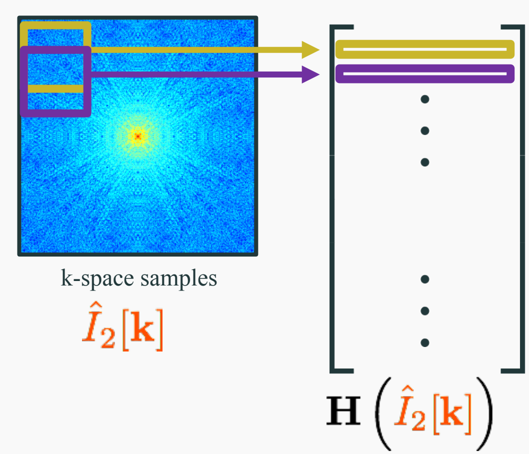

Smoothness regularized multishot MRI

Multi-shot recovery

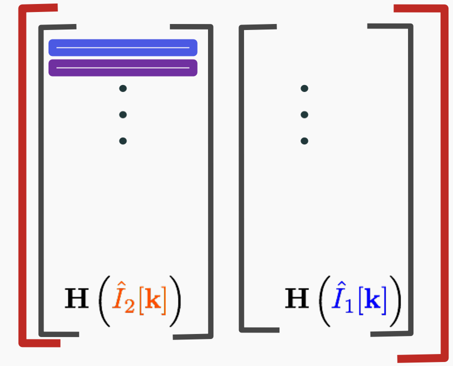

Smoothness regularization

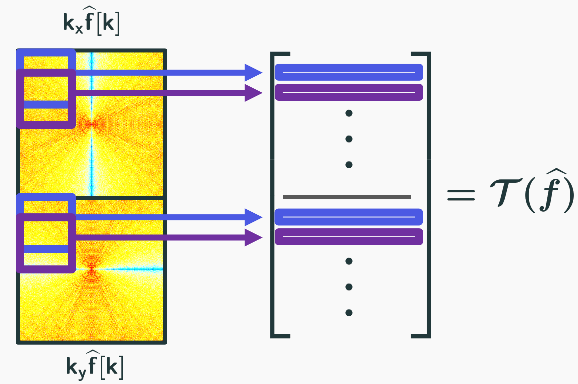

Combine the matrix liftings

Structured low-rank recovery

$$\|\mathcal{A}(I_1, I_2) - \mathbf{b}\|^2 + \lambda\|\mathcal{G}(I_1, I_2)\|_*$$

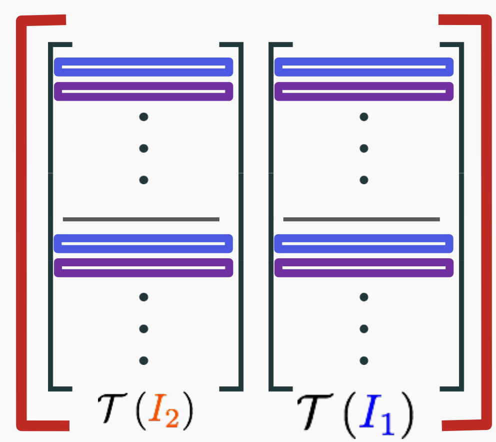

Mani & Jacob, Magnetic Resonance Medicine, in press

Structured low-rank recovery: MUSSELS

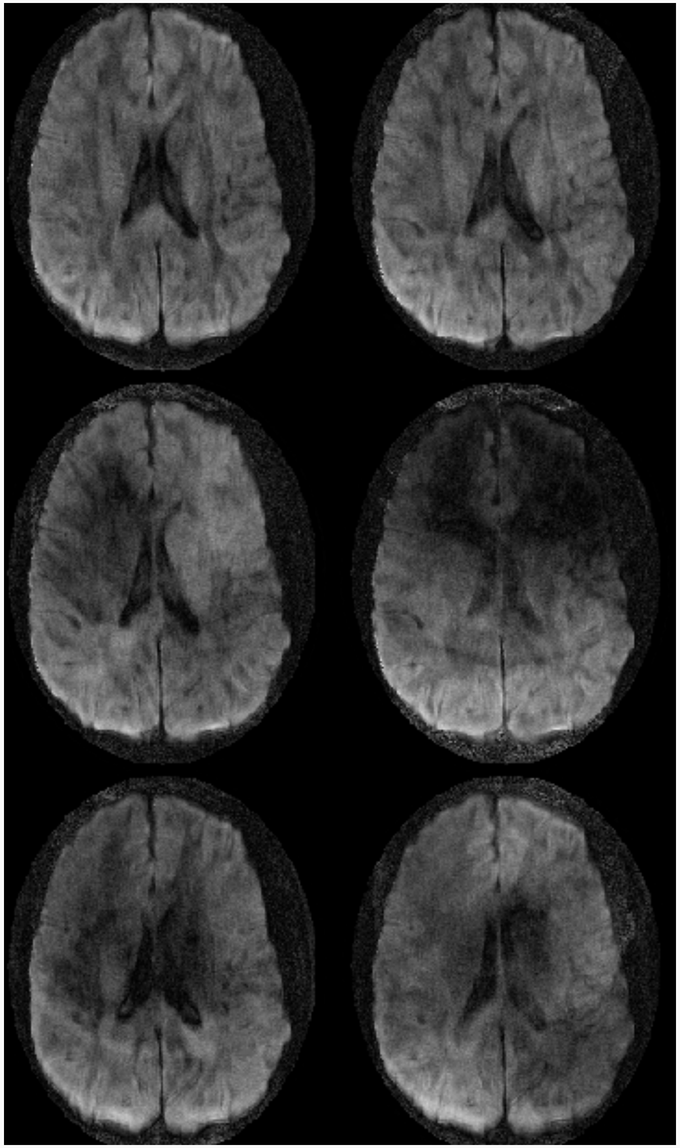

MUSE

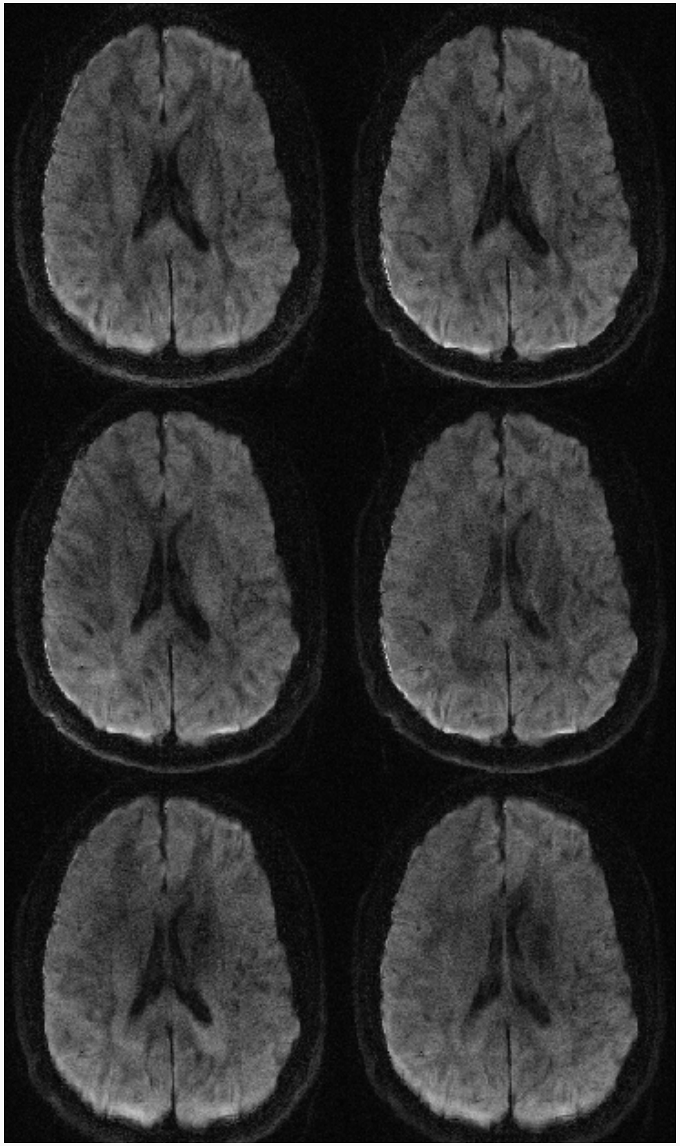

MUSSELS

Comparison with MUSE (state of the art)

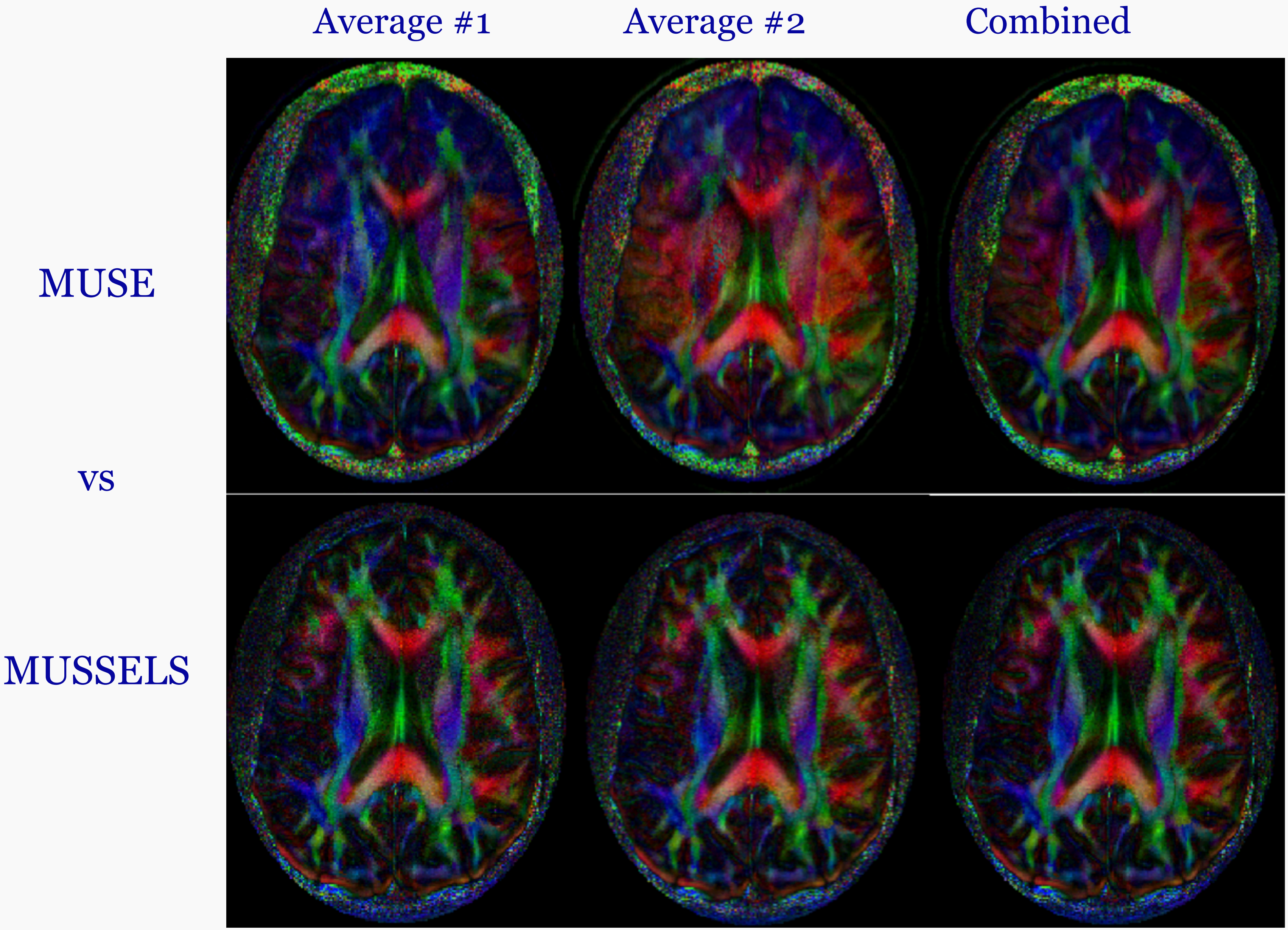

[Mani & Jacob, Magnetic Resonance Medicine, in press]()

Odd even shifts & partial Fourier in EPI

Multishot & partial Fourier

Improved SNR & reduced distortion

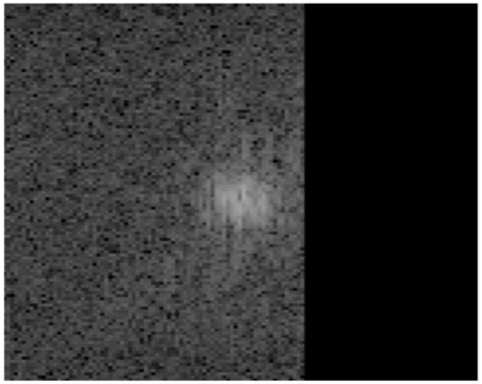

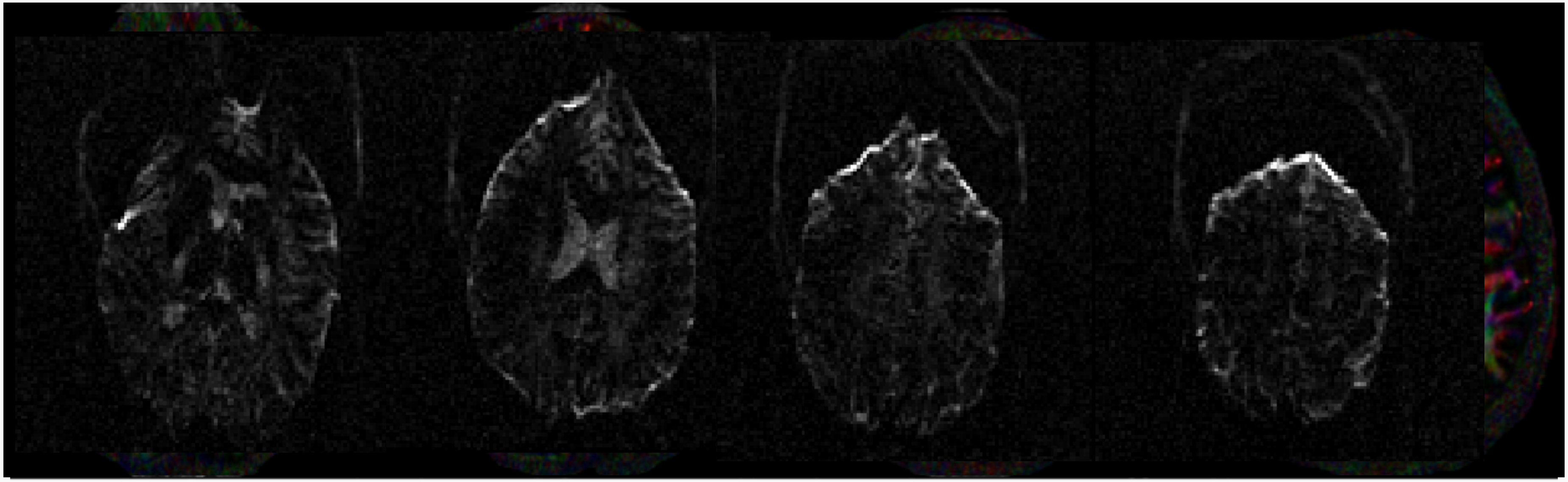

0.8 x 0.8 x 2mm; 3 avgs; 25 directions; b=700

Mani & Jacob, Magnetic Resonance Medicine, in press, EMBC 2016

Radial trajectory correction

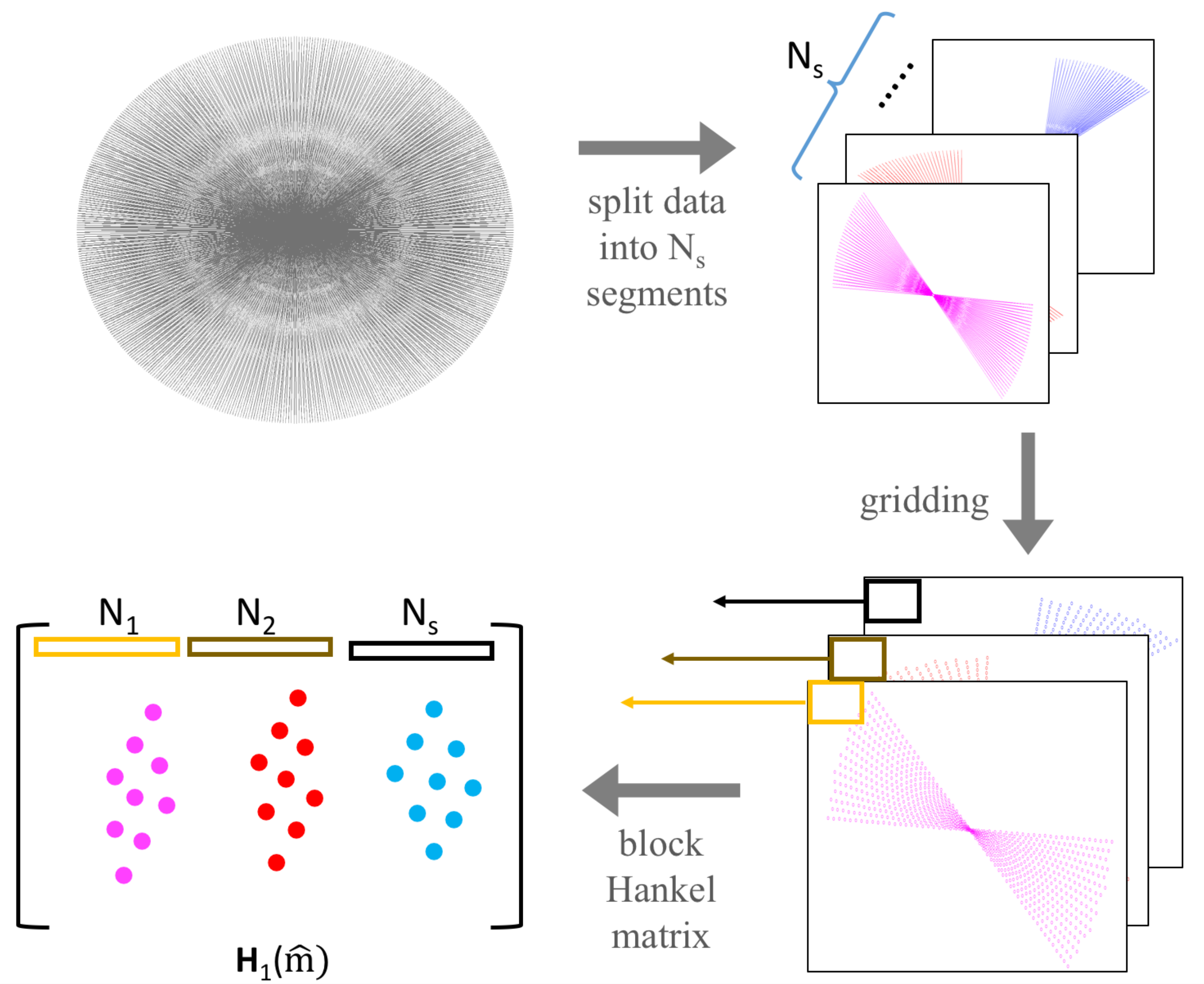

Results: MUSSELS based radial traj. correction

➢ Radial data:

- 3T GE scanner
- 256 spokes
- 154 points per spoke
- partial Fourier acq.
- 32 channels

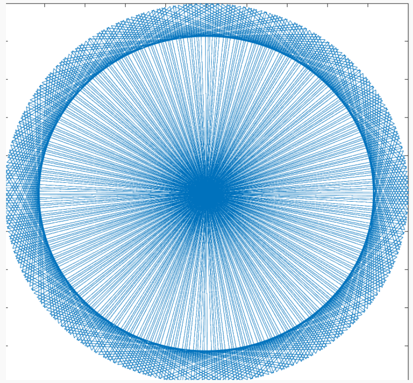

Ideal Radial trajectory

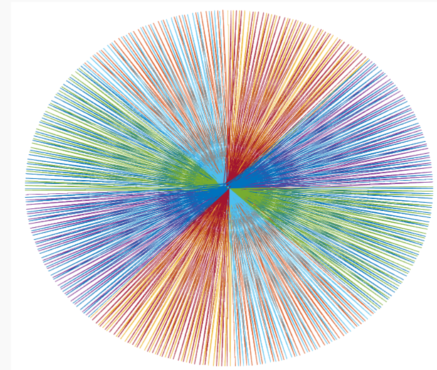

The 8 segments

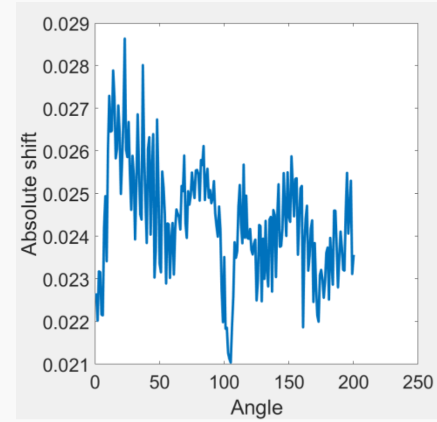

Plot of trajectory shift vs angle

Recon using NUFFT

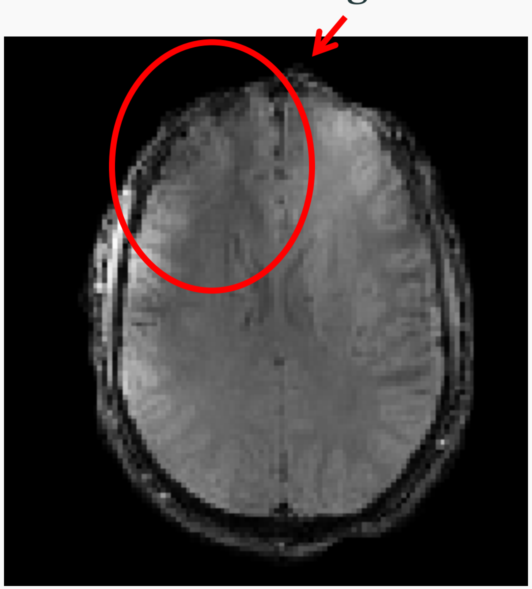

Recon using MUSSELS

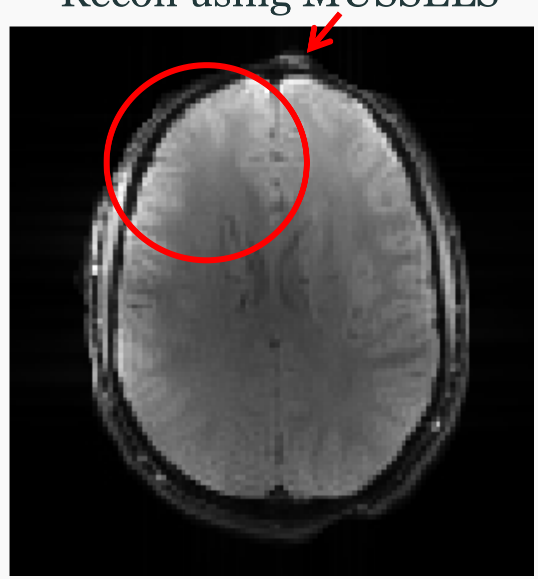

Recon using TrACR

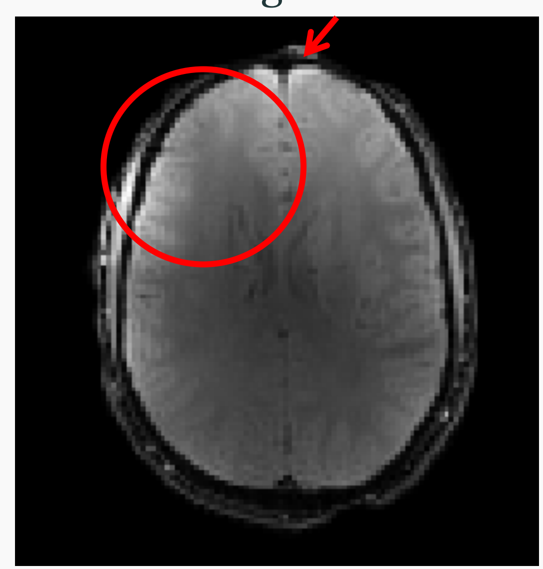

Results: MUSSELS based radial traj. correction

Radial data:

- 3T Siemens scanner
- 512 spokes
- 512 points per spoke
- 5 channels

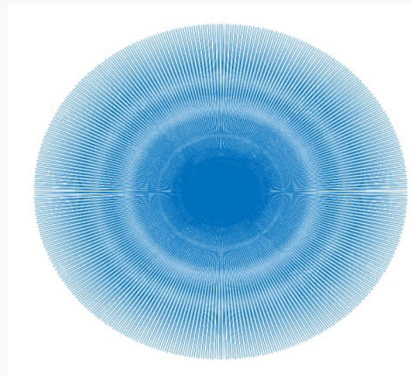

Ideal Radial trajectory

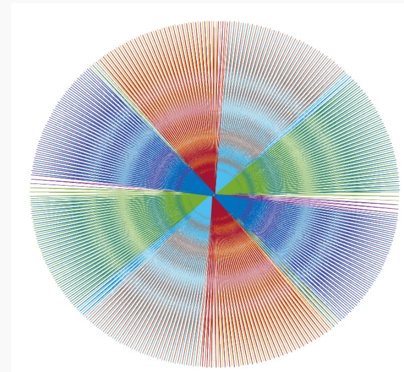

The 8 segments

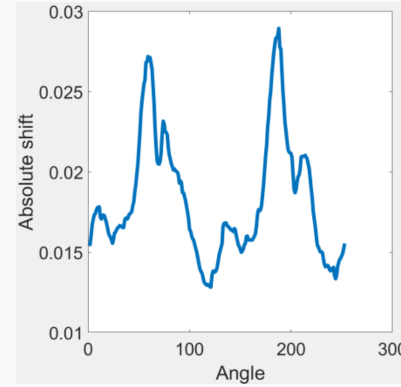

Plot of trajectory shift vs angle

Recon using NUFFT

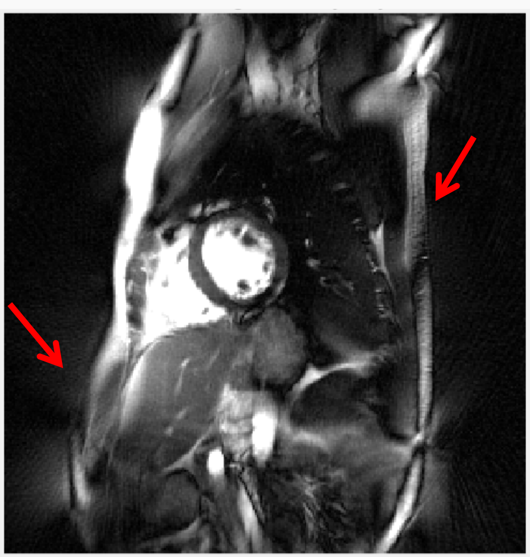

Recon using MUSSELS

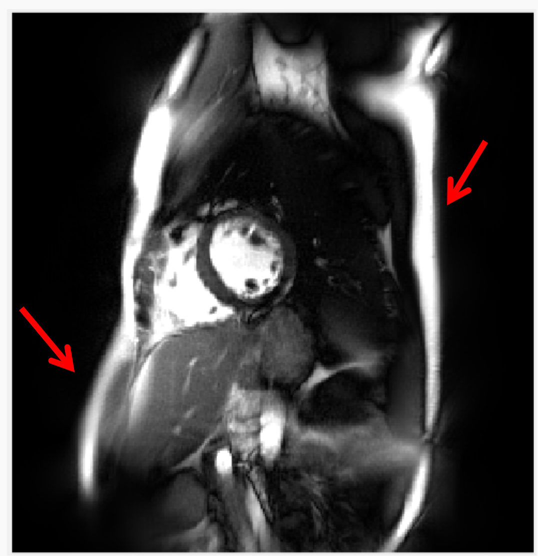

Recon using TrACR

Results: MUSSELS based radial traj. correction

- Radial data:
  - 3T Siemens scanner
  - 512 spokes
  - 512 points per spoke
  - 5 channels

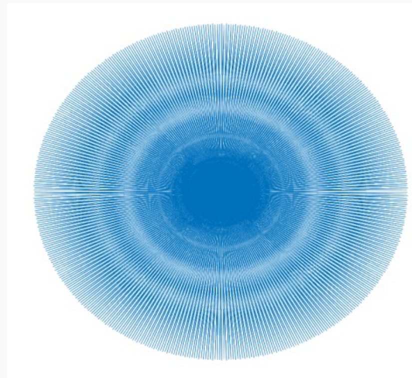

Ideal Radial trajectory

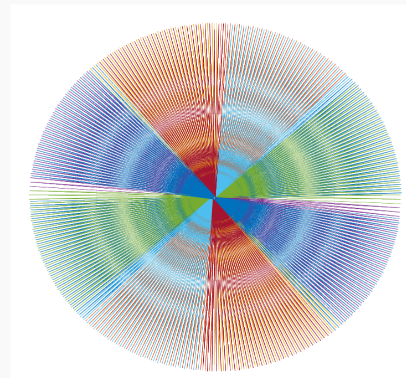

The 8 segments

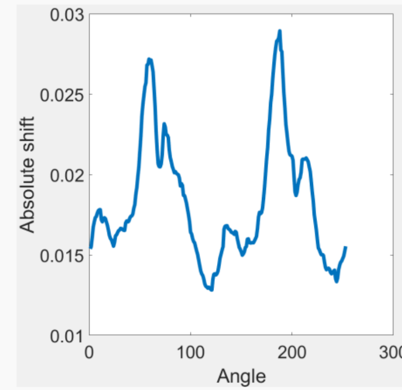

Plot of trajectory shift vs angle

Recon using NUFFT

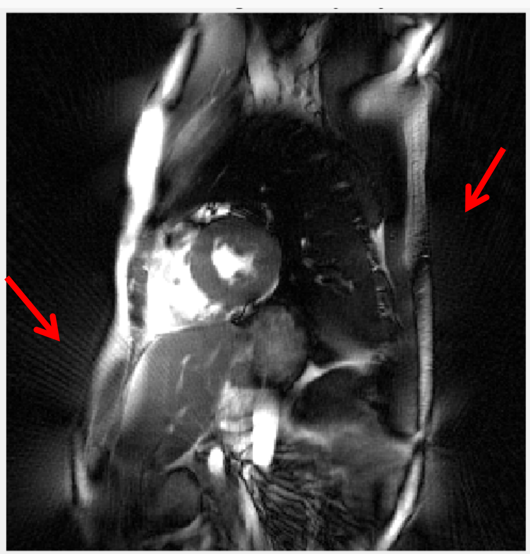

Recon using MUSSELS

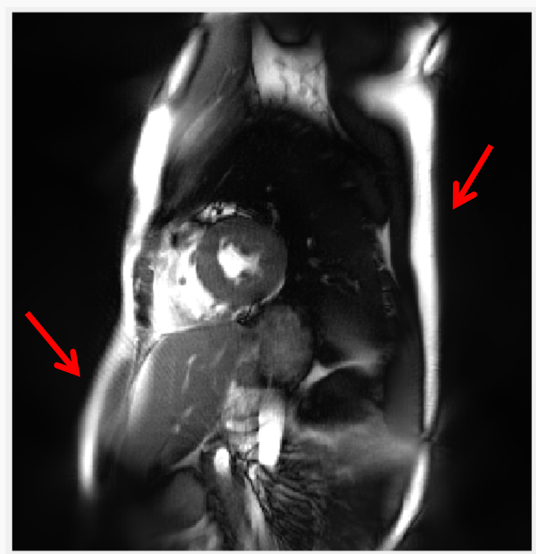

Recon using TrACR

MR artifacts

- What is MR artifacts?

  During acquisition, external interruptions (ex. fluctuation power supply of gradient, motion of object, etc.) distort signals.

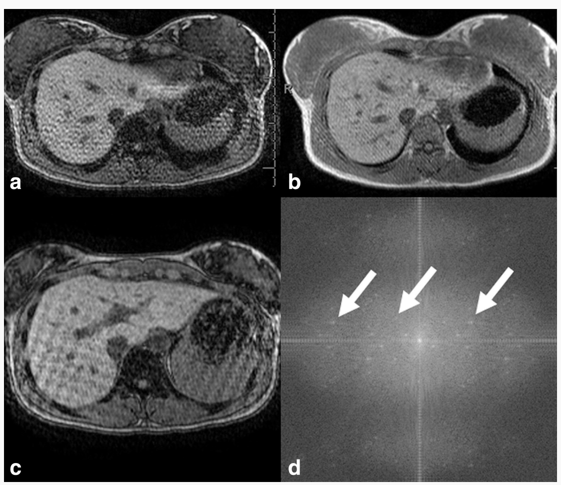

Spike noise

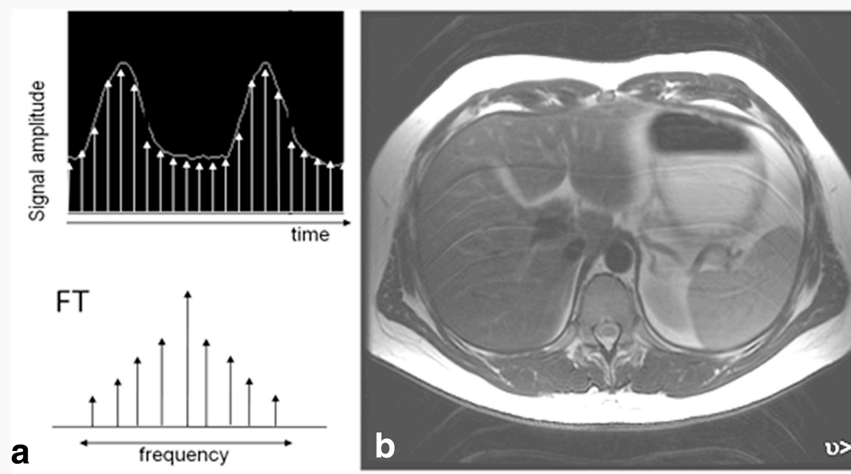

Respiratory motion

M. Graves, et. al., JMRI (2013)

Motivation

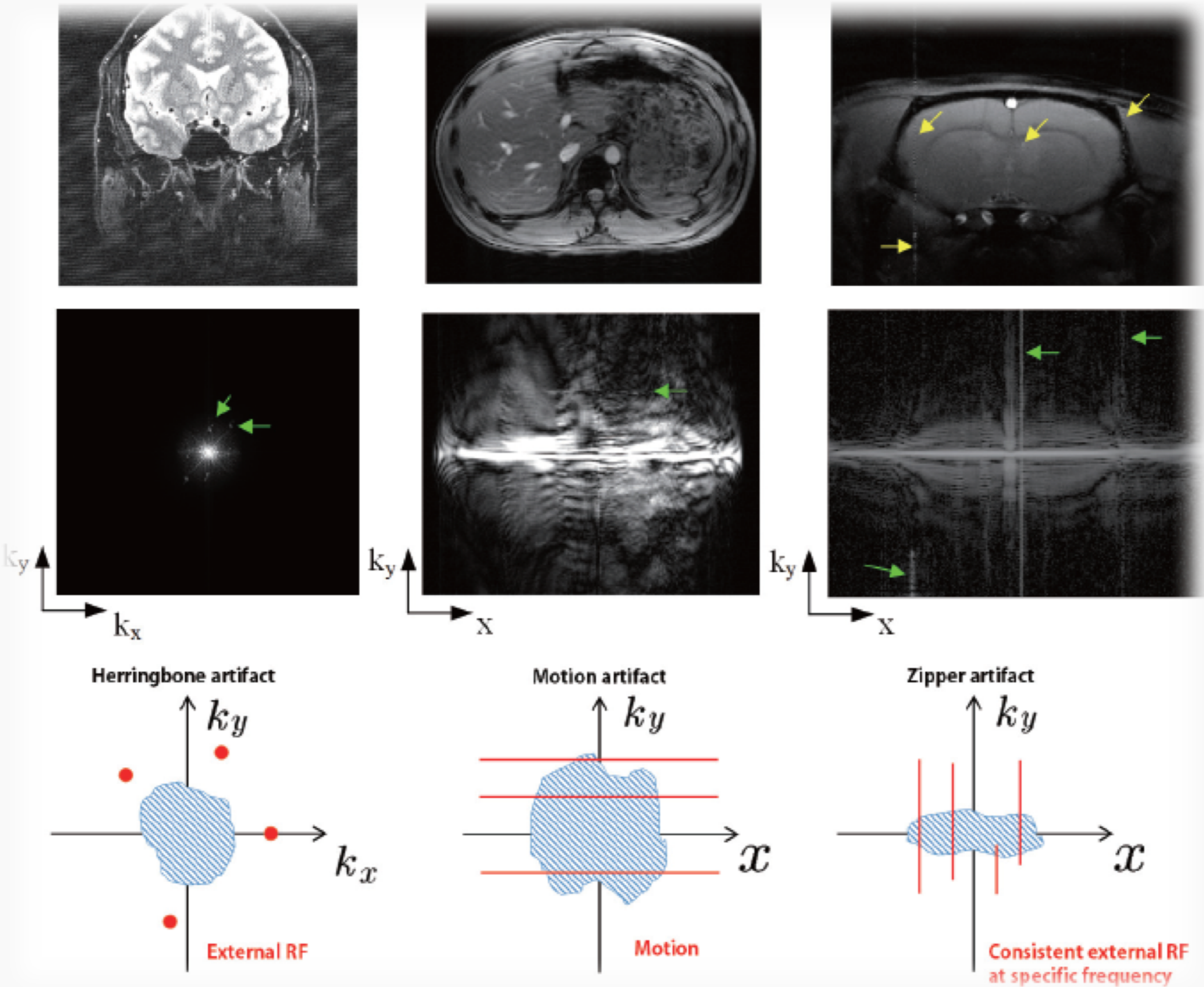
ky
kx
ky
x
ky
x
Herringbone artifact
k_y
k_x
External RF
Motion artifact
k_y
x
Motion
Zipper artifact
k_y
x
Consistent external RF
at specific frequency

Motivations: MR artifacts as sparse outliers

✓ Herringbone (spikes 2-D k-space)

$$\widetilde{M}(k_x, k_y) = \widehat{M}(k_x, k_y) + \underbrace{\sum_{j=1}^{S} \epsilon_j \delta[k_x - k_{x_j}, k_y - k_{y_j}]}_{\text{sparse outliers}},$$

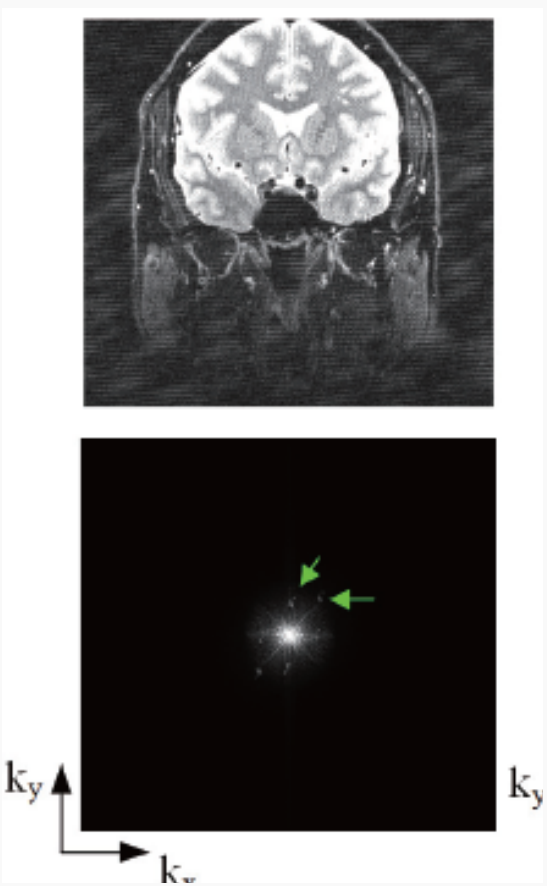

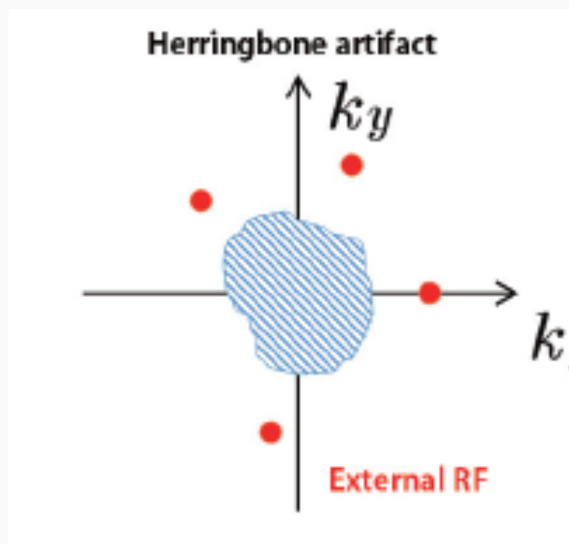

Motivations: MR artifacts as sparse outliers

✓ Motion artifact (spikes 1-D k-space parallel to readout)

$$\widetilde{M}(x,k_y) = \begin{cases} \widehat{M}(x,k_y)\exp(j2\pi k_y d(k_y)), & \text{when } k_y \in \{k_{y_1},\cdots,k_{y_S}\} \\ \widehat{M}(x,k_y), & \text{otherwise} \end{cases}$$

$$= \widehat{M}(x,k_y) + \underbrace{\sum_{j=1}^{S}\widehat{M}(x,k_y)(\exp(j2\pi k_y d(k_y))-1)\delta[k_y-k_{y_j}]}_{\text{sparse outliers}}$$

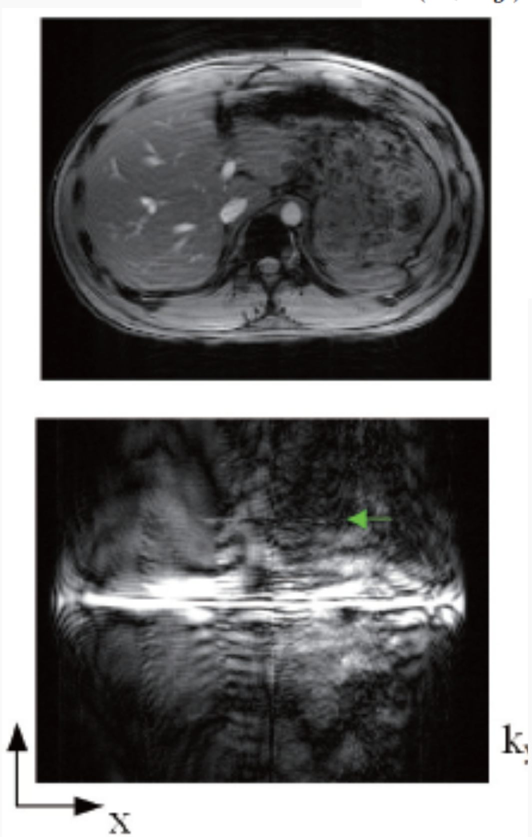

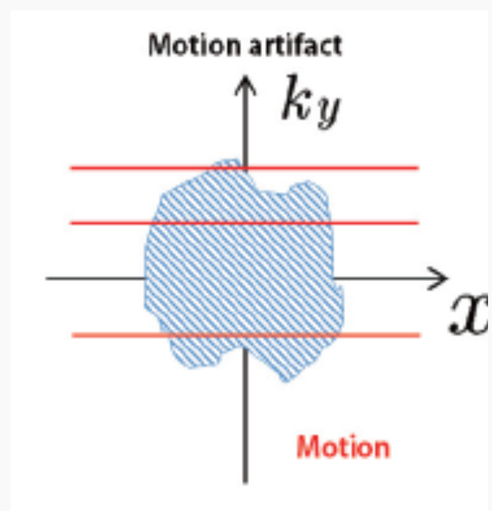

Motivations: MR artifacts as sparse outliers

Zipper artifact (spikes 1-D k-space perpendicular to readout)

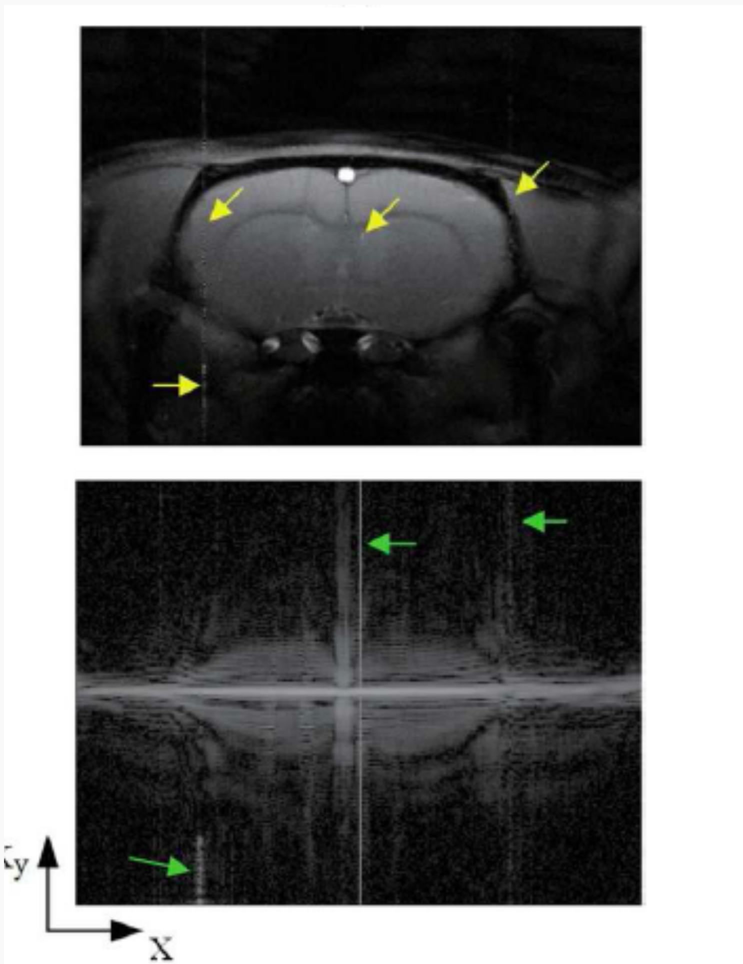

$$\widetilde{M}(x, k_y) = \widehat{M}(x, k_y) + \underbrace{\sum_{j=1}^{S} \epsilon_j \delta[x - x_j]}_{\text{sparse outliers}},$$

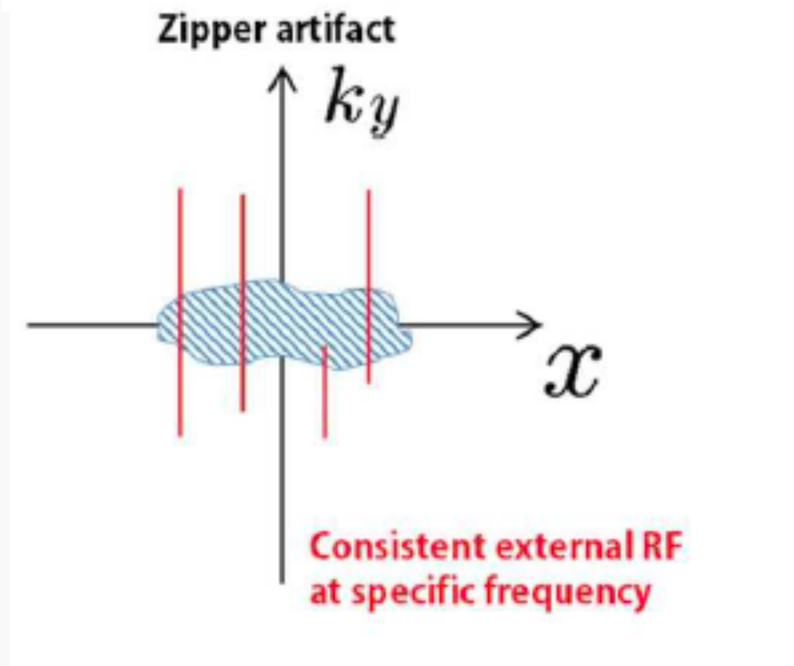

Key Observation : Sparse outliers

*** Sparse outlier is still sparse in weighted Hankel matrix**

ALOHA* + **Sparse MR artifact**

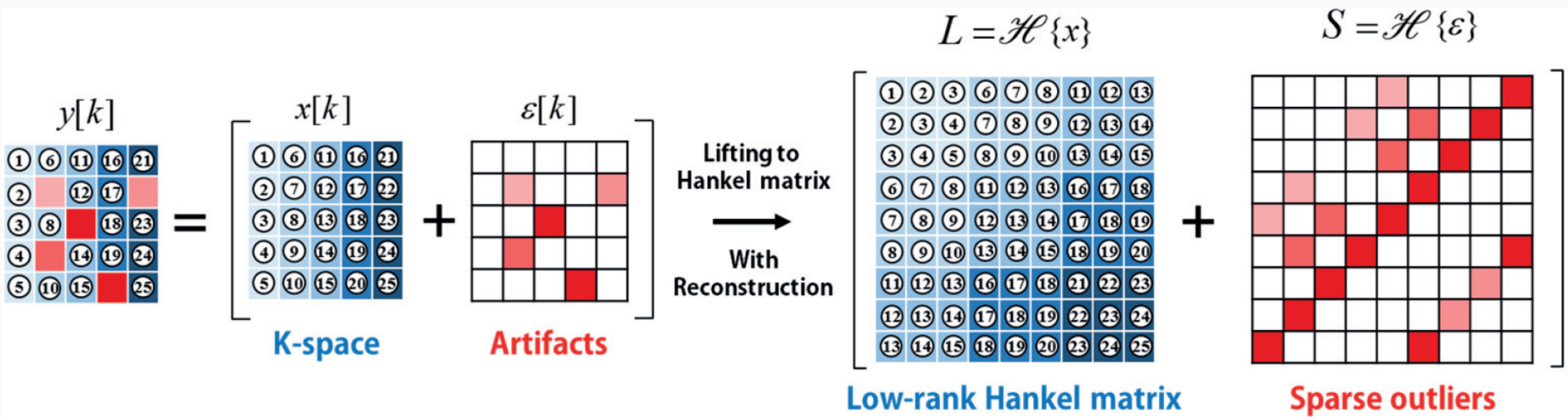

- **ALOHA: Annihilating filter based LOw rank Hankel matrix Approach**

† E. Candes, et. al, JACM (2011), R. Otazo, et. al, MRM (2015)
*K.H. Jin, et. al, IEEE TIP (2015), K.H. Jin, et. al, arXiv (2015), J. C. Ye, et. al, arXiv (2015), J. Lee, et. al, MRM (2016), D. Lee, et. al, MRM (2016)

Robust ALOHA

RPCA for weighted Hankel matrix

$$\min_{\mathbf{M},\mathbf{E}} \quad \|\mathscr{H}\{\mathbf{M}\}\|_* + \tau\|\mathbf{E}\|_1$$

$$\text{subject to} \quad \mathbf{P}_\Omega\left(\widehat{\mathbf{W}} \odot \hat{\mathbf{L}}\right) = \mathbf{P}_\Omega(\mathbf{M}+\mathbf{E}),$$

signal

Sparse outlier

K-space weighting

✓ *Extension of ALOHA for decomposition of sparse outliers (E) out of mixed signal**

✓ *Can be addressed ADMM†*

✓ *K-space weighting*

* E. Candes, et. al, JACM (2011), R. Otazo, et. al, MRM (2015)

† S. Boyd, et. al., Foundations and Trends in Machine Learning (2011)

‡ Z. Wan, et. al., Mathematical Programming Computation (2012)

Algorithm Flowchart

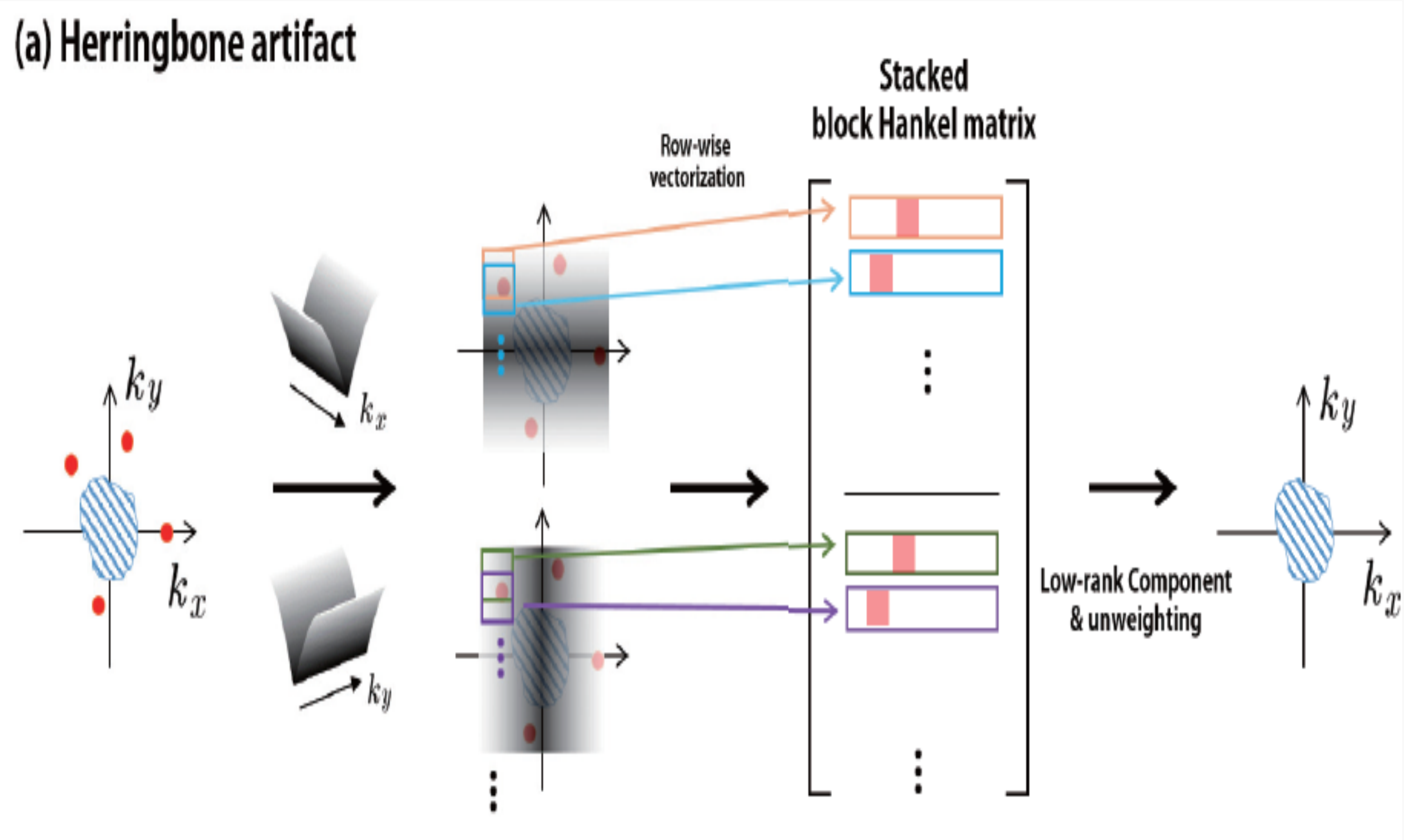

Retrospective results

High intensity
Spike noise

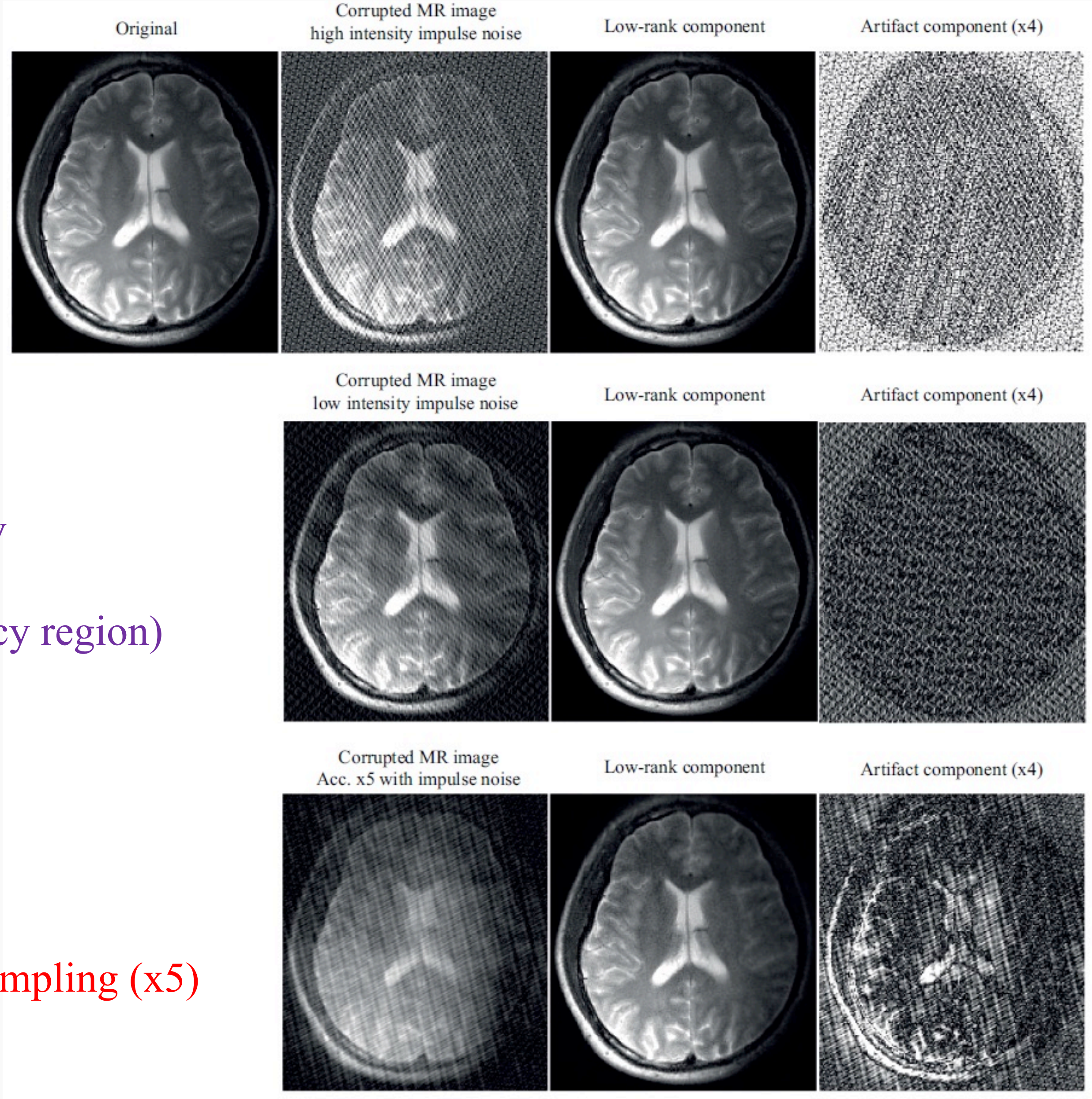

Low intensity
Spike noise
(low frequency region)

Spike noise
with down sampling (x5)

In Vivo Motion artifact

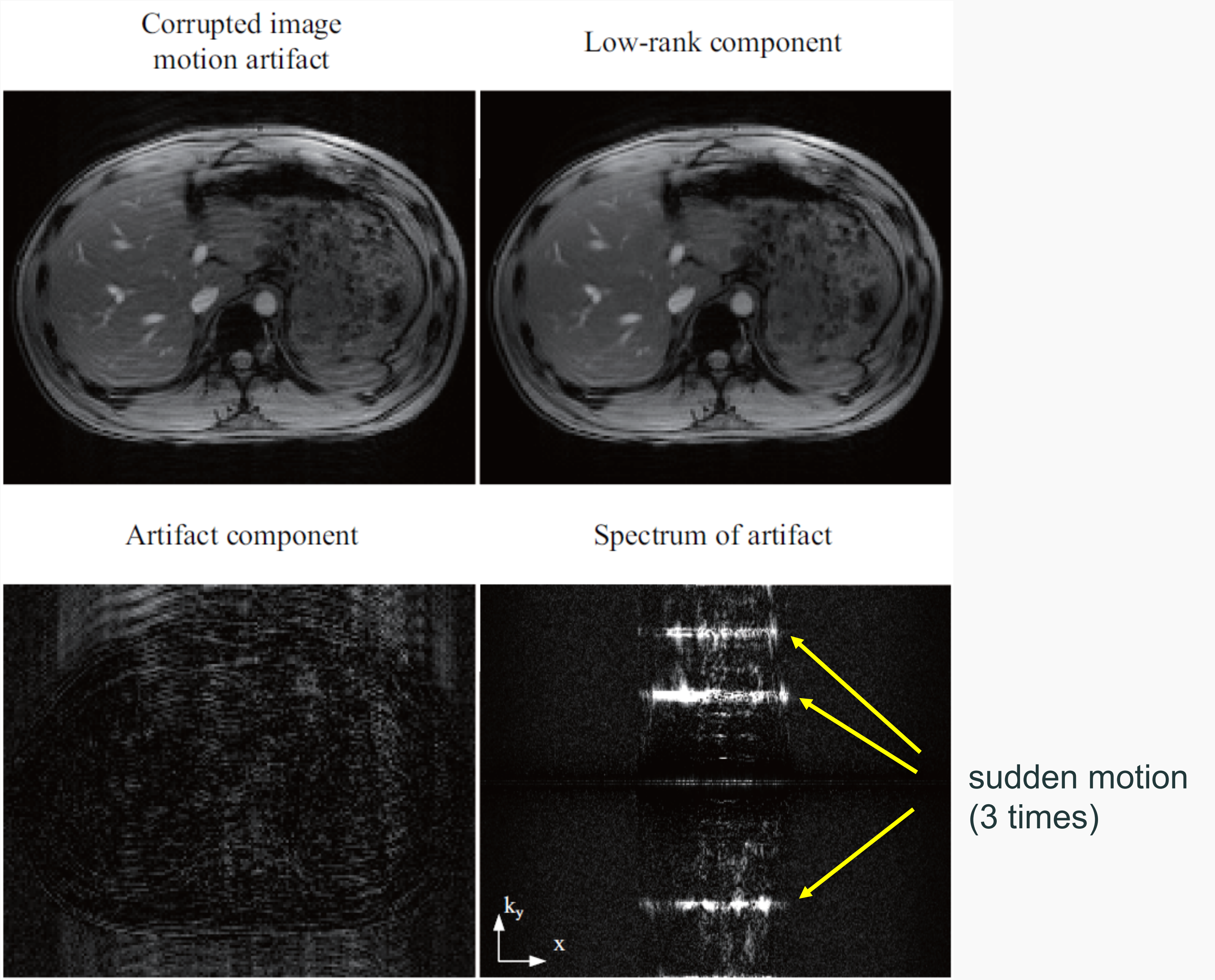

Cardiac Motion artifact

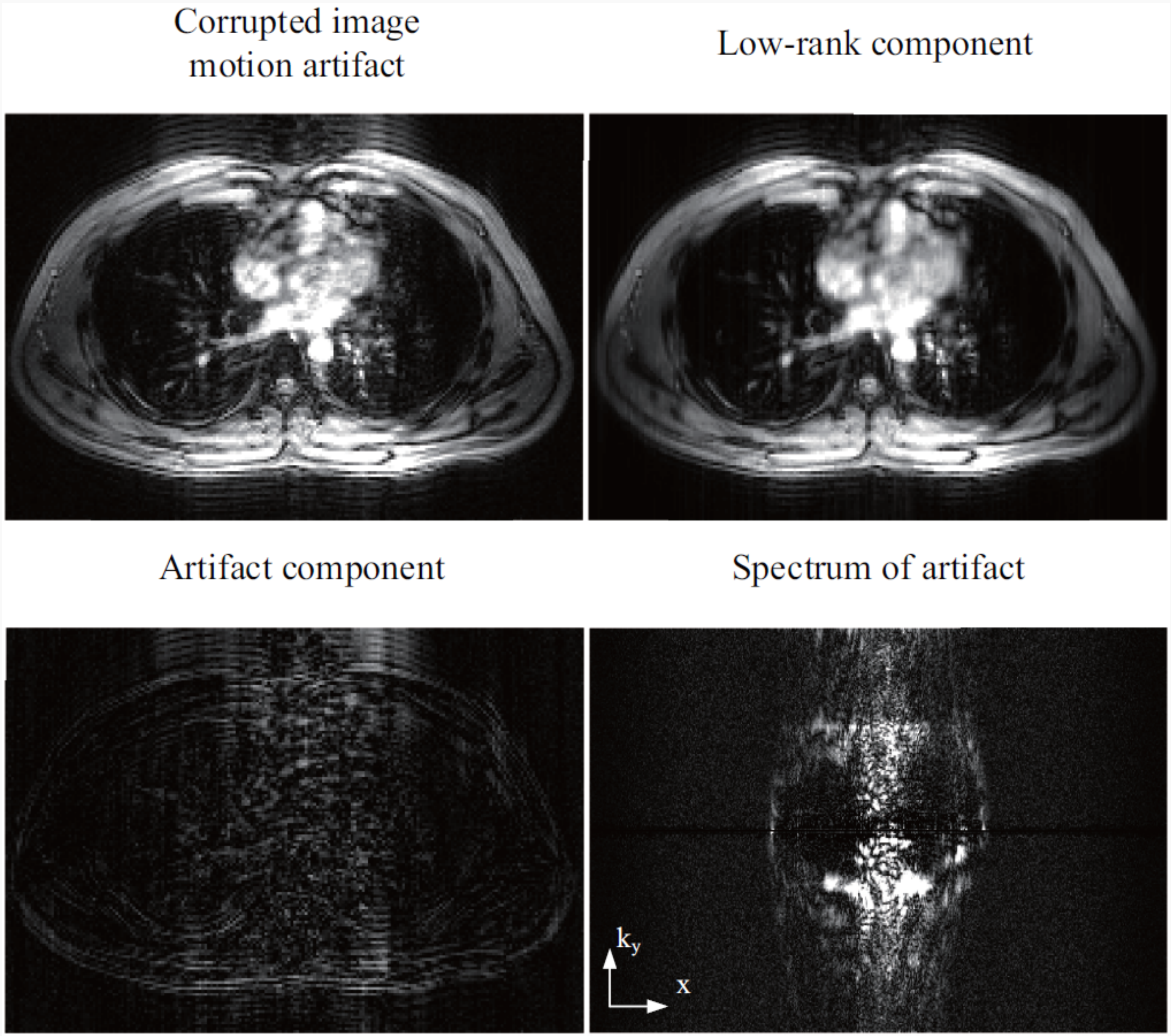

Zipper artifact

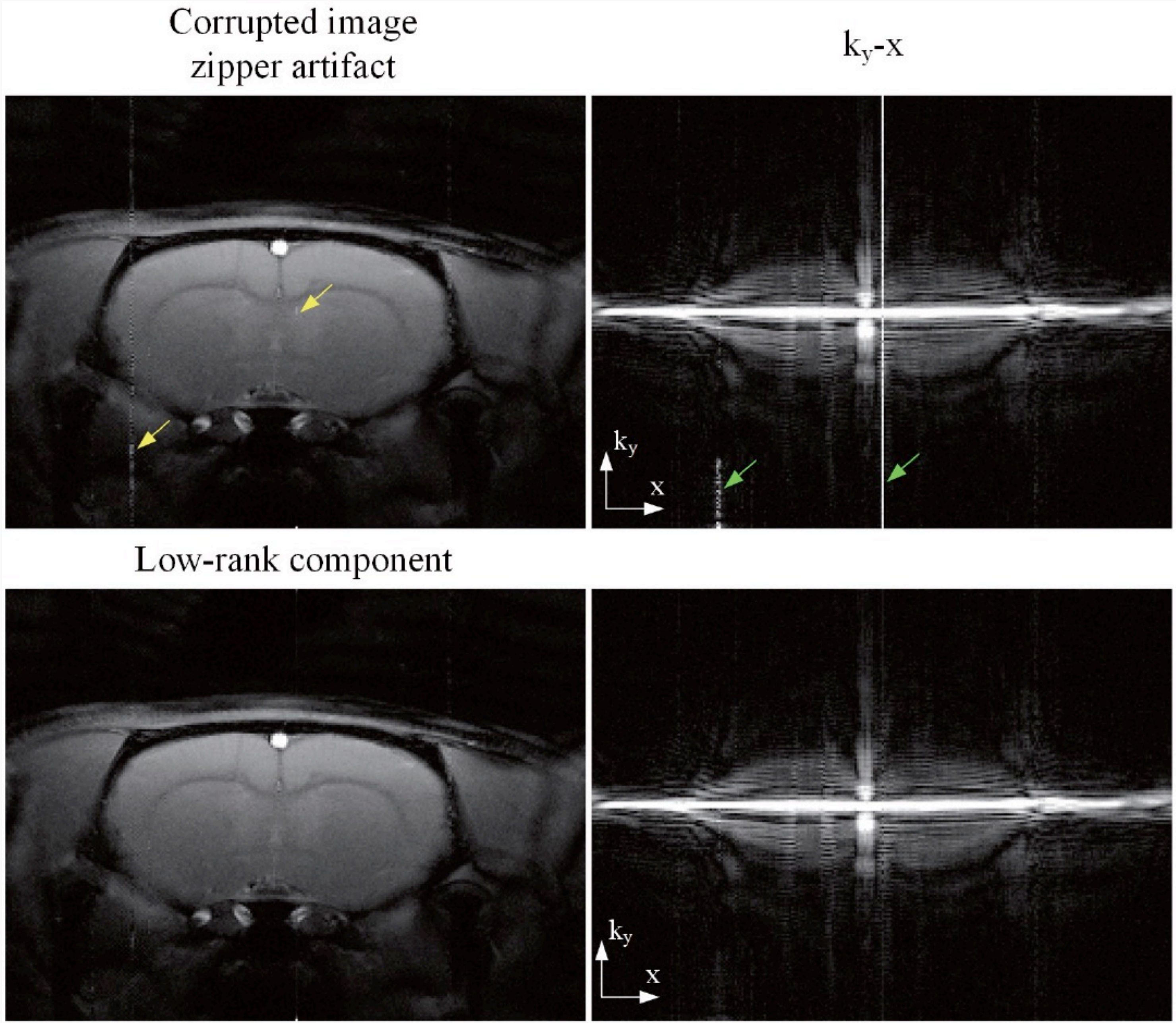

2-D herringbone (in-vivo)

before

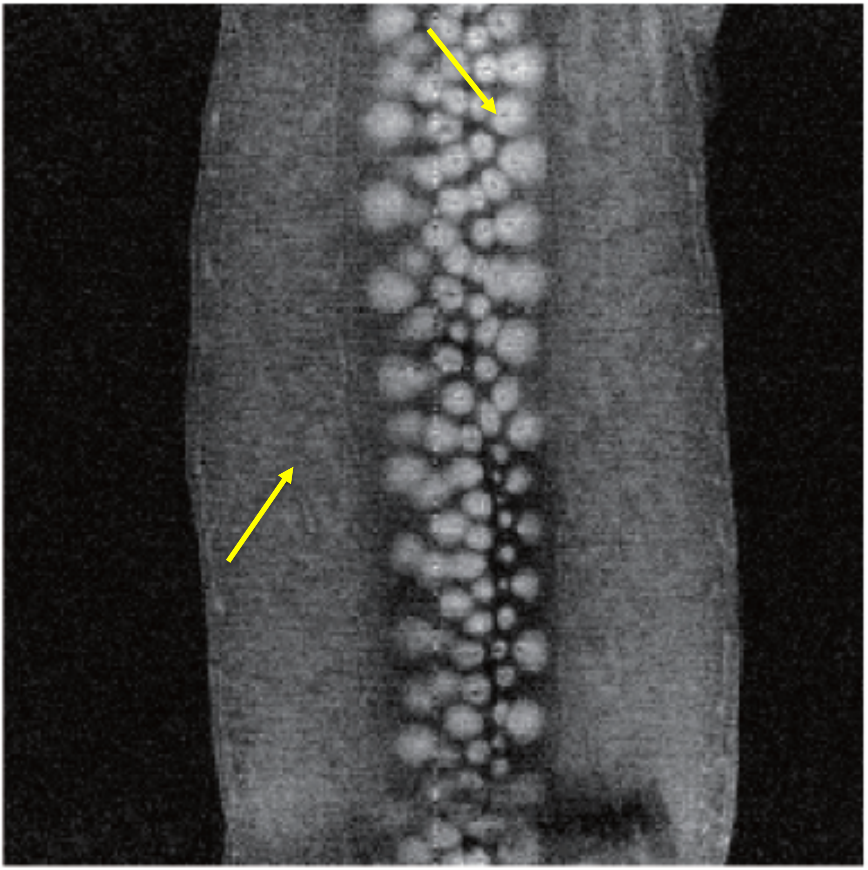

after

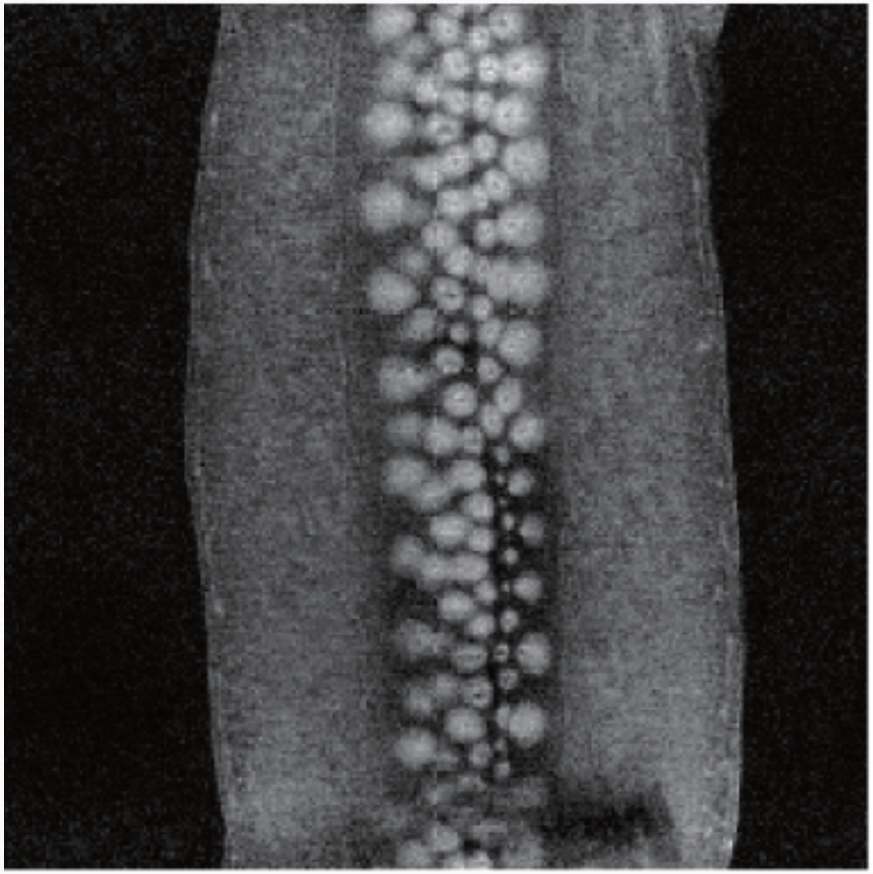

2-D herringbone (in-vivo)

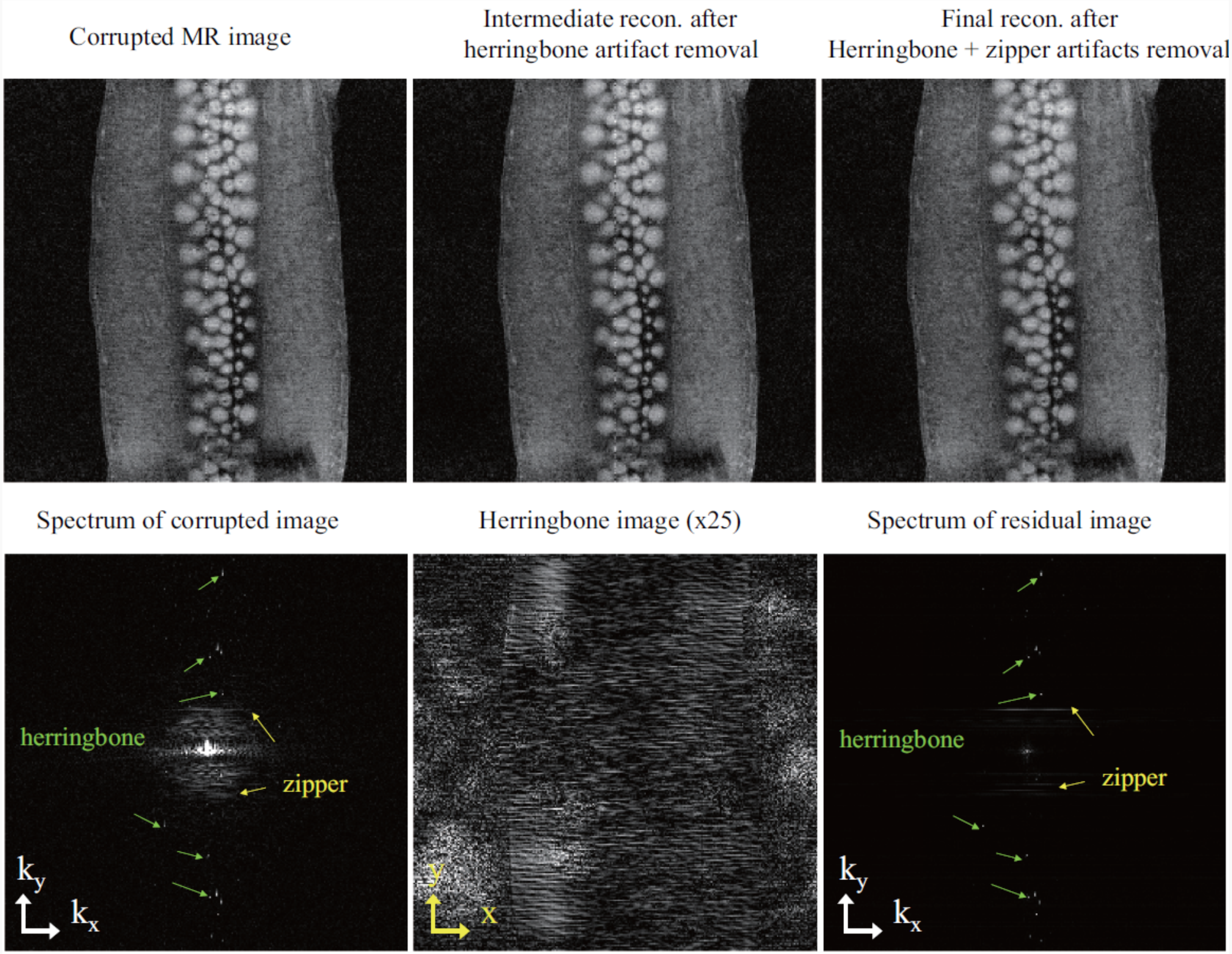

EPI Ghost artifact

In EPI, Gradient is distorted by eddy currents and this causes phase shift

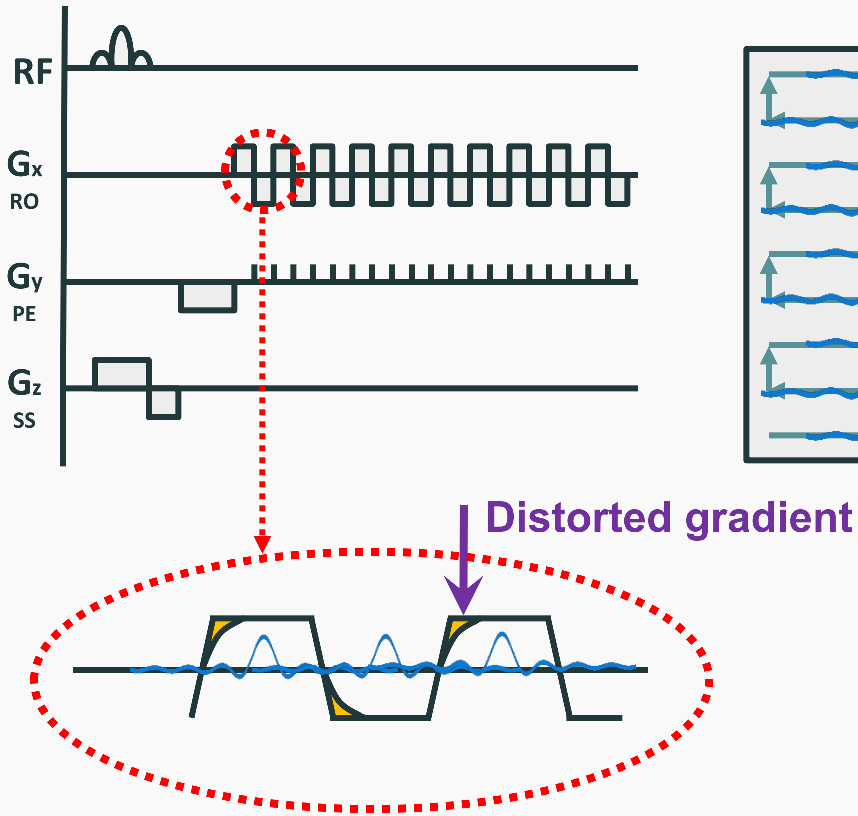

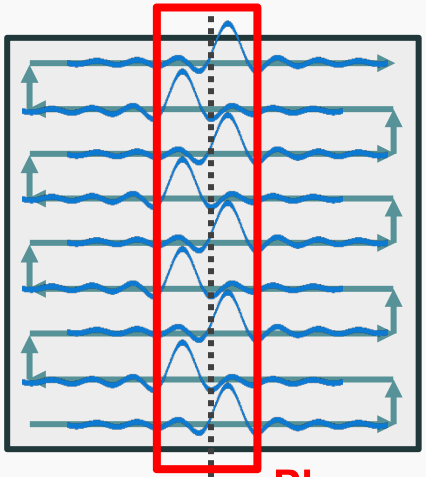

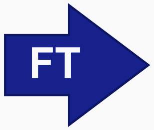

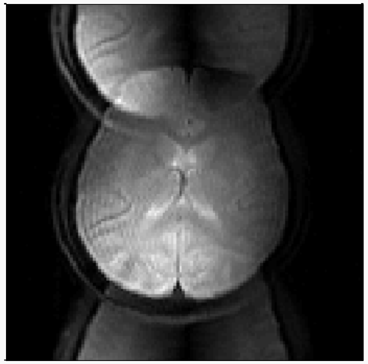

Even and odd echo mismatch causes ghost artifact!

Conventional correction

- **Navigator : pre-scan or reference scan**

Navigator-based

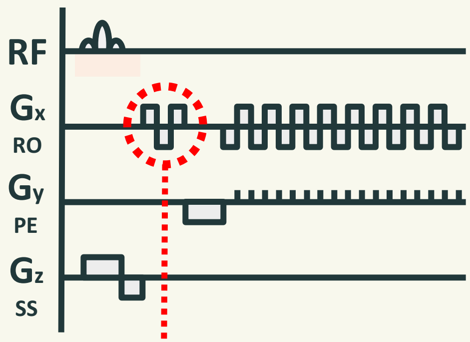

Without PE gradient

Calculate **difference** of phase between 1st -2nd line, 2nd -3rd line

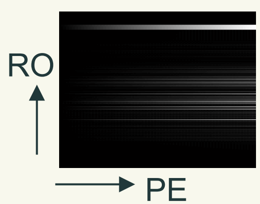

Make phase difference map

only possible to ***linear phase correction***

Navigator-free

- **Pulse sequence compensation**[1)]
- **Without any modification**[2)]
  - Using Parallel Imaging Information
  - others

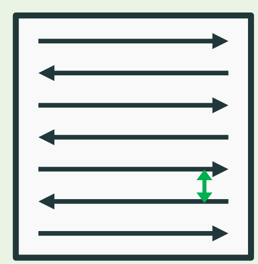

Calculate
Phase disparity
from EPI data itself

lower performance compared to the reference-based approaches

1) Xiang QS et al., MRM, 2007
Poser BA et al., MRM, 2013
2) Zhang et al., MRM, 2004
Kim YC et al., JMRI, 2007

EPI model

EPI data can be expressed as

N : Total # of echoes
n : Index of each line
x : Read-out
y : Phase-encoding

Echo time

$$S_n(k_x, k_y) = \int\int m(x,y) e^{j2\pi[\Delta f(x,y)((TE+(n-N/2)ESP)+(-1)^n(\frac{k_x}{\gamma G_x}))+k_x x+k_y y]} dxdy$$

Image intensity　Frequency offset　Echo spacing (time between each echo)

$$S_{n,+}(k_x, k_y) = \int\int m(x,y) e^{j2\pi[\Delta f(x,y)((TE+(n-N/2)ESP)+(\frac{k_x}{\gamma G_x}))+k_x x+k_y y]} dxdy$$

Virtual k-space (**even** signals)

$$= \int\int A\, e^{\left(j2\pi\Delta f(x,y)\frac{k_x}{\gamma G_x}\right)} \cdot e^{j2\pi(k_x x+k_y y)} dxdy$$

$$S_{n,-}(k_x, k_y) = \int\int m(x,y) e^{j2\pi[\Delta f(x,y)((TE+(n-N/2)ESP)-(\frac{k_x}{\gamma G_x}))+k_x x+k_y y]} dxdy$$

Different!

Virtual k-space (**odd** signals)

$$= \int\int A\, e^{\left(-j2\pi\Delta f(x,y)\frac{k_x}{\gamma G_x}\right)} \cdot e^{j2\pi(k_x x+k_y y)} dxdy$$

where $A = m(x,y)\exp\left(j2\pi\left[\Delta f(x,y)\left((TE+(n-N/2)ESP)\right)\right]\right)$

Sparsity of difference

The ghost generating phase term can be changed into a sine term

$$S_{n,\Delta}(k_x, k_y) = S_{n,+}(k_x, k_y) - S_{n,-}(k_x, k_y)$$

$$= \int\int A(x,y)\left(e^{j2\pi\Delta f(x,y)\frac{k_x}{\gamma G_x}} - e^{-j2\pi\Delta f(x,y)\frac{k_x}{\gamma G_x}}\right)e^{j2\pi(k_x x + k_y y)}\,\mathrm{d}x\mathrm{d}y$$

$$= \int\int A(x,y)2j\sin\left(2\pi\Delta f(x,y)\frac{k_x}{\gamma G_x}\right)e^{j2\pi(k_x x + k_y y)}\,\mathrm{d}x\mathrm{d}y$$

$$\sin\left(2\pi\Delta f(x,y)\frac{k_x}{\gamma G_x}\right) \simeq 2\pi\Delta f(x,y)\frac{k_x}{\gamma G_x}$$

$$S_{n,\Delta}(k_x, k_y) \simeq j2\pi k_x \int\int \frac{2}{\gamma G_x} A(x,y)\Delta f(x,y) e^{j2\pi(k_x x + k_y y)}\,\mathrm{d}x\mathrm{d}y$$

$$= \frac{2}{\gamma G_x}\mathcal{F}\left[\frac{\partial A(x,y)\Delta f(x,y)}{\partial x}\right]$$

Sparse

➪ **How can we use this sparsity?**

Sparsity of difference (Cont.)

$$S_{n,\Delta}(k_x, k_y) = \mathcal{F}(\textit{Sparse signal})$$

⇒ **Hankel structure matrix constructed by $S_{n,\Delta}(k_x, k_y)$ is low-ranked**

$$\mathscr{H}(S_{n,\Delta})\mathfrak{h} = (\mathscr{H}(S_{n,+}) - \mathscr{H}(S_{n,-}))\mathfrak{h} = \mathbf{0}$$

$$\Downarrow$$

$$\begin{bmatrix} \mathscr{H}(S_{n,+}) & \mathscr{H}(S_{n,-}) \end{bmatrix} \begin{bmatrix} \mathfrak{h} \\ -\mathfrak{h} \end{bmatrix} = \mathbf{0}$$

Low rank structured matrix completion algorithm

EPI ghost correction Problem → **k-space interpolation Problem using low rank structure**

Reconstruction flow

- **SE-EPI in-vivo data, 128x128 matrix size, 6/8 partial Fourier**

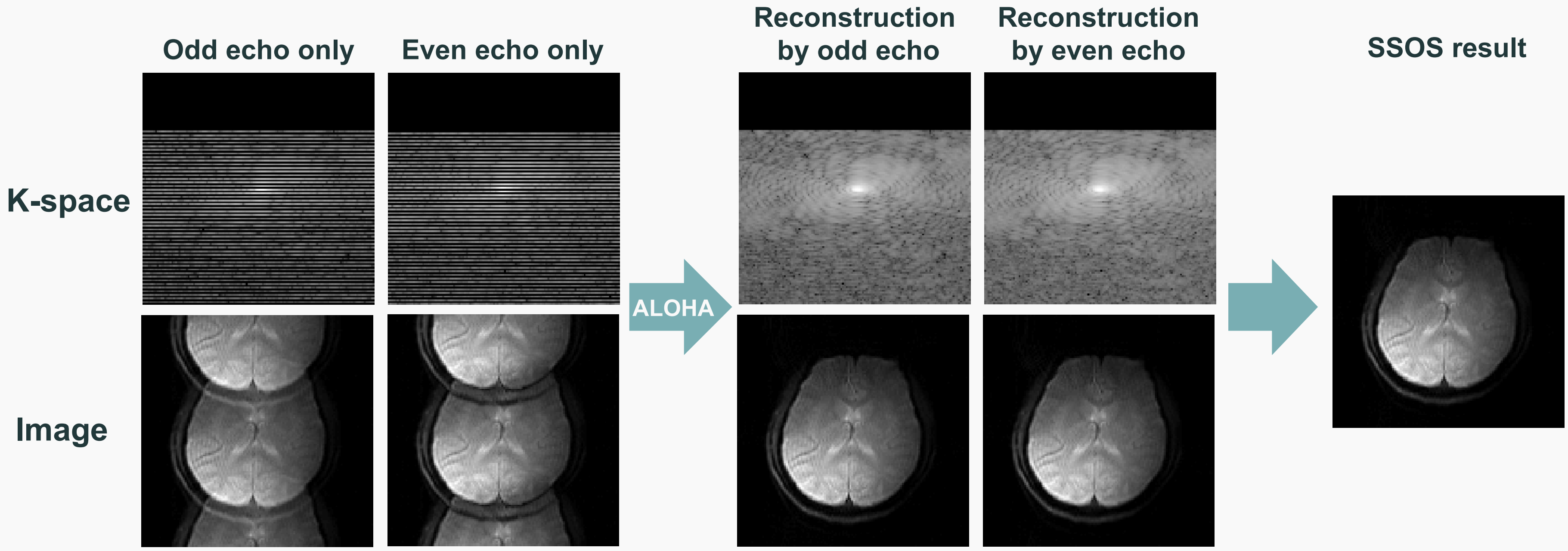

Result : GRE-EPI in-vivo

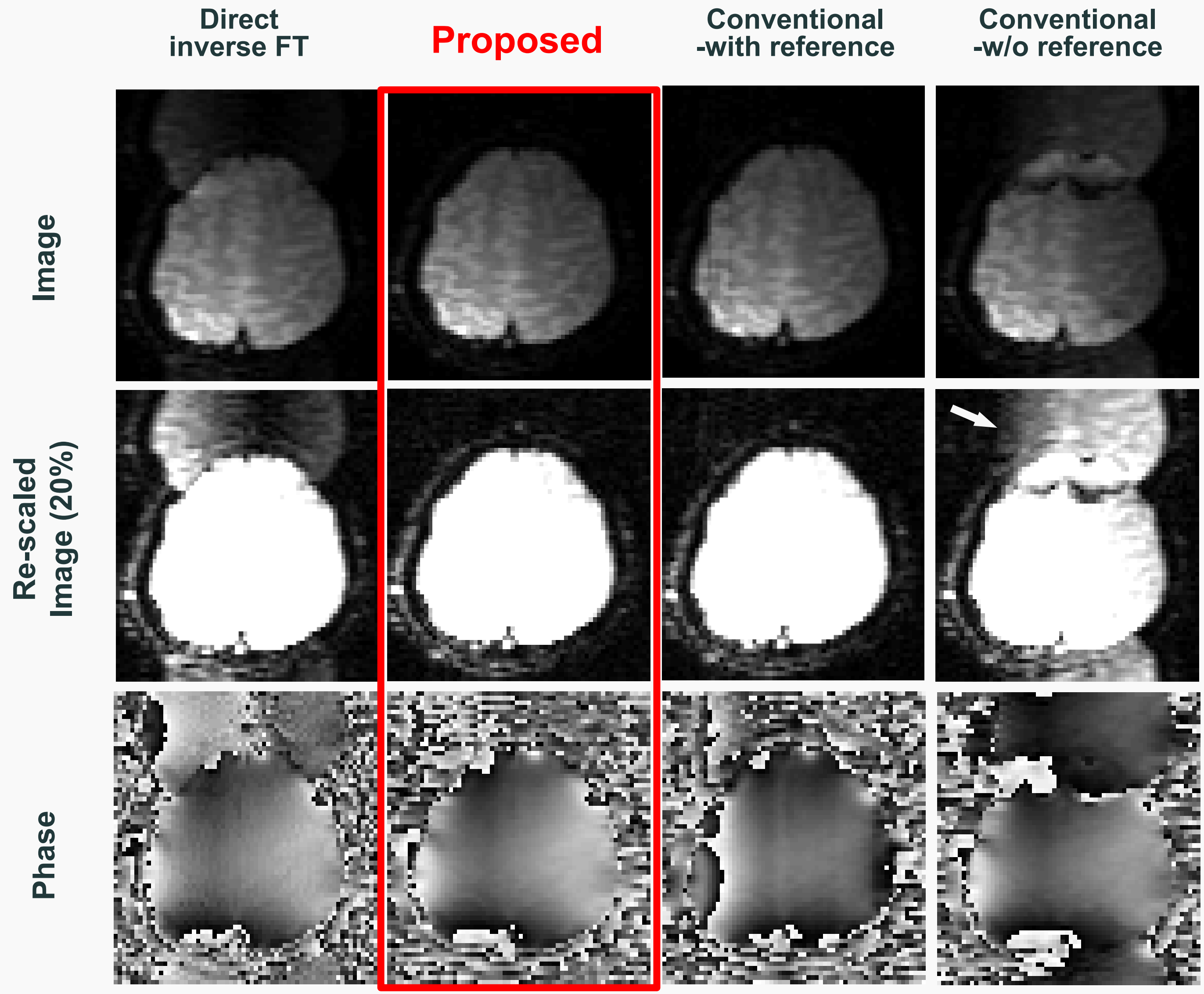

Result : fMRI analysis

fMRI analysis of GRE-EPI using SPM

- Pair hand squeezing stimulation
  ⇒ Motor cortex activation
- Familywise error, $p \leq 0.05$

Conventional

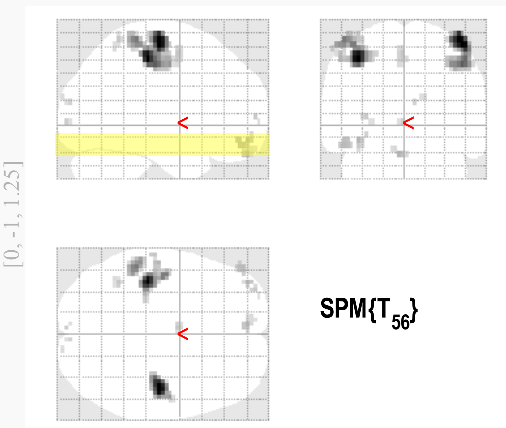

Proposed

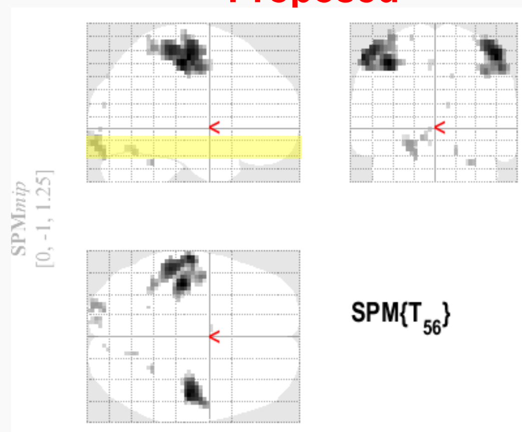

Conventional

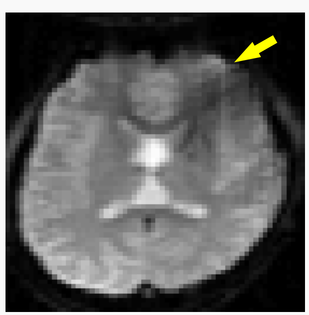

Proposed (multi-coil)

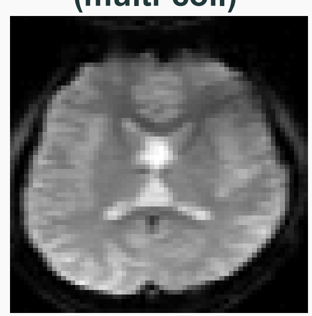

Proposed (single-coil)

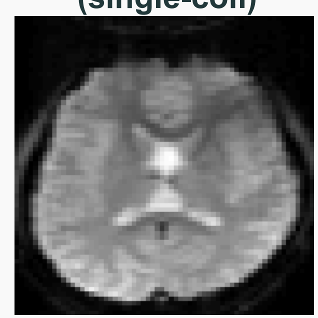

Applications to Image Processing

Inpainting & Impulse noise removal

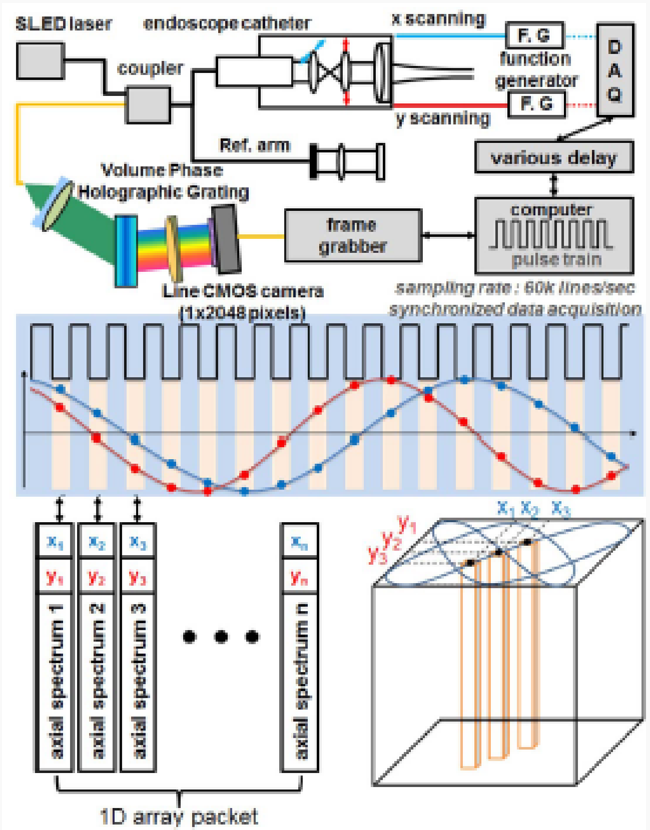

ig. 2. (Color online) 3D SD-OCT image reconstruction

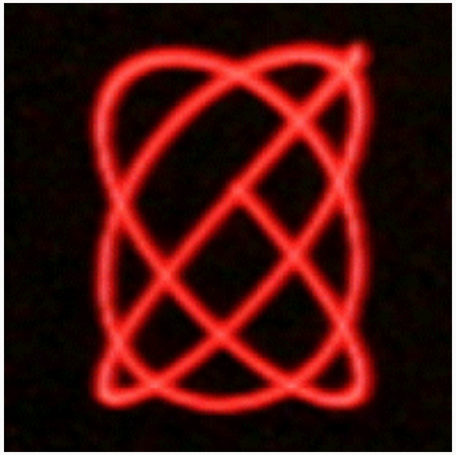

Spectral Domain Sparsity

Smoothness, texture, pattern

Sparse spectrum

Smooth patch

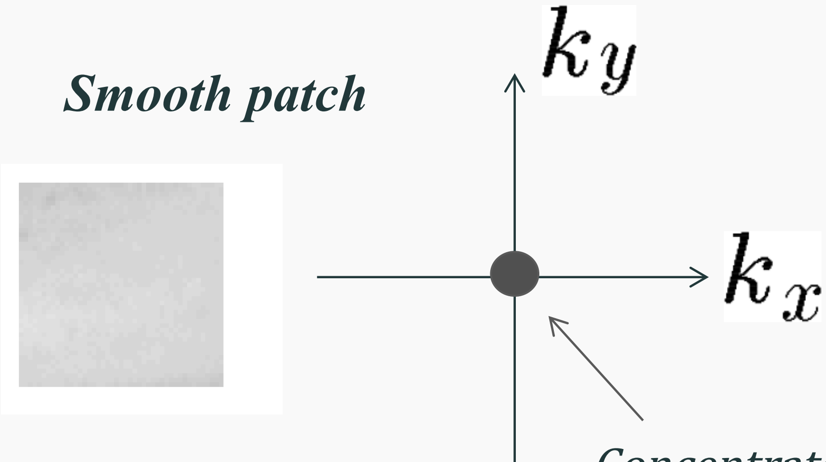

Concentrated at DC

Edge patch

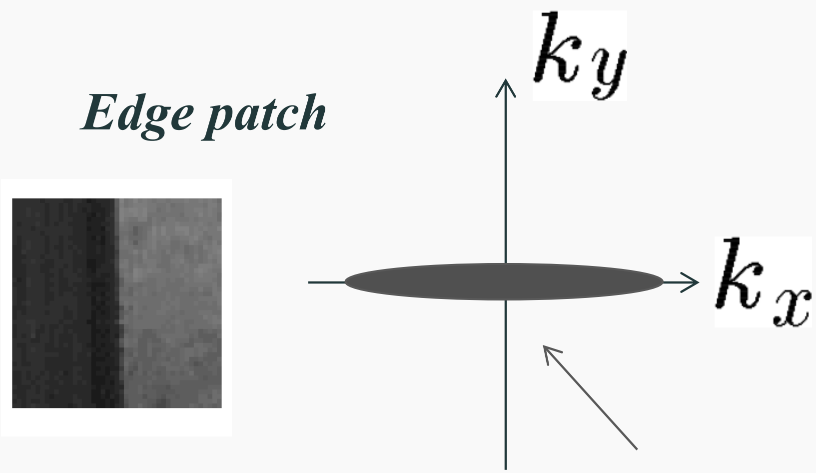

Elongated along Perpendicular to edge

Texture patch

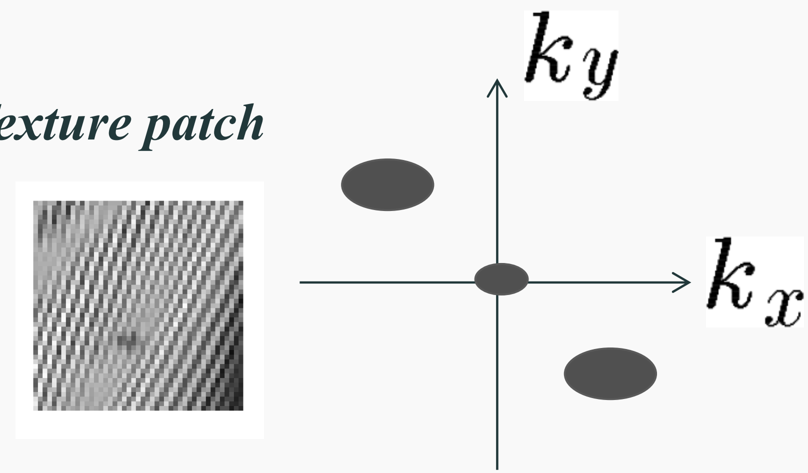

Distributed orthogonally w.r.t. texture

2-D Hankel matrix

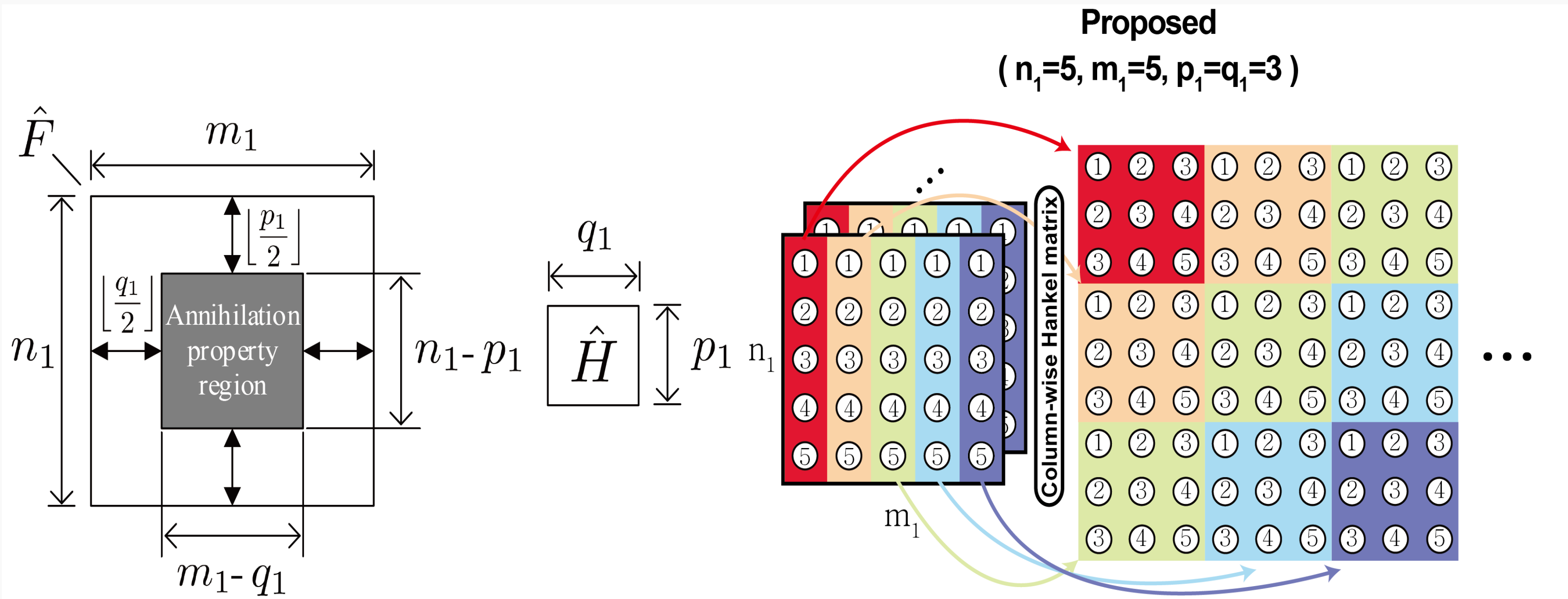

Hankel Matrix construction

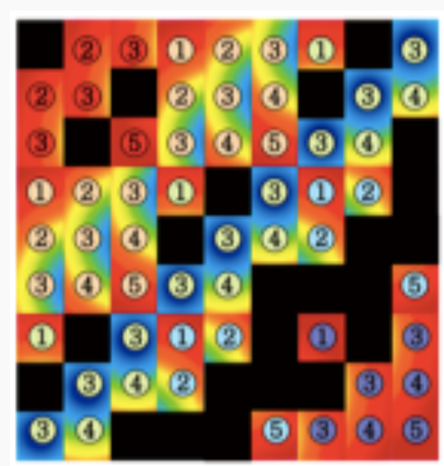

Why patch processing ?

- *Spectrum changes for each patch*
- *Need to adapt the local Image statistics*

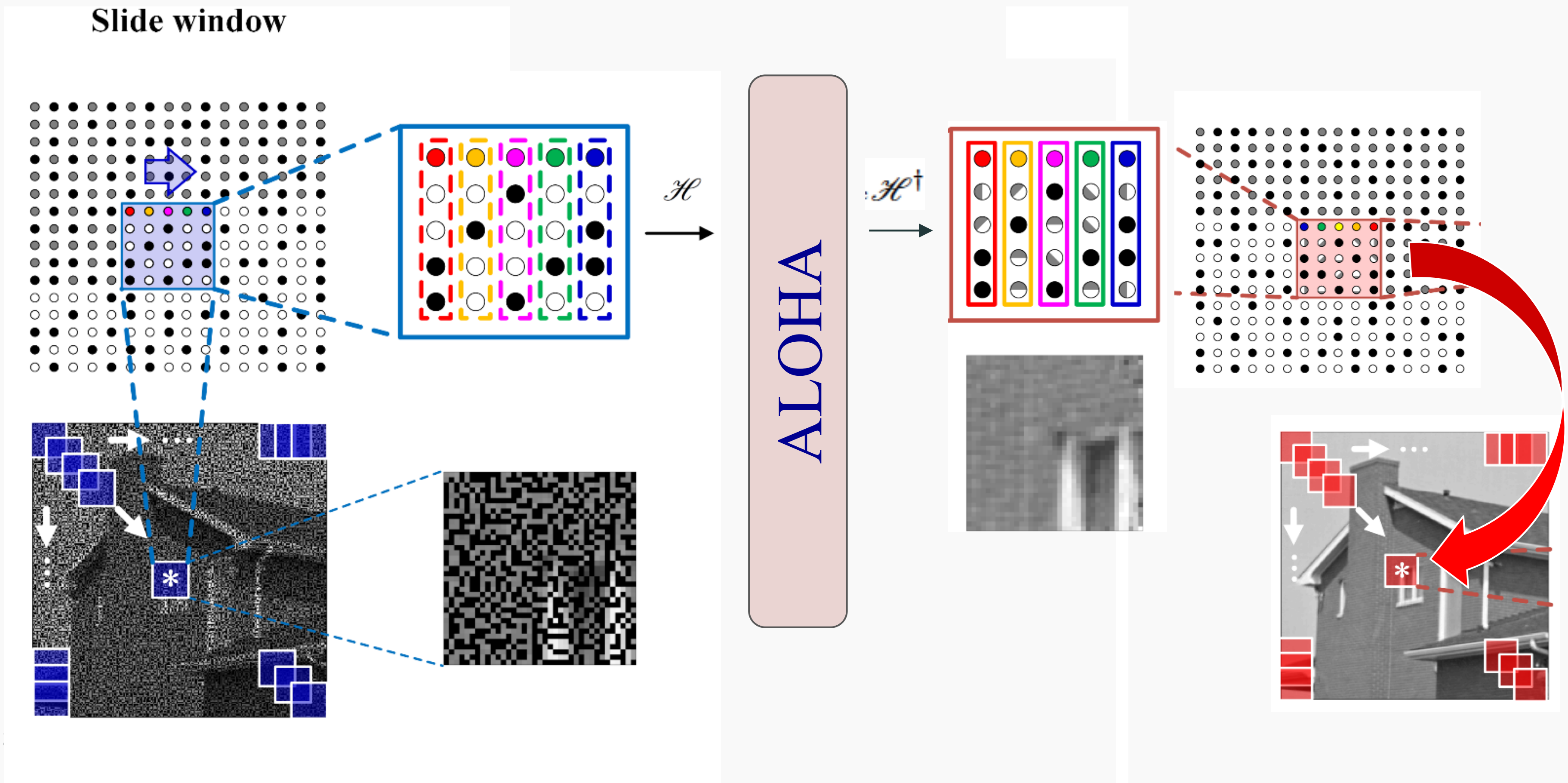

Rotation invariant sparsity

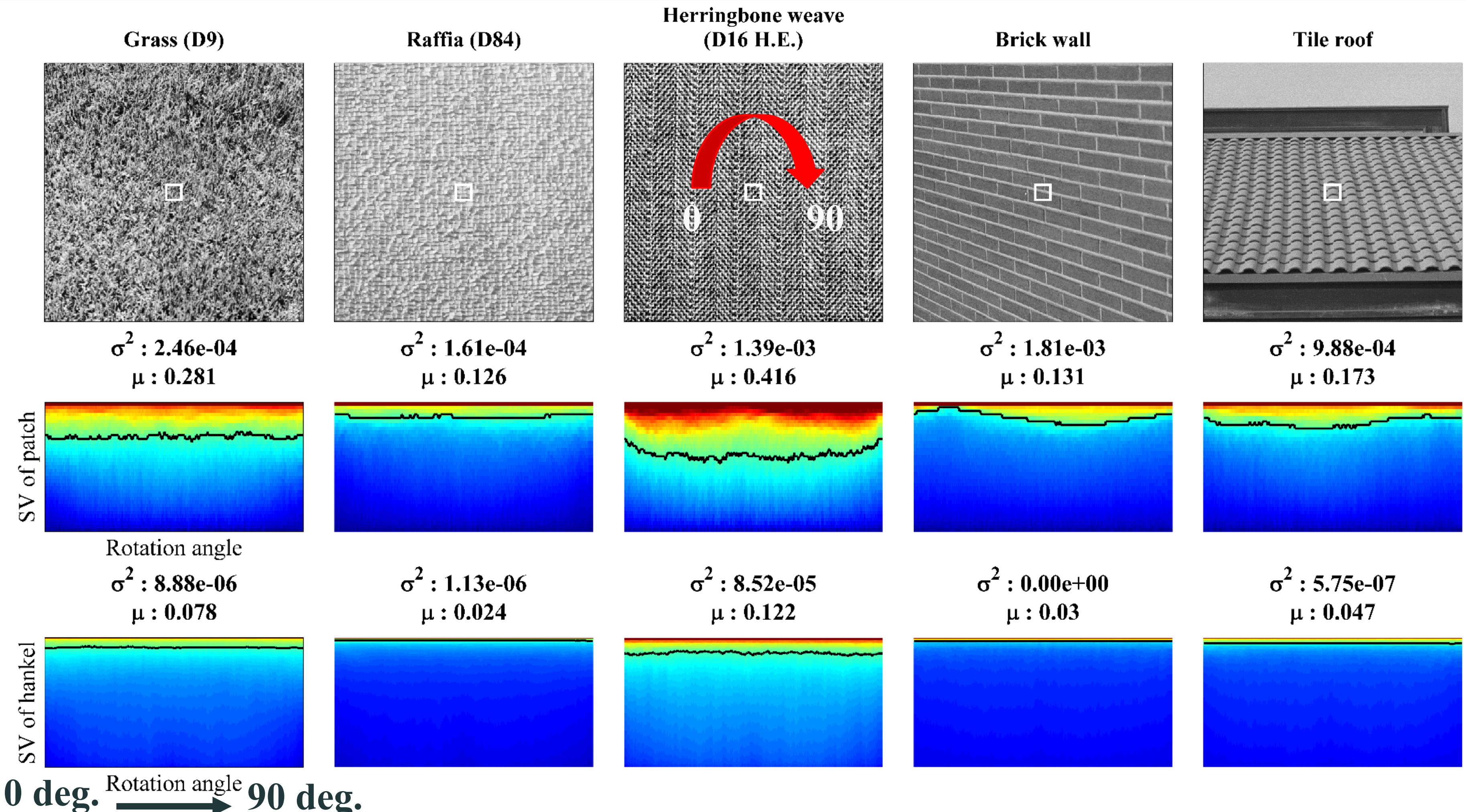

Hankel structured matrix is intrinsic low rank !!

Experimental results (x5)

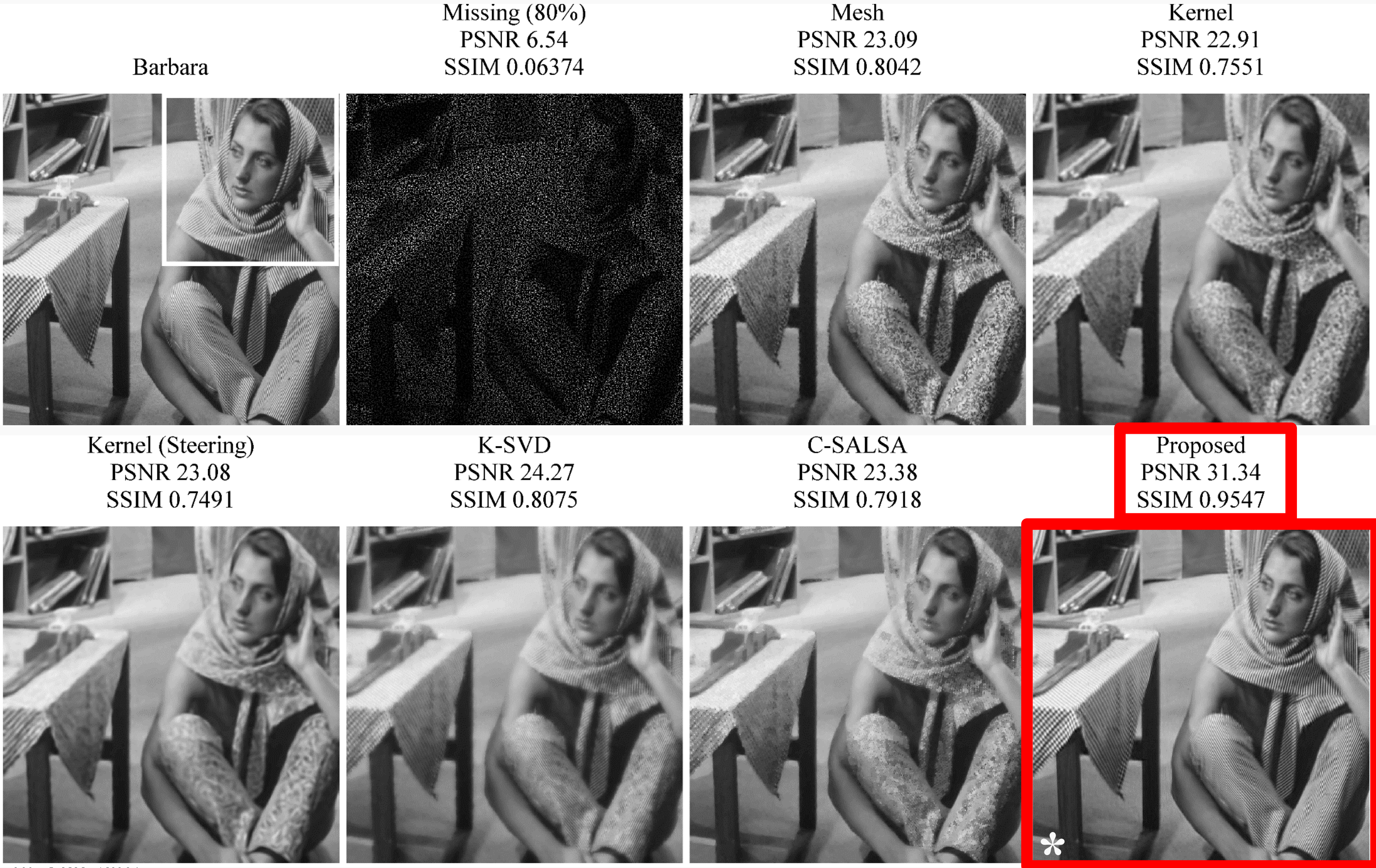

Experimental results (x5)

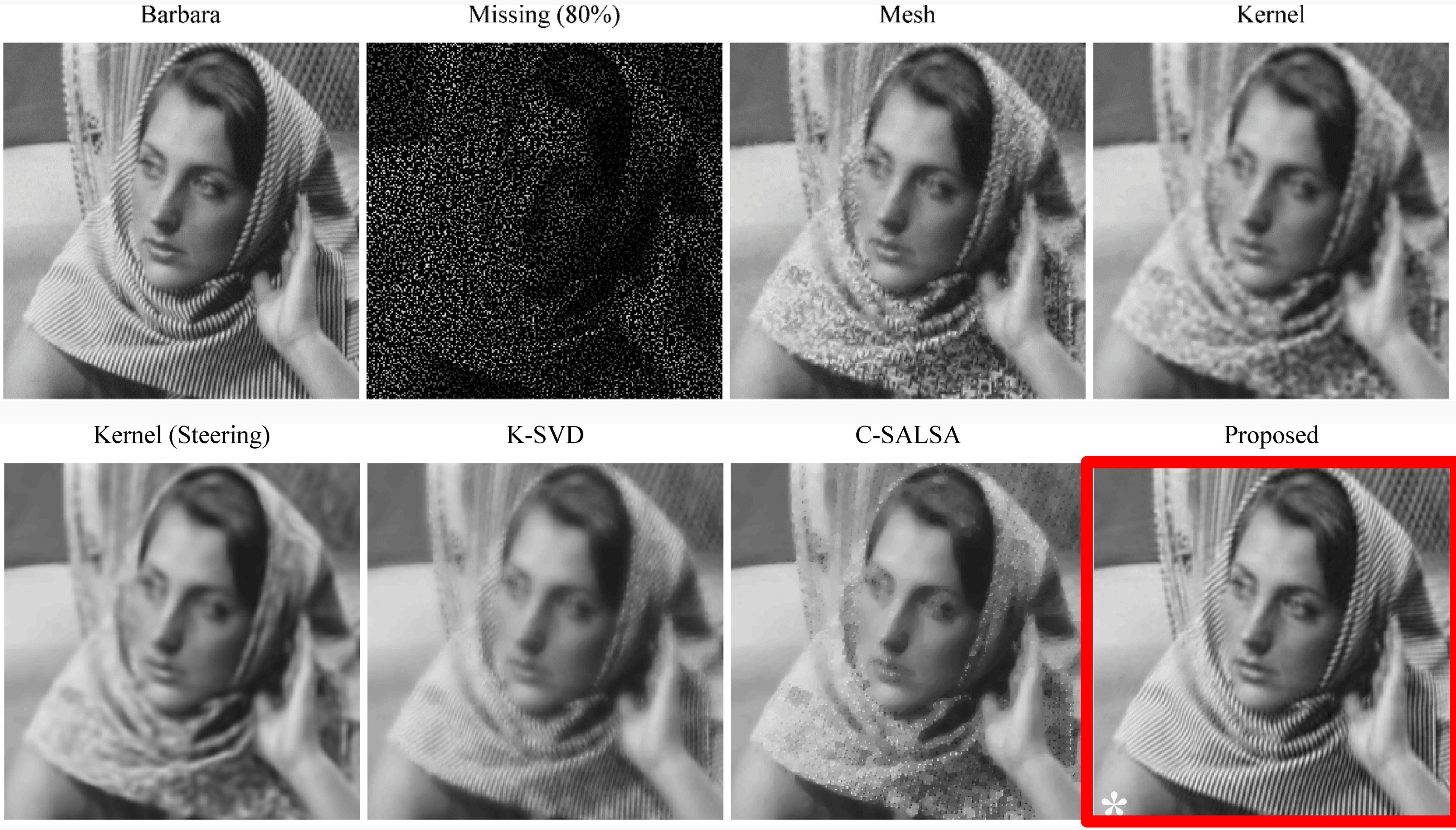

Text inlayed image reconstruction

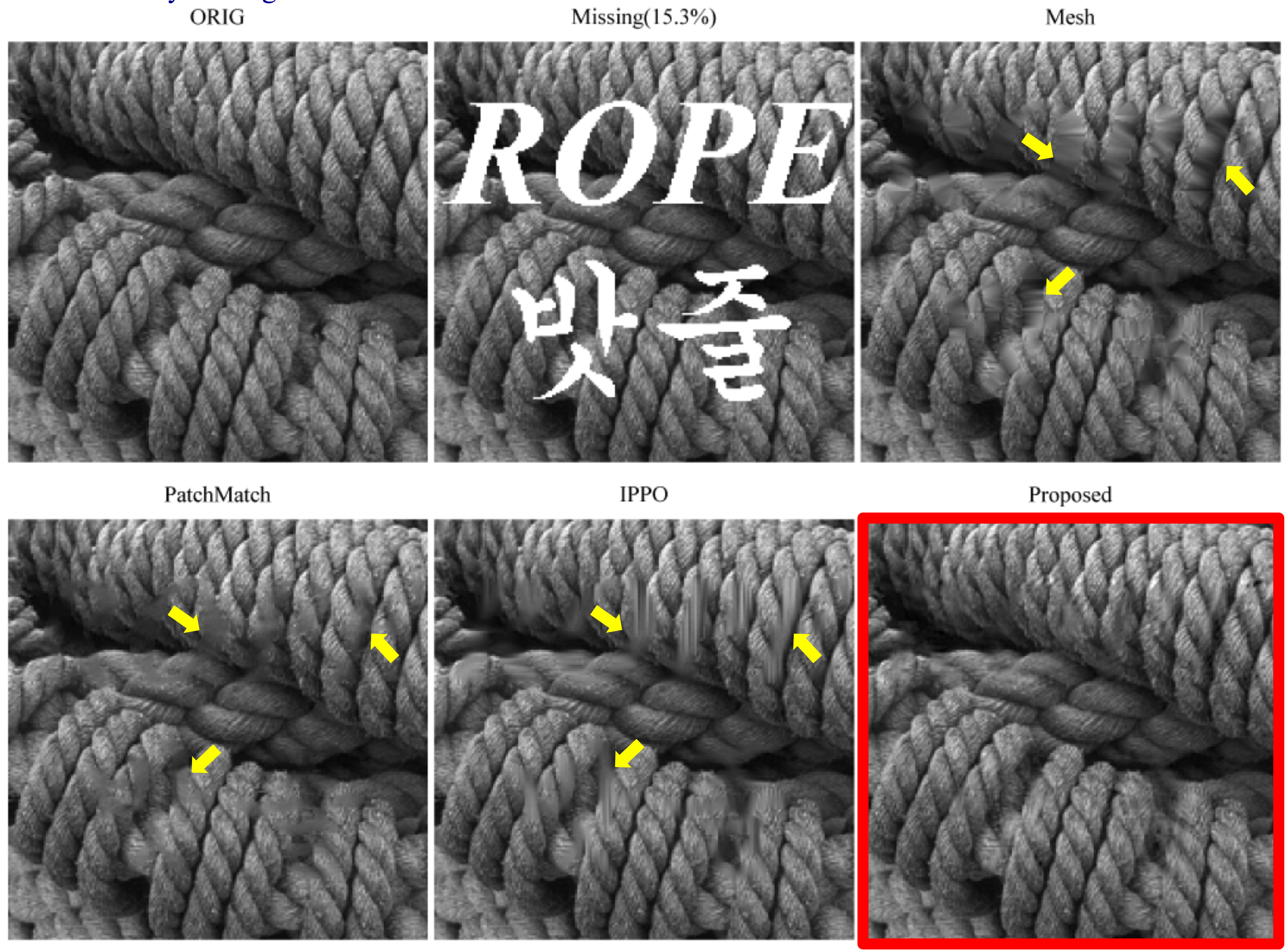

Line scratches

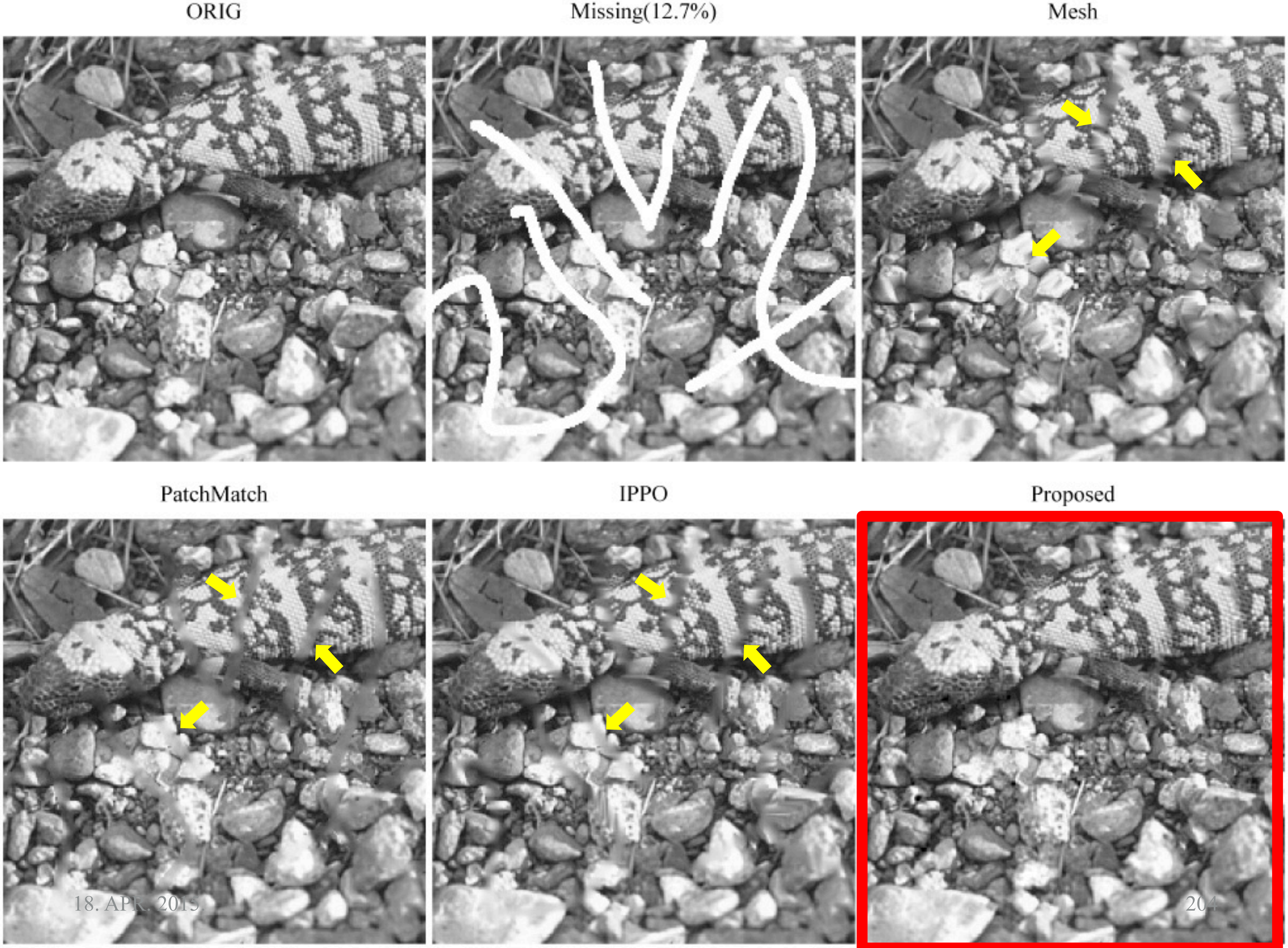

Object removal

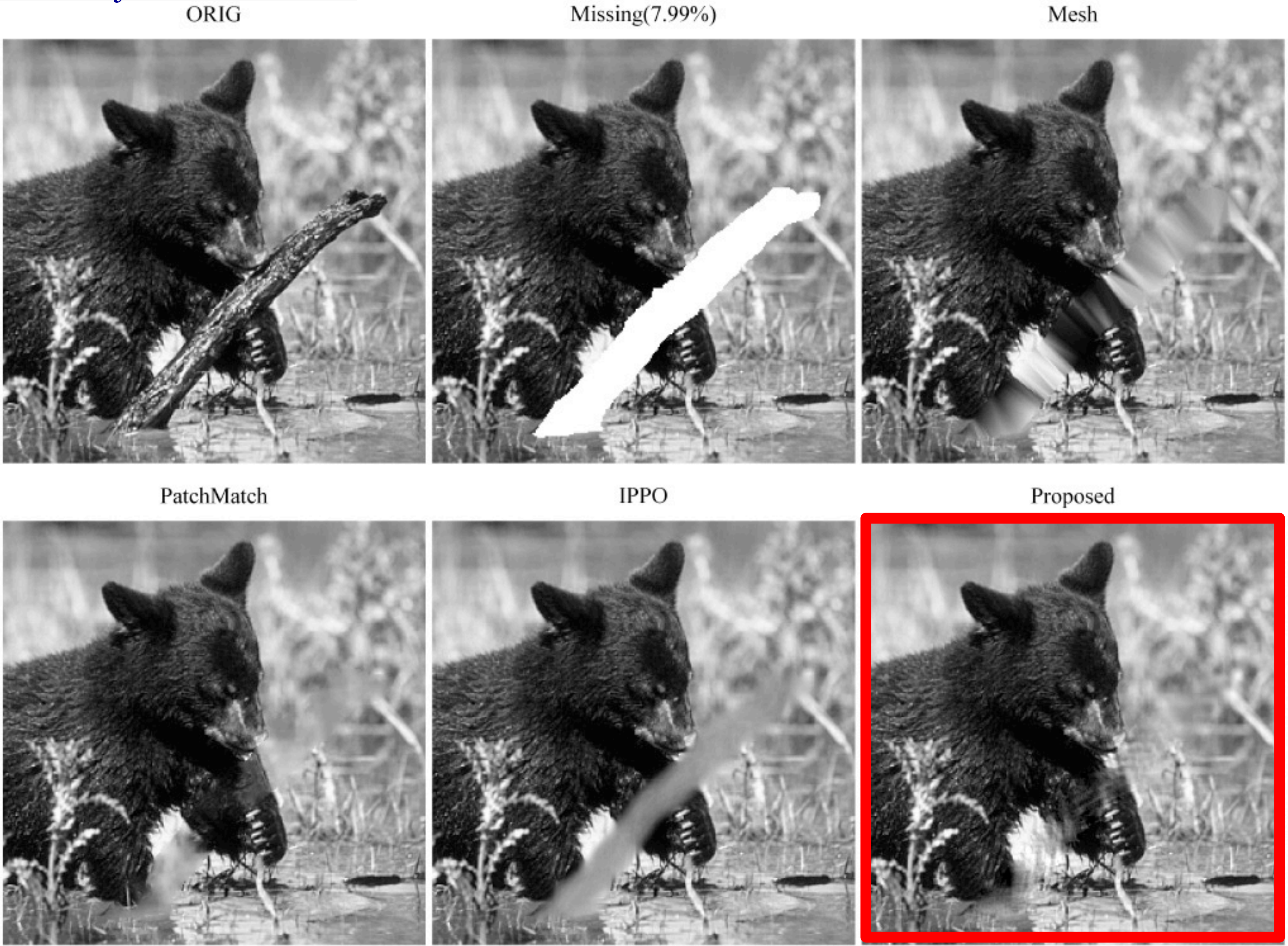

*K.H. Jin, et. al, IEEE TIP (2015)

Impulse Noise Removal

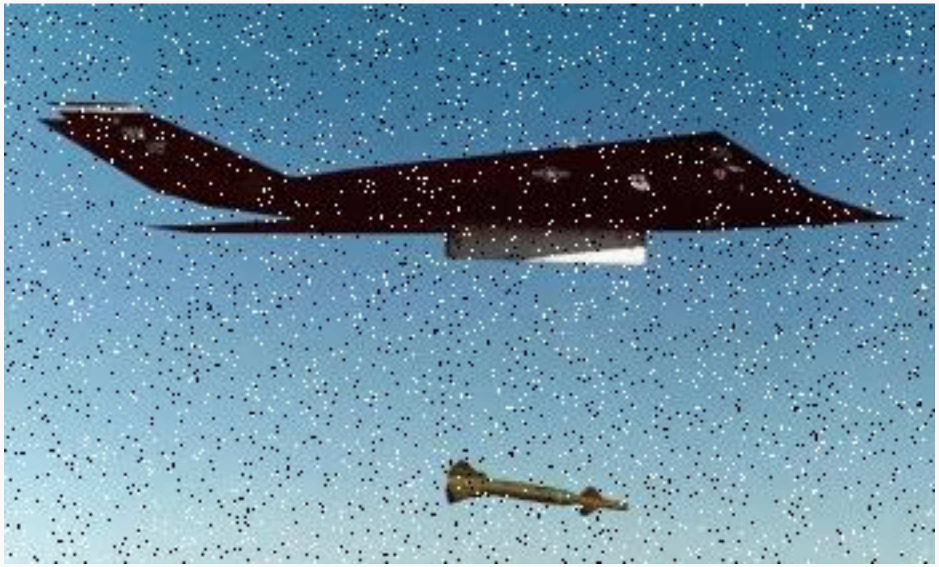

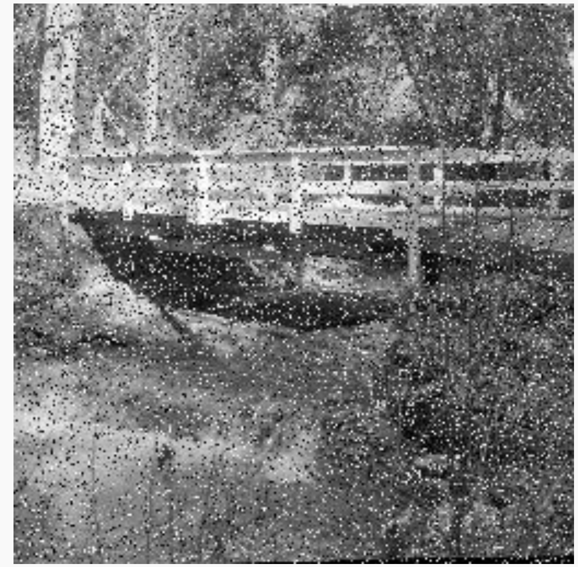

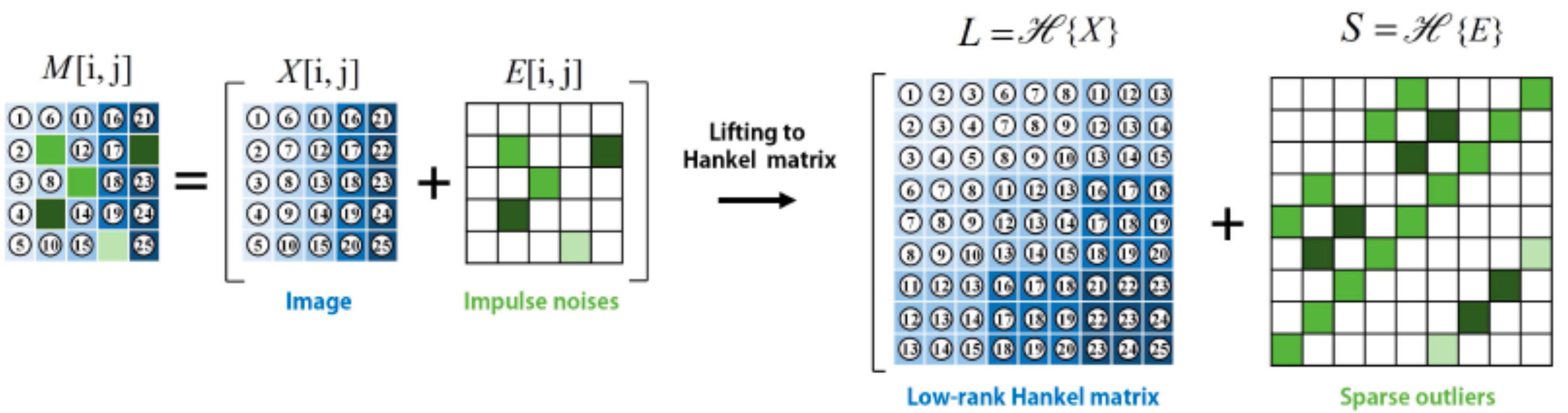

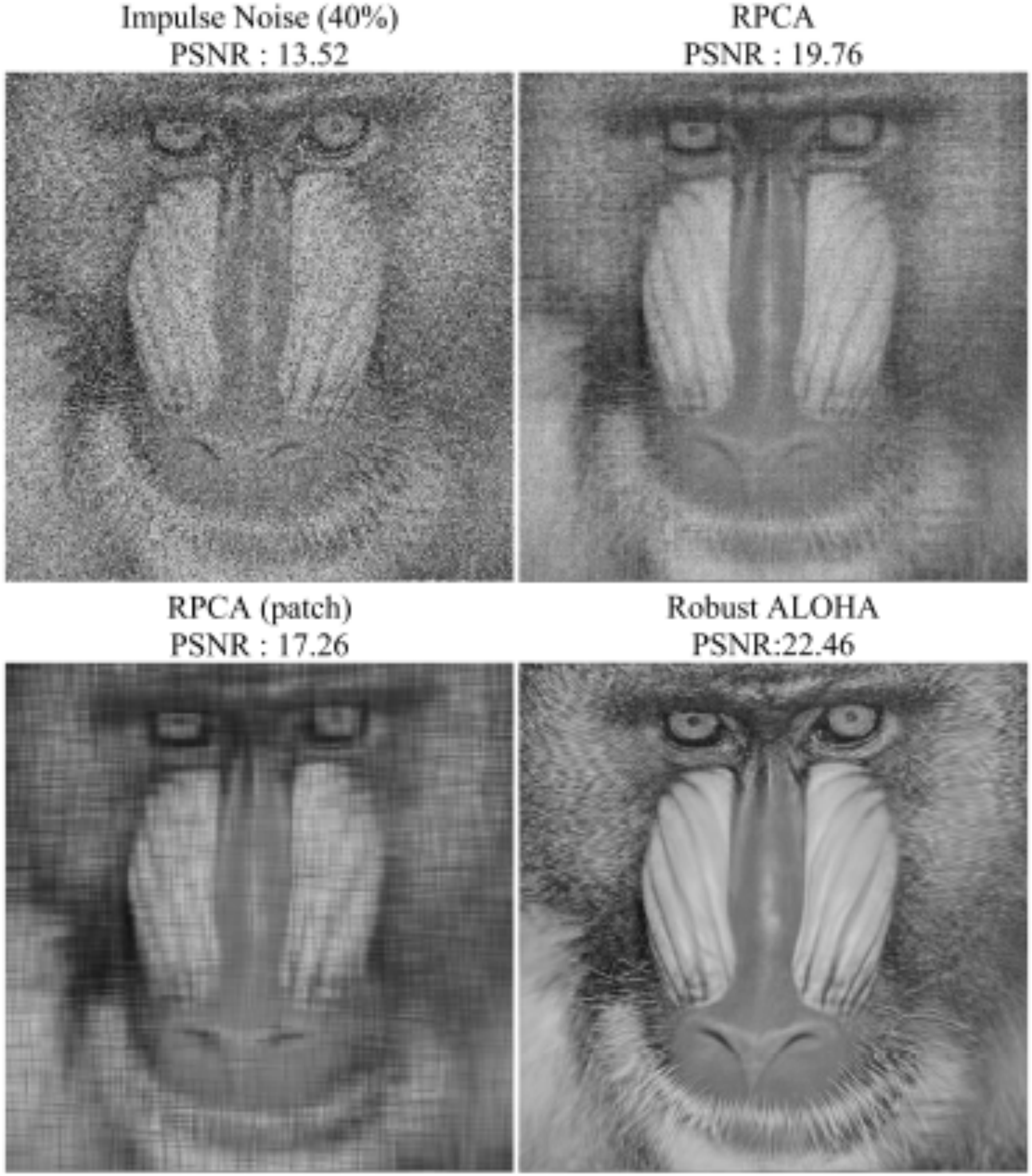
Impulse Noise (40%)
PSNR : 13.52
RPCA
PSNR : 19.76
RPCA (patch)
PSNR : 17.26
Robust ALOHA
PSNR:22.46

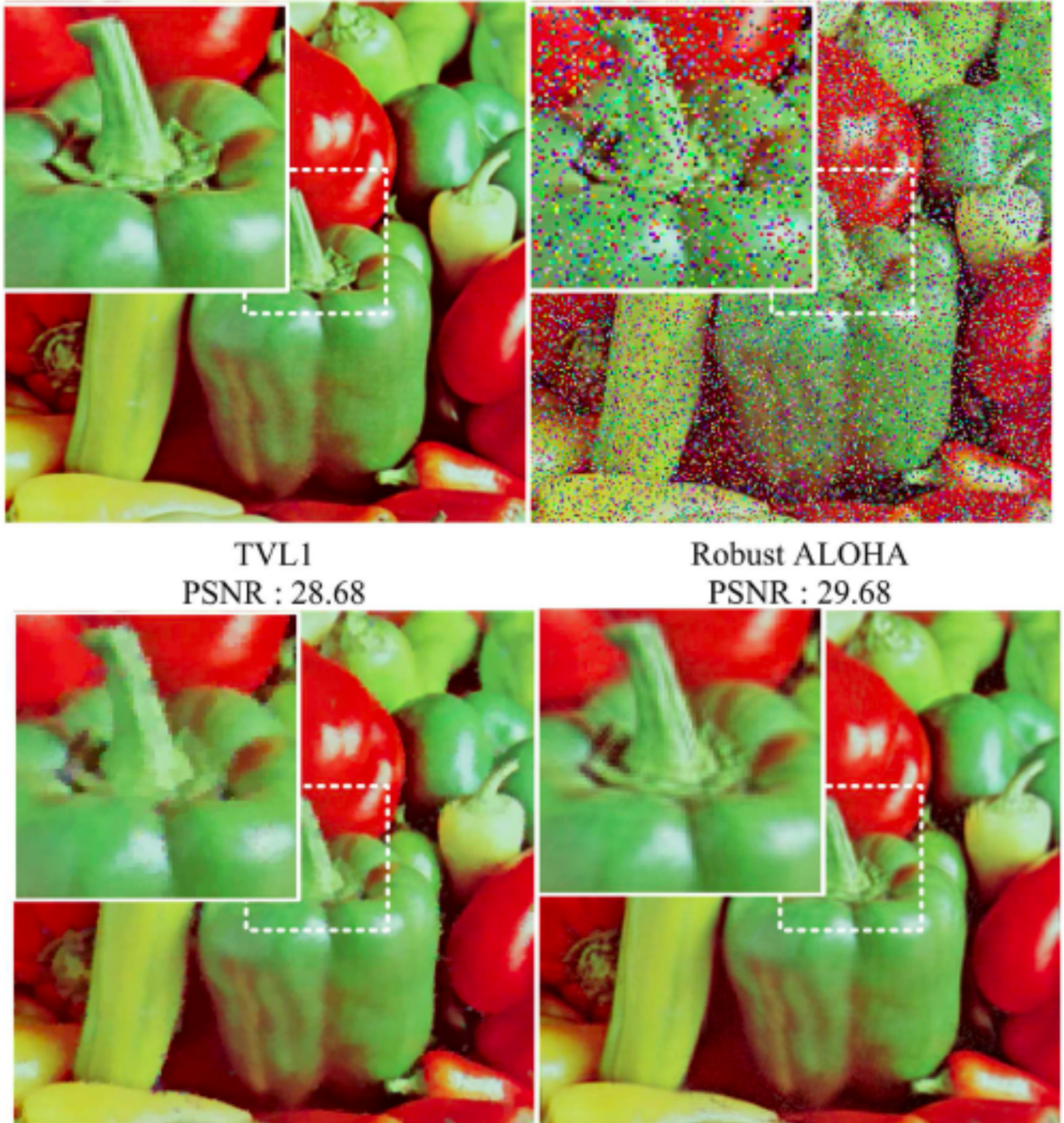
TVL1
PSNR : 28.68
Robust ALOHA
PSNR : 29.68

Application to B-mode US Imaging

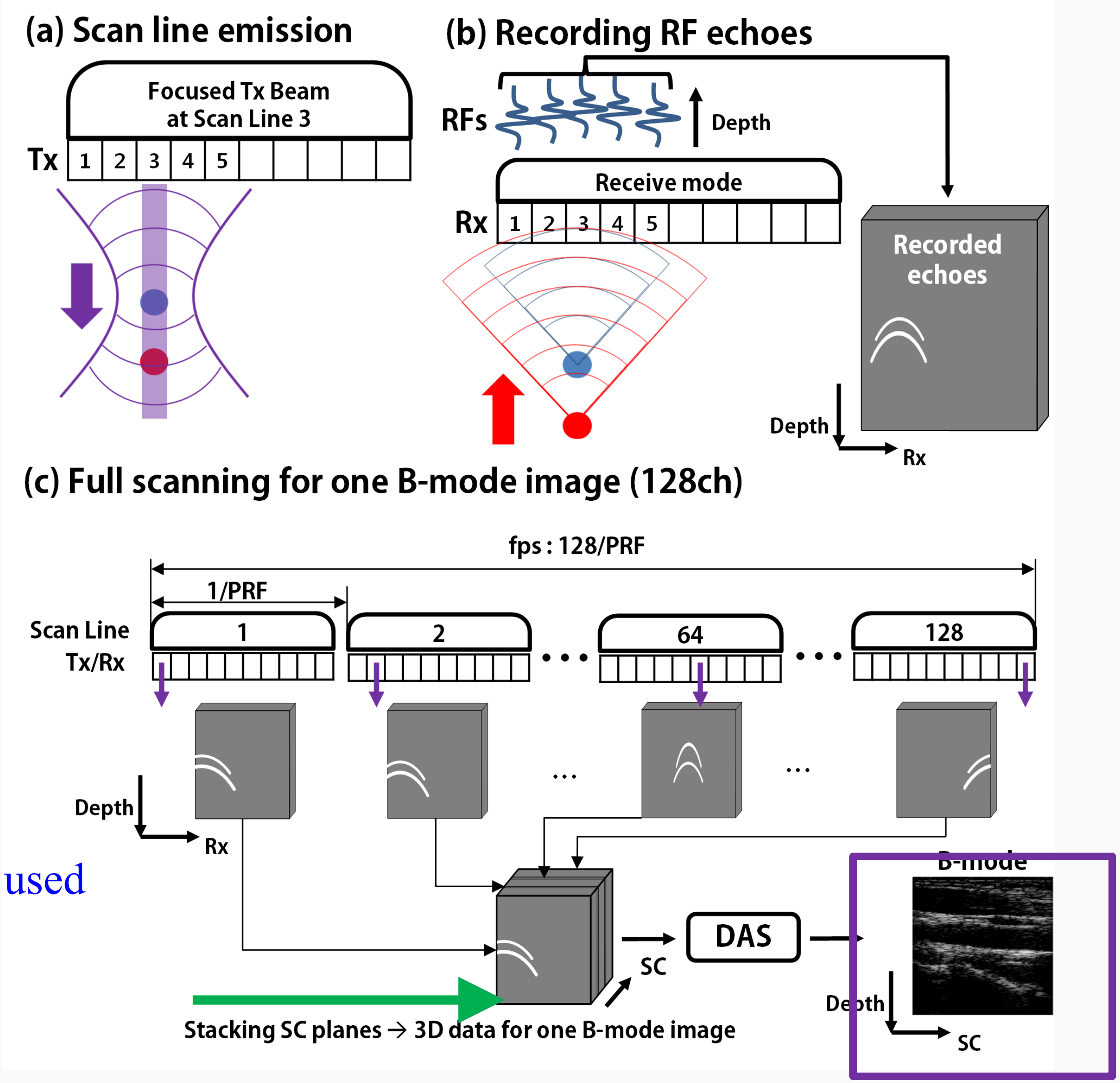

All Rx should be used

→ high power consumption, High data rate

1. Probes deliver beamformed B-mode image, only.

2. After DAS, raw measurements discarded.

Sub-sampled Dynamic Aperture B-mode Imaging

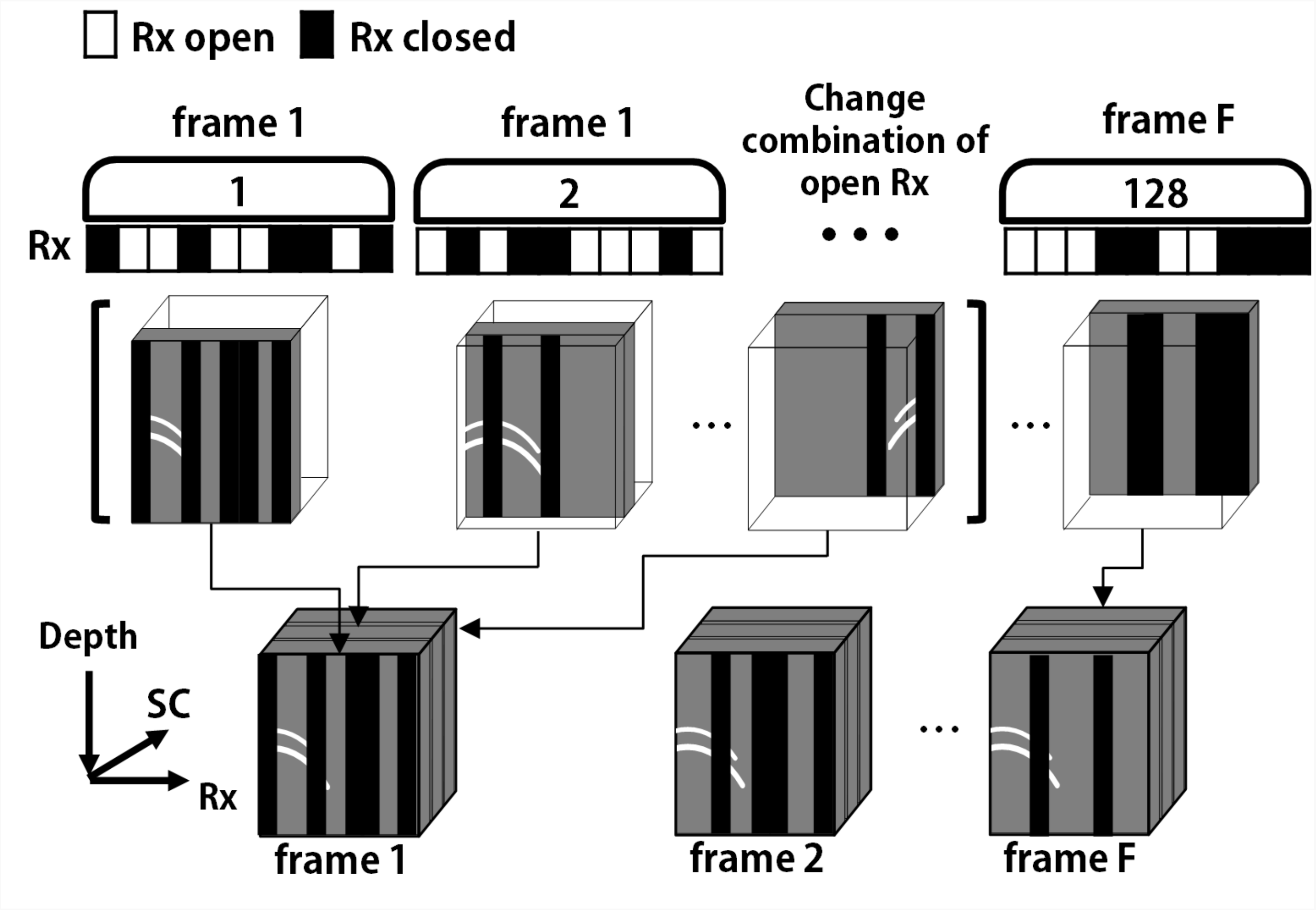

Low-Rankness of B-mode US Data

Temporal slices of
Pre-beamformed RF data

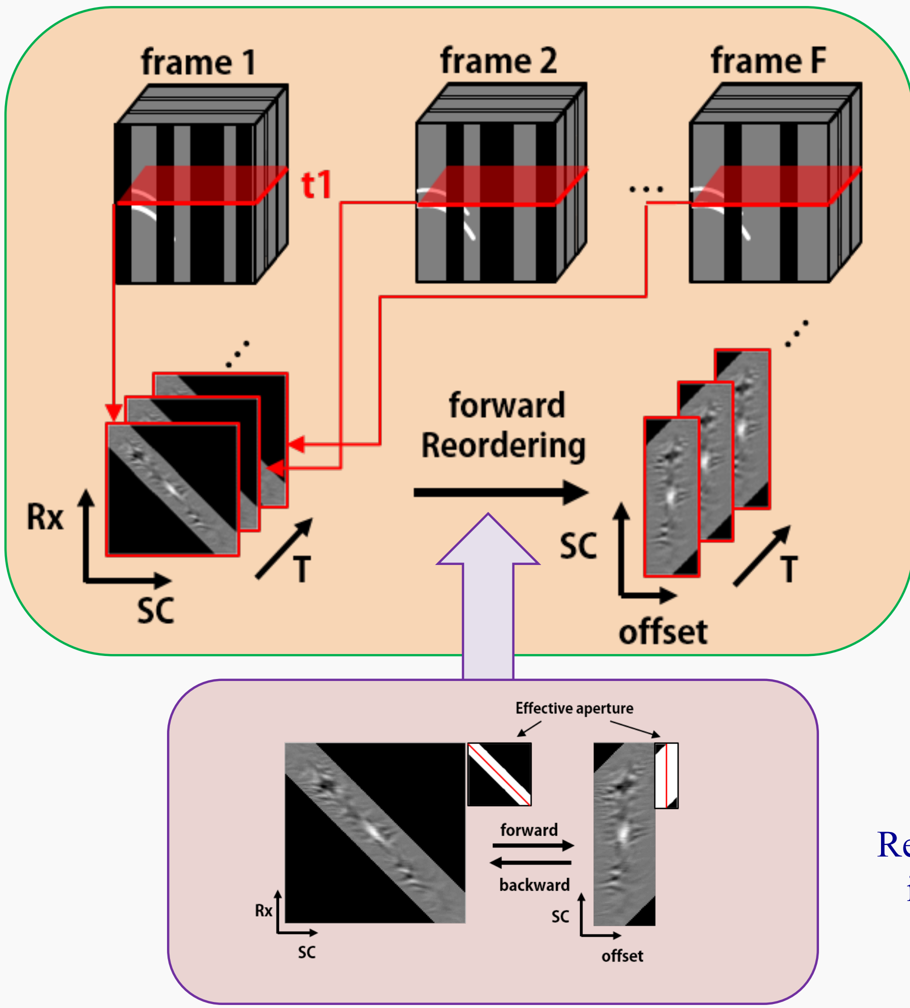

Series of
reordered data
→
Stacked
Hankel matrix

Multi-channel
ALOHA
Interpolation

Reordering of pre-beamformed
into scanline-offset domain
for low-rank property

Sparsity of the Spectrum

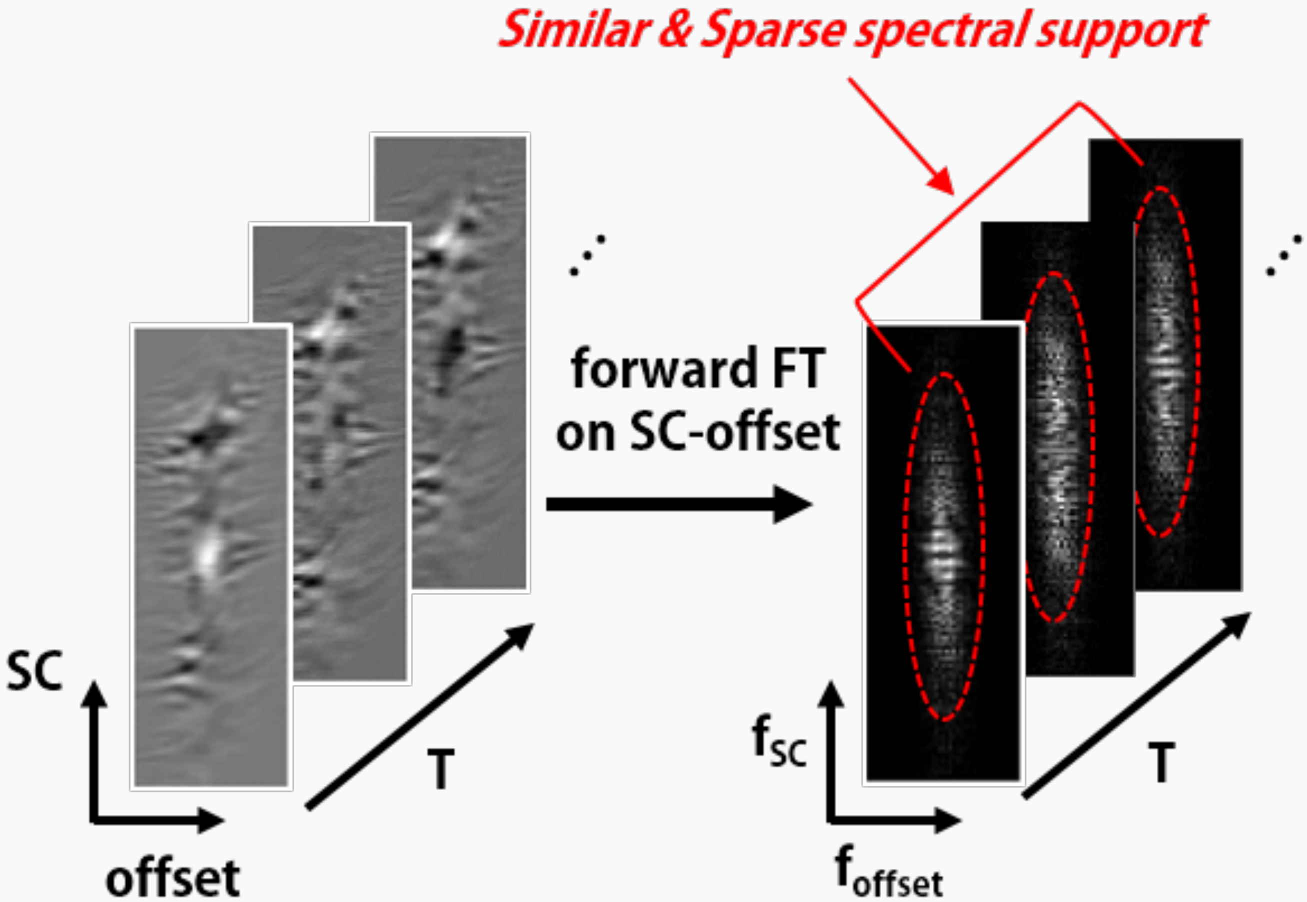

Low-Rankness of B-mode US Data

Exploiting Temporal Redundancy

→ inter-temporal annihilating filter

$$\min_{\mathcal{X}} \quad \|\mathcal{Z}\{\mathcal{X}\}\|_*$$

$$\text{subject to} \quad \mathcal{Z}\{\mathcal{X}\} = [\mathscr{H}\{\mathbf{X}_1\} \ \cdots \ \mathscr{H}\{\mathbf{X}_F\}] .$$

$$X_i(j,k) = M_i(j,k),$$

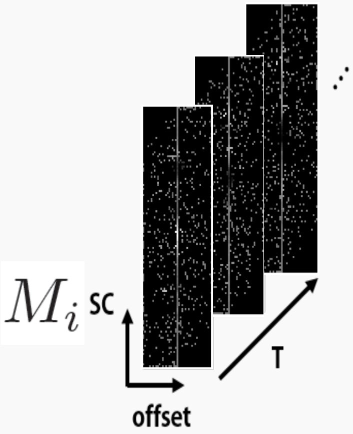

Reordered *subsampled pre-beamformed* data

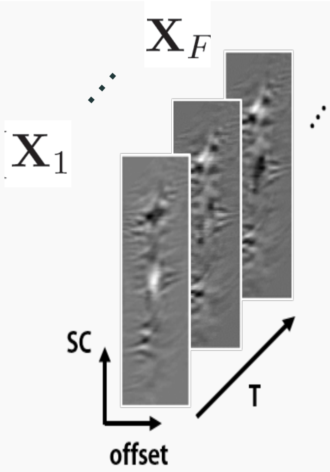

Reconstructed slices

Low-Rankness of B-mode US Data

Matrix →Hankel matrix

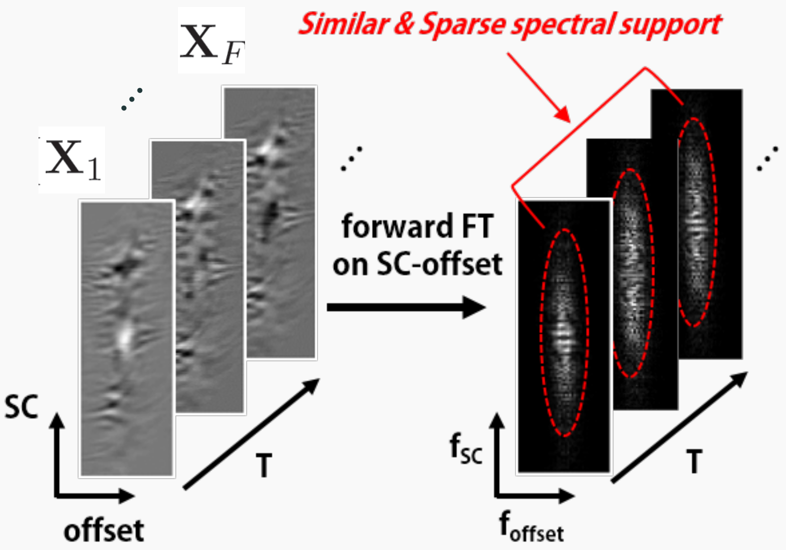

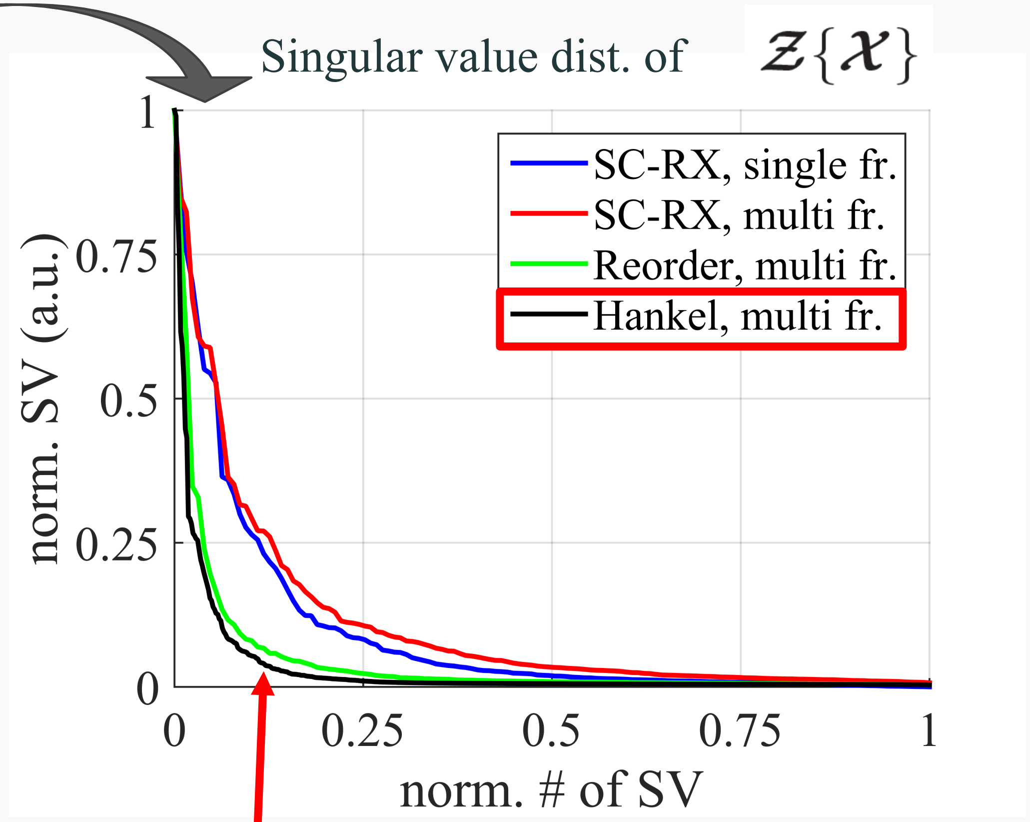

Spatio-temporal redundancy

→ achieved by multichannel Hankel matrix

Lowest rank over several settings!

In-vivo Acquisition

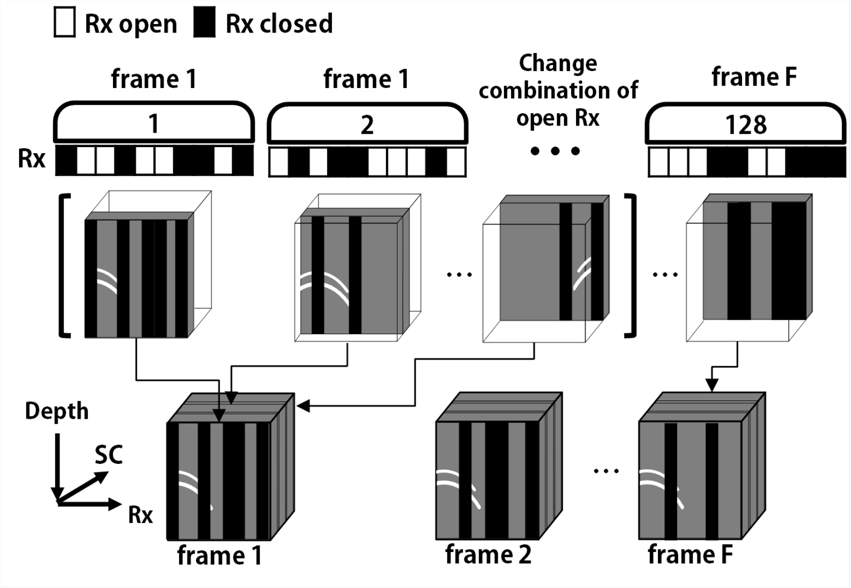

- Verasonics system with a Linear type probe (L7-4)
- Center freq:5MHz
- Sampling:20 MHz.
- 128 scanlines (SC) x 128 RX channels
- RX element
  - Width:133um
  - space between RX elements : 158um

Snapshot image from dynamic scan

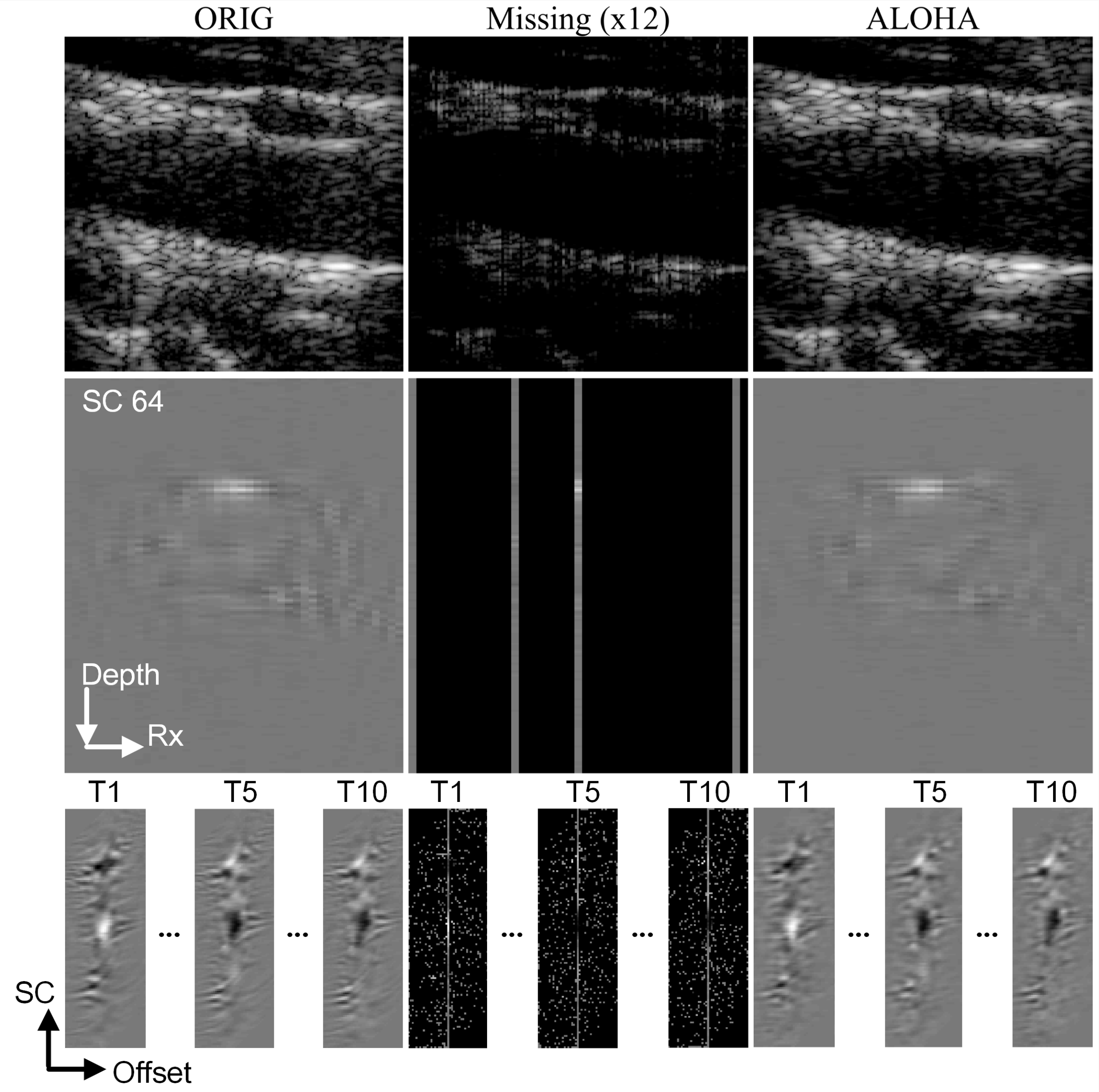

Dynamic reconstruction (x2)

Full Sampling

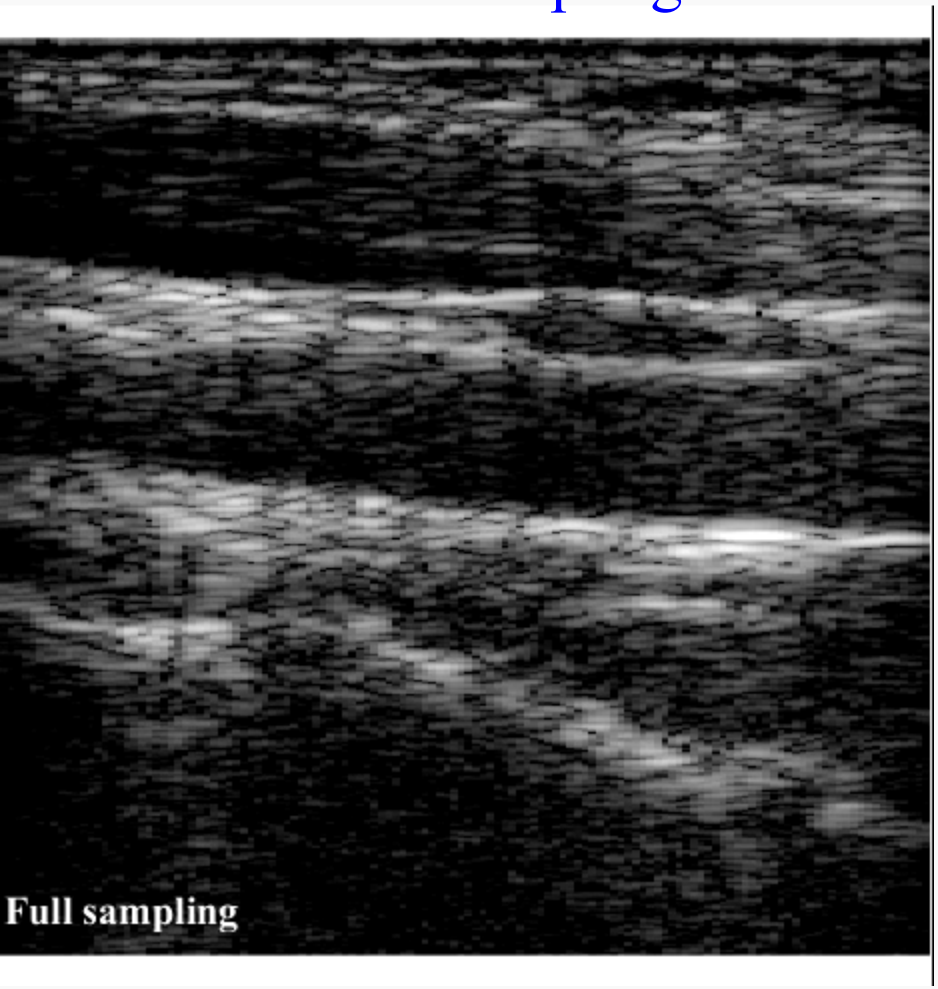

Beam forming

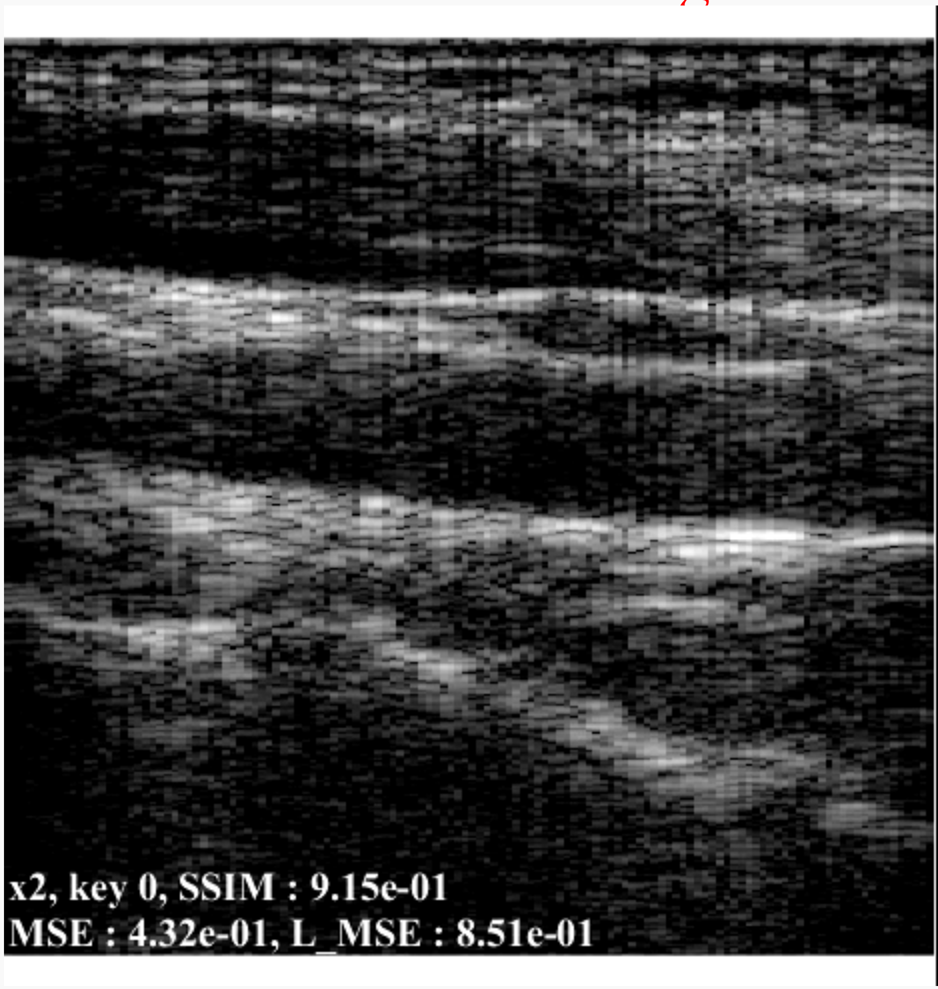

Dynamic reconstruction (x2)

Full Sampling

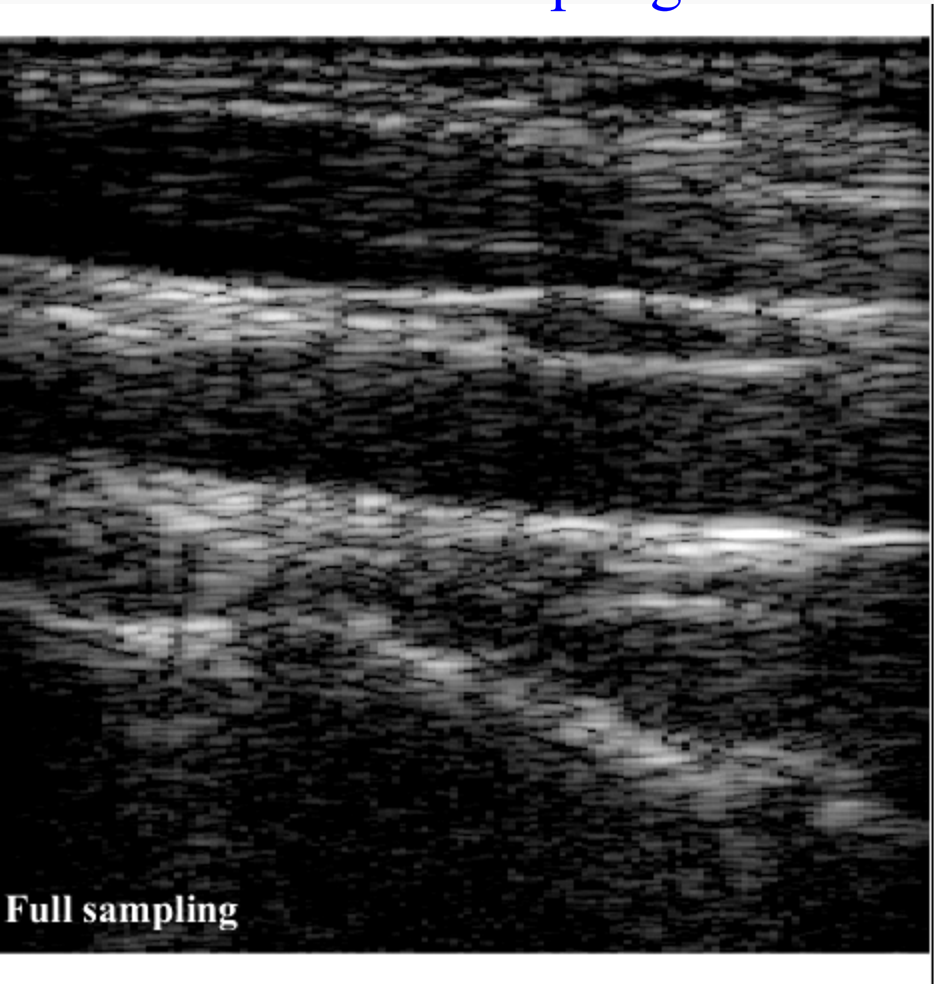

ALOHA

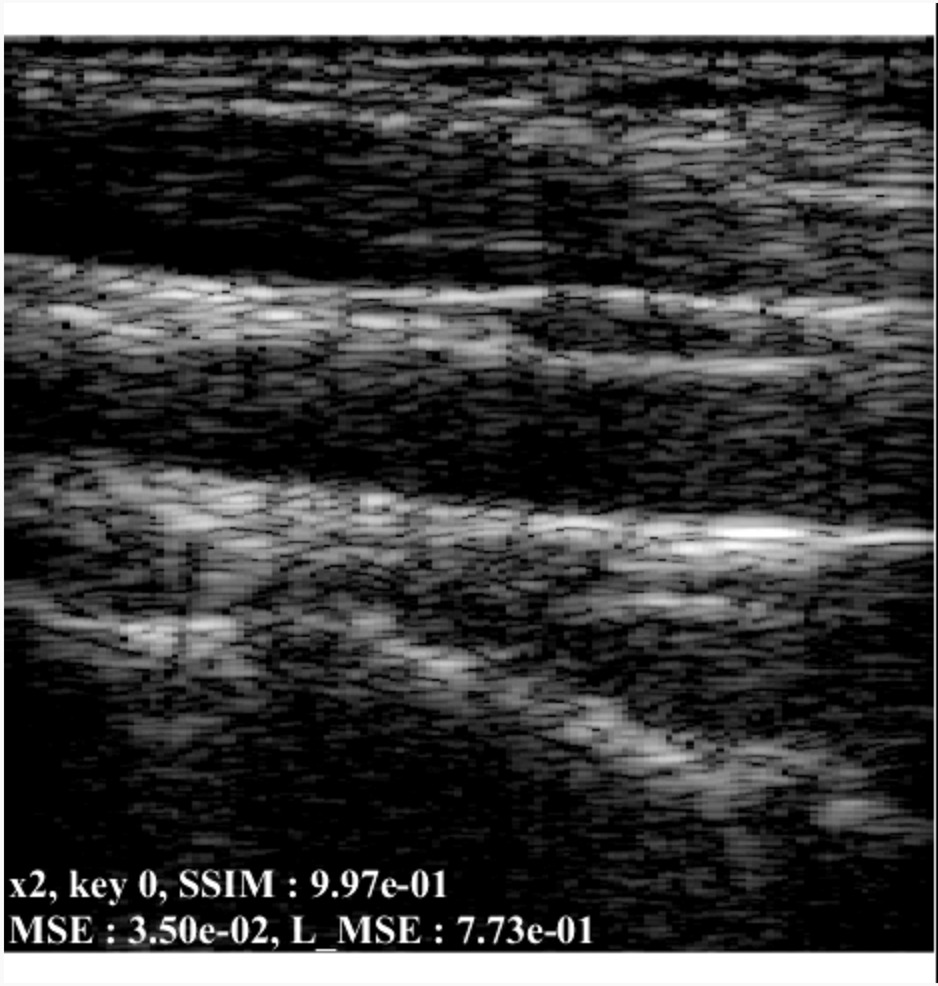

Dynamic reconstruction (x8)

Full Sampling

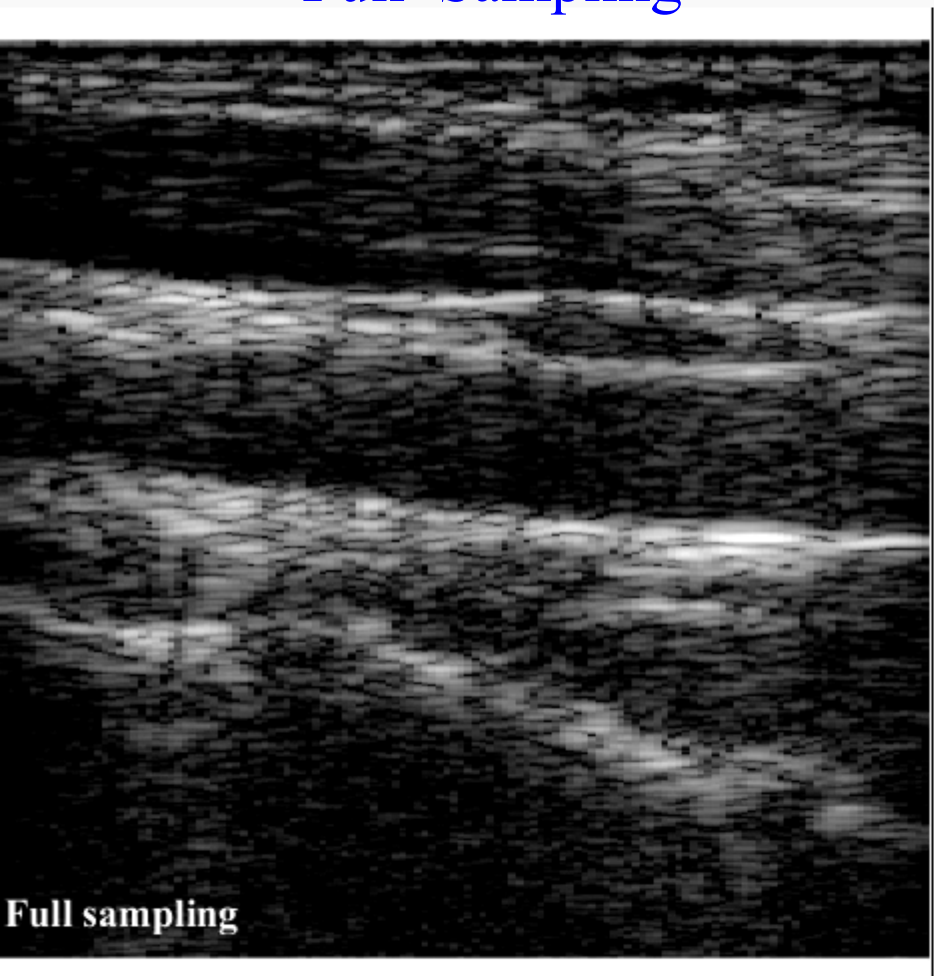

Beam forming

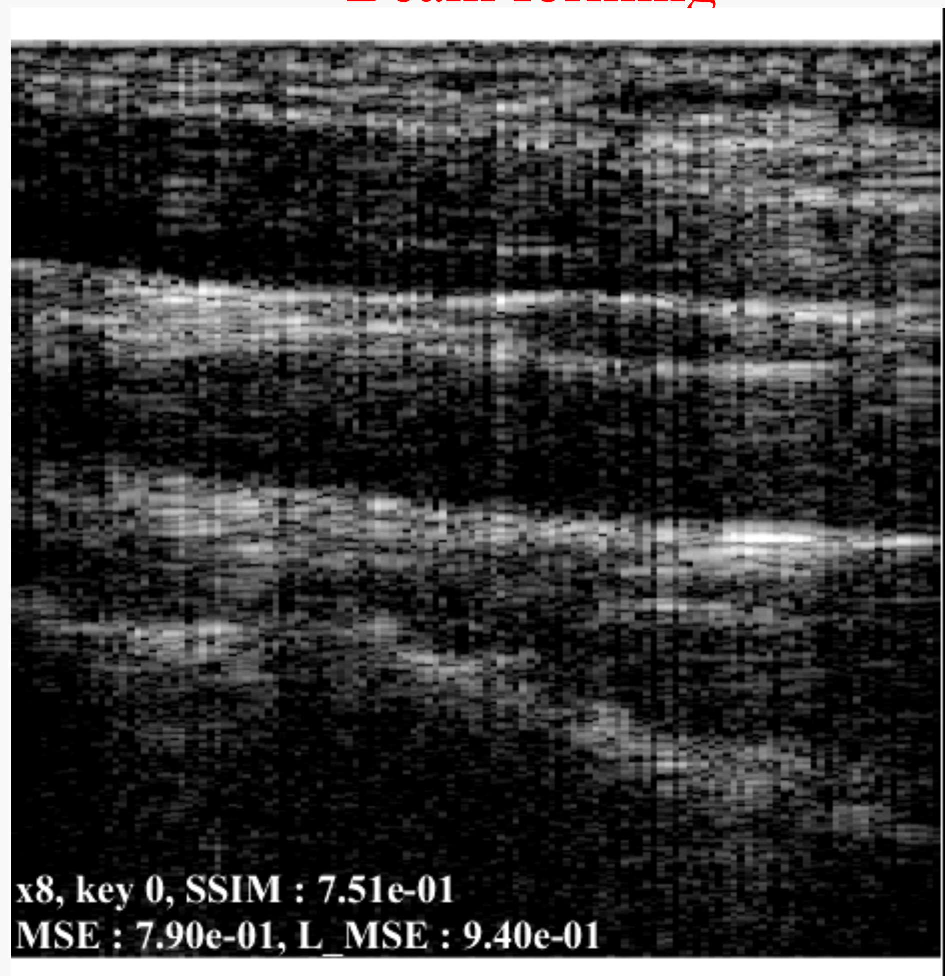

Dynamic reconstruction (x8)

Full Sampling

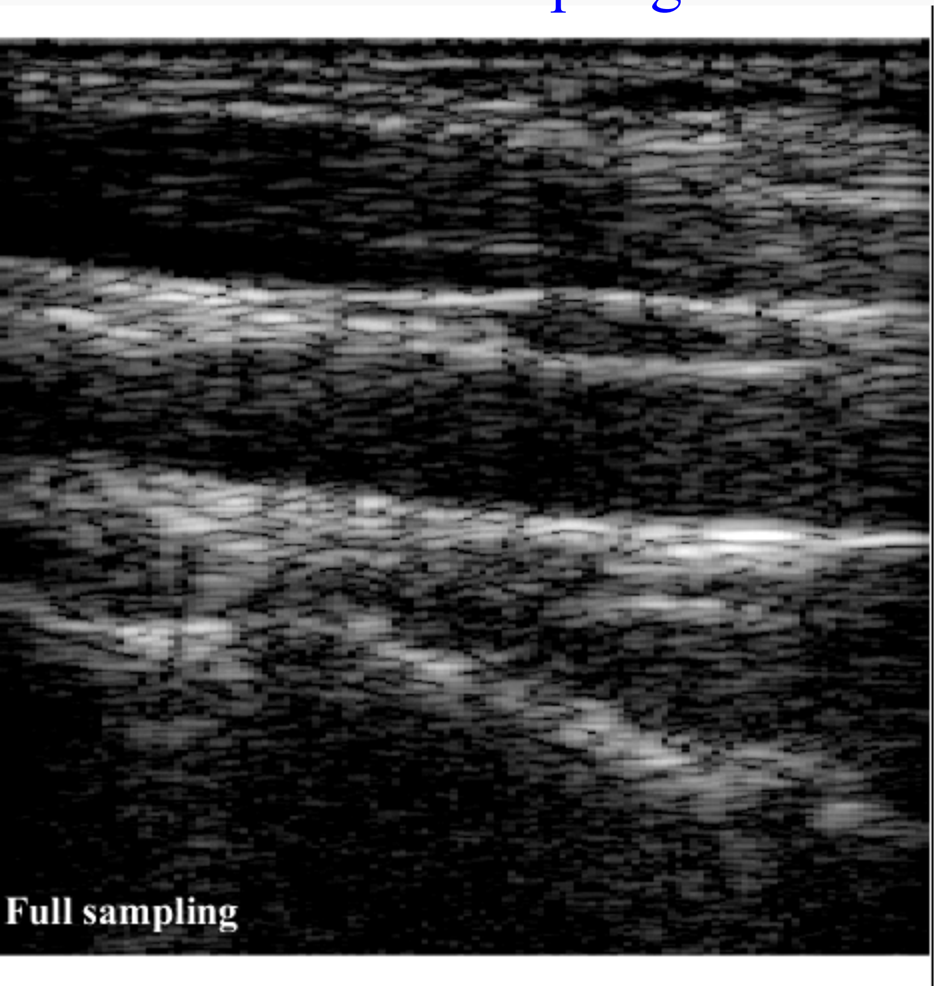

ALOHA

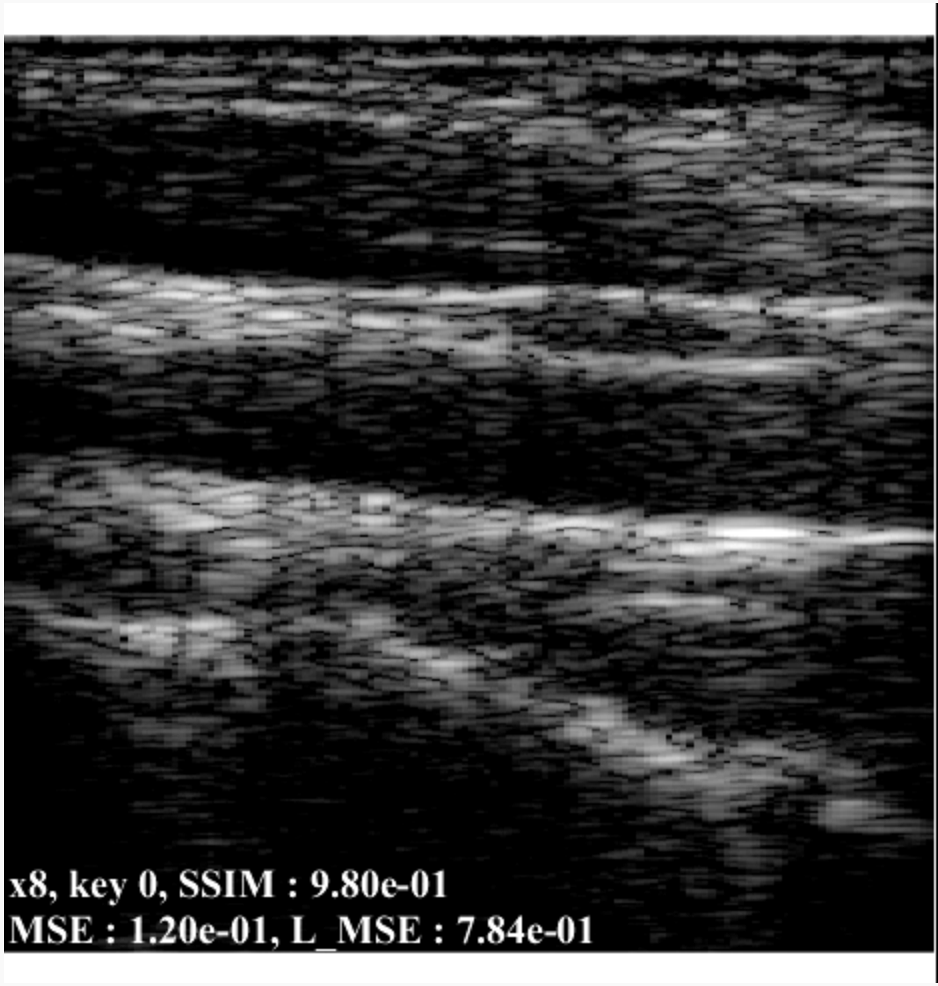

Dynamic reconstruction (x12)

Full Sampling

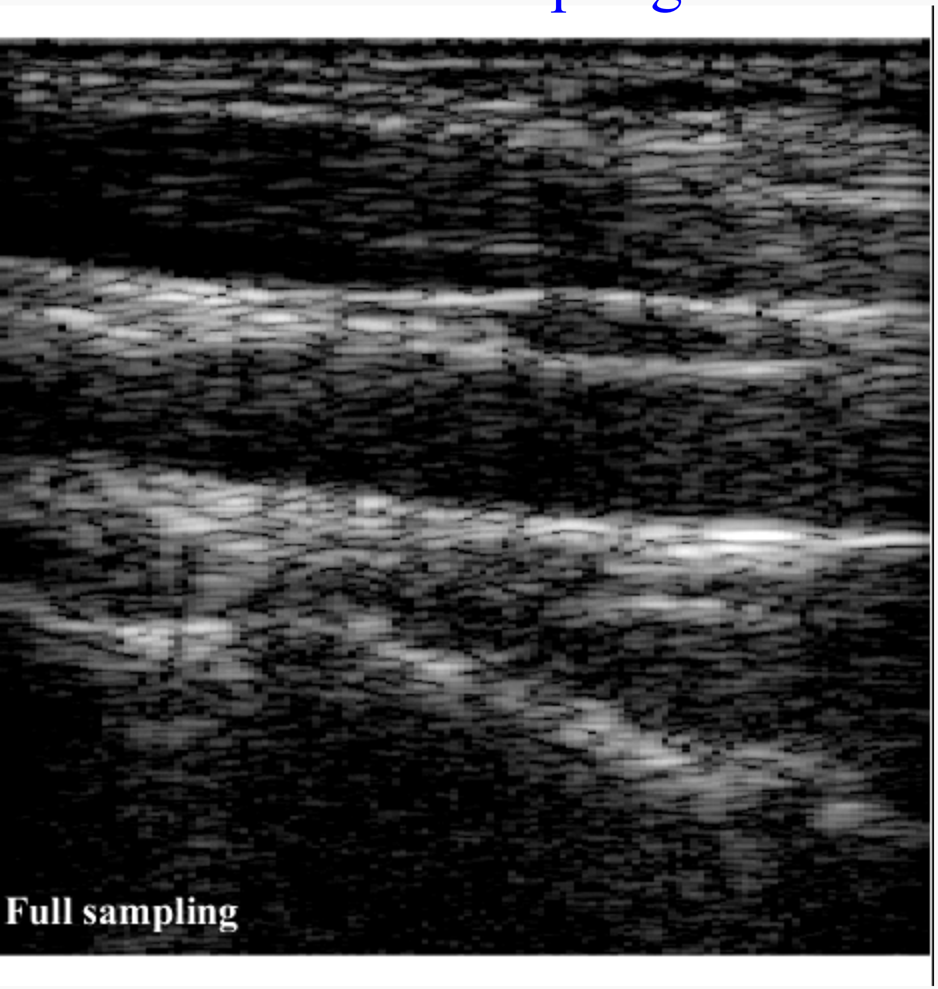

Beam forming

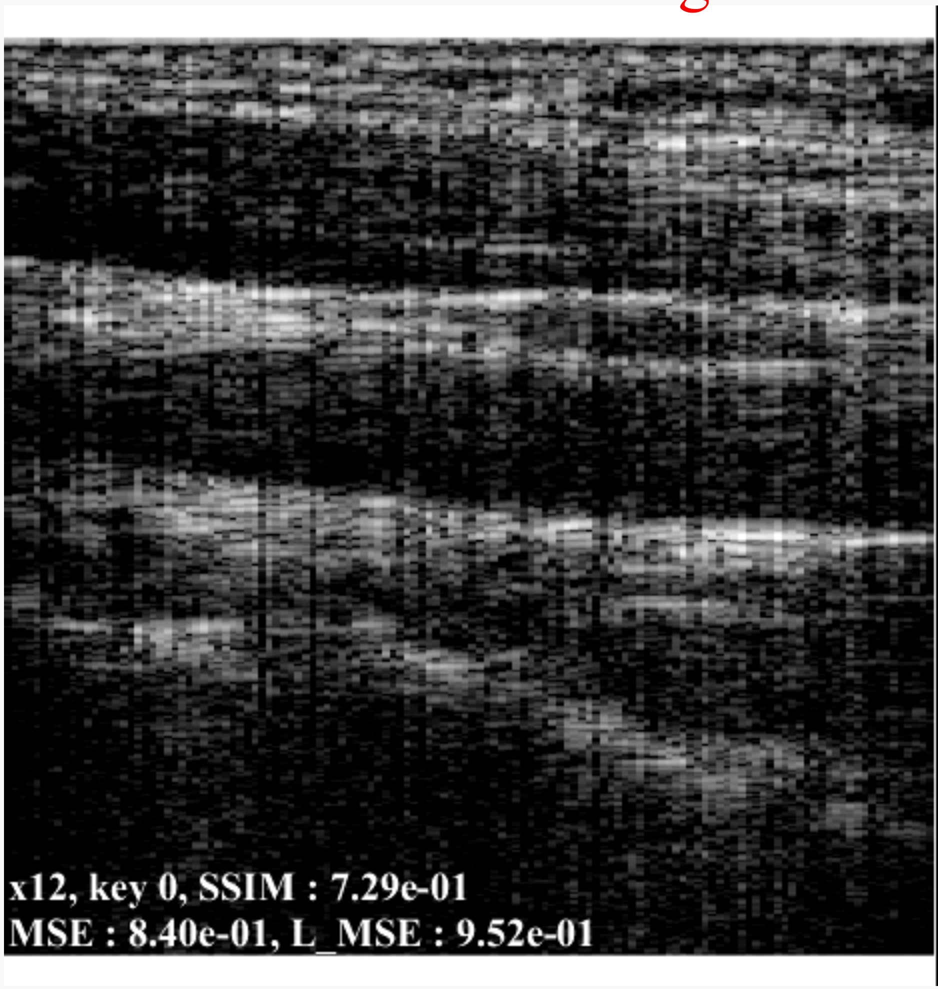

Dynamic reconstruction (x12)

Full Sampling

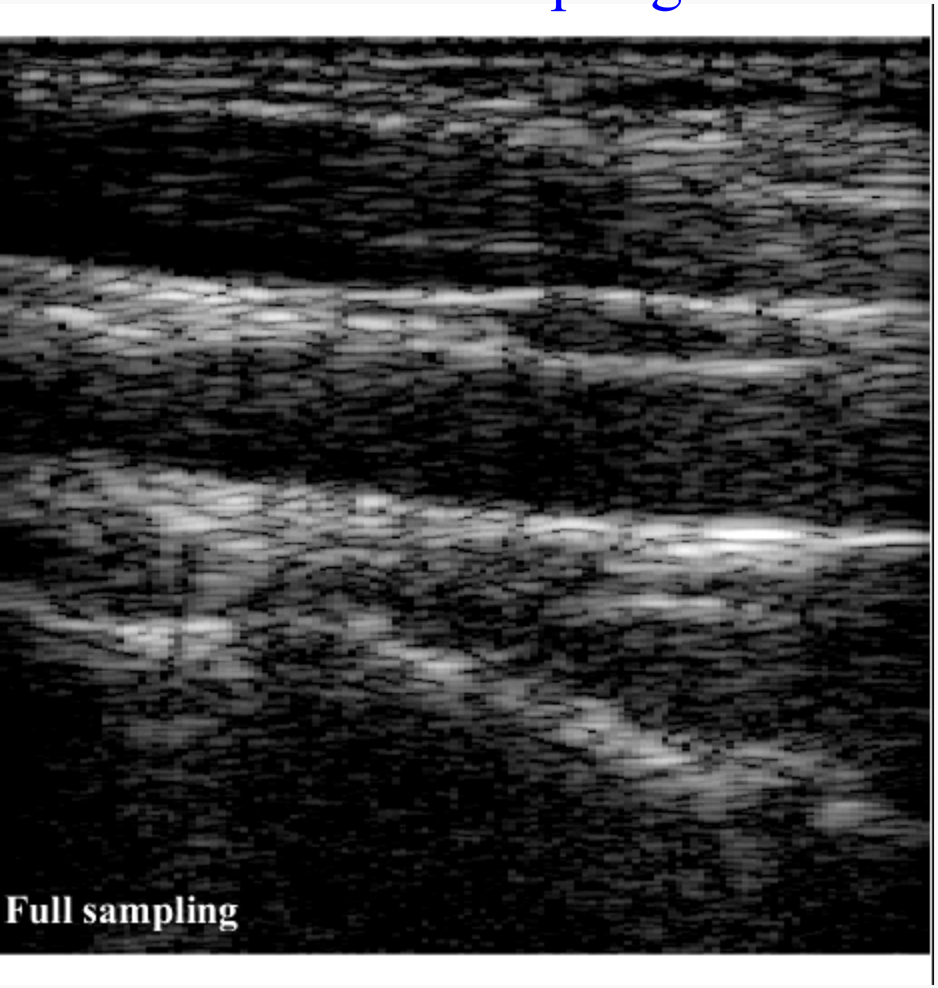

ALOHA

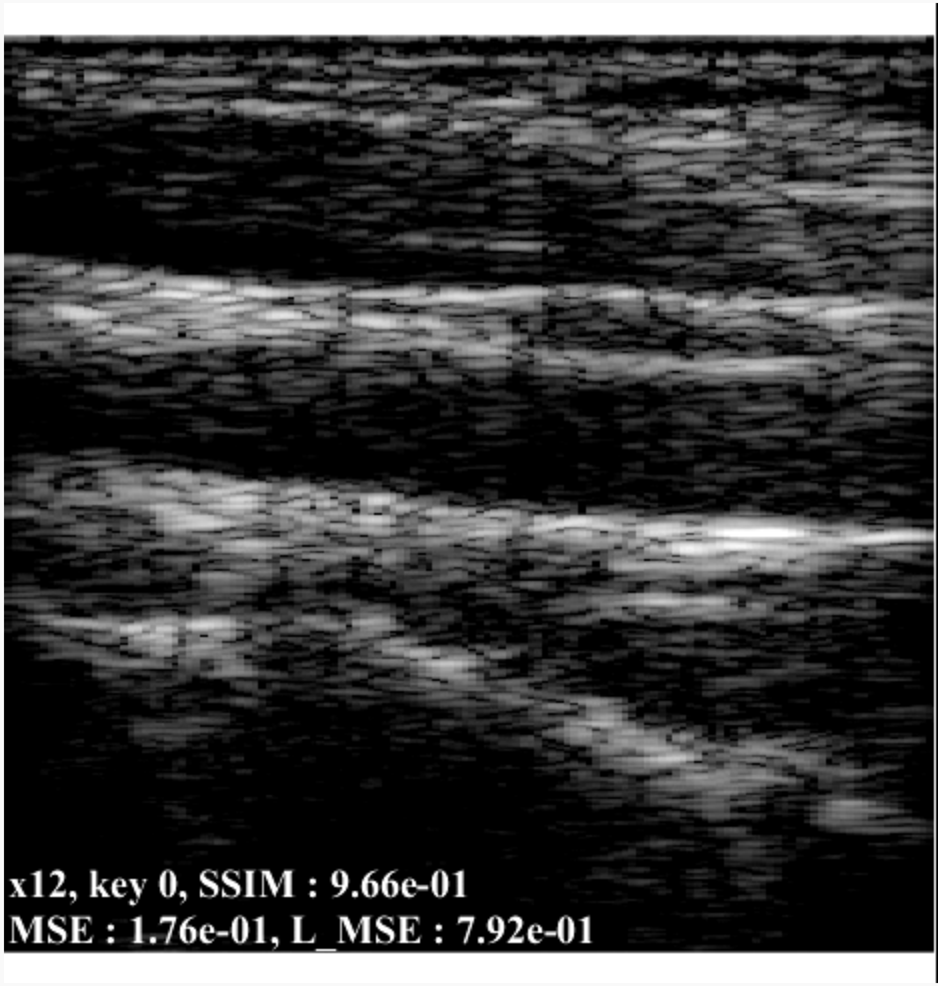

Localization microscopy

- Nanoscopy based on localization
  - Localization precision is not diffraction limited
  - Sparsely activated probes + localization => super-resolution image

$$\sigma_{\mu_i} = \sqrt{\left(\frac{s_i^2}{N} + \frac{a^2/12}{N} + \frac{8\pi s_i^4 b^2}{a^2 N^2}\right)}$$

Thompson et al. BPJ 2002

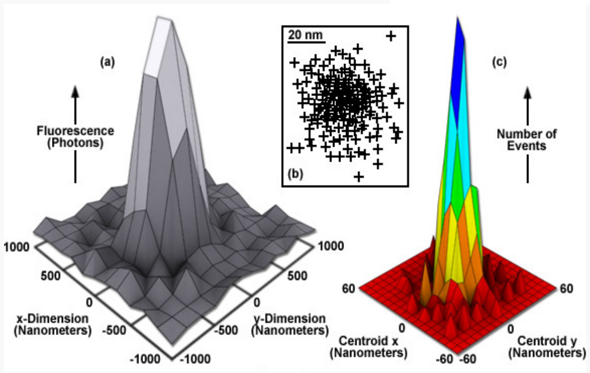

- However, sparse activation scheme has too slow temporal resolution for live imaging
  - Tens of seconds or several minutes
- High-density imaging for fast live imaging
  - Require a robust localization algorithm and system

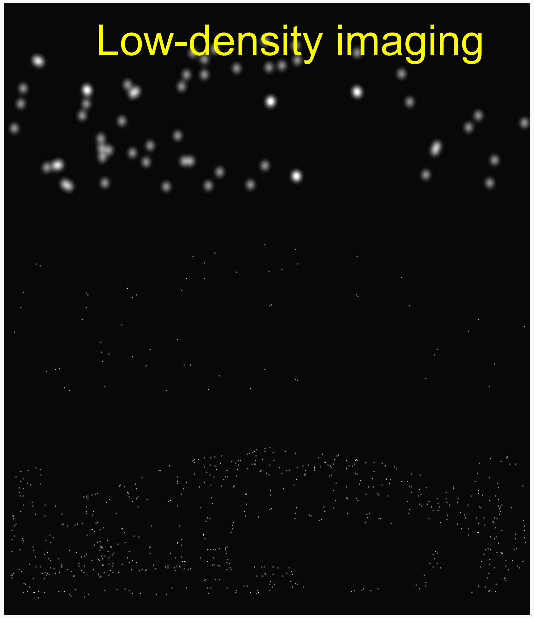

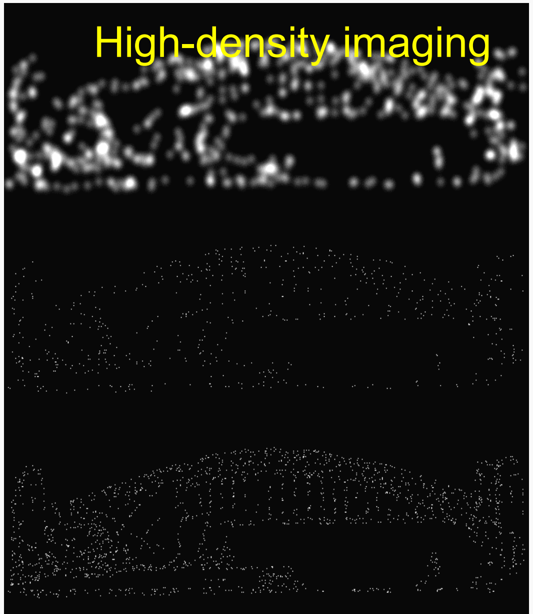

Existing high density algorithm

Greedy approach

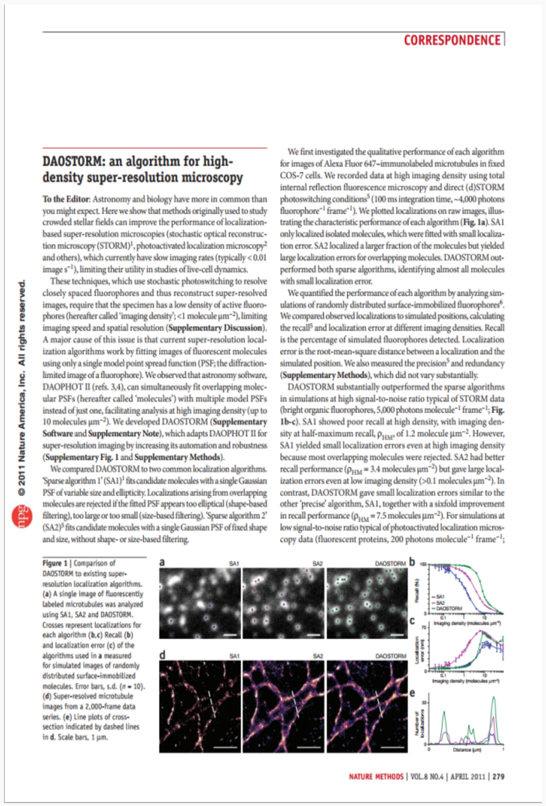

Holden, S.et al, Nat Methods, 2011

Sparsity based approach

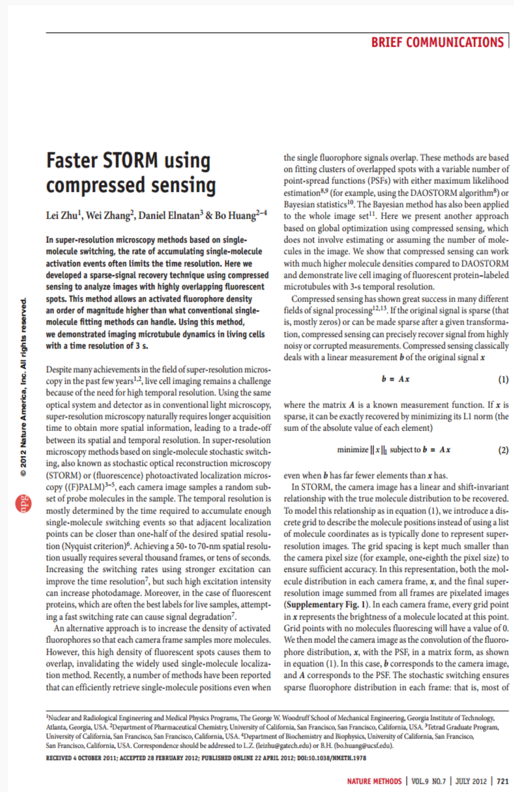

Zhu, L.et al, Nat Methods, 2012

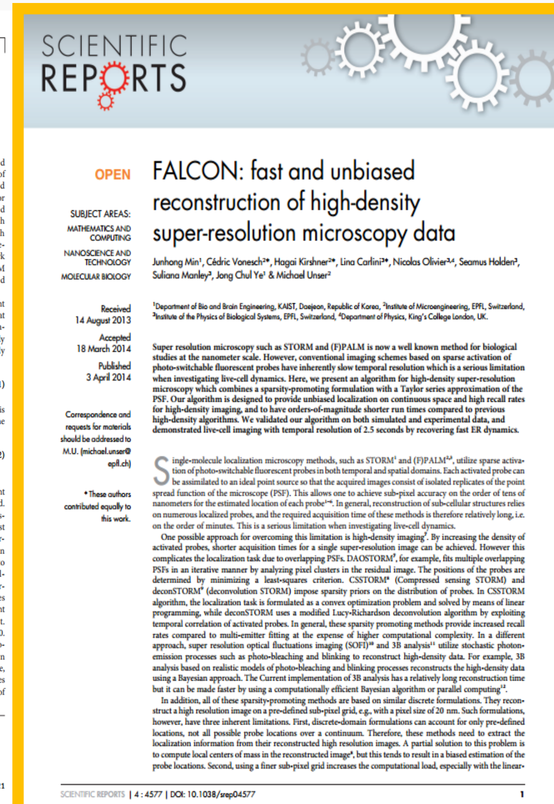

Min, J.et al, Sci. Rep, 2014

Better Localization Performance

ALOHA for localization microscopy

ALOHA principle

Image: $g = h * f$ f: Sparse

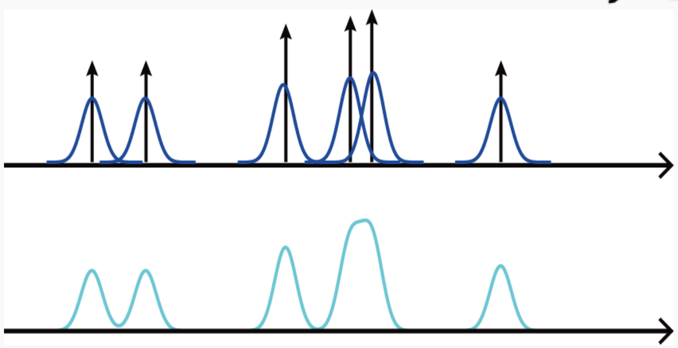

Fourier: $\hat{g} = \hat{h} \odot \hat{f}$ $\hat{f}$: Low-rank Hankel matrix

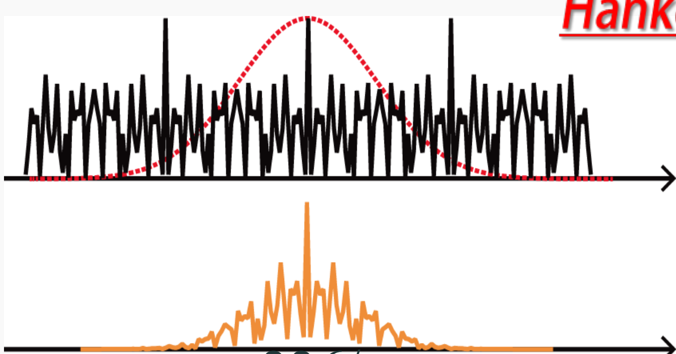

- ✓ *PSF estimation*
- ✓ *Deconvolution*
- ✓ *Grid-free localization*

PSF estimation

- HD localization algorithms usually assume that PSF is *known and fixed*
  - Requiring additional training low-density data set
  - *In live experiment, PSF is varying in time and space both.*

Key idea: ***Optimal PSF h^* => minimum rank of Hankel matrix***

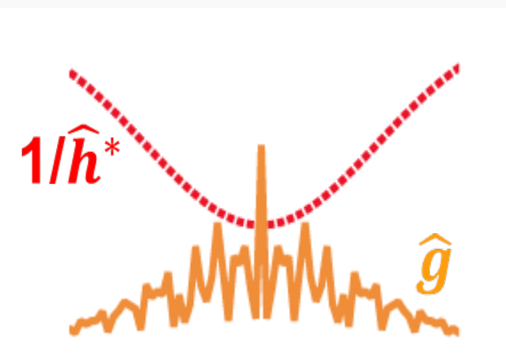

$\cong$

Minimum

$$\textbf{Rank}\left(\mathcal{H}\{\hat{g} \odot \hat{h}^{-1}\}\right)$$

- Under symmetric Gaussian PSF model, its width (σ) is estimated by minimizing Schatten norm

$$\sigma^* = \min_{\sigma} \left\| \left(\mathcal{H}\{\hat{g} \odot \widehat{h_\sigma}^{-1}\} \right) \right\|_{P\ (p<1)}$$

Grid-free localization

- Now, we have entire Fourier spectrum $\hat{f}$
- *Localization is nothing but spectral estimation problem!*

$$\hat{f}(m,n) = \sum_i c_i e^{-j2\pi\left(\frac{mx_i}{M}+\frac{ny_i}{N}\right)} = \sum_i c_i p_i^m q_i^n$$

- We used ACMP (algebraically coupled matrix pencils) algorithm (Vanpoucke et al, 1994)
- Data matrix $Z^{M\times N}$ of rank k, having no shared harmonics of p_i, q_i

$$\mathrm{Z}^{M\times N} = P^{M\times k}\, C^{k\times k}\, Q'^{N\times k}$$

- In Matrix form: $\mathrm{Z}^{M\times N} = P^{M\times k}\, C^{k\times k}\, Q'^{N\times k}$
- *P,Q are Vandermonde matrix*, C is diagonal

Algorithm procedure

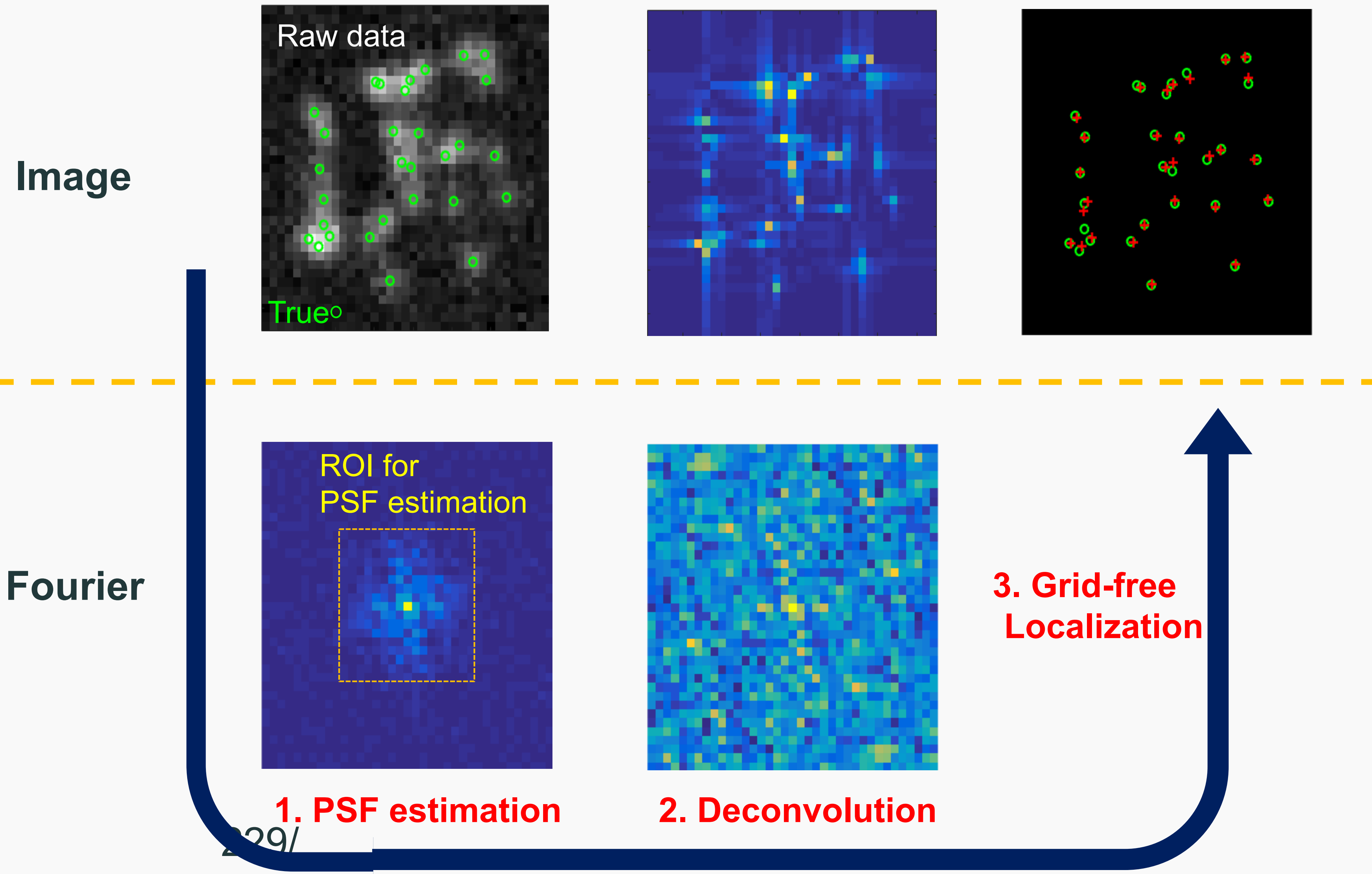

PSF variation along time

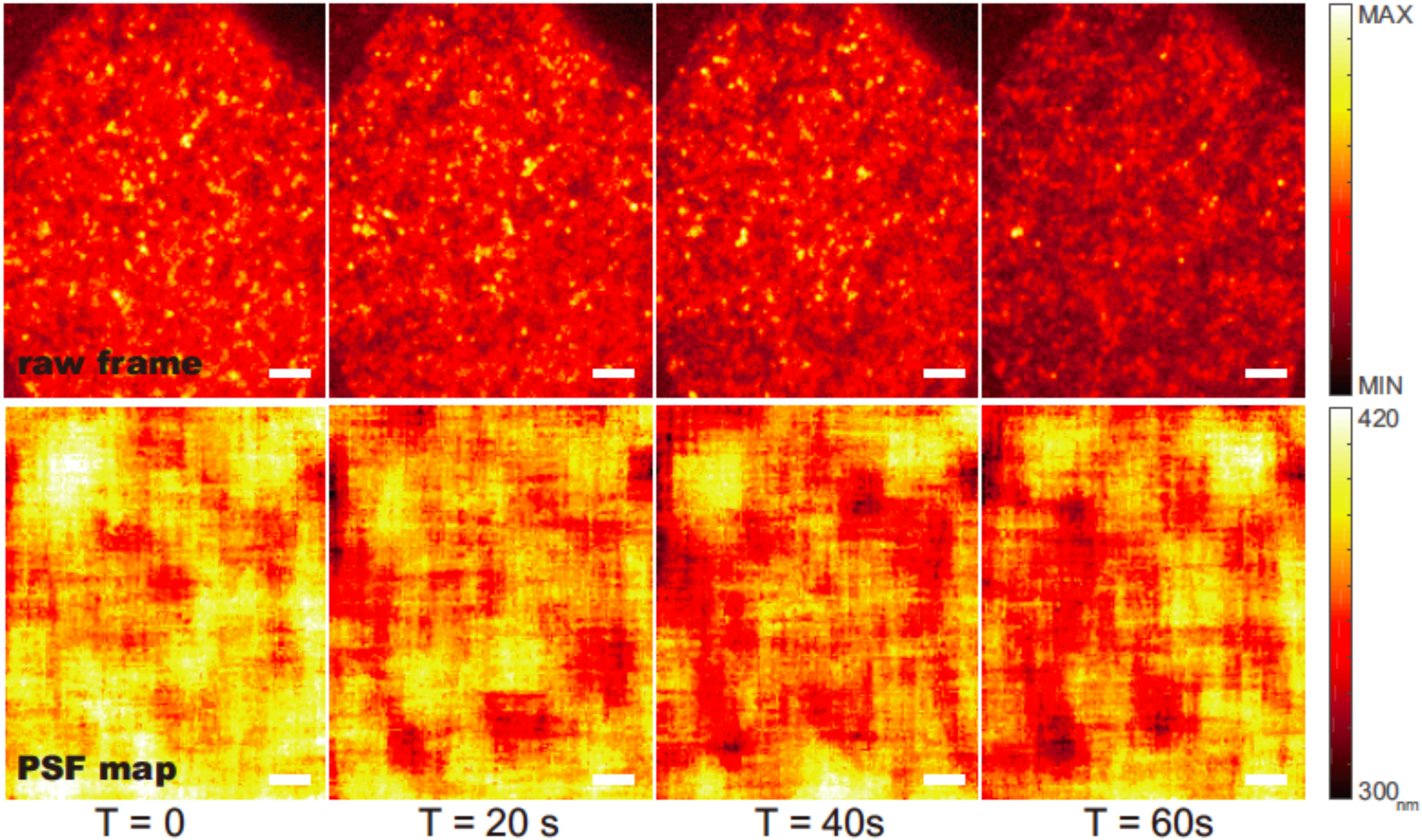

Reconstruction

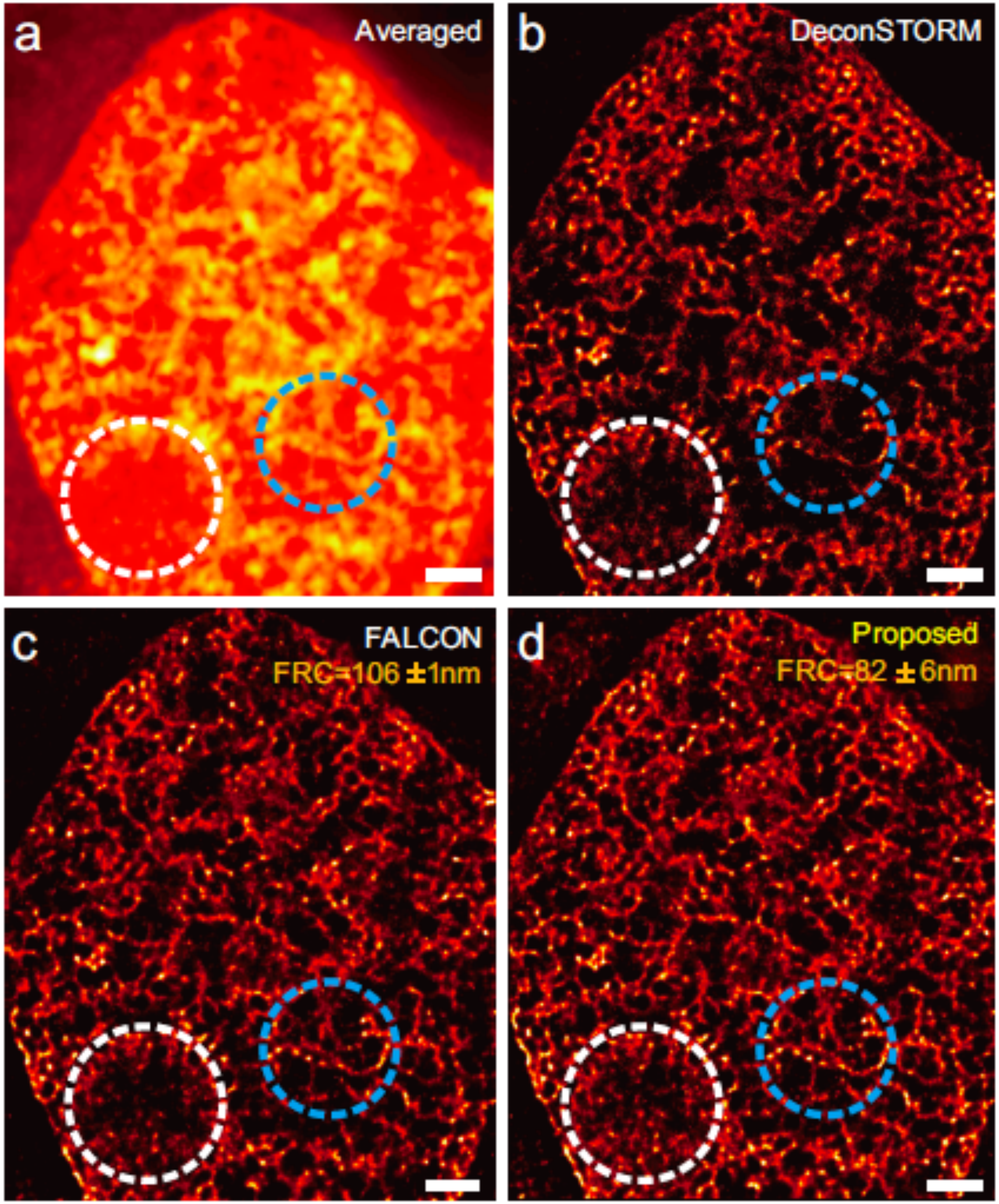

Localization bias

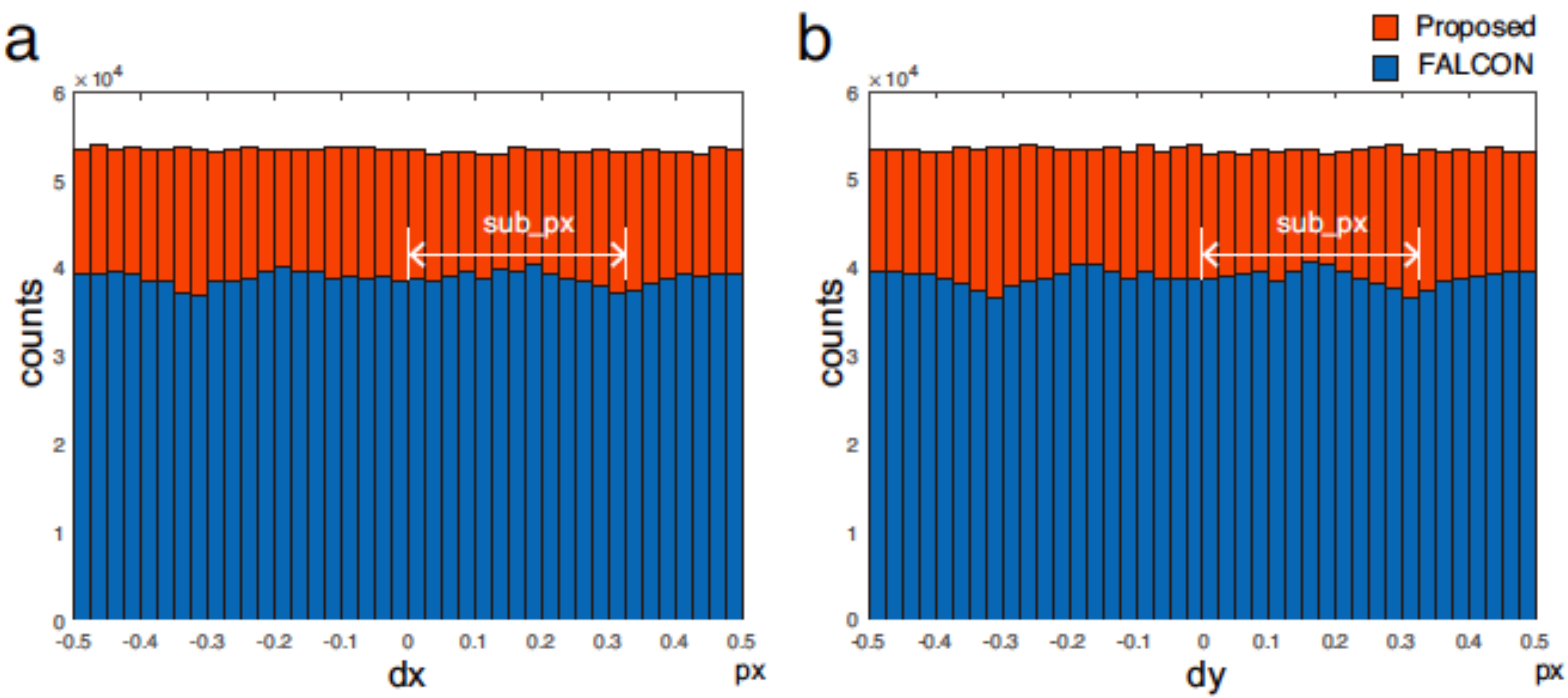

Free MATLAB software available

https://research.engineering.uiowa.edu/cbig/software

http://bispl.weebly.com/aloha-for-mri.html

Conclusions

- Off-the-grid = Continuous domain representation
- *Compressive* off-the-grid *imaging*:

  Exploit continuous domain modeling to improve image recovery from few measurements
- Two realizations: extrapolation, interpolation
  - Extrapolation: FRI theory
  - Interpolation: Structured low-rank matrix completion
- Performance guarantee for structured low-rank approach
  - 1D, 2D theory → near optimal performance guarantee

Conclusions (cont.)

- Extensive applications
  - MRI
    - Compressed sensing MRI, parallel MRI
    - Super-resolution MRI
    - MR artifact removal
  - Image processing: inpainting, impulse noise denoising
  - Other imaging applications
    - US imaging
    - Optics
- A missing link between analytic recon and CS ?

Joint work by several authors

CBIG, Univ. Iowa

1. Dr. Gregory Ongie
2. Dr. Merry Mani
3. Mr. Arvind Balachandrasekaran
4. Ms. Ipshita Bhattacharya
5. Ms. Sampurna Biswas

KAIST

1. Dr. Kyong Hwan Jin
2. Mr. Juyoung Lee
3. Dongwook Lee
4. Junhong Min

References

- Jong Chul Ye, Jong Min Kim, Kyong Hwan Jin and Kiryung Lee, "Compressive sampling using annihilating filter-based low-rank interpolation", IEEE Trans. on Information Theory, vol. 63, no. 2, pp.777-801, Feb. 2017.

- Kyong Hwan Jin, Dongwook Lee, and Jong Chul Ye. "A general framework for compressed sensing and parallel MRI using annihilating filter based low-rank hankel matrix," IEEE Trans. on Computational Imaging, vol 2, no. 4, pp. 480 - 495, Dec. 2016.

- Kyong Hwan Jin, Ji-Yong Um, Dongwook Lee, Juyoung Lee, Sung-Hong Park and Jong Chul Ye, " MRI artifact correction using sparse + low-rank decomposition of annihilating lter-based Hankel matrix", Magnetic Resonance in Medicine (in press), 2016

- Juyoung Lee, Kyong Hwan Jin, and Jong Chul Ye, "Reference-free single-pass EPI Nyquist ghost correction using annihilating filter-based low rank Hankel matrix (ALOHA)", Magnetic Resonance in Medicine, 10.1002/mrm.26077, Feb. 17, 2016.

References

- Dongwook Lee,, Kyong Hwan Jin, Eung Yeop Kim, Sung-Hong Park and Jong Chul Ye, "Acceleration of MR parameter mapping using annihilating filter-based low rank Hankel matrix (ALOHA)", Magnetic Resonance in Medicine, 10.1002/mrm.26081, Jan. 1, 2016.

- Kyong Hwan Jin and Jong Chul Ye, "Annihilating filter based low rank Hankel matrix approach for image inpainting", IEEE Trans. Image Processing, 2015 Nov;24(11):3498-511.

- KH Jin, JC Ye, Sparse+ low rank decomposition of annihilating filter-based Hankel matrix for impulse noise removal, arXiv preprint arXiv:1510.05559
- Min, J., Carlini, L., Unser, M., Manley, S., & Ye, J. C. (2015, September). Fast live cell imaging at nanometer scale using annihilating filter-based low-rank Hankel matrix approach. In SPIE Optical Engineering+ Applications (pp. 95970V-95970V). International Society for Optics and Photonics.

- Jin, Kyong Hwan, Yo Seob Han, and Jong Chul Ye. "Compressive dynamic aperture B-mode ultrasound imaging using annihilating filter-based low-rank interpolation." Biomedical Imaging (ISBI), 2016 IEEE 13th International Symposium on. IEEE, 2016.

References

- G. Ongie, M. Jacob, Off-the-Grid Recovery of Piecewise Constant Images from Few Fourier Samples, SIAM Journal on Imaging Sciences, in press.

- G. Ongie, S. Biswas, M. Jacob, Convex recovery of continuous domain piecewise constant images from non-uniform Fourier samples, https://arxiv.org/abs/1703.01405

- Ongie, M. Jacob, GIRAF: A Fast Algorithm for Structured Low-Rank Matrix Recovery, https://arxiv.org/abs/1609.07429

- M. Mani, M. Jacob, D. Kelley, V. Magnotta, Multishot sensitivity encoded diffusion data recovery using structured low rank matrix completion (MUSSELS), Magnetic Resonance in Medicine, in press.

- G. Ongie, S. Biswas, M. Jacob, Structured matrix recovery of piecewise constant signals with performance guarantees, International Conference on Image Processing, 2016.

- A. Balachandrasekaran, G. Ongie, M. Jacob, Accelerated dynamic MRI using structured matrix completion, International Conference on Image Processing, 2016.

References

- G. Ongie, M. Jacob, A fast algorithm for stuctured low rank matrix recovery with applications to undersampled MRI reconstruction, ISBI, Prague, Czech Republic, 2016.

- G. Ongie, M. Jacob, Recovery of piecewise smooth images from few Fourier samples, Sampling Theory and Applications (SampTA), Washington D.C., 2015.

- G. Ongie, M. Jacob, Super-resolution MRI using finite rate of innovation curves, IEEE ISBI, New York City, USA, 2015.

- M. Mani, V. Magnotta, D. Kelley, M.Jacob, Comprehensive reconstruction of multishot multichannel diffusion MRI data using MUSSELS, Engineering in Biology and Medicine Conference, 2016.